A characterisation of genes involved in apoptosis resistance

by

Tanja Davis

Thesis presented in partial fulfilment of the requirements for the degree Master of Science in Genetics at Stellenbosch University

Supervisor: Mr M. F. February

Faculty of Science

Department of Genetics

Collaborator: Dr M. Meyer

Department of Biotechnology

University of Western Cape

March 2013

The financial assistance of the National Research Foundation (NRF) towards this research is hereby acknowledged. Opinions expressed and conclusions arrived at, are those of the author and are not necessarily to be attributed to the NRF.

Declaration

By submitting this thesis/dissertation electronically, I declare that the entirety of the work contained therein is my own, original work, that I am the sole author thereof (save to the extent explicitly otherwise stated), that reproduction and publication thereof by Stellenbosch University will not infringe any third party rights and that I have not previously in its entirety or in part submitted it for obtaining any qualification.

March 2013

“Life is pleasant. Death is peaceful. It’s the transition that’s troublesome.”

Prof Isaac Asimov (1920 – 1992), scholar and novelist

Abstract

Apoptosis represents a finely orchestrated and highly conserved natural form of cell death. It exhibits unique morphological and biochemical characteristics which culminate in the controlled dismantling of a cell from within followed by its discreet removal by phagocytic cells. Apoptosis is vital for the preservation of cell and tissue homeostasis but also performs several defensive and protective functions. Owing to its importance, apoptosis is highly regulated and a large number of proteins have been shown to mediate and safeguard the process. Furthermore, deregulated or altered levels of apoptosis can have severe pathological consequences; indeed, apoptosis has been shown to play a central role in several diseases, including neurological and autoimmune diseases as well as a variety of cancers. Consequently, the search for apoptotic-based therapies has received much attention and of vital importance to this quest is the characterisation of the specific mediators of apoptosis and their regulation as well as the identification of novel genes or proteins that can have a regulatory effect on apoptosis. It is thus the aim of this study to assist in this characterisation and also to identify novel candidate genes potentially involved in apoptosis.

In a previously performed pilot study, three novel candidate genes potentially involved in apoptosis were identified by performing promoter-trap mutagenesis experiments. These genes were *lipoic acid synthetase* (*LIAS*), *cyclophilin A* (*CYPA*) and *ribosomal protein L9* (*RPL9*). Since the methodology for this pilot study involved the use of functionally haploid cells, it was aimed in this study to verify these results in a diploid mouse cell line. Candidate gene knockdown was achieved by means of RNA interference and apoptosis assays were performed. A potential role for *LIAS* and *CYPA* in apoptosis was successfully verified in this study; however this could not be achieved for *RPL9* and the gene was thus excluded from further study. In addition, nucleotide sequences isolated during the promoter-trap mutagenesis experiments in the pilot study were also investigated in order to identify additional novel candidate genes involved in apoptosis. By performing nucleotide BLAST searches, two potential candidate genes were identified, namely *AHNAK nucleoprotein* (*AHNAK*) and *serum amyloid A-like 1* (*SAAL1*). Further bioinformatic analyses were performed with the four candidate genes in order to ascertain possible associations with apoptosis or cancer. Lastly, to further characterise the four candidate genes, the relative gene expression was investigated by means of quantitative PCR in two cancer and control cell lines. The results revealed significant differential expression for the majority of genes in the cancer cell lines when compared to the control cell lines.

In conclusion, this study identified and characterised four novel genes potentially involved in apoptosis. Results obtained during this study can aid in the complete characterisation and functional annotation of these genes. Potential ties to apoptosis and associations with cancer are

discussed for all four candidate genes and the possibilities of therapeutic strategies for anticancer treatments involving these candidate genes are noted.

Opsomming

Apoptose verteenwoordig ‘n fyn georganiseerde en hoogs gekonserveerde natuurlike vorm van seldood. Dit vertoon unieke morfologiese and biochemiese eienskappe wat uitloop in die beheerde afbreek van ‘n sel vanuit die binnekant waarna dit onopsigtelik deur fagositiese selle verywder word. Apoptose is uiters belangrik vir die bewaring van sel en weefsel homeostase, maar dit vervul ook menigde afwerende and beskermde funksies. Vanweë sy noodsaaklikheid is apoptose hoogs gereguleer and ‘n groot aantal proteïene is al aangewys as bemiddelaars en beskermers van die proses. Verder, wangereguleerde en veranderde vlakke van apoptose kan ernstige patalogiese nagevolge hê; inderdaad, ‘n sentrale rol vir apoptose in verskeie siektes is al bevestig, insluitend neurologiese en outo-immuun siektes asook ‘n verskeidenheid van kankers. As gevolg hiervan ontvang die soektogte vir apoptose-gebaseerde terapieë vele aandag en uiters noodsaaklik vir hierdie soektogte is die karakterisering van die spesifieke bemiddelaars van apoptose en hul regulering asook die identifisering van nuwe gene of proteïene wat ‘n regulerende effek kan hê op apoptose. Dit is dus die doel van hierdie studie om by te dra tot hierdie karakterisering en ook om nuwe kandidaat gene wat moontlik betrokke kan wees in apoptose te identifiseer.

In ‘n vorige loodsprojek is drie gene moontlik betrokke in apoptose geïdentifiseer deur middel van promoter-strik mutagenese eksperimente. Hierdie gene is *lipoic acid synthetase* (*LIAS*), *cyclophilin A* (*CYPA*) en *ribosomal protein L9* (*RPL9*). Aangesien die metodiek in the loodsprojek gebruik gemaak het van funksionele haploïede selle, was dit die doel van hierdie studie om die resultate te bevestig in ‘n diploïede muis sellyn. Ribonukleïensuur (RNS) steuring is uitgevoer vir die uitklopping van die kandidaat gene en apoptose toetse is ook gedoen. Die bevestiging van ‘n moontlike rol vir *LIAS* en *CYPA* in apoptose was suksesvul in hierdie studie; alhoewel dit was nie bereikbaar vir *RPL9* nie en hierdie geen is dus uitgesluit in verdere studies. Bykomend is nukleotied volgordes wat geïsoleer is tydens die promoter-strik mutagenese eksperimente in die loodsprojek ook nagesien om moontlike addisionele nuwe kandidaat gene te identifiseer wat moontlik betrokke kan wees by apoptose. Twee potensiële kandidaat gene, naamlik *AHNAK nucleoprotein* (*AHNAK*) en *serum amyloid A-like 1* (*SAAL1*), was geïdentifiseer deur middel van nukleotied BLAST soektogte. Addisionele bioinformatiese analises is uitgevoer op die vier kandidaat gene om moontlike redes vir ‘n assosiasie met apoptose of kanker vas te stel. Laastens, om die kandidaat gene verder te karakteriseer, is daar ondersoek ingestel op die relatiewe geen uitdrukking van die kandidaat gene in twee kanker en twee normale sellyne. Die resultate het betekenisvolle differensiële regulering getoon vir meeste van die gene in die kanker sellyne in vergelyking met die normale sellyne.

Ten slotte, vier kandidaat gene moontlik betrokke in apoptose is in die huidige studie geïdentifiseer en gekarakteriseer. Die resultate verwerf in hierdie studie kan moontlik bydra tot die volkome

karakterisering en funksionele annotering van die kandidaat gene. Moontlike skakels met apoptose en assosiasies met kanker is bepreek vir die vier kandidaat gene en die moontlikheid van terapeutiese strategieë gebaseer rondom die kandidaat gene word ook genoem.

Acknowledgements

I would hereby like to thank the following persons and institutions, in no particular order, for supporting me during this study and for offering valuable guidance and advice:

- Mr M. F. February, for giving me the opportunity to be part of this study and for his supervision
- Prof D. Brink, for immeasurable amount of guidance, support and motivation
- Prof L. Warnich, Lundi Korkie and the rest of lab 231, for welcoming me into their lab and providing me with a healthy and friendly working environment
- The National Research Foundation (NRF), for providing me with personal funding
- My husband, family and friends, for continued support throughout my studies
- Dr Mervin Meyer, Dr Keith Gould and Dr A. Madiehe for their valuable contributions to this study

Table of contents

Declaration ... ii
Abstract ... iv
Opsomming ... vi
Acknowledgements ... viii
Table of contents ... ix
List of abbreviations ... xii
List of figures ... xviii
List of tables ... xxv
Chapter 1: Literature review ... 1
1.1 Cell death ... 1
1.1.1 Types of cell death ... 2
1.2 Apoptosis ... 5
1.2.1 The apoptotic process ... 6
1.2.2 Molecular pathways in apoptosis ... 7
1.2.3 Apoptosis related molecules ... 11
1.2.4 The genetics of apoptosis related proteins – implications of mutations ... 14
1.2.5 Implications of mismanaged apoptosis ... 15
1.2.6 Apoptosis-based therapies – contributing to the fight against cancer ... 17
1.3 Aims and objectives ... 20
1.4 Background to the current study ... 20
1.5 References ... 28
Chapter 2: Investigating the role of three novel candidate genes in apoptotic resistance ... 36
2.1 Introduction ... 36
2.1.1 RNA interference ... 36
2.1.2 Apoptosis Assays ... 38
2.1.3 Apoptotic Inducers ... 40
2.2 Materials and methods ... 41
2.2.1 Generation of stable knockdown cell lines for *LIAS*, *RPL9* and *CYPA* ... 41

2.2.1.1 Cell culture 41
2.2.1.2 Short hairpin-RNA (shRNA) design 41
2.2.1.3 Construction of expression vectors 41
2.2.1.4 Transfection 47
2.2.1.5 Visualisation of transfected cells 47
2.2.1.6 Total RNA extraction 47
2.2.1.7 First-strand cDNA synthesis 48
2.2.1.8 Validation of gene expression knockdown by means of quantitative PCR 48
2.2.2 Apoptosis Assays 49
2.2.2.1 APOPercentage™ Assay 49
2.2.2.2 Caspase-3/CPP32 Colourimetric Assay Kit 50
2.2.2.3 Analysis of results 50
2.3 Results and discussions 51
2.3.1 Generation of stable knockdown cell lines for *LIAS*, *RPL9* and *CYPA* 51
2.3.1.1 Construction of shRNA-expressing vectors 51
2.3.1.2 Transfection of NIH-3T3 cells with shRNA-expressing vectors 53
2.3.1.3 Validation of gene expression knockdown 54
2.3.2 Apoptosis assays 56
2.3.2.1 FACScan™ and CellQuest™ Pro analysis 56
2.3.2.2 Analysis of results 56
2.4 Conclusions 65
2.4.1 Potential roles for *LIAS* in apoptosis 65
2.4.2 Potential roles for *CYPA* in apoptosis 73
2.5 References 77
Chapter 3: A bioinformatic approach to identifying novel candidate genes involved in apoptosis .. 91
3.1 Introduction 91
3.2 Materials and methods 95
3.2.1 Identification of potential candidate genes 95
3.2.2 Bioinformatic analysis of selected candidate genes 96
3.3 Results and Discussion 97

3.3.1 Identification of potential candidate genes 97
3.3.2 Bioinformatic analysis of selected candidate genes 104
3.4 Conclusions 114
3.5 References 115
Chapter 4: Investigating the gene expression of the novel candidate genes in two cancer cell lines 118
4.1 Introduction 118
4.2 Materials and methods 120
4.2.1 Total RNA extraction and cDNA synthesis 120
4.3 Results and discussion 121
4.3.1 Quantitative PCR 121
4.4 Conclusions 124
4.5 References 129
Chapter 5: Conclusions 133
5.1 Final remarks and conclusions 133
5.2 References 136
Addendum A 139

List of abbreviations

%	percentage
<	less than
~	approximately
±	plus-minus
©	copyright
®	Registered Trademark
™	Trademark
$\Delta\Psi_m$	mitochondrial trans membrane potential
µg	microgram
µl	microliter
µM	micromolar
3D	three-dimensional
3’	three prime
5’	five prime
Aβ	amyloid beta
ADP	adenosine diphosphate
AIDS	acquired immunodeficiency syndrome
ALL	acute lymphoblastic leukaemia
ALPS	autoimmune lymphoproliferative syndrome
ALS	amyotrophic lateral sclerosis
AMP	adenosine monophosphate
ATL	adult T cell leukaemia
BCAA	branched-chain amino acids

BCKDH	branched-chain α-keto acid dehydrogenase
BH	Bcl-2 homology
BioGRID	Biological General Repository for Interaction Datasets
BLAST	Basic Local Alignment Search Tool
BLASTn	BLAST nucleotide search
BLASTp	BLAST protein search
bp	base pair
°C	degrees Celsius
CARD	caspase-recruitment domain
cDNA	complementary DNA
CHO	Chinese hamster ovary
CICD	caspase-independent cell death
CMV	cytomegalovirus
C_T	threshold cycle
CTL	cytotoxic T lymphocyte
CsA	cyclosporine A
CSR	cellular stress response
DAPI	4',6-diamidino-2-phenylindole
(d)ATP	(deoxy)-adenosine triphosphate
DD	death domain
DED	death effector domain
DEVD	aspartic acid – glutamic acid – valine – aspartic acid, peptide sequence
DISC	death-inducing signalling complex
DMEM	Dulbecco's Modified Eagle Medium
DNA	deoxyribonucleic acid

dpc	days post coitum
DR	death receptor
dsDNA	double-stranded DNA
dsRNA	double-stranded RNA
ETC	electron transport chain
FACS	fluorescence-activated cell sorting
FCS	fetal calf serum
FRET	fluorescence resonance energy transfer
GCS	glycine cleavage system
GFP	green fluorescent protein
GO	Gene Ontology
GTP	guanosine triphosphate
HCP	high confidence predictions
HGNC	HUGO Gene Nomenclature Committee
HIV	Human immunodeficiency virus
HSV-*TK*	Herpes simplex virus *thymidine kinase*
HRE	hypoxia-response elements
hrs	hours
ID	identity number
Ig	immunoglobulin
IMM	inner mitochondrial membrane
kDa	kilodalton
KEGG	Kyoto Encyclopaedia of Genes and Genomes
KGDH	α-ketoglutarate dehydrogenase
LB	Luria Broth

LCP	low confidence predictions
LTR	long terminal repeat
M	molar
MCP	medium confidence predictions
MCS	multiple cloning site
min	minutes
ml	millilitre
mM	millimolar
MLS	mitochondrial localisation signal
MMP	microsatellite mutator phenotype
MoMLV	Moloney murine leukaemia virus
MOMP	mitochondrial outer membrane permeabilisation
mRNA	messenger RNA
MSUD	maple syrup urine disease
N/A	not applicable
NADH	nicotinamide adenine dinucleotide (reduced form)
NADPH	nicotinamide adenine dinucleotide phosphate (reduced form)
NCBI	National Centre for Biotechnology Information
NCCD	Nomenclature Committee on Cell Death
ng	nanogram
NK	natural killer
NKH	non-ketotic hyperglycinemia
nm	nanometer
nM	nanomolar
No.	number

NRF	National Research Foundation
p	probability value
P	proline
PBS	phosphate buffer saline
PCD	programmed cell death
PDH	pyruvate dehydrogenase
PGDB	pathway/genome database
PCR	polymerase chain reaction
pmol	picomole
PPiase	peptidylproline *cis*-*trans*-isomerase
PS	phosphatidylserine
RFP	red fluorescent protein
RISC	RNA-induced silencing complex
RNA	ribonucleic acid
RNAi	RNA interference
ROS	reactive oxygen species
rpm	revolutions per minute
s	seconds
S	serine
SAP	shrimp alkaline phosphatase
shRNA	short hairpin RNA
siRNA	short interfering RNA
SMI	small molecule inhibitor
STRING	Search Tool for the Retrieval of Interacting Genes/Proteins
T_A	annealing temperature

TCA	tricarboxylic acid cycle
TEM	transmission electron microscopy
T_M	melting temperature
TUNEL	terminal deoxynucleotidyl transferase-mediated dUTP nick end labelling
U	units
ULS	UniPathway Linear Subpathway
UTP	uridine triphosphate
UWC	University of the Western Cape
v.	version
V	volt
w/v	weight per volume
x	times

List of figures

Figure 1.1: Transmission electron microscope images of A) an autophagosome showing the distinctive double-membrane structure surrounding a mitochondrion, indicated by A, (adapted from Wells 2005) and B) a necrotic cell showing the disrupted plasma membrane and preserved nucleus (Adapted from http://www.cyto.purdue.edu/archive/flowcyt/research/cytotech/apopto/data/chap10.htm)..... 4

Figure 1.2: The functional homologues, as indicated by the matching colours, of various apoptotic proteins found in nematodes, mammalians and fruit flies. Adapted from Riedl and Shi, 2004. 6

Figure 1.3: Scanning electron microscope image of a trophoblast cell undergoing apoptosis. A - Shrinkage of cells. B - Nuclear condensation. C - Further cellular shrinkage and packaging of cellular contents. D - Membrane blebbing. Arrow points to an apoptotic body. Obtained from http://www.reading.ac.uk/cellmigration/apoptosis.htm. 8

Figure 1.4: The extrinsic and intrinsic pathways of apoptosis. Adapted from http://www.hixonparvo.info/model.html. 9

Figure 1.5: Activation of the caspase cascade in the various apoptotic pathways. Adapted from Taylor et al., 2008. 10

Figure 1. 6: Protein structures of the caspase and Bcl-2 protein families. Adapted from Degterev and Yuan, 2008. 12

Figure 1.7: Schematic representation of the integration cassette used in the promoter-trap mutagenesis experiments. The cassette was transferred to the CHO22 cells by means of the MoMLV. LTR – long terminal repeat; U3 – promoter element; $Hygro^R$ – Hygromycin B resistance gene; Neo^R – Neomycin resistance gene; tk – thymidine kinase gene from the Herpes simplex virus. 21

Figure 1.8: Results of testing for resistance to apoptosis in promoter-trapped cell lines, as compared to wild type CHO22 cells, by means of the APOPercentage™ assay following treatment with C_2-ceramide for 24 hrs. Values are the averages ± standard deviation from triplicate experiments. * Indicates significantly different from wild type for $p < 0.05$. 22

Figure 1.9: Results of testing for resistance to apoptosis in promoter-trapped cell lines, as compared to wild type CHO22 cells, by means of the Annexin-V assay following treatment with Camptothecin for 24 hrs. Values are the averages ± standard deviation from triplicate experiments. * Indicates significantly different from wild type for $p < 0.05$. 22

Figure 1.10: Results of testing for resistance to apoptosis in promoter-trapped cell lines, as compared to wild type CHO22 cells, by means of the Caspase-3/CPP32 assay following treatment with C_2-ceramide for 24 hrs. Values are the averages ± standard deviation from triplicate experiments. * Indicates significantly different from wild type for $p < 0.05$. 23

Figure 1.11: Line graph showing results from CTL killing assay performed with recombinant J-cell lines isolated from promoter-trap mutagenesis experiments, with % specific cell lysis referring to the amount (in percentage) of cells dying due to CTL killing at various effector: target ratios. (Effector – CTL; Target – cells from respective J-cell line). 24

Figure 1.12: A simplified schematic representation of inverse PCR as performed in the pilot study. 1) Enzymatic digestion of genomic DNA with frequently cutting enzyme, followed by self-ligation to form circular fragments. 2) Linearization of circular fragments with a specific enzyme cutting within known sequences. (LTR – long terminal repeat; $Hygro^R$ – Hygromycin B resistance gene; U3 – promoter element; tk – thymidine kinase gene; Neo^R – Neomycin resistance gene). 25

Figure 1.13: Results obtained from the BLAST search for the genomic sequence generated from CHO-J304 showing a significant match to the mouse *lipoic acid synthetase* (*LIAS*) gene. 26

Figure 1.14: Results obtained from the BLAST search for the genomic sequence generated from CHO-J308 showing a significant match to the mouse *ribosomal protein L9* (*RPL9*) gene. 26

Figure 1.15: Results obtained from the BLAST search for the genomic sequence generated from CHO-J612 showing a significant match to the mouse *peptidylprolyl isomerase A* (*PPIA*) gene, also known as *cyclophilin A* (*CYPA*). 27

Figure 2.1: An illustration of RNAi process. Adapted from Rutz and Scheffold, 2004. 37

Figure 2.2: Typical example of a shRNA construct. U6 – a type of promoter; Term. – Termination signal. Obtained from http://www.addgene.org/tools/protocols/plko/..... 38

Figure 2.3: Representative example of the shRNA constructs designed with iRNAi. The sense target sequence for *LIAS* KD1 is represented. Colours represent the different parts of the shRNA construct: red – vector sequence forming part of restriction enzyme cut site, with *Bgl* II (non-functional) at the 5' end and *Hind* III at the 3' end on the sense strand; orange – shRNA sequence forming part of the respective restriction enzyme cut sites; black – spacer sequences and termination sequence (3' end of top strand); blue – target sequence complementary to the respective genes (in this example *LIAS* KD1); green – hairpin loop sequence. 42

Figure 2.4: Vector maps of the pEGFP-C1 (A) and pDsRed-Express-C1 (B) vectors. The images show the *Ase* I restriction enzyme cut site used for the cloning of the U6 promoter as well as the MCS. These images were created with the freely available SnapGene™ Viewer software version 1.3.3 (GSL Biotech LLC) in conjunction with the sequence and map files of the vectors, as created by SnapGene (www.snapgene.com/resources). 45

Figure 2.5: Sequences of the MCS regions of the pEGFP-C1 (A) and pDsRed-Express-C1 (B) vectors. The region removed by means of digestion with *Bgl* II and *BamH* I is highlighted. These images were created with the freely available SnapGene™ Viewer software version 1.3.3 (GSL Biotech LLC) in conjunction with the sequence and map files of the vectors, as created by SnapGene (www.snapgene.com/resources). 46

Figure 2.6: Representative example of the successful deletion of the MCS region between the *Bgl* II and *Hind* III cut sites in the expression vectors as confirmed by colony PCR and agarose gel electrophoresis. Lane 1 – pTZ molecular marker; Lane 2-8 - colonies showing successful deletion of the MCS region from the GFP vector; Lane 9 – control GFP vector. 52

Figure 2.7: Representative example of the successful cloning of the U6 promoter fragment into the expression vectors as confirmed by colony PCR and agarose gel electrophoresis. Lane 1 – pTZ molecular marker; Lane 2-5 – colonies showing the U6 promoter fragment cloned into the GFP vector; Lane 6 – negative control; Lane 7-10 – colonies showing the U6 promoter fragment cloned into the RFP vector. 52

Figure 2.8: Representative example of the successful cloning of shRNA constructs into the expression vectors as confirmed by colony PCR and agarose gel electrophoresis. Lane 1 – pTZ molecular marker; Lane 2 – control GFP vector; Lanes 3-7 – colonies showing successful cloning of *LIAS* shRNA constructs into the GFP vector; Lanes 8-10 – colonies showing successful cloning of *CYPA* shRNA constructs into the GFP vector. 53

Figure 2.9: Representative example of the final product following vector construction. Illustrated in the figure is a GFP vector containing a shRNA construct for *LIAS* driven by the U6 promoter..... 53

Figure 2.10: Representative photographs, taken with a Zeiss fluorescent microscope, of NIH-3T3 cells transfected with the shRNA-containing vectors. A – NIH-3T3 transfected cells counterstained with DAPI; B – NIH-3T3 cells transfected with RFP vector containing a shRNA for *LIAS*; C – NIH-3T3 transfected cells counterstained with DAPI; D – NIH-3T3 cells transfected with GFP vector containing a shRNA for *RPL9*. 54

Figure 2.11: Representative example for determining the integrity of extracted total RNA as confirmed with the Agilent 2100 Bioanalyzer. The image shows the 18S and 28S peaks of RNA extracted from a *LIAS* knockdown cell line transfected with a GFP vector 55

Figure 2.12: Relative expression ratio plot produced by the REST© software used for the analysis of the qPCR results for the validation of candidate gene expression knockdown. Bars indicate the ratios of the collective KD1 and KD2 expression levels, as measured in a $\log_2$ scale, for each candidate gene in the knockdown cell lines as compared to the normal expression levels of each gene in the wild type NIH-3T3 cells. Values are the averages ± standard error from duplicate experiments. 55

Figure 2.13: Representative example of results obtained from the CellQuest™ Pro software following flow cytometry. Figures illustrate the cell plots of wild type NIH-3T3 cells and cells transfected with GFP vector containing a *LIAS* shRNA construct, both assayed with the APOPercentage™ assay. A – untreated *LIAS* knockdown NIH-3T3 cells; B – *LIAS* knockdown NIH-3T3 cell treated with 60 µM C_2-ceramide; C – untreated wild type NIH-3T3 cells; D – Wild type NIH-3T3 cells treated with 60 µM C_2-ceramide. M1 – region showing live cells; M2 – region showing dead cells..... 57

Figure 2.14: Results of testing for resistance to apoptosis in *LIAS* knockdown cell lines, as compared to wild type NIH-3T3 cells, by means of the APOPercentage™ assay following treatment of camptothecin for 24 hrs. Values are the averages ± standard deviation from triplicate experiments. * Indicates significantly different from wild type for $p < 0.05$. KD – knock down..... 59

Figure 2.15: Results of testing for resistance to apoptosis in *LIAS* knockdown cell lines, as compared to wild type NIH-3T3 cells, by means of the APOPercentage™ assay following treatment of C_2-ceramide for 24 hrs. Values are the averages ± standard deviation from triplicate experiments. * Indicates significantly different from wild type for $p < 0.05$. KD – knock down..... 59

Figure 2.16: Results of testing for resistance to apoptosis in *CYPA* knockdown cell lines, as compared to wild type NIH-3T3 cells, by means of the APOPercentage™ assay following treatment of camptothecin for 24 hrs. Values are the averages ± standard deviation from triplicate experiments. * Indicates significantly different from wild type for $p < 0.05$. KD – knock down..... 60

Figure 2.17: Results of testing for resistance to apoptosis in *CYPA* knockdown cell lines, as compared to wild type NIH-3T3 cells, by means of the APOPercentage™ assay following treatment of C_2-ceramide for 24 hrs. Values are the averages ± standard deviation from triplicate experiments. * Indicates significantly different from wild type for $p < 0.05$. KD – knock down..... 60

Figure 2.18: Results of testing for resistance to apoptosis in *RPL9* knockdown cell lines, as compared to wild type NIH-3T3 cells, by means of the APOPercentage™ assay following treatment of camptothecin for 24 hrs. Values are the averages ± standard deviation from triplicate experiments. * Indicates significantly different from wild type for $p < 0.05$. KD – knock down..... 61

Figure 2.19: Results of testing for resistance to apoptosis in *RPL9* knockdown cell lines, as compared to wild type NIH-3T3 cells, by means of the APOPercentage™ assay following treatment of C_2-ceramide for 24 hrs. Values are the averages ± standard deviation from triplicate experiments. * Indicates significantly different from wild type for $p < 0.05$. KD – knock down..... 61

Figure 2.20: Results of testing for resistance to apoptosis in *LIAS* knockdown cell lines, as compared to wild type NIH-3T3 cells, by means of the Caspase-3/CPP32 assay following treatment of Camptothecin for 24 hrs. Values are the averages ± standard deviation from triplicate experiments. * Indicates significantly different from wild type for $p < 0.05$. KD – knock down..... 62

Figure 2.21: Results of testing for resistance to apoptosis in *LIAS* knockdown cell lines, as compared to wild type NIH-3T3 cells, by means of the Caspase-3/CPP32 assay following treatment of C_2-ceramide for 24 hrs. Values are the averages ± standard deviation from triplicate experiments. * Indicates significantly different from wild type for $p < 0.05$. KD – knock down..... 62

Figure 2.22: Results of testing for resistance to apoptosis in *CYPA* knockdown cell lines, as compared to wild type NIH-3T3 cells, by means of the Caspase-3/CPP32 assay following treatment of Camptothecin for 24 hrs. Values are the averages ± standard deviation from triplicate experiments. * Indicates significantly different from wild type for $p < 0.05$. KD – knock down..... 63

Figure 2.23: Results of testing for resistance to apoptosis in *CYPA* knockdown cell lines, as compared to wild type NIH-3T3 cells, by means of the Caspase-3/CPP32 assay following

treatment of C_2-ceramide for 24 hrs. Values are the averages ± standard deviation from triplicate experiments. * Indicates significantly different from wild type for $p < 0.05$. KD – knock down. 63

Figure 2.24: Results of testing for resistance to apoptosis in *RPL9* knockdown cell lines, as compared to wild type NIH-3T3 cells, by means of the Caspase-3/CPP32 assay following treatment of Camptothecin for 24 hrs. Values are the averages ± standard deviation from triplicate experiments. * Indicates significantly different from wild type for $p < 0.05$. KD – knock down. 64

Figure 2.25: Results of testing for resistance to apoptosis in *RPL9* knockdown cell lines, as compared to wild type NIH-3T3 cells, by means of the Caspase-3/CPP32 assay following treatment of C_2-ceramide for 24 hrs. Values are the averages ± standard deviation from triplicate experiments. * Indicates significantly different from wild type for $p < 0.05$. KD – knock down. 64

Figure 2.26: Pathway for LA metabolism according to the KEGG Pathway Database (hsa00785, accessed 25/07/2012) 66

Figure 2.27: Illustration of the *cis-trans* isomerisation reaction catalysed by PPIases. P – proline; S – serine. Adapted from Lu et al., 2002. 75

Figure 3.1: BLAST search results of sequence RM118 showing verification of *AHNAK* as a candidate gene. Sequence was obtained from promoter-trap mutagenesis experiments and BLAST searched against the human genomic and transcript database using the BLASTn tool in the NCBI webpage. 104

Figure 3.2: BLAST search result of sequence RM289 showing verification of *SAAL1* as a candidate gene. Sequence was obtained from promoter-trap mutagenesis experiments and BLAST searched against the human genomic and transcript database using the BLASTn tool in the NCBI webpage. 104

Figure 4.1: Illustration of an amplification plot obtained in qPCR depicting the estimation of the C_T value. Obtained from http://www.langfordvets.co.uk/lab_pcr_ct_values.htm. 120

Figure 4.2: Representative example of an amplification plot (A) and melt curve (B) obtained during the qPCR reactions. The triplicate reactions for *LIAS* quantification in the lung cancer sample are displayed. Rn – normalised fluorescence. 123

Figure 4.3: Relative expression ratio plot produced by the REST-384© software showing the absolute regulation of the target genes in a $\log_2$ scale in lung cancer as compared to lung control. Values are the averages ± standard error of triplicate experiments. Target gene expression was normalised with the *UBC* reference gene. * indicates significant results for $p < 0.05$. 125

Figure 4.4: Relative expression ratio plot produced by the REST-384© software showing the absolute regulation of the target genes in a $\log_2$ scale in kidney cancer as compared to kidney control. Values are the averages ± standard error of triplicate experiments. Target gene expression was normalised with the *GAPDH* reference gene. * indicates significant results for $p < 0.05$. 126

List of tables

Table 1.1: Common chemotherapeutic drugs used in the treatment of cancers 18

Table 2.1: Target sequences of the shRNA constructs designed for each of the three novel candidate genes 42

Table 2.2: Details of primers used for colony PCRs performed during vector construction 44

Table 2.3: Details of primers used for qPCR performed for the validation of candidate gene expression knockdown 49

Table 2.4: Homologs of enzymes involved in LA metabolism across various species[a] 66

Table 3.1: Results obtained from the BLAST searches performed with sequences isolated from the pilot study 98

Table 3.2: Results obtained from the Genecards® database for each candidate gene identified by the BLAST searches 100

Table 3.3: Results obtained from the bioinformatic analysis investigating the protein interactions for AHNAK 106

Table 3.4: Results obtained from the bioinformatic analysis investigating the protein interactions for SAAL1 108

Table 3.5: Results obtained from the bioinformatic analysis investigating the protein interactions for CYPA 110

Table 3.6: Results obtained from the bioinformatic analysis investigating the protein interactions for LIAS 113

Table 4.1: Details of primers used for qPCR experiments 122

Table 4.2: Descriptive results for the analysis of the relative gene expression of the seven target genes in the lung cancer sample as compared to the lung control sample 125

Table 4.3: Descriptive results for the analysis of the relative gene expression of the seven target genes in the kidney cancer sample as compared to the kidney control sample 126

Table A1: Descriptive statistics for APOPercentage™ assay as calculated with Microsoft® Excell® 139

Table A2: Descriptive statistics for the Caspase-3/CPP32 assay as calculated with Microsoft® Excell® 143

Table A3: Previously calculated qPCR efficiencies of primers for target genes and reference genes 147

Chapter 1: Literature review

1.1 Cell death

When animals find themselves under a stressful and/or dangerous situation, the well-known “fight-or-flight” response is set into motion (Cannon, 1929). On an organismal level, this represents a complex process, regulated by a multitude of systems and hormones (Charmandari et al., 2005). In terms of a cellular level, a somewhat similar response can be expected; fight-comply-or-flight. The cellular stress response (CSR) can entail a series of offence and defence mechanisms, aimed at survival, or a temporary increase in tolerance levels. As a last resort, the flight response serves to remove damaged cells through cell death pathways when the applied stress is too severe (Kültz, 2005). Cellular stress can be explained as any state that threatens homeostasis and examples of stresses that can lead to the drastic step mentioned above includes hypoxia (oxygen limiting conditions), DNA damage, starvation, synthetic drugs, radiation and increased generation of reactive oxygen species (ROS) (Chrousos, 1992; Fulda, 2010; Kültz, 2005). Cell death, however, is not limited to the CSR but also fulfils other vital roles. Numerous examples of cell death in embryonic development and organogenesis emphasizes the crucial role of cell death in the specific removal of cells in a spatial and temporal manner, where the most famous examples is likely the removal of interdigital webs on the limbs of amniotes (e.g. humans, mice and birds) and the removal of the tail section in tadpoles (Penaloza et al., 2006). Equally important is the role of cell death in physiological cell and tissue homeostasis (Lockshin and Zakeri, 2007). As cells reach the end of their lifespan, new cells are produced to replace them and it is this intricate balance between cell death and cell proliferation that maintains cellular homeostasis (King and Cidlowski, 1998; Lawen, 2003). Interestingly, this can occur at quite an alarming pace in the human body, with erythrocytes showing the fastest exchange rate with about 360 billion cells dying each day, that is more than 4 million cells per second (Bratosin et al., 2002; Lockshin and Zakeri, 2007). In more physical terms, if humans were to constantly produce new cells without removing the old ones, an 80-year-old person would have an intestine of approximately 16 km in length and bone marrow and lymph nodes with a total weight of 2 tons (Melino, 2001). Owing to its importance, the decision to initiate cell death, as well as the particular method behind its execution, is tightly controlled and several escape routes are available until a certain event or phase is reached that fatally commits the cell to death. This switch from reversible to irreversible cell death has been adequately termed the “point-of-no-return”; however pinpointing and describing this “point” has been proven difficult due to discrepancies in literature (Galluzzi et al., 2007; Kroemer et al., 2005; Kroemer et al., 2009). Certain biochemical events have been proposed, including large-scale caspase (a family of cysteine proteases) activation, sustained loss of the mitochondrial trans membrane potential ($\Delta\Psi_m$), complete mitochondrial outer membrane permeabilisation (MOMP) and the display of phosphatidylserine (PS) residues on the outside of the cell, although these

events can occur independently of cell death and without any serious consequences. In the light of this shortcoming, a set of morphological characteristics has been suggested by the Nomenclature Committee on Cell Death (NCCD) that states that a cell is perceived as 'dead' when at least one of the following criteria is met: 1) the integrity of the cell membrane is significantly compromised, 2) cellular and nuclear fragmentation has occurred and 3) the resulting fragments are removed by adjacent cells (Galluzzi et al., 2007; Kroemer et al., 2005; Kroemer et al., 2009). In view of the above mentioned criteria, it is important to note that the definition of a 'dying' cell can be different to that of a 'dead' cell. The process of dying can take place through several pathways or mechanisms, each having their own set of characteristics. At the end, the different pathways or mechanisms can converge to produce one or more of the above mentioned criteria for a 'dead' cell (Kroemer et al., 2005; Kroemer et al., 2009).

1.1.1 Types of cell death

Several different types of cell death exist. Aiding in their characterisation, each type of cell death can be described in terms of functionality, morphology, immunology and enzymology (Kroemer et al., 2009). When classifying the different types of cell death, it has been suggested to rely on the major morphological characteristics of each type, since other characteristics has been shown to exhibit non-exclusivity in addition to a general lack of clear cut distinction in terms of biochemical properties (Galluzzi et al., 2007). There are three widely recognised types of cell death, namely apoptosis, autophagy and necrosis. Historically, roman numerals were assigned to each of these, designating apoptosis, autophagy and necrosis as type I, II and III cell death respectively; however the use of this nomenclature has been discouraged by the NCCD (Kroemer et al., 2009). One aspect that has led to some discrepancies with regards to the nomenclature of cell death types is the interchangeable use of programmed cell death (PCD) and apoptosis. PCD refers to cell death that is specifically genetically predetermined or implicitly physiological and although this mostly occurs by means of apoptosis, it is not to be used as a synonym (Galluzzi et al., 2007). Evidence supporting this statement includes the ability of apoptosis to be induced, for example by natural or synthetic apoptotic inducers, and the realisation that necrosis, originally thought of as accidental and pathological, can also be predetermined (Galluzzi et al., 2007). In an attempt to distinguish above mentioned from truly accidental necrosis, the terms "programmed necrosis" and "necroptosis" was coined (Degterev et al., 2005; Moquin and Chan, 2010).

The different types of cell death will be discussed briefly below, while apoptosis, the focus of this study, will be discussed in more detail in the section to follow.

Autophagy

Autophagy is a self-degradative process where a cell literally eats itself, as described by its meaning derived from the Greek words "autos" (self) and "fageo" (eat). The process is

morphologically characterised by massive vacuolisation of the cytoplasm and its contents in double-membraned structures, referred to as autophagosomes, without being accompanied by chromatin condensation (Fig. 1.1) (Hotchkiss et al., 2009; Kroemer et al., 2005). This key event is followed by fusion of the autophagosomes with lysosomes, forming autolysosomes. Lysosomes contain acid hydrolases capable of digesting the contents of the autophagosomes, thus producing metabolic substrates (Giansanti et al., 2011; Hotchkiss et al., 2009). The functional role of autophagy in the cellular environment is however under heavy debate with the two options representing opposing views. Autophagy is suggested to be critical for cell survival under conditions of nutrient deprivation owing to its ability to provide the cell with essential metabolites, amino acids and energy by recycling redundant or non-essential macromolecular components or organelles (Debnath et al., 2005; Degterev and Yuan, 2008; Hotchkiss et al., 2009). In addition, autophagy assists in cellular differentiation and development, in maintaining intracellular homeostasis by removing damaged or dysfunctional organelles and also forms one of the two major protein degradation pathways in the cell (Debnath et al., 2005; Degterev et al., 2005; Mizushima and Levine, 2010). In contrast, autophagy is also viewed as a method of cell death. Evidence for this statement includes the presence of autophagic vacuoles in dying cells as well as the ability to perform non-apoptotic cell death in apoptosis-deficient cells (Debnath et al., 2005; Shimizu et al., 2004). An important aspect to consider when investigating the role of autophagy in cell death is to determine if the observed cell death occurs *through* autophagy or *with* autophagy (Galluzzi et al., 2007).

Necrosis

Necrosis is traditionally described as an unregulated, passive and messy form of cell death (Edinger and Thompson, 2004; Hotchkiss et al., 2009). The pathway is often classified in a negative manner, that is, a form of cell death lacking characteristics of both apoptosis and autophagic cell death, but prominent morphological features has provided a more positive definition (Denecker et al., 2001; Golstein and Kroemer, 2007). This includes cellular and organelle swelling leading to the early rupture of the plasma membrane (Fig. 1.1) (Golstein and Kroemer, 2007). As a result, cellular contents are spilled into the surrounding area and an inflammatory response is initiated through the activation of antigen-presenting cells by, for example, calreticulin, the heat shock protein Hsp70 and oligonucleosomes (Melcher et al., 1999; Proskuryakov et al., 2003). Cells normally undergo necrosis after severe physical and physicochemical (detergents, heat, cold, irradiation etc.) injuries, infections (bacterial, viral and protozoan), toxic insults or acute hypoxia and was hence suggested to be an accidental form of cell death (Denecker et al., 2001; Edinger and Thompson, 2004; Hotchkiss et al., 2009; Proskuryakov et al., 2003). However, accumulating evidence suggests otherwise. This includes the involvement of extracellular mediators, ligands and receptors in the induction of necrosis, mediation of the process by

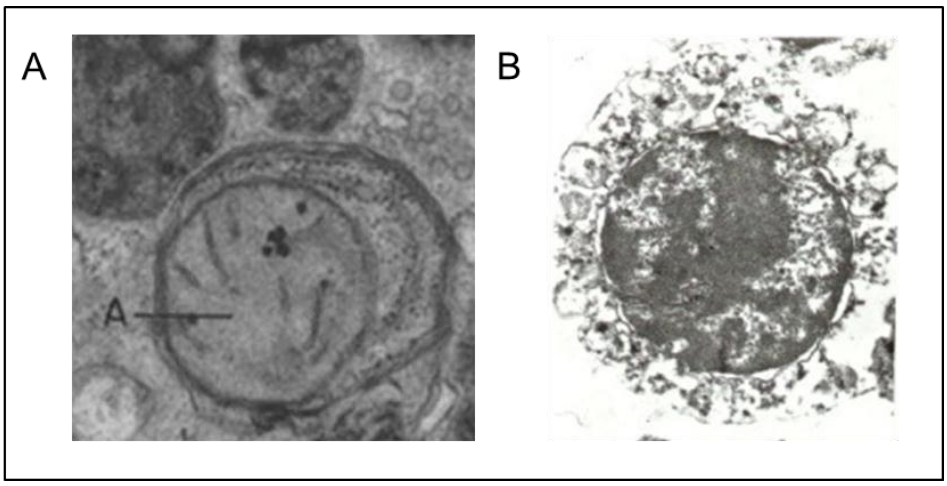

Figure 1.1: Transmission electron microscope images of A) an autophagosome showing the distinctive double-membrane structure surrounding a mitochondrion, indicated by A, (adapted from Wells 2005) and B) a necrotic cell showing the disrupted plasma membrane and preserved nucleus (Adapted from http://www.cyto.purdue.edu/archive/flowcyt/research/cytotech/apopto/data/chap10.htm).

key kinases and proteases, cross-talk with other cell death types and a proposed capability to serve as a substitute in cases of apoptosis-deficient cells (Denecker et al., 2001; Hotchkiss et al., 2009; Moquin and Chan, 2010; Proskuryakov et al., 2003). In addition, the pro-inflammatory response initiated by the leaked cellular contents may be important in enforcing an antitumour or antiviral response, suggesting that cell death by necrosis might take place with a specific purpose (Denecker et al., 2001; Hotchkiss et al., 2009). The terms “programmed necrosis” and “necroptosis” has since been coined to distinguish the traditional, accidental form of necrosis from a more controlled, specific version; with “programmed” implying that necrosis can be induced on specific cues or signals, which is subsequently followed by signalling pathways (Degterev et al., 2005; Edinger and Thompson, 2004; Moquin and Chan, 2010).

Other types of cell death

Apart from apoptosis, autophagy and necrosis, there are many other ways for a cell to die. Many of these types are less well known and not as frequently studied as the above mentioned types. Alternative cell death types include mitotic catastrophe, anoikis, excitotoxicity, Wallerian degeneration, paraptosis, pyroptosis, pyronecrosis, entosis and cornification (Kroemer et al., 2005; Kroemer et al., 2009). Most of these cell death types only take place in certain cell types and/or is dependent on a specific set of circumstances, for example, cornification only occurs in cells of the epidermis while pyroptosis involves distinct routes of caspase 1 activation. Some of these cell death types resemble apoptosis, autophagy or necrosis in some way or another, including sharing some morphological features; thus, their classification as individual cell death types is still a matter of debate (Kroemer et al., 2005; Kroemer et al., 2009).

1.2 Apoptosis

The existence of a mechanism serving as a counterbalance for mitosis was suggested as early as 1914 (Majno and Joris, 1995). It was only 57 years later that the critical experiment, displaying a discrete drop-off in cells, was performed by John Kerr, who coined the term “apoptosis” a year later (Kerr, 1971; Kerr et al., 1972; Majno and Joris, 1995). The term “apoptosis” stems from the ancient Greek language and describes the “falling of petals/leaves from flowers/trees” (Kerr et al., 1972). The initial characterisation of the apoptotic process took place in PCD studies in the nematode *Caenorhabditis elegans* (Degterev and Yuan, 2008). In 1993, Yuan *et al.* presented a molecular mechanism for PCD in the nematode and also suggested conservation of this mechanism in mammals. Since then the four individual apoptosis genes in *C. elegans* has each been expanded into large and much more complex multi-protein families in mammalians (Fig. 1.2) (Degterev and Yuan, 2008). The *C. elegans* apoptosis genes and their conserved mammalian protein families, respectively, are *egl-1* and BH3-only proteins; *ced-9* and the anti-apoptotic Bcl-2 family proteins; *ced-4* and Apaf-1 and related proteins; and *ced-3* and the caspase protein family (Lawen, 2003). High homology in key regions suggests that the mammalian counterparts of the *ced* and *egl-1* genes most likely arose through gene duplication events which were subsequently followed by selection and specification (Degterev and Yuan, 2008). Specification of the individual genes allows for different apoptotic responses from different apoptotic signals, mediated by different apoptotic regulators. It also provides the apoptotic process with a back-up plan; if, for example, the activity of one caspase is lost, the up-regulation of another can potentially compensate for this loss (Degterev and Yuan, 2008). Apoptosis shows a remarkable level of conservation ranging from nematodes to humans and exploring the process in the model organism *Drosophila melanogaster*, which possesses a similar mechanism for the execution of apoptosis, has proven useful in modelling human diseases (Hay et al., 2004; Vernooy et al., 2000).

In 1972 John Kerr and colleagues referred to apoptosis as a “vital biological phenomenon”; in the years to follow numerous studies have shown just how vital this form of cell death is (Hay et al., 2004). The ability of apoptosis to control cell numbers is crucial for sculpting structures and organs during embryonic development, while in adults it functions to maintain normal tissue homeostasis (Baehrecke, 2002; Lockshin and Zakeri, 2007; Penaloza et al., 2006). Apoptosis also provides a protective function by removing gametes or other embryonic cells with damaged DNA or aberrant chromosomal contents during development and by removing pathogen-infected cells, damaged cells or cells displaying inappropriate proliferation in adult tissues (Baehrecke, 2002; Benedict et al., 2002; Green and Evan, 2002).

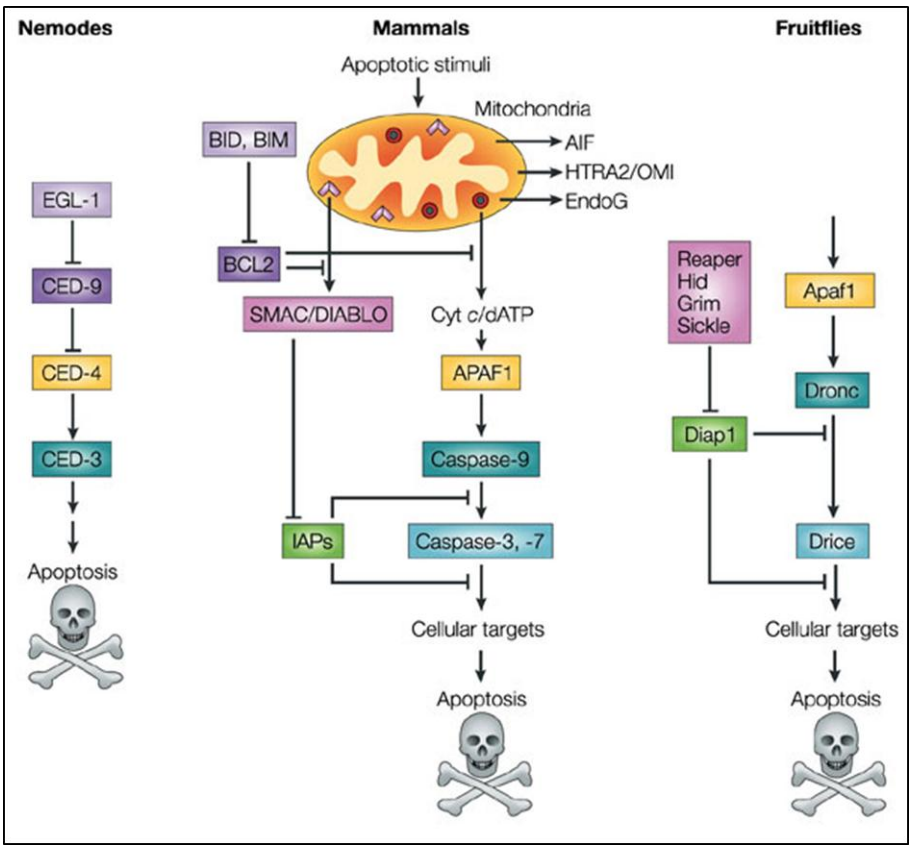

Figure 1.2: The functional homologues, as indicated by the matching colours, of various apoptotic proteins found in nematodes, mammalians and fruit flies. Adapted from Riedl and Shi, 2004.

1.2.1 The apoptotic process

The controlled demolition of a building has been used as a metaphor to describe the apoptotic process; being dismantled from within, the destruction of the cell rarely, if not at all, affects the surrounding cells (Taylor et al., 2008). The process has several characteristics, both biochemical and morphologic, that can distinguish it from other cell death types. Morphologically, the process begins with shrinkage of the cell, in contrast to necrosis where swelling of the cell occurs (Fadeel and Orrenius, 2005; Lawen, 2003). The apoptotic cell begins to loose contact with neighbouring cells and pseudopods are retracted (Kroemer et al., 2005; Lawen, 2003; Taylor et al., 2008). While the cellular organelles remain intact throughout the process, with only dilation of the endoplasmic reticulum and swelling of cisternae have been reported, several changes occur within the nucleus (Fadeel and Orrenius, 2005; Kroemer et al., 2005; Lawen, 2003). Compact masses of condensed chromatin undergo large-scale DNA fragmentation by endonucleases, producing a typical “DNA ladder” when the extracted DNA is analysed on an agarose gel (Kroemer et al., 2005; Lawen, 2003). The high level of DNA fragmentation is a distinctive event in apoptosis and, along with the observation that cellular organelles remain unaffected, it represents another noticeable contrast to necrosis (Fadeel and Orrenius, 2005; Taylor et al., 2008). Fragmentation of the nuclear DNA is followed by convolution of the nucleus, which ultimately buds off into several fragments (Lawen, 2003). In a similar manner, the plasma membrane becomes active and undergoes a prolonged

period of dynamic blebbing where pieces of the membrane buds off, encapsulating cellular contents, including intact organelles and nuclear fragments, and forming small vesicles known as apoptotic bodies (Fig. 1.3) (Fadeel and Orrenius, 2005; Lawen, 2003; Taylor et al., 2008). During this process, the plasma membrane can also be modified by the externalisation of PS residues (Lawen, 2003). Lastly, the resulting apoptotic bodies are effectively and quietly removed through engulfment by phagocytic cells and/or neighbouring cells (Fadeel and Orrenius, 2005; Lawen, 2003; Taylor et al., 2008). Since the contents of the apoptotic cell is neatly contained within the apoptotic bodies and discretely removed, there is little or no leakage into the surrounding area; thus preventing the inflammatory response seen in necrosis (Fadeel and Orrenius, 2005). The complete apoptotic process, including corpse clearance, can take place within a matter of hours and is said to occur at a rate 20 times faster than that of mitosis; making sightings of a dying cell a rare event (Fadeel and Orrenius, 2005; Melino, 2001).

Apoptotic stimuli can be divided into four main groups based on the method of apoptosis induction (Kam and Ferch, 2000). The first group is DNA damage stimuli and includes ionising radiation. The second group employs receptor-based mechanisms to induce apoptosis and entails the binding of ligands to death receptors or the withdrawal of growth factors. The third group functions to stimulate the apoptosis pathway and consist of biochemical agents like phosphatases and kinase inhibitors. Lastly, stimuli like ultraviolet light, heat and free radicals belong to the group that results in physical cell damage (Kam and Ferch, 2000). In addition, the signalling pathway activated within a cell by a specific stimulus can also depend on the specific cell type (Kolesnick and Krönke, 1998).

1.2.2 Molecular pathways in apoptosis

Apoptosis can follow one of two main signalling pathways, namely the extrinsic or intrinsic pathways (Fig. 1.4), while cytotoxic T lymphocytes (CTLs) and natural killer (NK) cells have a third option known as the Perforin/Granzyme B pathway (Fadeel and Orrenius, 2005; Lawen, 2003). The extrinsic pathway, also known as the death-receptor pathway, is stimulated by receptor-based mechanisms as well as certain chemotherapeutic drugs and is said to play a pivotal role in conserving tissue homeostasis, particularly in the immune system (Fadeel and Orrenius, 2005; Fulda and Debatin, 2006). The extrinsic pathway is initiated outside the cell through the binding of a membrane-bound death receptor (DR) and its corresponding ligand (Lawen, 2003). Death receptors involved in this pathway are members of the tumour necrosis factor (TNF) receptor gene superfamily and includes Fas (also known as CD95), TNF receptor (TNFR) and TNF-related apoptosis-inducing ligand-receptor (TRAIL-R). The corresponding ligand for each receptor, respectively, are Fas-L (CD95L), TNFα and TRAIL (Fulda and Debatin, 2006; Kam and Ferch, 2000). In order to facilitate downstream signal transduction, a region of approximately 80 amino

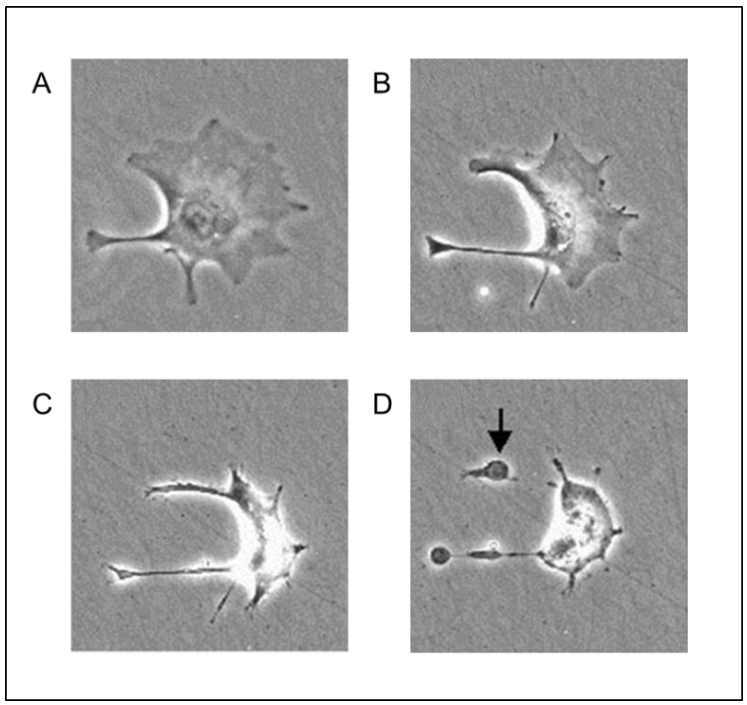

Figure 1.3: Scanning electron microscope image of a trophoblast cell undergoing apoptosis. A - Shrinkage of cells. B - Nuclear condensation. C - Further cellular shrinkage and packaging of cellular contents. D - Membrane blebbing. Arrow points to an apoptotic body. Obtained from http://www.reading.ac.uk/cellmigration/apoptosis.htm.

acids, which has been termed the death domain (DD), is shared between these receptors (Kidd, 1998). The binding of the ligand to the corresponding receptor sets in motion a series of events; firstly, the receptor undergoes trimerisation and DDs are clustered together, which is followed by the recruitment of an adapter molecule such as the Fas-associated death domain (FADD) and TNF-receptor-associated death domain (TRADD) proteins (Fulda and Debatin, 2006; Kam and Ferch, 2000; Lawen, 2003) . In addition to a DD, the adaptor molecules also contain another unique domain, known as the death effector domain (DED) (Kidd, 1998; Lawen, 2003). Once it is recruited to the membrane receptor, the adaptor molecule in turn facilitates the recruitment of either pro-caspase 8 or 10 (Fulda and Debatin, 2006; Kidd, 1998). The pro-caspase contains a similar DED in its pro-domain and an interaction is established through this domain with the corresponding DED of the adaptor molecule (Kidd 1998). This final recruitment completes the formation of the death-inducing signalling complex (DISC) (Fulda and Debatin, 2006; Lawen, 2003). The DISC facilitates transactivation of the pro-caspase molecules by bringing them in close proximity to each other (Lawen, 2003). Once activated, the caspases are free to activate downstream pro-caspases, initiating a caspase cascade (see figures 1.4 and 1.5) (Lawen, 2003).

In contrast to the extrinsic pathway, the intrinsic pathway is initiated from within the cell. The pathway is also known as the mitochondrial pathway as this organelle plays a central role in executing apoptosis through this pathway (Fadeel and Orrenius, 2005). The pathway is stimulated by intracellular stresses such as oxidative stress and DNA damage but can also be induced by

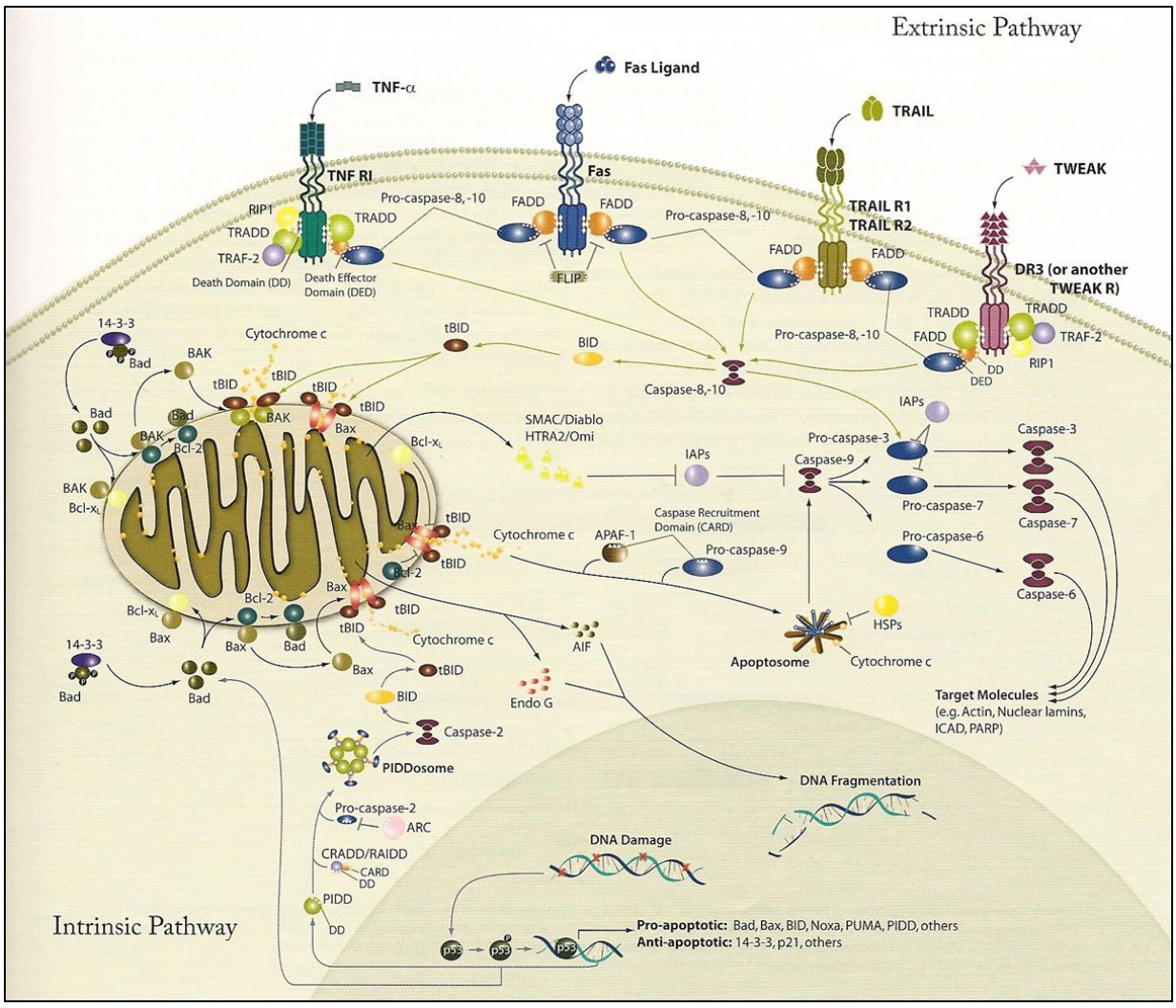

Figure 1.4: The extrinsic and intrinsic pathways of apoptosis. Adapted from http://www.hixonparvo.info/model.html.

chemotherapeutic drugs (Fadeel and Orrenius, 2005; Fulda and Debatin, 2006). Upon stimulation, an attack is launched on the mitochondria, presumably mediated by members of the Bcl-2 protein family, resulting in permeabilisation of the outer membrane, (Green and Kroemer, 2004). As a result, proteins normally found within the intermembrane space of the mitochondria are released into the cytosol (Green and Kroemer, 2004). One such protein is cytochrome c; which upon release binds apoptotic protease activating factor-1 (Apaf-1) in the cytosol (Lawen, 2003). Pro-caspase 9 is also recruited and the apoptosome complex is formed. The complex is rather large in size, approximately 1 MDa, and consists of seven molecules of each of its building blocks as well as seven (deoxy)-adenosine triphosphate ((d)ATP) molecules (Lawen, 2003). A similar type of homotypic interaction takes place here as with DISC formation in the extrinsic pathway. Both Apaf-1 and pro-caspase 9 contain a nucleotide binding domain known as the caspase-recruitment domain (CARD) and it is a CARD-CARD interaction that allows for the conversion of pro-caspase 9 to the active caspase 9 state (Fadeel and Orrenius, 2005; Fulda and Debatin, 2006). Similarly to caspase 8 and 10 in the extrinsic pathway, active caspase 9 now has the ability to further activate downstream pro-caspases 3, 6 and 7 (see figures 1.4 and 1.5) (Lawen, 2003). The mitochondria

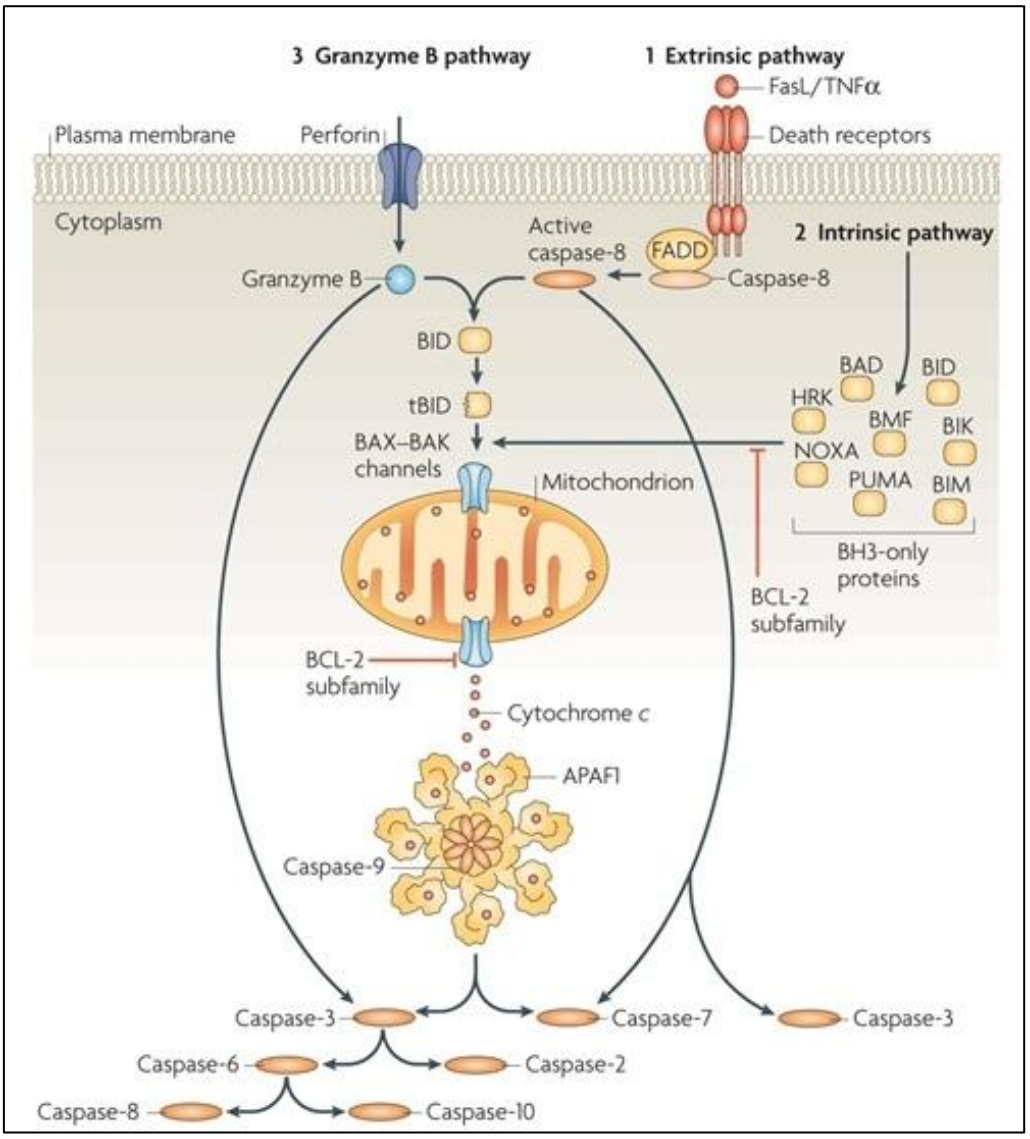

Figure 1.5: Activation of the caspase cascade in the various apoptotic pathways. Adapted from Taylor et al., 2008.

can also contribute to caspase-independent apoptosis through the release of apoptosis inducing factor (AIF) and endonuclease G (EndoG) from the intermembrane space. When released, these proteins translocate to the nucleus and contributes to chromatin condensation and DNA fragmentation (Fig. 1.4) (Fadeel and Orrenius, 2005; Fulda and Debatin, 2006).

A third pathway in apoptosis-mediated cell death is restricted to CTLs and NK cells and mainly functions during an immune response by targeting virally infected or transformed cells (Barry et al., 2000; Goping et al., 2003; Trapani and Smyth, 2002). The granzyme B, or perforin/granzyme B, pathway initiates with the transfer of cytoplasmic granules, containing, amongst other proteins, perforin and granzyme B, to the target cell (Barry et al., 2000; Trapani and Smyth, 2002). The particular delivery method of the granules and its contents is however under debate and several different mechanisms have been proposed (Trapani and Smyth, 2002). The perforin protein is referred to as a lytic molecule, since it is known to disrupt the cell membrane by means of pore

formation, while granzyme B belongs to a family of structurally related serine proteinases displaying a unique substrate specificity and capacity to cleave at aspartic residues (Barry et al., 2000; Goping et al., 2003; Trapani and Smyth, 2002). Granzyme B has the ability to cleave and activate pro-caspases 3 and 8, hence activating the caspase cascade which culminates in cell death. In addition, granzyme B also holds the ability to cleave and activate the pro-apoptotic molecule Bid, which upon activation translocate to the mitochondria where it stimulates MOMP (Fig. 1.5) (Barry et al., 2000; Goping et al., 2003).

1.2.3 Apoptosis related molecules

Of major importance to the process of apoptosis is caspases, a large protein family of cysteine proteases which is highly conserved (Hengartner, 2000; Turk and Stoka, 2007). Caspases share a characteristic cysteine residue in their active site and cleaves their substrates after an aspartic acid residue (Hengartner, 2000). To date, 11 different human caspases has been identified, which can be grouped according to their substrate preferences, functional or structural similarities (Hengartner, 2000; Ho and Hawkins, 2005; Turk and Stoka, 2007). Caspases can either function in apoptosis (caspases 2, 3, 6, 7, 8, 9 and 10), in the inflammatory response (caspases 1, 4 and 5) or in keratinocyte differentiation (caspase 14) (Turk and Stoka, 2007). Apoptotic caspases can further be categorised as initiator/activator caspases (caspases 2, 8, 9 and 10) or effector/executioner caspases (caspases 3, 6 and 7). A structure-function relationship is also present in apoptotic caspases; initiator caspases all share a long pro-domain containing either a DED or CARD domain, while the effector caspases are distinguished by shorter prodomains (Fig. 1.6) (Ho and Hawkins, 2005; Turk and Stoka, 2007). Caspases are synthesised as inactive zymogens, referred to as pro-caspases (Ola et al., 2011). Activation, which involves removal of the prodomain, can take place through one of three mechanisms; in most cases a pro-caspase undergoes proteolytic cleavage by another, active caspase, creating a caspase-cascade (Hengartner, 2000). Other mechanisms include an induced proximity model, which suggests the close proximity of multiple zymogens is sufficient to induce transactivation (for example activation of multiple pro-caspase 8 molecules in the DISC complex) and association with a regulatory subunit, which is apparently required for pro-caspase 9 activation. In the latter example, the apoptosome complex functions as a holoenzyme and the relevant subunits are seen as regulatory components rather than mere adaptors (Hengartner, 2000). As one can infer from the name, initiator caspases function during the initial stages of apoptosis, propagating the initial apoptotic stimuli, while effector caspases function during the later stages by cleaving approximately 400 different, but specific mammalian substrates (Green and Kroemer, 1998; Taylor et al., 2008). Cleavage of substrates like caspase-activated DNase (CAD), nuclear lamins, cytoskeletal proteins and epidermal growth factor directly

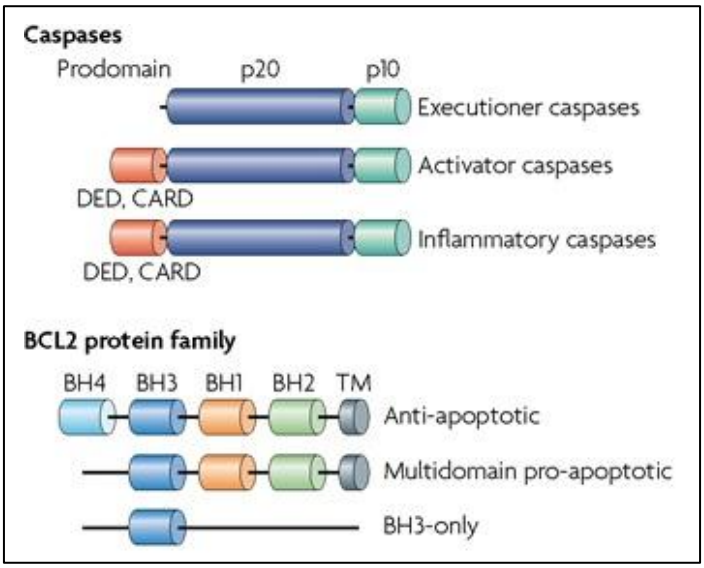

Figure 1. 6: Protein structures of the caspase and Bcl-2 protein families. Adapted from Degterev and Yuan, 2008.

results in some of the characteristic morphological features of apoptosis like DNA fragmentation, nuclear shrinking and budding and membrane blebbing (Devarajan et al., 2002; Hengartner, 2000).

Another important family regulating apoptosis is the Bcl-2 protein family. The family comprises of both pro-apoptotic and anti-apoptotic proteins and it is the ratio between these opposing proteins that determines which protein subfamily reigns in the cell (Kidd, 1998; Kroemer et al., 1998). The mammalian Bcl-2 family consists of 12 core members and can also be divided into three groups based on structural similarities (Coultas and Strasser, 2003; Ola et al., 2011; Youle and Strasser, 2008). All Bcl-2 family proteins share regions of homology known as the Bcl-2 homology (BH) regions, which are important for interactions between the family members. A total of four BH regions exist (BH1-4) and the structural grouping of a protein is based on the number and type of BH regions it contains (Fig. 1.6) (Coultas and Strasser, 2003; Ola et al., 2011). The first group of proteins contain all four BH regions and are anti-apoptotic in nature. Examples include Bcl-2, Bcl-X_L, Bcl-w, Mcl-1 and A1. The remaining two groups are pro-apoptotic and are distinguished by the number of BH regions they contain. One group of proteins contain either two or three BH regions, in any combination, and include the Bax, Bak, Bok, Bcl-X_S and Bcl-G_L proteins, while the last group of proteins contain only one specific BH region, namely BH3, and are thus also referred to as the BH3-only proteins. Members of this group include Bid, Bik, Hrk, Bim, Noxa and Puma (Coultas and Strasser, 2003; Giam et al., 2008; Ola et al., 2011; Youle and Strasser, 2008). Pro-apoptotic members function to induce apoptosis through permeabilisation of the mitochondrial outer membrane while anti-apoptotic members function to prevent this from happening and also by preventing caspase activation (Coultas and Strasser, 2003; Hengartner, 2000). However, the exact functional mechanism of the proteins is still unclear (Coultas and Strasser, 2003). What is known is that regulation of apoptosis by the Bcl-2 family proteins are mediated through their interaction with each other and two models has been proposed for the activation of Bax and Bak (Giam et al.,

2008; Ola et al., 2011). In the direct model, BH3-only proteins are divided into 'sensitizers' and 'activators', the latter being inactivated by anti-apoptotic proteins under normal physiological conditions. Apoptotic stimuli activate the sensitizers which bind and sequester the anti-apoptotic proteins, leaving the activator BH3-only proteins free to directly activate Bax and Bak, which in turn oligomerises and induces MOMP. In contrast, in the indirect model, anti-apoptotic proteins bind and inactivate Bax and Bak. Apoptotic stimuli signal the BH3-only proteins to bind the anti-apoptotic proteins, allowing Bax and Bak to oligomerise. In this model there is no interaction between the BH3-only proteins and Bax and Bak (Giam et al., 2008; Ola et al., 2011).

Even though caspases are seen as the central executioners of apoptosis and is responsible for many of the characteristic features, apoptosis without caspase activation is still possible (Hengartner, 2000; Tait and Green, 2008). In 2008, Tait and Green defined caspase-independent cell death (CICD) as "death that ensues when a signal that normally induces apoptosis fails to activate caspases", while Pradelli *et al.* (2010) took it one step further by defining CICD as any type of cell death, apart from necrosis, that ensues if apoptosis fails to take place. The former group implies that CICD can still be included under the classification of apoptosis, since it only depends on the failure of caspase activation. In contrast, the latter group suggests that caspase activation is synonymous with apoptosis; the one can not take place without the other. Typically, CICD displays a relatively varying phenotype, which includes features from apoptosis, autophagy and necrosis (Kroemer et al., 2009; Tait and Green, 2008). As previously mentioned, the intrinsic pathway of apoptosis can proceed without the activation of caspases and it is in this example of CICD that the flavoprotein AIF plays a crucial role (Modjtahedi et al., 2006; Tait and Green, 2008). AIF was the first protein identified as a major component of CICD and since then studies in model organisms such as *Saccharomyces cerevisiae*, *C. elegans*, *D. melanogaster* and *Mus musculus* have contributed to significant progression in the understanding of AIF's role in CICD (Susin et al., 1999). AIF is produced as a 67 kDa precursor protein containing a mitochondrial localisation signal (MLS) at its N-terminus (Hangen et al., 2009; Norberg et al., 2010). This MLS region is cleaved off upon import into the mitochondria and the resulting 62 kDa protein is embedded into the inner mitochondrial membrane (IMM) by means of a hydrophobic transmembrane region (Norberg et al., 2010; Yu et al., 2009). AIF exclusively exerts is apoptotic function when the cell death process is induced by certain stimuli; the protein is released from the IMM, most likely by calpains or cathepsins, to produce the soluble and mature 57 kDa form which is subsequently released into the cytoplasm by means of MOMP (Joza et al., 2009; Norberg et al., 2010). From here, AIF is targeted to the nucleus by two nuclear localisation signals where it induces chromatin condensation and large-scale DNA fragmentation (Joza et al., 2009; Norberg et al., 2010). The exact mechanism for this apoptotic activity remains unclear, however electrostatic interaction between AIF and DNA is known to be mediated by multiple positively charged amino acids and that the binding of AIF to DNA is not sequence-specific (Candé et al., 2002; Hangen et al., 2009;

Norberg et al., 2010). Interestingly, AIF is described as a bi-functional protein based on the observation that it also performs an important function in healthy cells (Candé et al., 2004; Hangen et al., 2009). Indeed, these two functions are restricted to different regions within the protein structure itself; the C-terminal region is required for apoptotic function of AIF, while internal regions are responsible for the non-apoptotic function (Hangen et al., 2009; Ye et al., 2002). The second function of AIF was elucidated upon discovery of significant homology with bacterial nicotinamide adenine dinucleotide (reduced, NADH) oxidases, that is, AIF performs important physiological redox functions, suggested to regulate and maintain respiratory complexes (Maté et al., 2002; Norberg et al., 2010; Wang et al., 2011; Ye et al., 2002). Specifically, AIF mainly acts upon complex I however associations with complexes III and IV have also been suggested (Hangen et al., 2009). The ability of AIF to induce apoptosis has been shown to be dependent on the cell type as well as the specific apoptotic stimulus involved (Joza et al., 2009; Norberg et al., 2010). With regards to the latter, the release of AIF from the IMM is likely to occur upon any stimulus that disrupts the intracellular Ca^{2+} homeostasis, since calpains are Ca^{2+}-dependent enzymes (Norberg et al., 2010). In addition, AIF has been shown to be the major facilitator of cell death following excessive activation of Poly(ADP-ribose) polymerase-1 (PARP-1) (Wang et al., 2011; Yu et al., 2009).

1.2.4 The genetics of apoptosis related proteins – implications of mutations

The p53 protein is notoriously associated with cancer since it is estimated that the corresponding gene, *TP53*, is mutated in 50% of all tumours; a statement that emphasises the importance and major role of genetics in cancer (Amaral et al., 2010). The genetic foundation of cancer, which is further complicated by environmental influences, and the realisation that tumour cells can harbour mutations that favour their survival, suggests that mutations in other apoptosis-related genes can also be of significance in the genesis, as well as progression, of tumours. Indeed, numerous studies have identified mutations in a variety of genes involved in the signalling pathways of apoptosis. It is however important to remember that no single genetic mutation should be seen as a ‘causative mutation’ but rather as a ‘contributing mutation’, since multiple mutations in different genes are required for the development of cancer (Vogelstein and Kinzler, 2004). In terms of the caspase family, mutation-screening studies have mainly focussed on *caspase 8*, with mutations being identified in cases of advanced gastric, invasive colorectal, hepatocellular and head and neck carcinomas (Olsson and Zhivotovsky, 2011). For other caspases, mutations have been observed in colon, oesophageal and head/neck carcinomas for *caspase 7*; multiple myeloma, hepatocellular and adenocarcinomas for *caspase 3*; breast, gastric, colon and adenocarcinomas for *caspase 5;* and gastric and colon carcinomas for *caspases 1* and *4* respectively (Ghavami et al., 2009). Even though the frequencies of these mutations were quite low, they contribute to the

substantial heterogeneity seen in different tumours. One also has to keep in mind that apart from mutations, post-translational modifications, altered gene expression and epigenetic modifications are also able to deregulate these proteins in tumour cells. Mutations in the *TRAIL-R1* and *TRAIL-R2* genes have previously been identified in metastatic breast cancers (Shin et al., 2001). These two genes are located on chromosome 8p21-22; a region that has recently been suggested to harbour a metastatic susceptibility locus for tumours (Macartney-Coxson et al., 2008). The second major protein family involved in apoptosis pathways, the Bcl-2 family, can also present with mutations in certain tumour types. A t(14:18) translocation between the heavy chain immunoglobulin (Ig) segments and the anti-apoptotic *Bcl-2* gene is known to be associated with follicular lymphomas (Müllauer et al., 2001). A second translocation with the light chain Ig genes on chromosomes 2 or 22 is also possible, however these occur less frequently. Both of these translocations result in the increased expression of *Bcl-2* and ultimately suppression of apoptosis (Müllauer et al., 2001). Frameshift mutations in the pro-apoptotic member *Bax* have been identified in colon adenocarcinomas with a microsatellite mutator phenotype (MMP) (Rampino et al., 1997). Tumours positive for MMP display significant genomic instability at microsatellites due to replication slippage. The *Bax* gene contains an eight-nucleotide deoxyguanosine track which was shown to contain frameshift mutations in 51% of MMP^+ colon adenocarcinomas; an alternation that was absent in MMP^- tumours. These frameshift mutations would render the *Bax* gene unresponsive to transcriptional activation by p53 (Rampino et al., 1997). The consequences of genetic mutations in apoptosis-related proteins is however not limited to cancers. Mutations in the death receptor *Fas* gene have been shown to be the causative factor for autoimmune lymphoproliferative syndrome (ALPS) type Ia while mutations in the Fas ligand gene (*Fas-L*) produces ALPS type Ib (Straus et al., 2001). Interestingly, mutations in *caspase 10* is associated with ALPS type II, suggesting that the disorder is a result of a defective pathway. ALPS is a disorder of lymphocyte homeostasis and symptoms include splenomegaly (enlarged spleen), chronic lymphadenopathy (enlarged lymph nodes), autoimmune phenomena and lymphoma (Straus et al., 2001).

1.2.5 Implications of mismanaged apoptosis

As previously mentioned, apoptosis is vital to maintain a normal, homeostatic state and stringent measures of control are in place to ensure appropriate levels of activity. Based on these facts, one can only assume that deregulation of apoptosis can have severe pathological consequences. In fact, it was estimated that inappropriate levels of apoptosis is a contributing factor in 50% of main medical illnesses lacking adequate preventative measures and therapies (Reed, 2002). Throughout decades of research deregulated apoptosis has been found to be associated with an array of pathological disorders and the mode of action in these diseases can be ascribed to either

too little apoptosis or too much. Disorders included in the former category include cancer, restenosis, autoimmune diseases and disorders of prolonged or chronic inflammation, while disorders from the latter category include neurodegenerative disorders (for example Alzheimer's, Parkinson's, and Huntington's disease), acquired immunodeficiency syndrome (AIDS), ischemia-reperfusion injury and heart failure (Fadeel and Orrenius, 2005; Hotchkiss et al., 2009; Lawen, 2003; Reed, 2002). Highlighted below is a disorder from each category.

It is said that defective apoptotic machinery can be found in more than 50% of malignant tumours (Hotchkiss et al., 2009). These tumours are characterised by uncontrolled proliferation paralleled by evasion of apoptosis (Green and Evan, 2002). Malignant cells can employ various mechanisms to evade apoptosis and these mechanisms can be directed at both the extrinsic and intrinsic pathway of apoptosis (Fulda, 2010). Evasion of the extrinsic pathway can involve down regulation of DR surface expression, abnormal expression of decoy DR (capable of binding the appropriate ligands but fails to initiate downstream signalling) and altered expression or phosphorylation of pro-caspase 8. In terms of the intrinsic pathway, malignant cells survive by altering the ratio of Bcl-2 family proteins to favour their survival, reduction of cytochrome c, thus rendering the molecule incapable of activating pro-caspase 9, and through down regulating Apaf-1 expression and/or activity (Fulda, 2010). However these mechanisms not only ensures the malignant cell's own survival and proliferation by resisting natural cellular defences but also results in apoptotic resistance towards many cancer therapies, as the objective of many of these therapies is to induce apoptosis (Fulda and Debatin, 2006; Fulda, 2010). Furthermore, genetic mutations in apoptosis-related genes, as discussed previously, have also been implicated in a variety of malignant tumours. The realisation of apoptosis' involvement in tumourigenesis has spurred many researchers to focus on unravelling the apoptotic process with the aim of developing new therapies for cancer treatment.

Increased levels of apoptosis have been implicated in various forms of neurodegenerative disorders. Alzheimer's disease is the most common of these disorders and is characterised by pronounced neuronal cell loss (Eckert et al., 2003). Also associated with Alzheimer's is the accumulation and oligomerisation of the amyloid beta (Aβ) peptide, forming plaques in the cerebral and brain vasculature (Eckert et al., 2003; Kam and Ferch, 2000). These Aβ plaques can lead to apoptotic neuronal cell death, most likely through the generation of free radicals like nitric oxide and ROS, resulting in increased oxidative stress (Eckert et al., 2003; Kam and Ferch, 2000; Takuma et al., 2005). Moreover, caspases 3, 8 and 9 have been implicated in Alzheimer's through the examination of post-mortem tissues while *Bcl-2* and *Bax* expression have been shown to be down- and up-regulated, respectively; both complications resulting in increased neuronal cell loss by means of apoptosis (Eckert et al., 2003; Olson and Kornbluth, 2001). Parkinson's disease is another neurodegenerative disorder characterised by neuronal cell loss, more specifically, a loss of dopaminergic neurons (Kam and Ferch, 2000; Olson and Kornbluth, 2001). As with Alzheimer's,

the cell loss is also believed to be due, at least in part, to increased ROS production and a combination of neurorestorative and anti-apoptotic therapies has been proposed to be of benefit to patients with Parkinson's (Eberhardt and Schulz, 2003; Olson and Kornbluth, 2001). Huntington's disease is characterised by a polyglutamine tract in the Huntingtin protein caused by the expansion of a cytosine-adenine-guanine (CAG) repeat in the corresponding gene (Fadeel and Orrenius, 2005). Accumulation of the aberrant protein is associated with neuronal cell loss, possible through the activation of pro-caspase 8, while knockout of caspase 1 in a mouse model displayed slower disease progression (Fadeel and Orrenius, 2005; Reed, 2002). Additional evidence supporting a possible role for apoptosis in neurodegenerative diseases can be concluded from imaging studies where apoptotic nuclei was observed in post-mortem tissues from Alzheimer's, Parkinson's and Huntington's patients (Olson and Kornbluth, 2001).

1.2.6 Apoptosis-based therapies – contributing to the fight against cancer

The ability of tumour cells to effectively evade the induction of apoptosis is a characteristic that has severely limited the progress in the fight against cancer. Furthermore, traditional therapeutic strategies such as chemotherapeutic drugs and radiotherapy have also been subjected to failure due to the tumour cell's ability to actively prevent apoptosis from taking place (Azmi et al., 2011). The most commonly used chemotherapeutic drugs are cytotoxic in nature and include drugs such as methotrexate, doxorubicin, carboplatin and vinca alkaloids (table 1.1) (Nussbaumer et al., 2011). As mentioned previously, tumour cells often harbour genetic alternations, such as mutations and genome aberrations, that lend them this unique ability; however, these alternations remain a continuing force that aims to initiate apoptotic pathways (Sayers, 2011). Thus, removing the blockade against apoptosis employed by tumour cells or, alternatively, activating other/additional apoptotic proteins/pathways has become an attractive approach in identifying new therapeutic protocols for cancer treatment. Additionally, the use of different strategies in combination has also received much attention (Azmi et al., 2011; Sayers, 2011). Since many chemotherapeutic drugs rely on the pro-apoptotic members of the Bcl-2 family to mediate apoptosis, the anti-apoptotic members which regulate the activity of these proteins have become prime targets for the development of novel cancer therapies to assist traditional methods (Yip and Reed, 2008). In addition, extensive research into the mechanisms of apoptosis resistance in tumour cells has revealed that the anti-apoptotic members of the Bcl-2 family are commonly overexpressed in tumours, especially in complex and aggressive cancers such as prostate, pancreatic, ovarian and metastatic breast cancers (Azmi et al., 2011; Yip and Reed, 2008). As a result, a variety of strategies aiming to reduce or inhibit these proteins has been devised, including the use of antisense oligonucleotides, antibodies, synthetic peptides and small molecule inhibitors (SMIs) (Azmi et al., 2011). Early success was seen in gene silencing strategies and phase III clinical trials

Table 1.1: Common chemotherapeutic drugs used in the treatment of cancers

Drug	Class	Function/stimulus for intrinsic apoptotic pathway	Commonly prescribed for
Methotrexate	Antimetabolites	Binds and inhibits dihydrofolate reductase (produces tetrahydrofolate) resulting in the inhibition of DNA, RNA, and protein synthesis	Maintenance therapy for childhood ALL; non-Hodgkin's lymphoma; choriocarcinoma; lung cancer
Doxorubicin	DNA interactive agent	Intercalating agent - binds between the base pairs of DNA, preventing DNA replication and protein synthesis	Broad spectrum – acute leukaemia; lymphomas; variety of solid tumours
Carboplatin	DNA interactive agent	Cross-linking agent - binds DNA to induce intra- and interstrand cross-linking of DNA	Advanced ovarian cancer; lung cancer
Vincristine	Antitubulin agent	Binds microtubules and spindle proteins to interfere with formation of mitotic spindle, resulting in cell cycle arrest	Lung cancer; breast cancer; lymphomas; acute leukaemia;
Etoposide	Topoisomerase inhibitor	Prevents DNA replication and repairs by binding and inhibiting topoisomerase II	Small-cell bronchial carcinoma; testicular cancer; certain lymphomas
5-Fluorouracil	Antimetabolite	Pyrimidine analogue – incorporates into RNA and inhibits RNA processing	Breast cancer; skin cancer; cancers of the gastrointestinal tract
Actinomycin-D	DNA interactive agent	Intercalating agent - binds between the base pairs of DNA, preventing DNA replication and protein synthesis	Paediatric cancers; testicular sarcomas; AIDS-related Kaposi's sarcoma
Bleomycin	DNA cleaving agent	Induces single- and double-strand DNA breaks	Head and neck cancer; testicular cancers; Hodgkin's and non-Hodgkin's lymphoma

ALL – acute lymphoblastic leukaemia. Information obtained from Nussbaumer et al., 2011 and the National Cancer Institute, http://www.cancer.gov/.

suggests that G3139, an antisense oligonucleotide targeting Bcl-2, shows great promise for the treatment of myeloid leukaemia. However, the strategy faces several hindrances, such as the short half-life of the oligonucleotides as well as enzymatic degradation, and chemical modifications are needed to improve the therapeutic potential of these antisense oligonucleotides (Azmi et al., 2011). Current research is now focussed on use of small molecule inhibitors (SMIs), low molecular mass organic molecules that function to inhibit the anti-apoptotic Bcl-2 proteins. SMIs are designed to bind and occupy the hydrophobic groove of these proteins, thereby preventing their heterodimerisation with pro-apoptotic family members. Currently, there are seven SMIs in various stages of clinical trials for the treatment of cancers such as lymphoma, multiple myeloma, leukaemia, pancreatic cancer, small cell lung cancer and head and neck cancer (Azmi et al., 2011).

The majority of traditional chemotherapeutic drugs, as well as radiotherapy, function to induce apoptosis by activating the intrinsic pathway (table 1.1); unfortunately though, this may result in the selection of tumour cells resistant to this pathway (Sayers, 2011). Designing therapeutic strategies targeting the extrinsic pathway is thus also of vital importance. In addition, activation of the extrinsic pathway may be advantageous in tumours where the intrinsic pathway signalling is limited, such as those harbouring mutations in the *TP53* gene. As mentioned previously, caspase 8 is activated in the extrinsic pathway, which in turn is able to cleave and activate Bid, a pro-apoptotic Bcl-2 family member that has the ability to facilitate MOMP by engaging Bax or Bak. This process serves as an alternative mechanism for the induction of the intrinsic pathway and importantly, is independent of p53 (Sayers, 2011). In terms of activating the extrinsic apoptotic pathway in tumour cells, the death ligand TRAIL is proving to be a promising candidate based on the observation that normal cells are relatively insensitive to apoptosis induction by TRAIL (Ashkenazi and Herbst, 2008; Sayers, 2011). TRAIL or TRAIL receptor agonists can be administered systemically or via non-replicating recombinant adenoviral vectors (Sayers, 2011). The TRAIL-mediated strategy is also amendable to use in a combination of strategies and ABT-737, one of the SMIs targeting Bcl-2 proteins currently in clinical trials, has been shown to greatly enhance the TRAIL-mediated apoptosis in pancreatic cancer cell lines (Huang and Sinicrope, 2008). An alternative method to administer death receptor ligands to a tumour cells would be to utilise immune effector cells, such as macrophages, T cells, dendritic cells and NK cells. These cells have the ability to express multiple death ligands and would make excellent delivery vehicles (Sayers, 2011). In fact, a recent study showed that adoptively transferred transgenic T cells was able to deliver Fas-L to renal cancer cells and that this step was essential to the observed therapeutic effect (Sayers, 2011; Shanker et al., 2009). Lastly a promising avenue in novel anti-cancer therapies that is currently being explored is the design and use of nanoparticles (Brannon-Peppas and Blanchette, 2012; Brigger et al., 2012). These submicronic colloidal systems could potentially serve as a mechanism of gene delivery as well as an improved mechanism for the

delivery of antisense oligonucleotides by providing increased stability and protection. In addition, nanoparticles are also capable of specifically targeting chemotherapeutic drugs to a cancer cell, which has the potential of improving drug efficacy while minimising harmful side-effects (Brannon-Peppas and Blanchette, 2012; Brigger et al., 2012).

1.3 Aims and objectives

The aim of this study is to aid in the characterisation of genes involved in apoptosis, as well as to identify novel candidate genes possibly involved in resistance to apoptosis. The following objectives were set out to achieve these aims:

- To verify the involvement of three novel candidate genes, identified in a previously performed pilot study, in resistance to apoptosis induced by C_2-ceramide and camptothecin by generating stable knockdown cell lines for each of the candidate genes and repeating the apoptosis assays as performed in the pilot study.
- To identify additional novel candidate genes possibly involved in resistance to apoptosis by analysing nucleotide sequences obtained in a previously performed pilot study.
- To characterise the identified novel candidate genes by using a bioinformatic approach.
- To investigate the gene expression levels of the novel candidate genes, as well as other genes known to be involved in apoptosis, in normal and cancer cell lines.

1.4 Background to the current study

This study builds on a previously performed pilot study that aimed to identify novel genes involved in resistance to apoptosis induced by C_2-ceramide in Chinese hamster ovary (CHO) cell lines. These cells were used due to their unique characteristic of being functionally haploid. The cell line was originally isolated in 1958 by Puck and colleagues and later described as functionally hemizygous (Siminovitch, 1976). The cell line thus provides an invaluable platform for functional studies: if the expression of a gene is abrogated either by disrupting its coding sequence or the sequences of its regulatory elements, a “knock-out” cell is effectively produced. In the pilot study, this was achieved by performing promoter trap mutagenesis experiments. The technique is based on the random insertion of an integration cassette, delivered by a retrovirus, into the host genome. The experiment is viewed as successful if insertion occurs within the promoter region of a gene. The integration cassette utilised in the pilot study was designed to provide dual-type positive selection in the form of Hygromycin B and Neomycin resistance genes, as well as negative selective by means of the Herpes simplex virus thymidine kinase gene (Fig. 1.7).

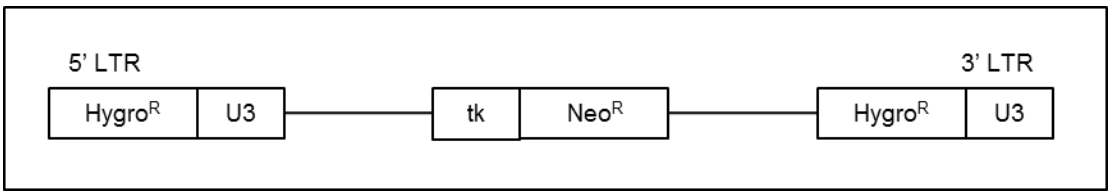

Figure 1.7: Schematic representation of the integration cassette used in the promoter-trap mutagenesis experiments. The cassette was transferred to the CHO22 cells by means of the MoMLV. LTR – long terminal repeat; U3 – promoter element; Hygro^R – Hygromycin B resistance gene; Neo^R – Neomycin resistance gene; tk – thymidine kinase gene from the Herpes simplex virus.

Expressing the ecotropic receptor for the Moloney murine leukaemia virus (MoMLV), CHO22 cells were infected with the retrovirus carrying the promoter-trap vector containing the integration cassette. Transfectants were placed on media containing Hygromycin B or G418 to select positive recombinants and then treated with either C_2-ceramide or camptothecin to induce apoptosis. Surviving colonies were screened and the top three colonies showing the highest level of resistance were isolated and cultured to obtain stable cell lines. The three cell lines were designated J304, J308 and J612. Apoptosis assays were performed to confirm apoptosis as the mode of cell death induced by the agents and to measure the resistance shown by the isolated J-cell lines. Both the APOPercentage™ Apoptosis assay (Biocolor LTD, UK) and the Annexin-V FITC Apoptosis Detection Kit (BD Biosciences) used in the pilot study exploits the structural cell membrane changes of apoptotic cells to detect and quantify apoptosis. In physiologically normal cells, phosphatidylserine molecules are located on the inside of the cell, on the inner cell membrane. However, upon apoptotic stimuli, these molecules are translocated to the outside of the cell by what has been described as a "flip-flop" mechanism (Fadok et al., 1992). The APOPercentage™ Apoptosis assay utilizes this "flip-flop" mechanism to import a purple-red dye into the dying cell, while the Annexin-V FITC Apoptosis Detection Kit contains fluorophore-labelled Annexin-V molecules which selectively binds to the exposed phosphatidylserine molecules. In addition, a Caspase 3 Colourimetric assay (BioVision Incorporated) was performed which allows detection of early/mid apoptosis. These assays allows for the quantification of the amount of apoptotic cells in a sample.

For the purpose of the pilot study, cell lines J304, J308 and J612, along with wild type CHO22 cells serving as a control, were treated for 24 hours with C_2-ceramide and camptothecin at concentrations ranging from 0-100 µM and 0-10 µg/ml respectively. The amount of apoptotic cells in each cell line sample were quantified with each of three apoptosis assays. These cell lines were subsequently analysed to determine if they displayed a significant level of resistance to apoptosis ($p < 0.05$). Figures 1.8 – 1.10 are examples of graphs generated during the analysis. Similar results were obtained in all three apoptosis assays. Compared to the wild type CHO22 cell line, the promoter-trapped cell lines displayed significant resistance to apoptosis upon treatment with both C_2-ceramide and camptothecin. The resistance persisted upon increasing concentrations of the apoptotic inducer, while the amount of CHO22 cells continued to decrease dramatically. In

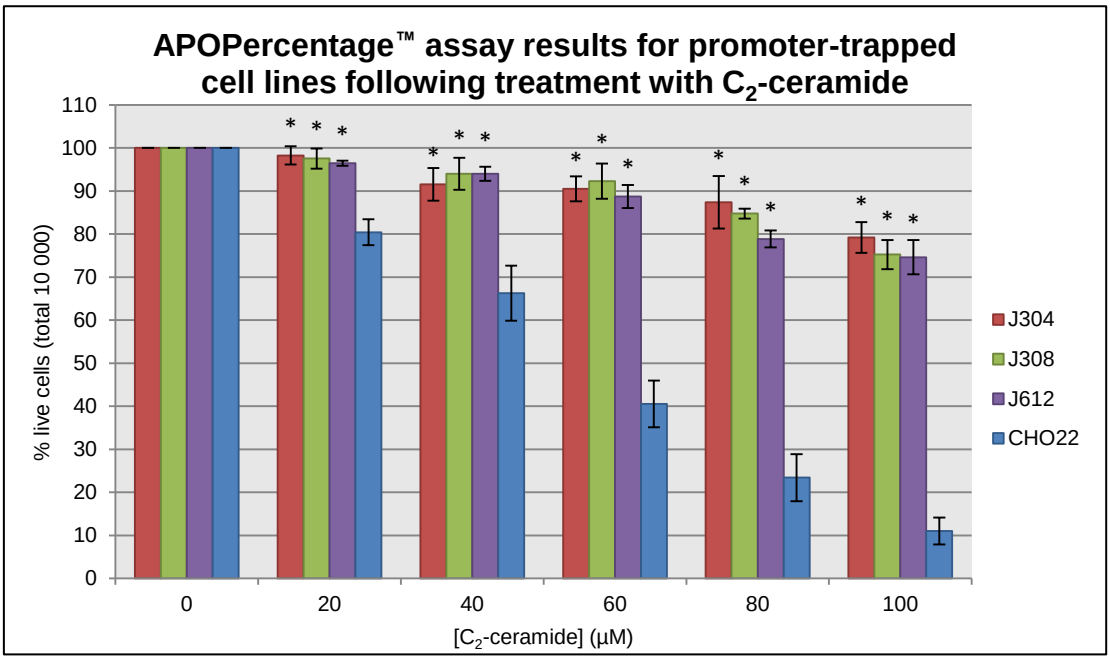

Figure 1.8: Results of testing for resistance to apoptosis in promoter-trapped cell lines, as compared to wild type CHO22 cells, by means of the APOPercentage™ assay following treatment with C_2-ceramide for 24 hrs. Values are the averages ± standard deviation from triplicate experiments. * Indicates significantly different from wild type for $p < 0.05$.

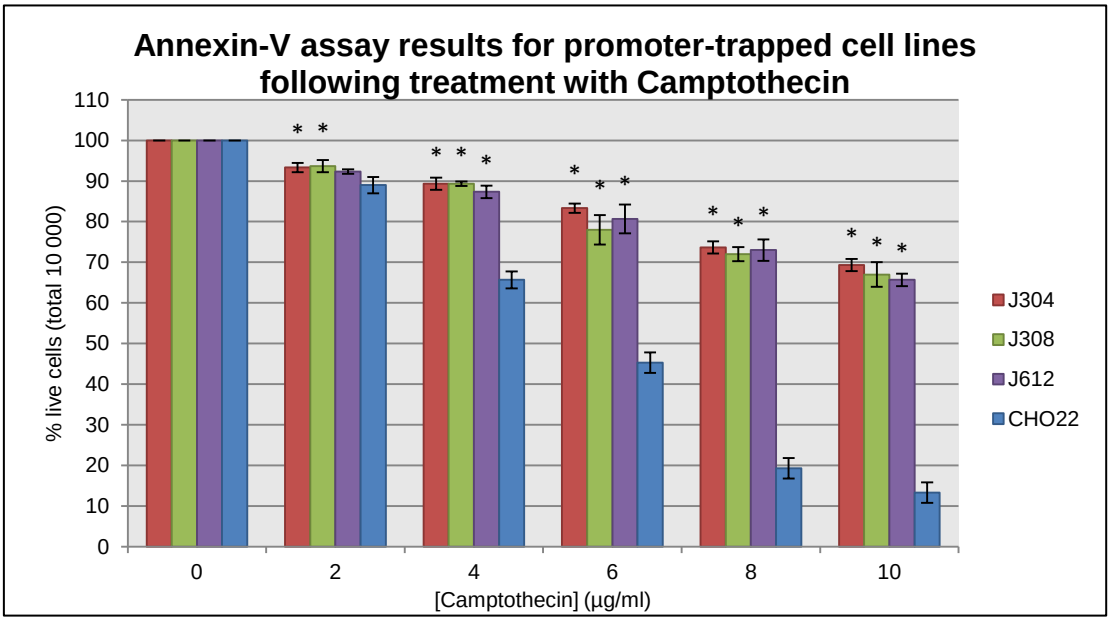

Figure 1.9: Results of testing for resistance to apoptosis in promoter-trapped cell lines, as compared to wild type CHO22 cells, by means of the Annexin-V assay following treatment with Camptothecin for 24 hrs. Values are the averages ± standard deviation from triplicate experiments. * Indicates significantly different from wild type for $p < 0.05$.

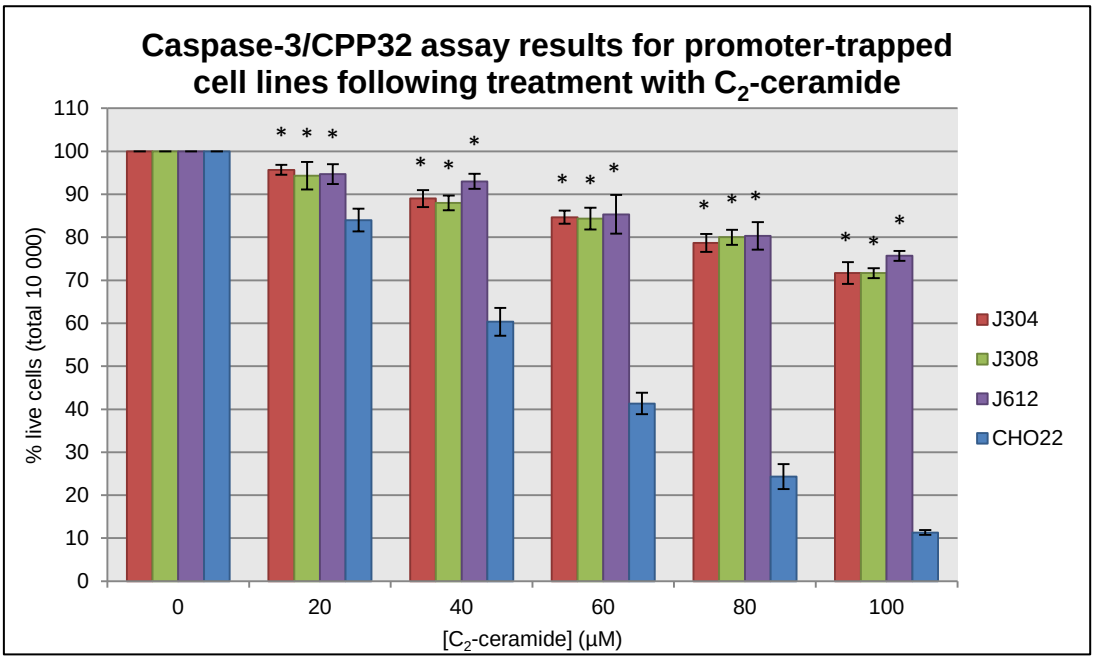

Figure 1.10: Results of testing for resistance to apoptosis in promoter-trapped cell lines, as compared to wild type CHO22 cells, by means of the Caspase-3/CPP32 assay following treatment with C_2-ceramide for 24 hrs. Values are the averages ± standard deviation from triplicate experiments. * Indicates significantly different from wild type for $p < 0.05$.

addition, results from the assays with C_2-ceramide as apoptotic inducer were also comparable to those of the assays with camptothecin treatment. The previously mentioned assays were specific for apoptosis. The success of the assays consequently excluded the presence of necrotic cell death since none of the assays is applicable to this form of cell death. However, it was necessary determine whether the recombinant cell lines delivered resistance to apoptosis *per se* or to CTL-mediated killing, which can lead to apoptosis (Groscurth and Filgueira, 1998). Thus, in order to exclude CTL killing as the method of cell death, a standard ^{51}Chromium (^{51}Cr) release CTL killing assay was performed in collaboration with Dr K. Gould at Imperial College London (UK). The assay measures the release of ^{51}Cr from ^{51}Cr-labelled target cells, in this case cells from each of the respective J-cell lines, upon lysis by CTL effector cells (Brunner et al., 1968; Wonderlich et al., 2001). The Y10 cell line, presenting an epitope recognised by the CTL on the major histocompatibility complex 1 (MHC1) receptor, was used as a reference for susceptibility to CTL killing, thus acting as a positive control. In contrast, the wild type CHO22 cells were used as a negative control since it lacks a recognisable epitope on the cell surface, making it resistant to CTL killing. All three J-cell lines followed the Y10 cell line across all effector: target ratios (1.25:1 – 10:1), indicating susceptibility to CTL killing (Fig. 1.11). In order to obtain the unknown hamster sequences surrounding the retrovirus integration site, a modified polymerase chain reaction PCR technique, namely inverse PCR, was performed. In this technique, established by Saiki and colleagues in 1985, unknown genomic areas flanking known sequences are amplified by allowing self-ligation of genomic DNA fragments following restriction enzyme digestion with a frequent cutter. The circular fragments are linearized by a specific restriction enzyme that cuts within the

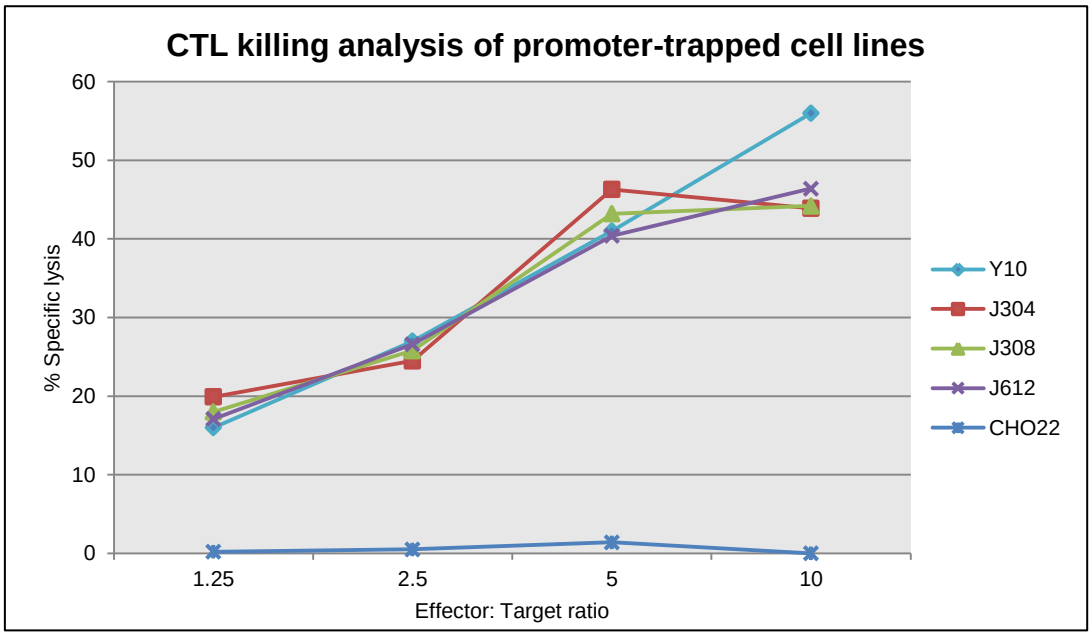

Figure 1.11: Line graph showing results from CTL killing assay performed with recombinant J-cell lines isolated from promoter-trap mutagenesis experiments, with % specific cell lysis referring to the amount (in percentage) of cells dying due to CTL killing at various effector: target ratios. (Effector – CTL; Target – cells from respective J-cell line).

known retrovirus sequence. PCR primers are designed to complement the known sequences and anneal at either ends of the linear fragment. Amplified products consist of two types of fragments; one of a specific size containing the known sequence and one of unknown size containing the unknown flanking sequences. The latter product can now be subjected to sequencing. A schematic representation of inverse PCR, as performed in the pilot study, is shown in figure 1.12. Products obtained from the inverse PCR technique were sequenced and the resulting sequences were aligned to the mouse genome using BLAST on the NCBI website. Three alignments to genes were made, one in each cell line. The particular genes were *Lipoic Acid Synthetase* (*LIAS*) in cell line J304 (Fig. 1.13), *Ribosomal Protein L9* (*RPL9*) in cell line J308 (Fig. 1.14) and *Cyclophilin A* (*CYPA*) in cell line J612 (Fig. 1.15). *RPL9* and *LIAS* are located on chromosome 4p13 and 4p14 respectively, while *CYPA* maps to chromosome 7p11.2-p13. These genes are discussed further in chapter two.

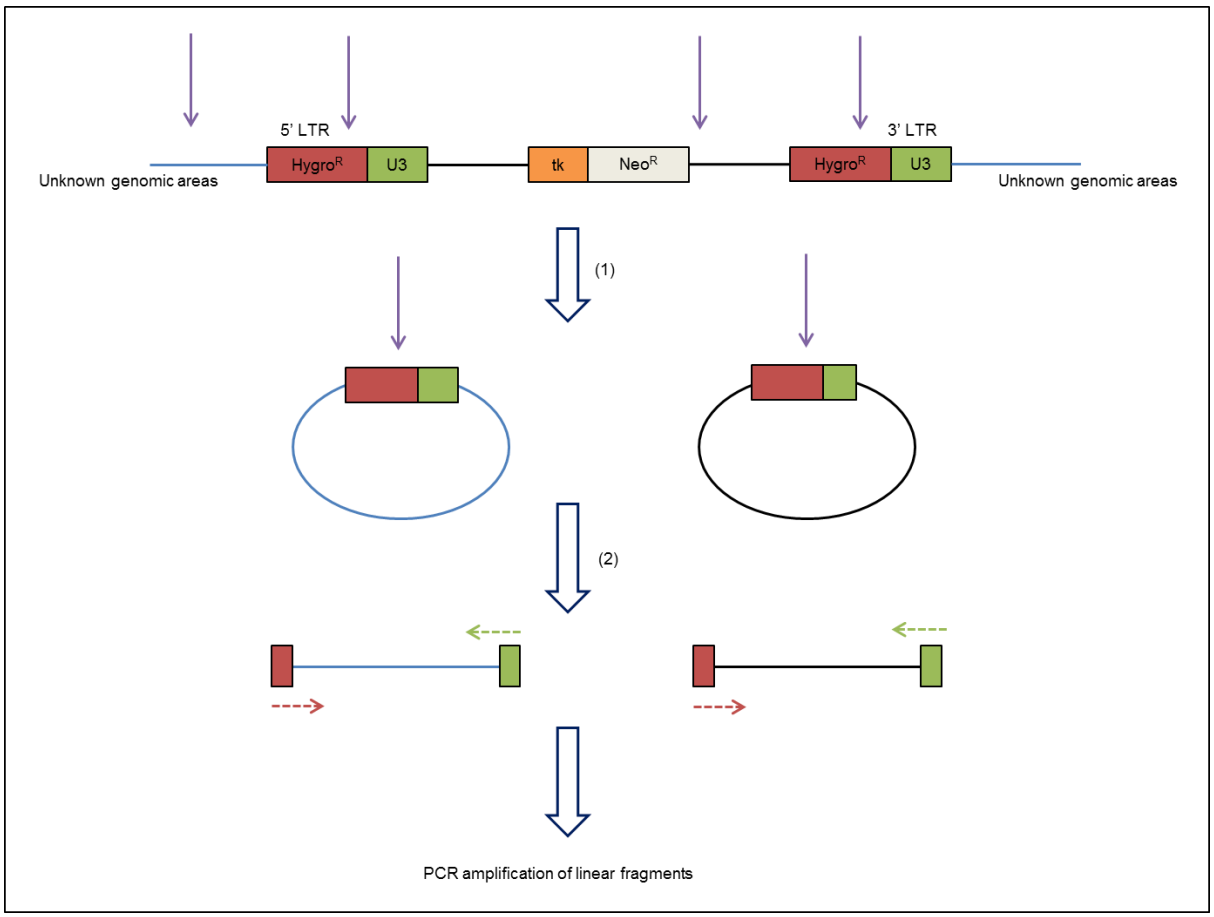

Figure 1.12: A simplified schematic representation of inverse PCR as performed in the pilot study. 1) Enzymatic digestion of genomic DNA with frequently cutting enzyme, followed by self-ligation to form circular fragments. 2) Linearization of circular fragments with a specific enzyme cutting within known sequences. (LTR – long terminal repeat; $Hygro^R$ – Hygromycin B resistance gene; U3 – promoter element; tk – thymidine kinase gene; Neo^R – Neomycin resistance gene).

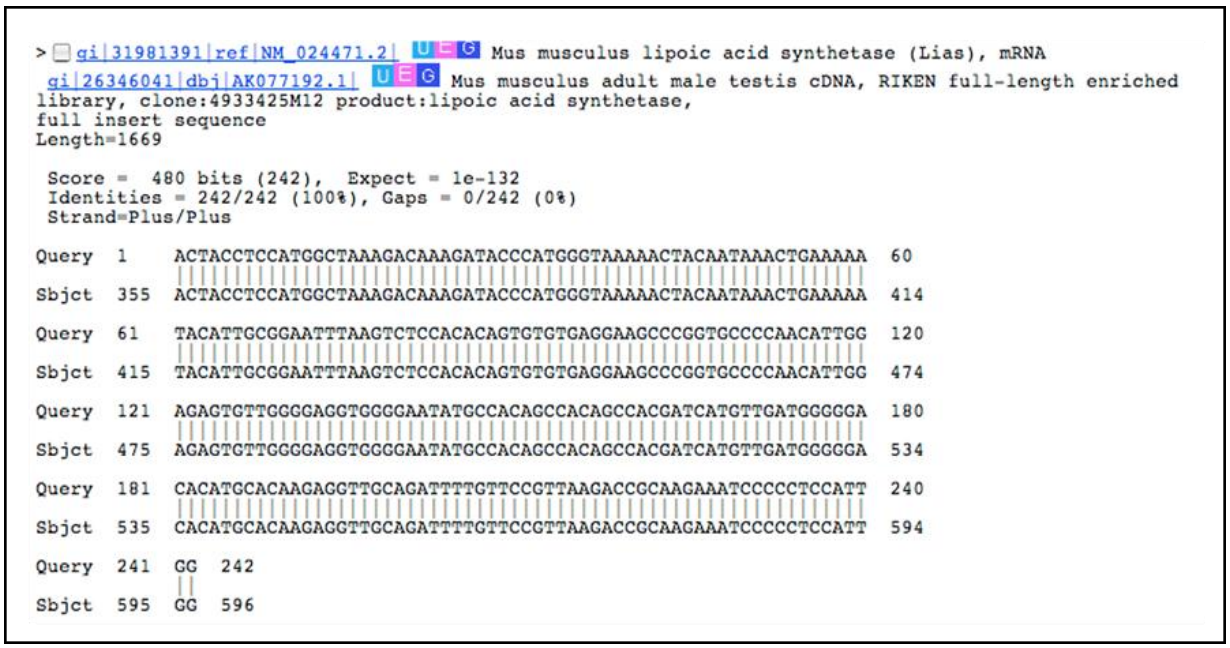

```
> gi|31981391|ref|NM_024471.2|  Mus musculus lipoic acid synthetase (Lias), mRNA
 gi|26346041|dbj|AK077192.1|  Mus musculus adult male testis cDNA, RIKEN full-length enriched
library, clone:4933425M12 product:lipoic acid synthetase,
full insert sequence
Length=1669

 Score =  480 bits (242),  Expect = 1e-132
 Identities = 242/242 (100%), Gaps = 0/242 (0%)
 Strand=Plus/Plus

Query  1    ACTACCTCCATGGCTAAAGACAAAGATACCCATGGGTAAAAACTACAATAAACTGAAAAA  60
            ||||||||||||||||||||||||||||||||||||||||||||||||||||||||||||
Sbjct  355  ACTACCTCCATGGCTAAAGACAAAGATACCCATGGGTAAAAACTACAATAAACTGAAAAA  414

Query  61   TACATTGCGGAATTTAAGTCTCCACACAGTGTGTGAGGAAGCCCGGTGCCCCAACATTGG  120
            ||||||||||||||||||||||||||||||||||||||||||||||||||||||||||||
Sbjct  415  TACATTGCGGAATTTAAGTCTCCACACAGTGTGTGAGGAAGCCCGGTGCCCCAACATTGG  474

Query  121  AGAGTGTTGGGGAGGTGGGGAATATGCCACAGCCACAGCCACGATCATGTTGATGGGGGA  180
            ||||||||||||||||||||||||||||||||||||||||||||||||||||||||||||
Sbjct  475  AGAGTGTTGGGGAGGTGGGGAATATGCCACAGCCACAGCCACGATCATGTTGATGGGGGA  534

Query  181  CACATGCACAAGAGGTTGCAGATTTTGTTCCGTTAAGACCGCAAGAAATCCCCCTCCATT  240
            ||||||||||||||||||||||||||||||||||||||||||||||||||||||||||||
Sbjct  535  CACATGCACAAGAGGTTGCAGATTTTGTTCCGTTAAGACCGCAAGAAATCCCCCTCCATT  594

Query  241  GG  242
            ||
Sbjct  595  GG  596
```

Figure 1.13: Results obtained from the BLAST search for the genomic sequence generated from CHO-J304 showing a significant match to the mouse *lipoic acid synthetase* (*LIAS*) gene.

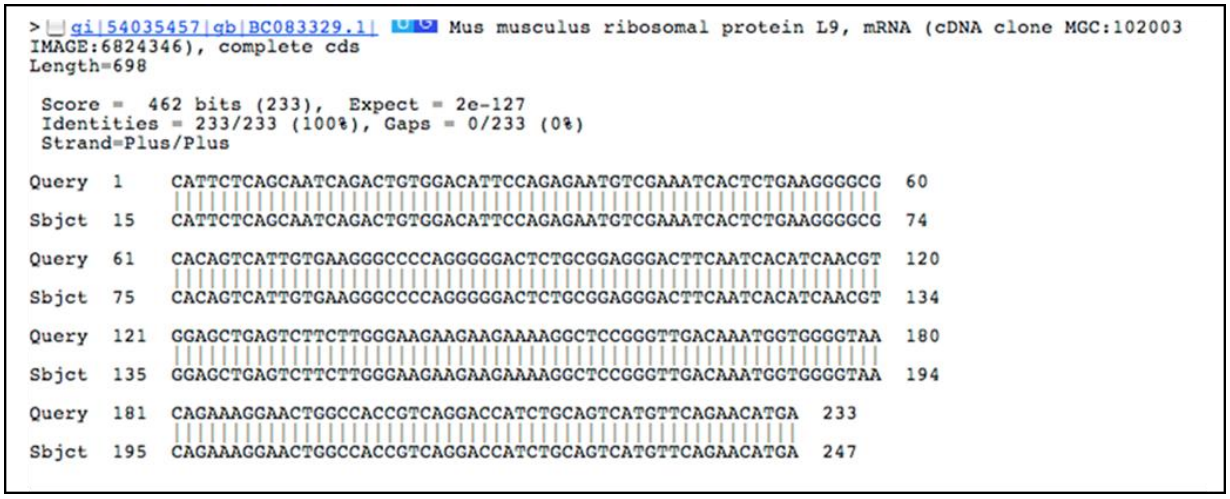

```
> gi|54035457|gb|BC083329.1|  Mus musculus ribosomal protein L9, mRNA (cDNA clone MGC:102003
IMAGE:6824346), complete cds
Length=698

 Score =  462 bits (233),  Expect = 2e-127
 Identities = 233/233 (100%), Gaps = 0/233 (0%)
 Strand=Plus/Plus

Query  1    CATTCTCAGCAATCAGACTGTGGACATTCCAGAGAATGTCGAAATCACTCTGAAGGGGCG  60
            ||||||||||||||||||||||||||||||||||||||||||||||||||||||||||||
Sbjct  15   CATTCTCAGCAATCAGACTGTGGACATTCCAGAGAATGTCGAAATCACTCTGAAGGGGCG  74

Query  61   CACAGTCATTGTGAAGGGCCCCAGGGGGACTCTGCGGAGGGACTTCAATCACATCAACGT  120
            ||||||||||||||||||||||||||||||||||||||||||||||||||||||||||||
Sbjct  75   CACAGTCATTGTGAAGGGCCCCAGGGGGACTCTGCGGAGGGACTTCAATCACATCAACGT  134

Query  121  GGAGCTGAGTCTTCTTGGGAAGAAGAAGAAAAGGCTCCGGGTTGACAAATGGTGGGGTAA  180
            ||||||||||||||||||||||||||||||||||||||||||||||||||||||||||||
Sbjct  135  GGAGCTGAGTCTTCTTGGGAAGAAGAAGAAAAGGCTCCGGGTTGACAAATGGTGGGGTAA  194

Query  181  CAGAAAGGAACTGGCCACCGTCAGGACCATCTGCAGTCATGTTCAGAACATGA  233
            |||||||||||||||||||||||||||||||||||||||||||||||||||||
Sbjct  195  CAGAAAGGAACTGGCCACCGTCAGGACCATCTGCAGTCATGTTCAGAACATGA  247
```

Figure 1.14: Results obtained from the BLAST search for the genomic sequence generated from CHO-J308 showing a significant match to the mouse *ribosomal protein L9* (*RPL9*) gene.

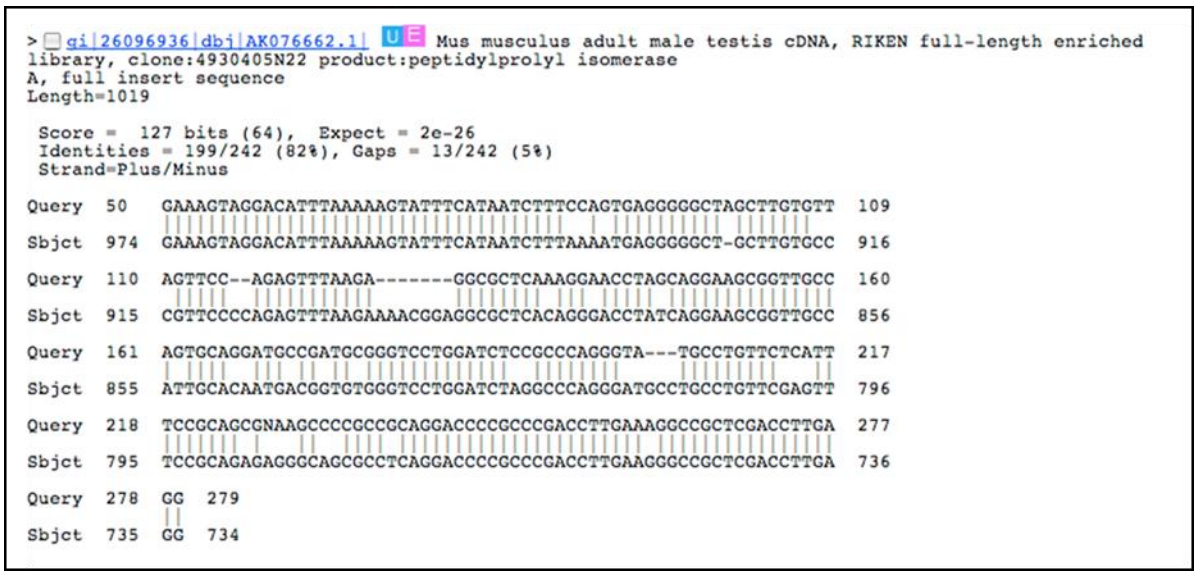

Figure 1.15: Results obtained from the BLAST search for the genomic sequence generated from CHO-J612 showing a significant match to the mouse *peptidylprolyl isomerase A* (*PPIA*) gene, also known as *cyclophilin A* (*CYPA*).

1.5 References

Amaral, J., Xavier, J., Steer, C., and Rodrigues, C. (2010). Targeting the p53 pathway of apoptosis. Curr. Pharm. Des. *16,* 2493-2503.

Ashkenazi, A., and Herbst, R. (2008). To kill a tumor cell: the potential of proapoptotic receptor agonists. J. Clin. Invest. *118,* 1979-1990.

Azmi, A.S., Wang, Z., Philip, P.A., Mohammad, R.M., and Sarkar, F.H. (2011). Emerging Bcl-2 inhibitors for the treatment of cancer. Expert Opin. Emerging Drugs *16,* 59-70.

Baehrecke, E. (2002). How death shapes life during development. Nat. Rev. Mol. Cell Biol. *3,* 779-787.

Barry, M., Heibein, J.A., Pinkoski, M.J., Lee, S., Moyer, R.W., Green, D.R., and Bleackley, R.C. (2000). Granzyme B short-circuits the need for caspase 8 activity during granule-mediated cytotoxic T-lymphocyte killing by directly cleaving Bid. Mol. Cell. Biol. *20,* 3781-3794.

Benedict, C., Norris, P., and Ware, C. (2002). To kill or be killed: viral evasion of apoptosis. Nat. Immunol. *3,* 1013-1018.

Brannon-Peppas, L., and Blanchette, J.O. (2012). Nanoparticle and targeted systems for cancer therapy. Adv. Drug Deliv. Rev. *64,* 206-212.

Bratosin, D., Estaquier, J., Ameisen, J.C., and Montreuil, J. (2002). Molecular and cellular mechanisms of erythrocyte programmed cell death: impact on blood transfusion. Vox Sang. *83,* 307-310.

Brigger, I., Dubernet, C., and Couvreur, P. (2012). Nanoparticles in cancer therapy and diagnosis. Adv. Drug Deliv. Rev. *64,* 24-36.

Brunner, K.T., Mauel, J., Ceronttini, J., and Chapuis, B. (1968). Quantitative assay of the lytic action of immune lymphoid cells on ^{51}Cr-labelled allogeneic target cells *in vitro*; inhibition by isoantibody and by drugs. Immunology *14,* 181-196.

Candé, C., Cecconi, F., Dessen, P., and Kroemer, G. (2002). Apoptosis-inducing factor (AIF): key to the conserved caspase-independent pathways of cell death? J. Cell Sci. *115,* 4727-4734.

Candé, C., Vahsen, N., Garrido, C., and Kroemer, G. (2004). Apoptosis-inducing factor (AIF): caspase-independent after all. Cell Death Differ. *11,* 591-595.

Cannon, W.B. (1929). Bodily changes in pain, hunger, fear and rage (Oxford, England: Appleton).

Charmandari, E., Tsigos, C., and Chrousos, G. (2005). Endocrinology of the stress response. Annu. Rev. Physiol. *67,* 259-284.

Chrousos, G.P. (1992). The concepts of stress and stress system disorders: overview of physical and behavioral homeostasis. J. Am. Med. Assoc. *267,* 1244-1252.

Coultas, L., and Strasser, A. (2003). The role of the Bcl-2 protein family in cancer. Semin. Cancer Biol. *13,* 115-123.

Debnath, J., Baehrecke, E.H., and Kroemer, G. (2005). Does autophagy contribute to cell death? Autophagy *1,* 66-74.

Degterev, A., Huang, Z., Boyce, M., Li, Y., Jagtap, P., Mizushima, N., Cuny, G., Mitchison, T., Moskowitz, M., and Yuan, J. (2005). Chemical inhibitor of nonapoptotic cell death with therapeutic potential for ischemic brain injury. Nat. Chem. Biol. *1,* 112-119.

Degterev, A., and Yuan, J. (2008). Expansion and evolution of cell death programmes. Nat. Rev. Mol. Cell Biol. *9,* 378-390.

Denecker, G., Vercammen, D., Declercq, W., and Vandenabeele, P. (2001). Apoptotic and necrotic cell death induced by death domain receptors. Cell. Mol. Life Sci. *58,* 356-370.

Devarajan, E., Sahin, A., Chen, J., Krishnamurthy, R., Aggarwal, N., Brun, A., Sapino, A., Zhang, F., Sharma, D., Yang, X., Tora, A., and Mehta, K. (2002). Down-regulation of caspase 3 in breast cancer: a possible mechanism for chemoresistance. Oncogene *21,* 8843-8851.

Eberhardt, O., and Schulz, J.B. (2003). Apoptotic mechanisms and antiapoptotic therapy in the MPTP model of Parkinson's disease. Toxicol. Lett. *139,* 135-151.

Eckert, A., Keil, U., Marques, C.A., Bonert, A., Frey, C., Schüssel, K., and Müller, W.E. (2003). Mitochondrial dysfunction, apoptotic cell death, and Alzheimer's disease. Biochem. Pharmacol. *66,* 1627-1634.

Edinger, A.L., and Thompson, C.B. (2004). Death by design: apoptosis, necrosis and autophagy. Curr. Opin. Cell Biol. *16,* 663-669.

Fadeel, B., and Orrenius, S. (2005). Apoptosis: a basic biological phenomenon with wide-ranging implications in human disease. J. Intern. Med. *258,* 479-517.

Fadok, V., Voelker, D., Campbell, P., Cohen, J., Bratton, D., and Henson, P. (1992). Exposure of phosphatidylserine on the surface of apoptotic lymphocytes triggers specific recognition and removal by macrophages. J. Immunol. *148,* 2207-2216.

Fulda, S., and Debatin, K. (2006). Extrinsic versus intrinsic apoptosis pathways in anticancer chemotherapy. Oncogene *25,* 4798-4811.

Fulda, S. (2010). Evasion of apoptosis as a cellular stress response in cancer. Int. J. Cell Biol. *2010,* 370835-1-370835-6.

Galluzzi, L., Maiuri, M., Vitale, I., Zischka, H., Castedo, M., Zitvogel, L., and Kroemer, G. (2007). Cell death modalities: classification and pathophysiological implications. Cell Death Differ. *14,* 1237-1243.

Ghavami, S., Hashemi, M., Ande, S.R., Yeganeh, B., Xiao, W., Eshraghi, M., Bus, C.J., Kadkhoda, K., Wiechec, E., Halayko, A.J., and Los, M. (2009). Apoptosis and cancer: mutations within caspase genes. J. Med. Genet. *46,* 497-510.

Giam, M., Huang, D., and Bouillet, P. (2008). BH3-only proteins and their roles in programmed cell death. Oncogene *27,* S128-S136.

Giansanti, V., Torriglia, A., and Scovassi, A.I. (2011). Conversation between apoptosis and autophagy: "Is it your turn or mine?". Apoptosis *16,* 321-333.

Golstein, P., and Kroemer, G. (2007). Cell death by necrosis: towards a molecular definition. Trends Biochem. Sci. *32,* 37-43.

Goping, I.S., Barry, M., Liston, P., Sawchuk, T., Constantinescu, G., Michalak, K.M., Shostak, I., Roberts, D.L., Hunter, A.M., Korneluk, R., *et al.* (2003). Granzyme B-induced apoptosis requires both direct caspase activation and relief of caspase inhibition. Immunity *18,* 355-365.

Green, D., and Kroemer, G. (1998). The central executioners of apoptosis: caspases or mitochondria? Trends Cell Biol. *8,* 267-271.

Green, D., and Evan, G. (2002). A matter of life and death. Cancer Cell *1,* 19-30.

Green, D., and Kroemer, G. (2004). The pathophysiology of mitochondrial cell death. Science *305,* 626-629.

Groscurth, P., and Filgueira, L. (1998). Killing mechanisms of cytotoxic T lymphocytes. News Physiol. Sci. *13,* 17-21.

Hangen, E., Kroemer, G., and Modjtahedi, N. (2009). Vital functions of apoptosis inducing factor (AIF). Gastroenterol. Hepatol. Bed Bench *2,* S66-S70.

Hay, B.A., Huh, J.R., and Guo, M. (2004). The genetics of cell death: approaches, insights and opportunities in Drosophila. Nat. Rev. Genet. *5,* 911-922.

Hengartner, M. (2000). The biochemistry of apoptosis. Nature *407,* 770-776.

Ho, P., and Hawkins, C.J. (2005). Mammalian initiator apoptotic caspases. FEBS J. *272,* 5436-5453.

Hotchkiss, R., Strasser, A., McDunn, J., and Swanson, P. (2009). Cell death. N. Engl. J. Med. *361,* 1570-1583.

Huang, S., and Sinicrope, F.A. (2008). BH3 mimetic ABT-737 potentiates TRAIL-mediated apoptotic signaling by unsequestering Bim and Bak in human pancreatic cancer cells. Cancer Res. *68,* 2944-2951.

Joza, N., Pospisilik, J.A., Hangen, E., Hanada, T., Modjtahedi, N., Penninger, J.M., and Kroemer, G. (2009). AIF: not just an apoptosis-inducing factor. Ann. N. Y. Acad. Sci. *1171,* 2-11.

Kam, P.C.A., and Ferch, N.I. (2000). Apoptosis: mechanisms and clinical implications. Anaesthesia *55,* 1081-1093.

Kerr, J.F.R. (1971). Shrinkage necrosis: a distinct mode of cellular death. J. Pathol. *105,* 13-20.

Kerr, J., Wyllie, A., and Currie, A. (1972). Apoptosis: a basic biological phenomenon with wide-ranging implications in tissue kinetics. Br. J. Cancer *26,* 239-257.

Kidd, V. (1998). Proteolytic activities that mediate apoptosis. Annu. Rev. Physiol. *60,* 533-573.

King, K., and Cidlowski, J. (1998). Cell cycle regulation and apoptosis. Annu. Rev. Physiol. *60,* 601-617.

Kolesnick, R.N., and Krönke, M. (1998). Regulation of ceramide production and apoptosis. Annu. Rev. Physiol. *60,* 643-665.

Kroemer, G., Dallaporta, B., and Resche-Rigon, M. (1998). The mitochondrial death/life regulator in apoptosis and necrosis. Annu. Rev. Physiol. *60,* 619-642.

Kroemer, G., El-Deiry, W., Golstein, P., Peter, M., Vaux, D., Vandenabeele, P., Zhivotovsky, B., Blagosklonny, M., Malorni, W., Knight, R.*, et al.* (2005). Classification of cell death: recommendations of the Nomenclature Committee on Cell Death. Cell Death Differ. *12,* 1463-1467.

Kroemer, G., Galluzzi, L., Vandenabeele, P., Abrams, J., Alnemri, E., Baehrecke, E., Blagosklonny, M., El-Deiry, W., Golstein, P., Green, D.*, et al.* (2009). Classification of cell death: recommendations of the Nomenclature Committee on Cell Death 2009. Cell Death Differ. *16,* 3-11.

Kültz, D. (2005). Molecular and evolutionary basis of the cellular stress response. Annu. Rev. Physiol. *67,* 225-257.

Lawen, A. (2003). Apoptosis - an introduction. Bioessays *25,* 888-896.

Lockshin, R.A., and Zakeri, Z. (2007). Cell death in health and disease. J. Cell. Mol. Med. *11,* 1214-1224.

Macartney-Coxson, D., Hood, K., Shi, H., Ward, T., Wiles, A., O'Connor, R., Hall, D., Lea, R., Royds, J., Stubbs, R., *et al.* (2008). Metastatic susceptibility locus, an 8p hot-spot for tumour progression disrupted in colorectal liver metastases: 13 candidate genes examined at the DNA, mRNA and protein level. BMC Cancer *8,* 187-198.

Majno, G., and Joris, I. (1995). Apoptosis, oncosis, and necrosis. an overview of cell death. Am. J. Pathol. *146,* 3-15.

Maté, M., Ortiz-Lombardía, M., Boitel, B., Haouz, A., Tello, D., Susin, S., Penninger, J., Kroemer, G., and Alzari, P. (2002). The crystal structure of the mouse apoptosis-inducing factor AIF. Nat. Struct. Biol. *9,* 442-446.

Melcher, A., Gough, M., Todryk, S., and Vile, R. (1999). Apoptosis or necrosis for tumor immunotherapy: what's in a name? J. Mol. Med. (Heidelberg, Ger.) *77,* 824-833.

Melino, G. (2001). The Sirens' song. Nature *412,* 23.

Mizushima, N., and Levine, B. (2010). Autophagy in mammalian development and differentiation. Nat. Cell Biol. *12,* 823-830.

Modjtahedi, N., Giordanetto, F., Madeo, F., and Kroemer, G. (2006). Apoptosis-inducing factor: vital and lethal. Trends Cell Biol. *16,* 264-272.

Moquin, D., and Chan, F.K. (2010). The molecular regulation of programmed necrotic cell injury. Trends Biochem. Sci. *35,* 434-441.

Müllauer, L., Gruber, P., Sebinger, D., Buch, J., Wohlfart, S., and Chott, A. (2001). Mutations in apoptosis genes: a pathogenetic factor for human disease. Mutat. Res. *488,* 211-231.

Norberg, E., Orrenius, S., and Zhivotovsky, B. (2010). Mitochondrial regulation of cell death: processing of apoptosis-inducing factor (AIF). Biochem. Biophys. Res. Commun. *396,* 95-100.

Nussbaumer, S., Bonnabry, P., Veuthey, J., and Fleury-Souverain, S. (2011). Analysis of anticancer drugs: a review. Talanta *85,* 2265-2289.

Ola, M., Nawaz, M., and Ahsan, H. (2011). Role of Bcl-2 family proteins and caspases in the regulation of apoptosis. Mol. Cell. Biochem. *351,* 41-58.

Olson, M., and Kornbluth, S. (2001). Mitochondria in apoptosis and human disease. Curr. Mol. Med. *1,* 91-122.

Olsson, M., and Zhivotovsky, B. (2011). Caspases and cancer. Cell Death Differ. *18,* 1441-1449.

Penaloza, C., Lin, L., Lockshin, R., and Zakeri, Z. (2006). Cell death in development: shaping the embryo. Histochem. Cell Biol. *126,* 149-158.

Pradelli, L., Bénéteau, M., and Ricci, J. (2010). Mitochondrial control of caspase-dependent and -independent cell death. Cell. Mol. Life Sci. *67,* 1589-1597.

Proskuryakov, S., Konoplyannikov, A., and Gabai, V. (2003). Necrosis: a specific form of programmed cell death? Exp. Cell Res. *283,* 1-16.

Puck, T.T., Cieciura, S.J., and Robinson, A. (1958). Genetics of somatic mammalian cells III: Long-term cultivation of euploid cells from human and animal subjects. J. Exp. Med. *108,* 945-956.

Rampino, N., Yamamoto, H., Ionov, Y., Li, Y., Sawai, H., Reed, J.C., and Perucho, M. (1997). Somatic frameshift mutations in the *Bax* gene in colon cancers of the microsatellite mutator phenotype. Science *275,* 967-969.

Reed, J. (2002). Apoptosis-based therapies. Nat. Rev. Drug Discov. *1,* 111-121.

Riedl, S., and Shi, Y. (2004). Molecular mechanisms of caspase regulation during apoptosis. Nat. Rev. Mol. Cell Biol. *5,* 897-907.

Saiki, R., Scharf, S., Faloona, F., Mullis, K., Horn, G., Erlich, H., and Arnheim, N. (1985). Enzymatic amplification of beta-globin genomic sequences and restriction site analysis for diagnosis of sickle cell anemia. Science *230,* 1350-1354.

Sayers, T. (2011). Targeting the extrinsic apoptosis signaling pathway for cancer therapy. Cancer Immunol. Immunother. *60,* 1173-1180.

Shanker, A., Brooks, A.D., Jacobsen, K.M., Wine, J.W., Wiltrout, R.H., Yagita, H., and Sayers, T.J. (2009). Antigen presented by tumors *in vivo* determines the nature of $CD8^+$ T-cell cytotoxicity. Cancer Res. *69,* 6615-6623.

Shimizu, S., Kanaseki, T., Mizushima, N., Mizuta, T., Arakawa-Kobayashi, S., Thompson, C., and Tsujimoto, Y. (2004). Role of Bcl-2 family proteins in a non-apoptotic programmed cell death dependent on autophagy genes. Nat. Cell Biol. *6,* 1221-1228.

Shin, M.S., Kim, H.S., Lee, S.H., Park, W.S., Kim, S.Y., Park, J.Y., Lee, J.H., Lee, S.K., Lee, S.N., Jung, S.S.*, et al.* (2001). Mutations of tumor necrosis factor-related apoptosis-inducing ligand receptor 1 (TRAIL-R1) and receptor 2 (TRAIL-R2) genes in metastatic breast cancers. Cancer Res. *61,* 4942-4946.

Siminovitch, L. (1976). On the nature of hereditable variation in cultured somatic cells. Cell *7,* 1-11.

Straus, S.E., Jaffe, E.S., Puck, J.M., Dale, J.K., Elkon, K.B., Rösen-Wolff, A., Peters, A.M.J., Sneller, M.C., Hallahan, C.W., Wang, J.*, et al.* (2001). The development of lymphomas in families with autoimmune lymphoproliferative syndrome with germline Fas mutations and defective lymphocyte apoptosis. Blood *98,* 194-200.

Susin, S., Lorenzo, H., Zamzami, N., Marzo, I., Snow, B., Brothers, G., Mangion, J., Jacotot, E., Costantini, P., Loeffler, M., *et al.* (1999). Molecular characterization of mitochondrial apoptosis-inducing factor. Nature *397,* 441-446.

Tait, S., and Green, D. (2008). Caspase-independent cell death: leaving the set without the final cut. Oncogene *27,* 6452-6461.

Takuma, K., Yan, S., Stern, D., and Yamada, K. (2005). Mitochondrial dysfunction, endoplasmic reticulum stress, and apoptosis in Alzheimer's disease. J. Pharmacol. Sci. *97,* 312-316.

Taylor, R., Cullen, S., and Martin, S. (2008). Apoptosis: controlled demolition at the cellular level. Nat. Rev. Mol. Cell Biol. *9,* 231-241.

Trapani, J., and Smyth, M. (2002). Functional significance of the perforin/granzyme cell death pathway. Nat. Rev. Immunol. *2,* 735-747.

Turk, B., and Stoka, V. (2007). Protease signalling in cell death: caspases versus cysteine cathepsins. FEBS Lett. *581,* 2761-2767.

Vernooy, S.Y., Copeland, J., Ghaboosi, N., Griffin, E.E., Yoo, S.J., and Hay, B.A. (2000). Cell death regulation in *Drosophila*: conservation of mechanism and unique insights. J. Cell Biol. *150,* F69-F76.

Vogelstein, B., and Kinzler, K. (2004). Cancer genes and the pathways they control. Nat. Med. *10,* 789-799.

Wang, Y., Kim, N., Haince, J., Kang, H., David, K., Andrabi, S., Poirier, G., Dawson, V., and Dawson, T. (2011). Poly(ADP-ribose) (PAR) binding to apoptosis-inducing factor is critical for PAR polymerase-1-dependent cell death (parthanatos). Sci. Signal. *4,* ra20.

Wells, W.A. (2005). Autophagy unveiled. J. Cell Biol. *168,* 676-677.

Wonderlich, J., Shearer, G., Livingstone, A., and Brooks, A. (2001). Induction and measurement of cytotoxic T lymphocyte activity. Curr. Protoc. Immunol. *72*, 3.11.1-3.11.23.

Ye, H., Cande, C., Stephanou, N., Jiang, S., Gurbuxani, S., Larochette, N., Daugas, E., Garrido, C., Kroemer, G., and Wu, H. (2002). DNA binding is required for the apoptogenic action of apoptosis inducing factor. Nat. Struct. Biol. *9,* 680-684.

Yip, K., and Reed, J. (2008). Bcl-2 family proteins and cancer. Oncogene *27,* 6398-6406.

Youle, R., and Strasser, A. (2008). The Bcl-2 protein family: opposing activities that mediate cell death. Nat. Rev. Mol. Cell Biol. *9,* 47-59.

Yu, S., Wang, Y., Frydenlund, D., Ottersen, O., Dawson, V., and Dawson, T. (2009). Outer mitochondrial membrane localization of apoptosis-inducing factor: mechanistic implications for release. ASN Neuro *1,* 275-281.

Yuan, J., Shaham, S., Ledoux, S., Ellis, H., and Horvitz, H. (1993). The *C. elegans* cell death gene *ced-3* encodes a protein similar to mammalian interleukin-1 beta-converting enzyme. Cell *75,* 641-652.

Chapter 2: Investigating the role of three novel candidate genes in apoptotic resistance

The practical methodology (excluding analysis of results) of this chapter was performed in collaboration with Dr Mervin Meyer at the University of Western Cape (UWC), Department of Biotechnology.

2.1 Introduction

During the pilot study three novel candidate genes were identified to potentially be involved in resistance to apoptosis induced by C_2-ceramide and camptothecin. This part of the current study aimed to verify their involvement in apoptosis by generating stable mouse knockdown cell lines for each of the respective genes, namely *LIAS*, *RPL9* and *CYPA*, and repeating the apoptosis assays performed in the pilot study. Stable knockdown cell lines were generated by taking advantage of the RNA interference (RNAi) process. This verification aims to build on the results obtained in the pilot study by making use of a diploid model compared to the haploid model used in the pilot study. In addition, a more specific method of gene expression knockdown will be used. A positive outcome would provide supporting evidence for either a direct or indirect role in the apoptotic pathway for the candidate genes.

2.1.1 RNA interference

RNAi is a process that occurs naturally in early developmental pathways and responses to viral infection in vertebrates, invertebrates and plants (Caplen et al., 2001; Elbashir et al., 2001; Sashital and Doudna, 2010). The process is mediated by short interfering RNAs (siRNAs) of about 21 nucleotides in length which is processed from double-stranded RNA (dsRNA) by the RNase III-like nuclease named Dicer (Elbashir et al., 2001; Hammond, 2000; Holen, 2005). These siRNAs associate with proteins from the Argonaute family to form the RNA-induced silencing complex (RISC). The sequence-specific siRNA is denatured and the guide strand is used by RISC to target the complementary mRNA in the host cell, while the passenger strand is degraded (Fig. 2.1) (Hammond, 2000; Sashital and Doudna, 2010; Shan, 2010). The process of RNAi became an important tool for functional gene studies upon the discovery that specific gene expression knockdown could be achieved through the successful introduction of 21 bp siRNAs into a cell (Elbashir et al., 2001; Shan, 2010). The delivery of siRNAs into a host cell can occur either directly by means of liposomes, electroporation, transfection or microinjection, or indirectly via a vector. In the latter methodology, the sense and antisense siRNA sequences can either be transcribed by

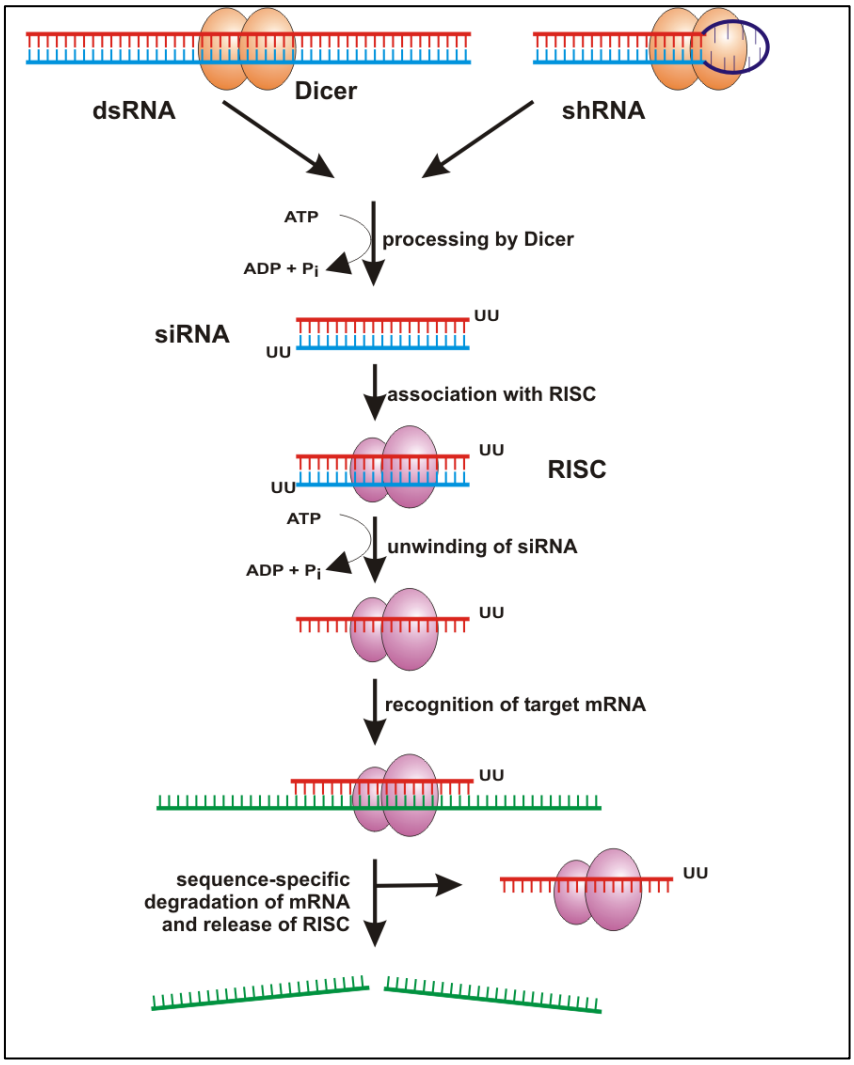

Figure 2.1: An illustration of RNAi process. Adapted from Rutz and Scheffold, 2004.

individual promoters or by a single promoter in the form of a short hairpin RNA (shRNA, Fig. 2.2) which is then subsequently processed by the native Dicer enzyme (Shan, 2010; Tuschl, 2002). Vector-mediated siRNA delivery holds the advantage of eliminating the danger of RNAse contamination compared to the direct delivery of synthetically synthesised siRNAs. However, the process of generating siRNA expression vectors, along with the transfection, might prove to be more time consuming and laborious (Tuschl, 2002). The current study employed the vector-mediated strategy in conjunction with the use of a shRNA construct, subsequently processed into the target specific siRNAs. Another advantage of the vector-mediated strategy is the production of a more stable and sustainable gene expression knockdown effect which, in addition, also allows for the generation of stable knockdown cell lines (Berns et al., 2004; Fraser, 2004; Hannon, 2002; Shan, 2010; Tuschl, 2002).

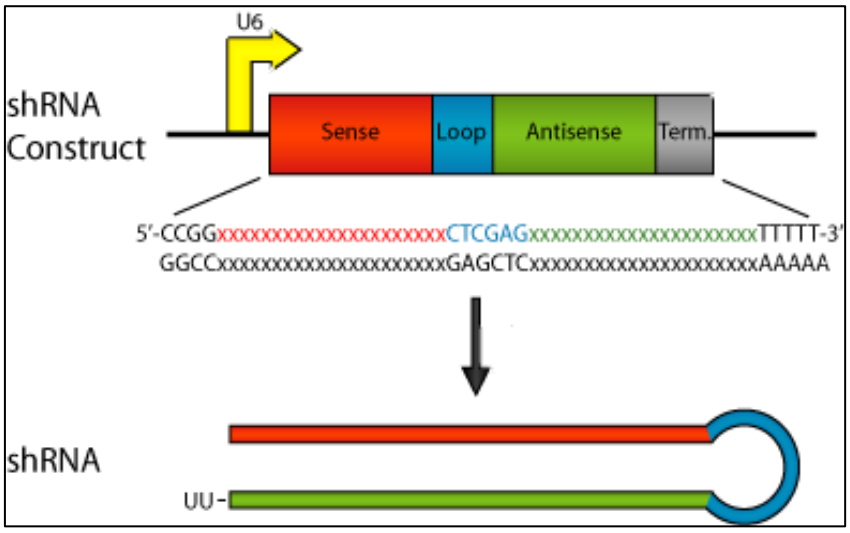

Figure 2.2: Typical example of a shRNA construct. U6 – a type of promoter; Term. – Termination signal. Obtained from http://www.addgene.org/tools/protocols/plko/.

2.1.2 Apoptosis Assays

In an editorial to Science journal in 1998, Pierre Golstein noted the publication of 20 000 articles on the topic of cell death within a time span of five years (Golstein, 1998). Recently, a literature search for 'apoptosis' in the title or abstract fields in the NCBI PubMed database produced 189 391 publications, with 76.34% of these published in the last decade (as on 19/07/12). Increased research and continued progress in this field have urged the improvement of traditional apoptosis detection methods as well as the development of new techniques. Currently, several apoptosis assays are available and many of these can be purchased commercially in the form of kits. Among the most popular are terminal deoxynucleotidyl transferase-mediated dUTP nick end labelling (TUNEL) assays, Annexin V binding assays, the APOPercentage™ assay and caspase 3 activity assays, of which the latter two are employed in this study. Apoptosis assays are designed around its unique characteristics, which includes the morphological and biochemical features.

The APOPercentage™ apoptosis assay (Biocolor LTD, UK) exploits the structural plasma membrane changes of apoptotic cells to detect and quantify apoptosis. In physiologically normal cells, PS molecules are located on the inside of the cell, on the inner plasma membrane. However, upon apoptotic stimuli, these molecules are translocated to the outside of the cell by what has been described as a "flip-flop" mechanism (Fadok et al., 1992). The APOPercentage™ assay utilizes this mechanism to import a purple-red dye into the dying cell. Traditionally, apoptotic cells were visualised by bright-field microscopy and quantified by spectrophotometric measurement, proving the technique to be quite laborious (Meyer et al., 2008). However, the assay has recently been modified to allow for the use of flow cytometry. In addition, the modification also rendered the assay more cost-effective, allowed for apoptosis detection of cells in suspension and also rendered the technique amendable to high-throughput analysis (Meyer et al., 2008).

Activation of the caspase cascade during apoptosis culminates in the activation of caspase 3 (Watanabe et al., 2002). This executioner caspase recognises its cellular substrates through the peptide sequence DEVD (aspartic acid – glutamic acid – valine – aspartic acid); proteolytic cleavage occurs after the second aspartic acid residue (Wang et al., 2005a). Apoptotic caspase activity assays involve the detection of active caspase 3 by utilising synthetic substrates. These substrates contain the DEVD-peptide sequence and traditionally contained fluorogenic tags based on coumarin dye (Wang et al., 2005a). Improvement of this technique includes the use of rhodamin-labelled substrates which has longer excitation and emission wavelengths (Wang et al., 2005a). The technique can also be performed as a colourimetric assay (Gurtu et al., 1997).

The TUNEL assay is designed to detect DNA fragmentation by modifying the 3' end of fragments with labelled nucleotides through transferase activity (Gavrieli et al., 1992; Watanabe et al., 2002). This allows for the visualisation of accumulated DNA fragments by either fluorescent microscopy or a colourimetric assay (Watanabe et al., 2002). The Annexin V assay is based on the Ca^{2+}-dependent binding of the annexin V protein to externalised PS residues (Vermes et al., 1995). The protein is also labelled to allow for the detection of cells with fluorescent microscopy (Watanabe et al., 2002). As PS externalisation also occurs in necrosis, the assay is used in conjunction with a dye exclusion test to determine the integrity of the plasma membrane; if the dye is excluded, the cell is undergoing apoptosis, as opposed to necrosis where permeabilisation of the plasma membrane is an early event (Vermes et al., 1995). Other methods of apoptosis detection include the visualisation of morphological characteristics by means of standard transmission electron microscopy (TEM) and various mitochondrial assays, for example the detection of cytochrome c release (Watanabe et al., 2002).

As with any molecular technique, certain advantages and limitations have been described for each of the apoptosis assays (Watanabe et al., 2002). Although TEM permits definitive identification of apoptotic cells, it's quite time consuming and only small regions of tissues can be assayed at a time. TUNEL assays can be performed on a variety of tissues but fails to distinguish between apoptosis and necrosis. The APOPercentage™ assay circumvents the problem associated with the Annexin V assay; since the former assay entails the uptake of a dye there is no need to determine plasma membrane integrity with a dye exclusion test as with the latter assay. A requirement for caspase 3 activity assays is homogenisation of the tissue; hence the specific apoptotic cell can't be identified. Even though limitations exist, many of these assays are well accepted and widely used in apoptosis research. It is however recommended that a combination of two assays, based on different principles, be used in a study to detect and confirm the presence of apoptosis (Watanabe et al., 2002).

2.1.3 Apoptotic Inducers

A plethora of apoptotic inducers is available today for research purposes and many of these have also been utilised in anticancer therapies. Inducers of apoptosis can take many different forms and can either be natural compounds or synthetically produced. Natural compounds capable of inducing apoptosis include dietary flavonoids (for example from grapes), extracts from various medicinal plants or trees, plant polyphenols and phenolic compounds (for example curcumin), lectins, terpenoids and isoprenoids (Chen et al., 2005; Taraphdar et al., 2001; Zhang et al., 2004). Various organic copper compounds have also been shown to induce apoptosis in human cancer cells (Daniel et al., 2004). Popular examples of synthetic apoptotic inducers are cytotoxic drugs and their derived analogues. These include doxorubicin, etoposide, cytarabine, methotrexate, cysplatin and taxol (Friesen et al., 1999; Taraphdar et al., 2001).

For the purposes of this study, two synthetic compounds were selected to serve as apoptotic inducers for each of the apoptosis assays performed, namely C_2-ceramide and camptothecin. Ceramide is bioactive sphingolipid that forms part of the sphingomyelin pathway, an evolutionary conserved pathway from yeast to humans (Andrieu-Abadie and Levade, 2002; Hannun and Obeid, 2008). Naturally produced ceramide species differ in the length of their fatty acid moiety, which ranges from C_{14} to C_{26}, however synthetic short chain analogues, such as C_2- or C_6-ceramide, has been produced and are frequently used in studies by means of exogenous administration (Huang et al., 2011a; Novgorodov et al., 2011). Apoptotic induction by ceramide is mediated by a variety of downstream targets; ceramide-induced activation of protein phosphatase 2A (PP2A) is capable of activating the pro-apoptotic Bax protein and inducing cytochrome c release while ceramide-induced activation of cathepsin D results in the truncation and activation of Bid, which is subsequently followed by cytochrome C release and caspase 9 and 3 activation (Heinrich et al., 2004; Xin and Deng, 2006). Other mediators of ceramide's pro-apoptotic effect include protein kinase Cζ and the c-JUN N-terminal kinase (JNK) pathway (Mathias et al., 1998; Wang et al., 2005b). Camptothecin is an alkaloid originally isolated from the *Camptotheca acuminate* tree indigenous to China (Hsiang et al., 1985). It displays potent antitumour activities and possesses several features that make it pharmacologically unique (Hsiang et al., 1985; Pommier, 2006). The sole target of camptothecin is topoisomerase I, an essential enzyme responsible for unwinding supercoiled DNA generated by replication, transcription and chromatin remodelling (Hsiang et al., 1985; Pommier, 2006). Inhibition of topoisomerase I by camptothecin results in significant DNA damage and subsequent apoptosis.

2.2 Materials and methods

2.2.1 Generation of stable knockdown cell lines for *LIAS*, *RPL9* and *CYPA*

2.2.1.1 Cell culture

NIH-3T3 cells were used during this study. This fibroblast cell line originates from a NIH Swiss mouse embryo and was first established by George Todaro and Howard Green in 1962 (Todaro and Green, 1963). Characteristics of the cell line include inhibition by temazepam and other benzodiazepines and sensitivity to leukaemia and sarcoma virus propagation. NIH-3T3 cells were obtained from Dr A. Madiehe at the Medical Research Council, South Africa. During the study the cells were cultured in Dulbecco's Modified Eagle Medium (DMEM) supplemented with 10% fetal calf serum (FCS) and maintained in an incubator at 37°C and 5% CO_2. Cells were cultured until a confluency of 70% were reached, upon which passaging were performed using sterile phosphate buffer saline (PBS, pH 7.0) and 0.125% trypsin solution pre-equilibrated to 37°C. All reagents, unless otherwise specified, were supplied by Gibco® (Life Technologies™).

2.2.1.2 Short hairpin-RNA (shRNA) design

Two shRNA constructs were designed for each of the novel candidate genes, namely *LIAS*, *RPL9* and *CYPA*. This was done by making use of iRNAi (v. 1.0, nucleobytes.com), a standalone software package designed to identify suitable shRNA constructs in your template sequence according to specified parameters. Selected parameters for shRNA design included a target size of 19 nucleotides, start and end points of AA and TT respectively as well as default sequences for the hairpin loop structures. Restriction enzyme cut sites for *Bgl* II (5' end) and *Hind* III (3' end) were incorporated in order to facilitate cloning of the constructs into vectors; however, the 5' end was designed in such a way that the *Bgl* II site would become non-functional upon ligation of the shRNA into the vector. In addition, scramble controls, mutated shRNA constructs that are non-specific, were also designed in order to serve as negative controls. Figure 2.3 contains an example of a complete shRNA while table 2.1 contains the sense target sequences for each of the novel candidate genes. The shRNA constructs were synthesised by Inqaba Biotech™.

2.2.1.3 Construction of expression vectors

Several techniques common to cloning experiments were performed during the preparation and construction of the expression vectors. This includes restriction enzyme digests, ligation reactions, colony PCRs and plasmid isolations. Below follows a short description of each of these techniques.

The restriction enzymes used in this section were purchased from Fermentas™ (Thermo Fisher Scientific) (*Hind* III and *Ase* I) and New England Biolabs Inc. (*Bgl* II and *BamH* I) and all digest reactions were performed according to the manufacturer's specifications. For the most part, the digest reactions were performed with 1 µg of vector DNA and 5 U of the restriction enzyme.

Figure 2.3: Representative example of the shRNA constructs designed with iRNAi. The sense target sequence for *LIAS* KD1 is represented. Colours represent the different parts of the shRNA construct: red – vector sequence forming part of restriction enzyme cut site, with *Bgl* II (non-functional) at the 5' end and *Hind* III at the 3' end on the sense strand; orange – shRNA sequence forming part of the respective restriction enzyme cut sites; black – spacer sequences and termination sequence (3' end of top strand); blue – target sequence complementary to the respective genes (in this example *LIAS* KD1); green – hairpin loop sequence.

Table 2.1: Target sequences of the shRNA constructs designed for each of the three novel candidate genes

shRNA	Sense target sequence
LIAS KD1	5' – TTGCAGAGTGGGGTCTGGA – 3'
LIAS KD2	5' – TGTGGAGACTGTCCCCGAG – 3'
RPL9 KD1	5' – ACACCGGCCCAAAGACAAC – 3'
RPL9 KD2	5' – TTACATCTGCTCTTAGAGC – 3'
CYPA KD1	5' – GTCCATCTATGGGGAGAAA – 3'
CYPA KD2	5' – GCATACGGGTCCTGGCATC – 3'

KD – knock down.

Following incubation for 2 hrs at the required temperature, a final inactivation step was performed by means of incubation for 20 min at 65°C. Digested vectors were used as is if the digestion produced non-compatible ends; however, if this was not the case, the vectors were treated with shrimp alkaline phosphatase (SAP, Roche Applied Sciences) in order to remove 5' phosphate groups, preventing self-ligation.

Ligation reactions were generally performed during the cloning of fragments into the respective vectors. These reactions, incubated overnight, were performed in a total volume 20 µl and contained 1.0 Weiss unit of T4 ligase, purchased from Fermentas™ (Thermo Fisher Scientific).

In order to perform the colony PCRs, competent *Escherichia coli* cells had to be transformed with the vectors. The *E. coli* MC1061 strain (Casadaban and Cohen, 1980) was used for this purpose and was prepared for competency by incubating the strain overnight at 37°C streaked out on a Luria Broth (LB) medium plate containing 10 mM $MgSO_4$. A single colony was then grown up by means of incubation at 37°C, with shaking, in 20 ml TYM broth (tryptone, yeast extract, NaCl and $MgCl_2$) until a desired optical density of 0.2 (measured at 550 nm) was reached. The incubation step was then repeated after transferring the cells to 100 ml TYM broth. A volume of 400 ml fresh TYM broth was then added and the cells were further incubated under the same conditions until an optical density between 0.4 and 0.6 was reached. Ice cold water was used to rapidly cool down the cells, which were then collected by centrifugation for 10 min at 3000 *g* in a 4°C room. 250 ml

ice cold transfection buffer 1 (potassium acetate, $MnCl_2$, KCl, $CaCl_2$ and glycerol) were added to the cells for resuspension, which was then incubated for 30 min at 0°C. Cells were then pelleted by centrifugation for 8 min at 6000 *g* and resuspended in 50 ml ice cold transfection buffer 2 (MOPS, $CaCl_2$, KCl and glycerol). For storage purposes, cell were frozen as 300 µl fractions in liquid nitrogen and stored at -80°C.

Bacterial transformations was performed by adding 100 µl of the competent cells, thawed on ice, to 10 µl of the vector DNA solution, gently mixing the solution and incubating it on ice for 30 min. Cells were heat-shocked by means incubation for 45 s at 42°C where after 500 µl of pre-warmed LB medium was added to the cells. To allow for the expression of the antibiotic resistance markers, the solution was first incubated for one hour at 37°C before plating out the cells on nutrient rich agar plates supplemented with 50 µg/ml kanamycin sulphate (Sigma-Aldrich®).

Recombinant cells were used as template for colony PCR reactions aimed at verifying the successful modification of the vector. The template solution was prepared by suspending a single recombinant colony, grown on agar plates, in 20 µl of sterile deionised water. A PCR reaction containing 1 µl of the template solution and 10 pmol/µl specific primers (table 2.2) was incubated for 35 cycles comprising of a denaturation (45 s at 95°C), annealing (45 s at a primer-specific annealing temperature (T_A)) and extension step (45 s at 72°C), followed by a final extension step (10 min at 72°C). Primers were synthesised by Inqaba Biotech™. PCR products were separated on a 1% agarose gel and sizes were determined by means of comparison with a pTZ molecular marker (pTZ18R vector digested with the restriction enzyme *Hinf* I).

A plasmid isolation protocol was followed in order to retrieve the modified vector construct following a successful colony PCR. For this isolation, an inoculum containing a single positive colony in 5 ml LB medium supplemented with 50 µg/ml kanamycin sulphate (Sigma-Aldrich®) was prepared and incubated overnight at 37°C with shaking. Following incubation, cells were obtained by centrifuging 1 ml of the culture for 5 min at 5000 *g*. 200 µl ice cold GTE buffer (glucose-tris-ethylenediaminetetraacetic acid) was added to the pellet for resuspension, which was then allowed to incubate for 5 min at room temperature. Next, 1 % sodium dodecyl sulphate (w/v) solution and 400 µl 0.2 M NaOH were added and after gentle mixing through inversion, the solution was incubated for 5 min on ice. This was followed by another 5 min incubation step on ice upon the addition of 300 µl ice cold potassium acetate (5 M, pH 5.5). A 10 min centrifugation step at 14 000 *g* was performed to remove all the cell debris while the supernatant containing the vector DNA was transferred to a new eppendorf tube to which 0.6 volumes of isopropanol had already been added. The vector DNA was precipitated by incubation for 30 min at -20°C and pelleted by centrifugation for 15 min at 14 000 *g*. A wash step was performed with 500 µl 70% ethanol, after which the pellet was dried and resuspended in 50 µl 1 x TE buffer (tris and ethylenediaminetetraacetic acid).

Table 2.2: Details of primers used for colony PCRs performed during vector construction

Primer name	Primer orientation	Sequence (5'-3')	Length (bp)	T_A (°C)
1-F	F	CTGGCCGTCGTTTTAC	16	58
1-R	R	CAGGAAACAGCTATGA	16	
2-F	F	ACTACTACGTGGACTCCAAGC	21	60
2a-R	R	TAGGTGGCATCGCCCTCG	18	
2b-R	R	TCGTAGGGGCGGCCCTC	17	
3-F	F	ACTACTACGTGGACTCCAAGC	21	60
3-R	F	ATTATGATCAGTTATCTAGATCC	23	

See text in section 2.3.1.1 for PCR product sizes. F – forward; R – reverse; bp – base pair; T_A – annealing temperature.

Two mammalian expression vectors were used in this study, namely pEGFP-C1 and pDsRed-Express-C1 (Fig. 2.4), and were purchased from Clontech. The pEGFP-C1 vector has been optimised for higher expression and brighter fluorescence in mammalian cells while the translation efficiency in eukaryotic cells was improved by converting the sequences flanking EGFP to a Kozak consensus translation initiation site. Selection of transfected eukaryotic cells with the G418 (neomycin sulphate) antibiotic is made possible by the presence of a resistance cassette consisting of the neomycin/kanamycin resistance gene, *Tn5*, and polyadenylation signals from the Herpes simplex virus *thymidine kinase* (HSV-*TK*) gene, driven by a SV40 early promoter. Cells transfected with this vector can also be easily identified by the fluorescent signal emitted by the expressed green fluorescent protein (GFP) using fluorescent microscopy. The pDsRed-Express-C1 expresses a variant of the *Discosoma sp.* red fluorescent protein which contains nine amino acid substitutions aimed at improving the solubility of the protein as well as detection time. As with the pEGFP-C1 vector, this vector contains a Kozak consensus translation initiation site and the resistance cassette. The presence of this vector can also be detected in cells by fluorescent microscopy since it expresses red fluorescent protein (RFP). The pEGFP-C1 and pDsRed-Express-C1 vectors are hereafter referred to as GFP and RFP vectors, respectively.

Since the multiple cloning site (MCS) in both of the vectors were not going to be used for the cloning of the shRNA constructs, the *Bgl* II and *Hind* III restriction enzyme cut sites in this region were removed to prevent inappropriate restriction enzyme digestions (see below). This was done by digesting the vectors with *Bgl* II and *BamH* I (Fig. 2.5). Since *Bgl* II and *BamH* I ends are compatible, re-circulisation of the vectors were allowed which would leave only a *BamH* I restriction site functional. Deletion of the *Bgl* II and *Hind* III restriction sites in the MCS were verified by means of colony PCR performed with the 1-F and 1-R primer pair (table 2.2).

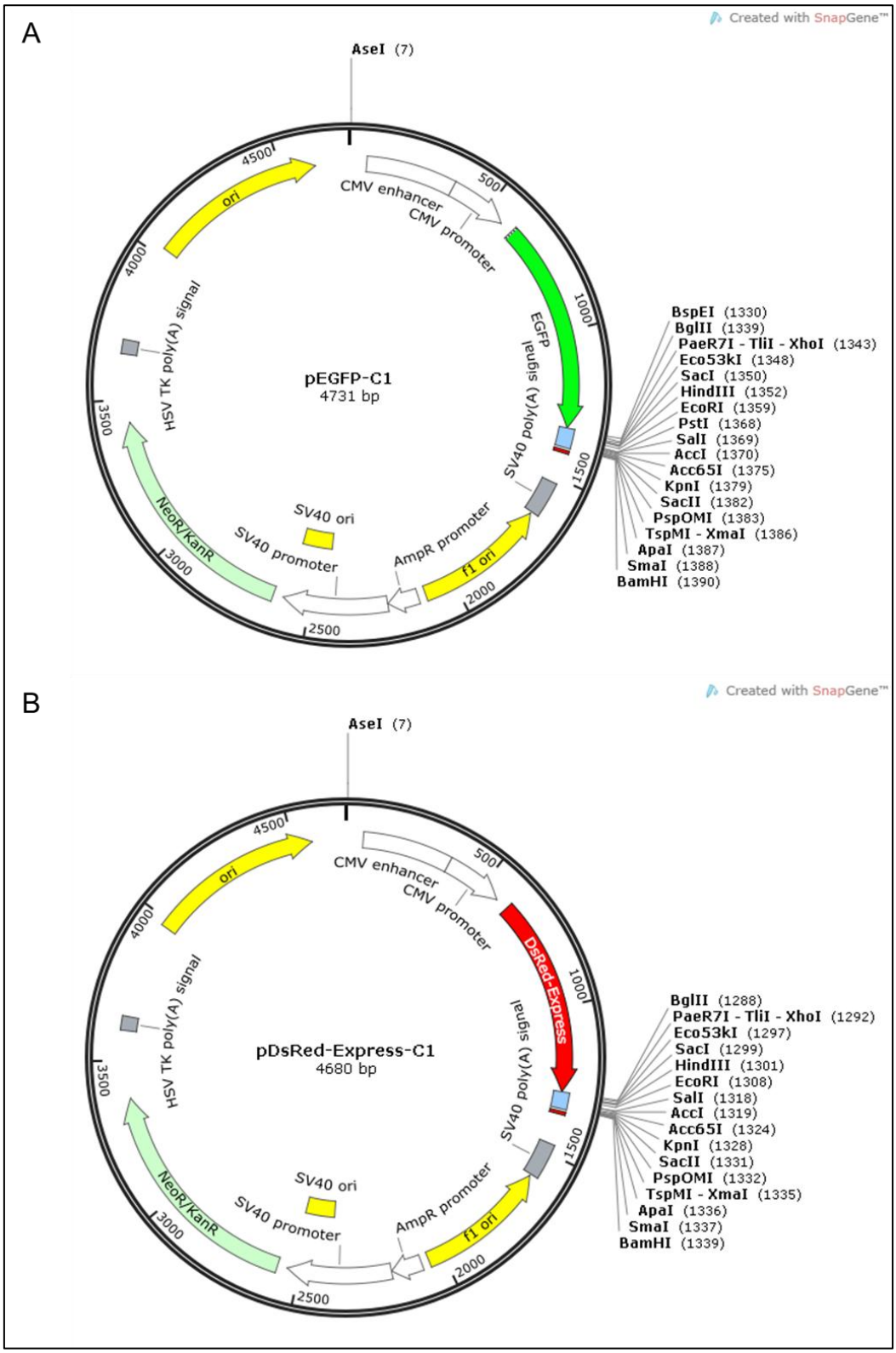

Figure 2.4: Vector maps of the pEGFP-C1 (A) and pDsRed-Express-C1 (B) vectors. The images show the *Ase* I restriction enzyme cut site used for the cloning of the U6 promoter as well as the MCS. These images were created with the freely available SnapGene™ Viewer software version 1.3.3 (GSL Biotech LLC) in conjunction with the sequence and map files of the vectors, as created by SnapGene (www.snapgene.com/resources).

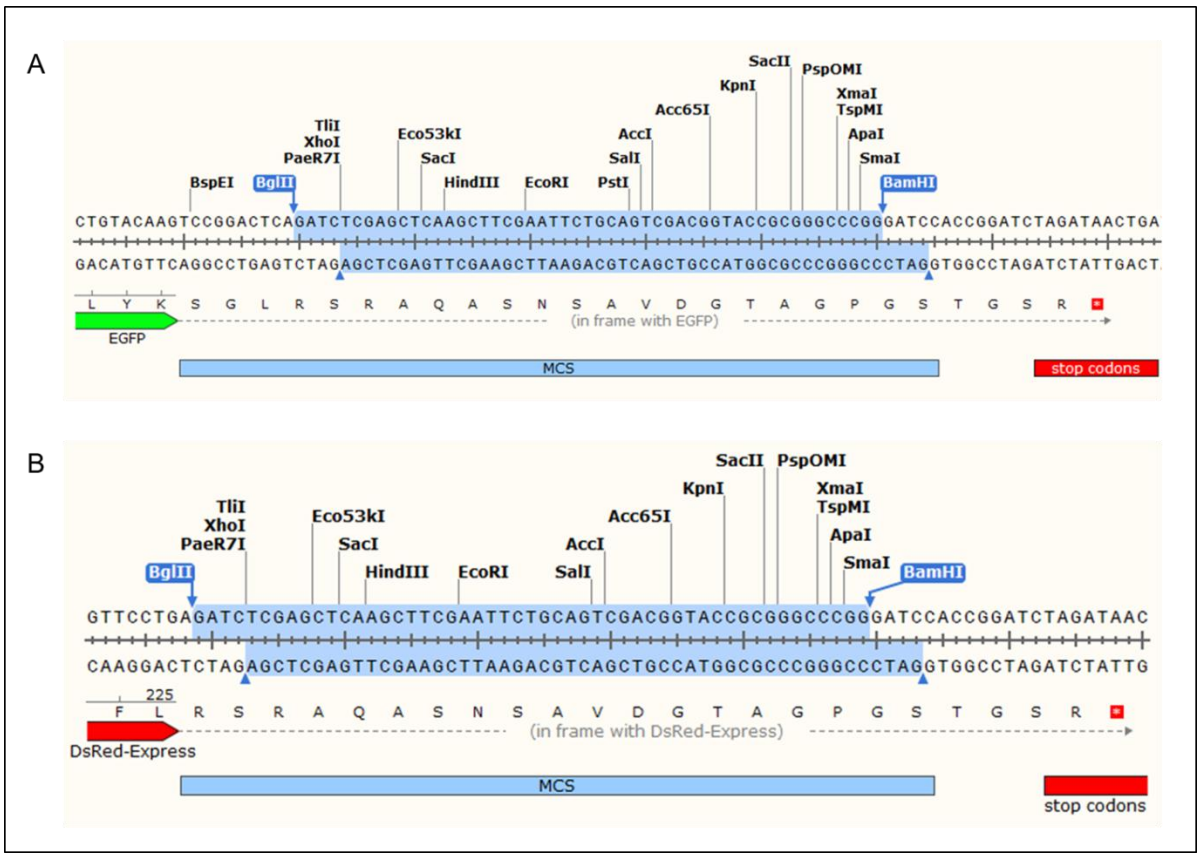

Figure 2.5: Sequences of the MCS regions of the pEGFP-C1 (A) and pDsRed-Express-C1 (B) vectors. The region removed by means of digestion with *Bgl* II and *BamH* I is highlighted. These images were created with the freely available SnapGene™ Viewer software version 1.3.3 (GSL Biotech LLC) in conjunction with the sequence and map files of the vectors, as created by SnapGene (www.snapgene.com/resources).

Both vectors were further modified by inserting a human U6 promoter sequence upstream of the fluorescent markers. A fragment containing the U6 promoter sequence was cloned into both vectors after digestion with *Ase* I. The fragment was generated by PCR amplification of the human U6 promoter region and was designed to contain recognition sites for *Bgl* II and *Hind* III downstream of the promoter sequence, which would allow for the cloning of the shRNA constructs into this site. Colony PCR, with primers 2-F and either 2a-R (GFP vector) or 2b-R (RFP vector) (table 2.2), was performed to verify the presence of the fragment in the vectors.

To allow for the cloning of the shRNA's constructs, 1 µg of both vectors were first digested overnight with 1 U *Hind* III, since this enzyme requires a larger overhang to digest properly, followed by digestion with 1 U *Bgl* II to remove the section between these two enzyme recognition sites. Digest products were separated on an 1% agarose gel and the appropriately sized linearized vector was obtained and purified by means of the GFX™ PCR DNA and Gel Band Purification Kit (Amersham Biosciences), performed according to the manufacturer's specifications. Purified vector DNA were diluted into aliquots with a final concentration of 10 ng/µl, which were then subsequently used for the cloning of the various shRNA's constructs into the vectors. For this 10 ng of the vector DNA was added to 1 U of T4 DNA ligase, 20 µM of double-stranded oligos and 10 x reaction buffer and incubated overnight. After ligation the constructed vectors were transformed in MC1061

competent cells as described earlier. Successful cloning was verified by means of colony PCR (primer pair 3-F and 3-R, table 2.2) and pure, high quality vector DNA was achieved by means of the Qiagen® Midi-prep Plasmid Purification Kit (SABiosciences™), performed according to manufacturer's specifications.

2.2.1.4 Transfection

Transient and stable transfection experiments were performed concurrently following the same protocol. NIH-3T3 cells used for transfection were cultured as described in section 2.3.1.1. The METAFECTENE® Lipid Reagent (Biontex) was used in all transfection experiments according to the manufacturer's specifications. A solution containing 10 µl METAFECTENE® reagent and 1 ml DMEM, without FCS, per 2 µg of vector construct was prepared and incubated at room temperature for 20 min to allow for the formation of DNA-lipid complexes. The solution was gently mixed with the cultured NIH-3T3 cells, previously washed with PBS, and incubated at 37°C for 24 hrs in a 5% CO_2 incubator to allow adequate time for transfection. Success of the transfection experiments, as described below, were determined for both transient (within 48 hrs) and stable transfections, while only stable transfections were selected for and maintained in DMEM containing 500 µg/ml G418 (Sigma-Aldrich®).

2.2.1.5 Visualisation of transfected cells

Fluorescent microscopy was performed in order to verify the presence of the respective vectors within the cells by means of detection of the fluorescent GFP and RFP signals from the GFP and RFP vectors respectively. Cells were also counterstained with 4',6-diamidino-2-phenylindole (DAPI, Sigma-Aldrich®) to locate and identify cells. Cells were placed on microscopic slides and mounted with VECTASHIELD® Hard-Set™ Mounting Medium as per manufacturer's specifications. Visualisation was performed on a Zeiss fluorescent microscope.

2.2.1.6 Total RNA extraction

The TRIzol® LS protocol was followed for total RNA extraction. An amount of 0.3-0.4 ml TRIzol® LS reagent per 10 cm^3 culture flask was added to homogenised monolayer-grown cells. Upon transfer to a 15 ml conical tube, 0.2 ml chloroform per 0.75 ml TRIzol® LS reagent was added to the homogenate where after the solution was shaken vigorously for 15 sec. The solution was incubated at room temperature for 10 min and centrifuged for 30 min at 3000 rpm at 4°C in order to complete the phase separation step. In a clean conical tube, 0.5 ml isopropyl alcohol per 0.75 ml TRIzol® LS reagent was mixed with the top aqueous phase obtained after centrifugation. Adequate RNA precipitation was achieved by allowing the mixture to incubate at room temperature for 15 min followed by centrifugation of the mixture for 30 min at 3000 rpm at 4°C. An amount of 1 ml 70% ethanol per 0.75 ml TRIzol® LS reagent was used to wash the RNA pellet where after it was dried at room temperature and subsequently resuspended in 100 µl diethylpyrocarbonate-treated water.

The Agilent 2100 Bioanalyzer (Agilent Technologies) was used to determine the concentration of the RNA (measured at 260 nm) as well as to analyse the integrity of the RNA. Isolated RNA was described as pure if the 260/280 nm ratio lied between 1.8 and 2.1. Gel electrophoresis (2% (w/v) denaturing agarose gel containing formaldehyde) was also performed. Total RNA was stored at -80°C as 20 µl aliquots.

2.2.1.7 First-strand cDNA synthesis

The Transcriptor First Strand cDNA Synthesis kit from Roche Applied Sciences was used to reverse transcribe the extracted total RNA into single strand cDNA. In a total volume of 20 µl, 1 µg total RNA was mixed with 2.5 µM Anchored-oligo$(dT)_{18}$ Primer, 1 x Transcriptor Reverse Transcriptase Reaction Buffer (containing 8 mM $MgCl_2$), 20 U Protector RNase Inhibitor, 4 mM Deoxynucleotide Mix and 10 U Transcriptor Reverse Transcriptase. The reaction was incubated at 55°C for 30 min followed by a final inactivation step of 5 min incubated at 85°C. The concentration of the synthesised cDNA was determined with a NanoDrop Spectrophotometer.

2.2.1.8 Validation of gene expression knockdown by means of quantitative PCR

Quantitative PCR (qPCR) was performed to verify the levels of gene expression for the candidate genes in the respective knockdown cell lines. Gene-specific primers were designed with the Primer3 (Rozen and Skaletsky, 2000) software using the default parameters. A blast search confirmed the specificity of the primers, which were also optimised beforehand with traditional end-point PCR. A T_A of 60°C was used for all primers; additional details for the primers are available in table 2.3. In all qPCR reactions, a standard reaction mix was prepared containing LightCycler® FastStart DNA Master^{PLUS} SYBR Green Reaction Mix (Roche Applied Science), 0.5 µM of each primer and 200 ng cDNA in a final volume of 20 µl which, following gentle mixing, was transferred to capillary tubes. Tubes were centrifuged for 5 sec at 700 g to eliminate any possible air bubbles. Non-template controls were included in all experiments. The qPCR were performed on the LightCycler® 1.5 instrument and the following cycling parameters were used in all runs: a pre-incubation step of 10 min at 95°C followed by 40 cycles of a three part amplification step consisting of denaturation for 15 sec at 95°C, annealing for 15 sec at a T_A dependent on the primer set and extension for 20 sec at 72°C. A melt curve, ranging from 60°C-95°C was also performed on completion of the amplification step.

The relative standard curve quantification method was followed to quantify the level of gene expression of the candidate genes. This method requires that the expression levels of the target and reference gene(s) be measured in a serial dilution format in order to construct a standard curve. Based on an analysis previously performed with the Microsoft® Excel®-based software BestKeeper (Pfaffl et al., 2004), two reference genes, namely *glyceraldehyde-3-phosphate*

Table 2.3: Details of primers used for qPCR performed for the validation of candidate gene expression knockdown

Gene	Primer orientation	Sequence (5'-3')	Length (bp)	Product length (bp)
LIAS	F	TTAAGACCGCAAGAAATCCC	20	102
	R	ACCGACGTCAGGACAACATA	20	
CYPA	F	CAGACGCCACTGTCGCTTT	19	132
	R	TGTCTTTGGAACTTTGTCTGCAA	23	
RPL9	F	CGGTCTGTGTACGCTCACTT	20	152
	R	ATCCTTCTGGGCTTGAGAGA	20	
GAPDH	F	GGTGGCAGAGGCCTTTG	17	215
	R	TGCCGATTTAGCATCTCCTT	20	
HPRT1	F	GACTGTAGATTTTATCAGACTG	22	89
	R	GTCTGGCCTGTATCCAACACTTC	23	

F – forward; R – reverse; bp – base pair.

dehydrogenase (*GAPDH*) and *hypoxanthine phosphoribosyltransferase 1* (*HPRT1*) were selected. Standard curves were constructed by generating a dilution series consisting of four points ranging from a 10 x dilution to a 10 000 x dilution of the synthesised cDNA. Primer sequences for the reference genes were sourced from validated primer database RTPrimerDB (Pattyn et al., 2003) (table 2.3). All primers were synthesised by Inqaba Biotech™. The freely-available Microsoft® Excel®-based software REST© (Pfaffl et al., 2002) was used to perform the analysis of the qPCR results.

2.2.2 Apoptosis Assays

Cells from each of the stable knockdown cell lines were cultured and maintained as described in section 2.3.1.1. For the apoptosis assays, approximately 2.5 x 10^4 cells were seeded into six well tissue culture plates. Both assays were performed in triplicate, at multiple concentration points for both C_2-ceramide (Sigma-Aldrich®) and camptothecin (Sigma-Aldrich®) and for each of the knockdown cell lines.

2.2.2.1 APOPercentage™ Assay

Cells from each of the knockdown cell lines were subjected to apoptosis induction by both inducers and subsequent analysis with the APOPercentage™ assay (Biocolor LTD, UK). Spent medium were removed from tissue culture plates containing cultured confluent cells and replaced with 2 ml fresh DMEM medium containing the apoptotic inducer. Concentrations ranged between 0 and 100 µM in intervals of 20 µM for C_2-ceramide and between 0 and 10 µg/ml in intervals of 2 µg/ml for camptothecin; zero concentration points served as negative controls. The medium was removed

after 24 hrs, where after the cells were washed with 1 ml PBS. Since one of the morphological characteristics in apoptosis is the “rounding up” of cells, it could result in some of the cells loosing adherence; hence, the collected medium was spun down to retrieve any cells that might have been removed along with the medium. The spent medium was removed from this collection and the cells were washed with PBS. Cells in the tissue culture plates, as well as the collected cells, were incubated in 1 ml APOPercentage™ dye for one hour at 37°C. Following removal of the dye, cells were washed with 1 ml PBS in order to remove any remaining dye. Cells in the tissue culture plates were harvested by means of trypsinisation (incubated with 1 ml 0.125% trypsin solution until cells became partially detached), resuspended in 1 ml ice-cold fluorescence-activated cell sorting (FACS) buffer and transferred to a FACS calibrated tube. Cells retrieved from the collected medium were also resuspended and added to the same tube. The cellular fluorescence of 10 000 cells per sample were measured by means of flow cytometry using the FL3 (red) channel on a FACScan™ (Becton Dickinson, BD) instrument, which, in conjunction with the CellQuest™ Pro (BD) software, allowed for the quantification of the amount of viable cells.

2.2.2.2 Caspase-3/CPP32 Colourimetric Assay Kit

As with the APOPercentage™ assay, cells from each of the knockdown cell lines were subjected to apoptosis induction, followed by analysis with the Caspase-3/CPP32 Assay Kit (BioVision Inc.). Spent medium were removed from tissue culture plates containing cultured confluent cells. 1 ml of a 0.125% trypsin solution was added to loosen the cells in the wells, where after the cells were resuspended in 2 ml fresh DMEM medium and recovered by centrifugation. A volume of 500 µl Cytofix/Cytoperm™ (BD) was added to the cells followed by incubation on ice for 20 min. Cells were recovered by centrifugation and washed twice with 100 µl Perm/Wash buffer™ (BD). Upon the second resuspension step in Perm/Wash™, 20 µl of the fluorescein isothiocyanate-conjugated polyclonal active caspase 3 antibody, provided in the kit, were added and the solution incubated in the dark at room temperature for 30 min. The solution was spun down and resuspended in 1 ml Perm/Wash™, followed by another centrifugation and resuspension in 500 µl Perm/Wash™. Finally, the solution was transferred to a FACS calibrated tube and a total of 10 000 cells per sample were analysed with the FACScan™ instrument using the FL1 (green) channel. As with the APOPercentage™ assay, the amount of viable cells was quantified with the CellQuest™ Pro software.

2.2.2.3 Analysis of results

Output from the CellQuest™ Pro software provides counts of the amount of cells displaying a fluorescent signal in a sample; from the counts, the percentage of live cells in each sample were then calculated by taking 10 000 cells as the total amount. Results were then subjected to basic statistical analysis in Microsoft Excel, which included the calculation of a sample-based estimate of standard deviation, standard error of the mean, two sample F-test for variances and two sample T-

tests. A p-value of less than 0.05 was seen as significant for the T-tests. Only data obtained from the knockdown cell lines transfected with the GFP vectors carrying shRNA constructs for each of the candidate genes were used for this analysis.

2.3 Results and discussions

2.3.1 Generation of stable knockdown cell lines for *LIAS*, *RPL9* and *CYPA*

2.3.1.1 Construction of shRNA-expressing vectors

The construction of the shRNA-expressing vectors involved various steps; firstly, the MCS regions in the GFP and RFP vectors had to be removed. Since the expression of the shRNA constructs were to be driven by a U6 promoter and not by the native cytomegalovirus (CMV) early promoter, a U6 promoter fragment cloned into both of the vectors upstream of the native promoters contained recognition sites for *Bgl* II and *Hind* III in order to allow for the cloning of the shRNA constructs downstream of the new promoter. However, the MCS region downstream of the CMV promoter also contained recognition sites for these enzymes; thus these sites had to be removed in order to prevent multiple digestions taking place during cloning of the shRNA construct into the vectors. This was accomplished by means of vector digestions with the restriction enzymes *Bgl* II and *BamH* I. The deletion of the MCS regions in both of the vectors were successful as verified with agarose gel electrophoresis following a colony PCR (Fig. 2.6). A PCR product confirming the deletion of the MCS had a size of 170 bp, while the control vector delivered a PCR product of 210 bp. Next, the U6 promoter fragment was cloned into both of the vectors, upstream of the CMV promoter. This RNA Polymerase III promoter have been shown to efficiently induce target-specific mRNA cleavage in eukaryotic cells without the need for downstream transcriptional elements while allowing transcription to be terminated by stretch of four or more tyrosine residues (Dykxhoorn et al., 2003; Yu et al., 2002). The presence of this fragment was successfully verified by means colony PCR and subsequent agarose gel electrophoresis, since it produced the appropriate band of 800 bp (Fig. 2.7). Lastly, the KD1 and KD2 shRNA constructs for each of the candidate genes were cloned into both of the vectors between the *Bgl* II and *Hind* III recognition sites downstream of the U6 promoter. Again, following the colony PCR, the agarose gel electrophoresis showed the successful uptake of these constructs into the vectors; producing PCR products of 530 bp compared to the 469 bp products of the control vector (Fig. 2.8). An example of the final vector product can be seen in figure 2.9.

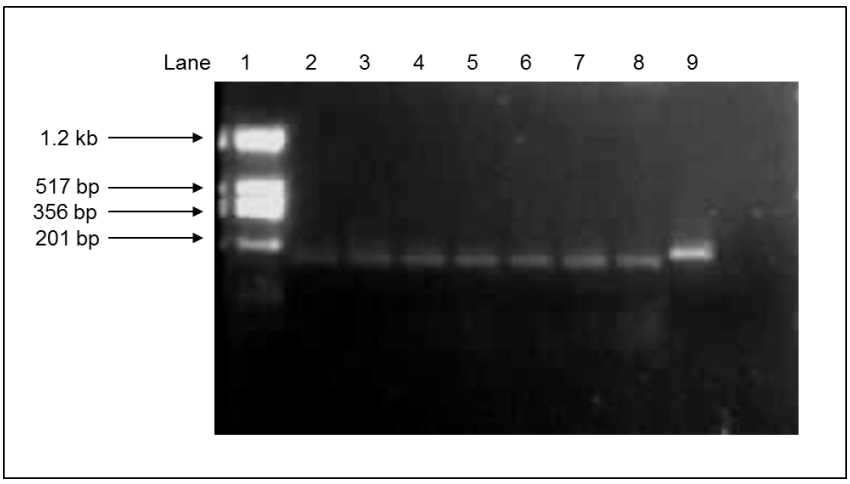

Figure 2.6: Representative example of the successful deletion of the MCS region between the *Bgl* II and *Hind* III cut sites in the expression vectors as confirmed by colony PCR and agarose gel electrophoresis. Lane 1 – pTZ molecular marker; Lane 2-8 - colonies showing successful deletion of the MCS region from the GFP vector; Lane 9 – control GFP vector.

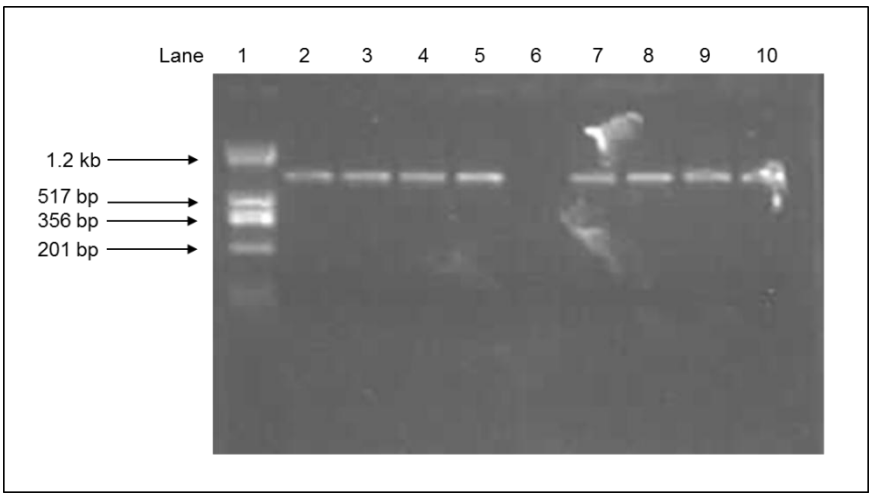

Figure 2.7: Representative example of the successful cloning of the U6 promoter fragment into the expression vectors as confirmed by colony PCR and agarose gel electrophoresis. Lane 1 – pTZ molecular marker; Lane 2-5 – colonies showing the U6 promoter fragment cloned into the GFP vector; Lane 6 – negative control; Lane 7-10 – colonies showing the U6 promoter fragment cloned into the RFP vector.

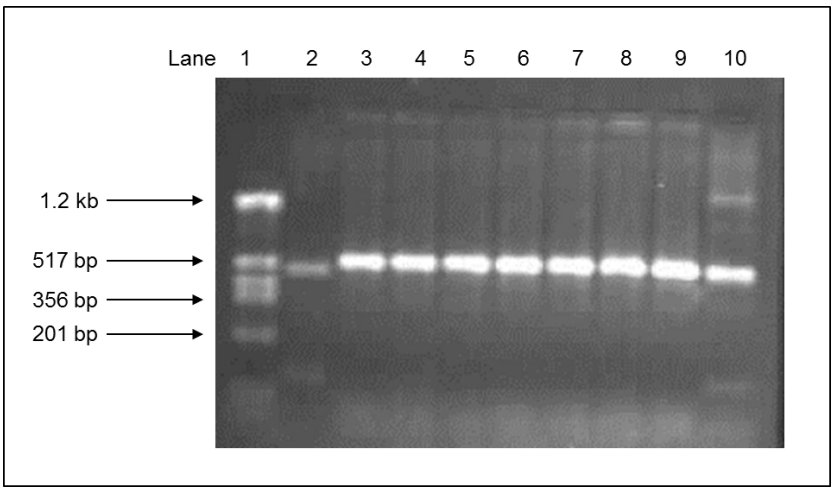

Figure 2.8: Representative example of the successful cloning of shRNA constructs into the expression vectors as confirmed by colony PCR and agarose gel electrophoresis. Lane 1 – pTZ molecular marker; Lane 2 – control GFP vector; Lanes 3-7 – colonies showing successful cloning of *LIAS* shRNA constructs into the GFP vector; Lanes 8-10 – colonies showing successful cloning of *CYPA* shRNA constructs into the GFP vector.

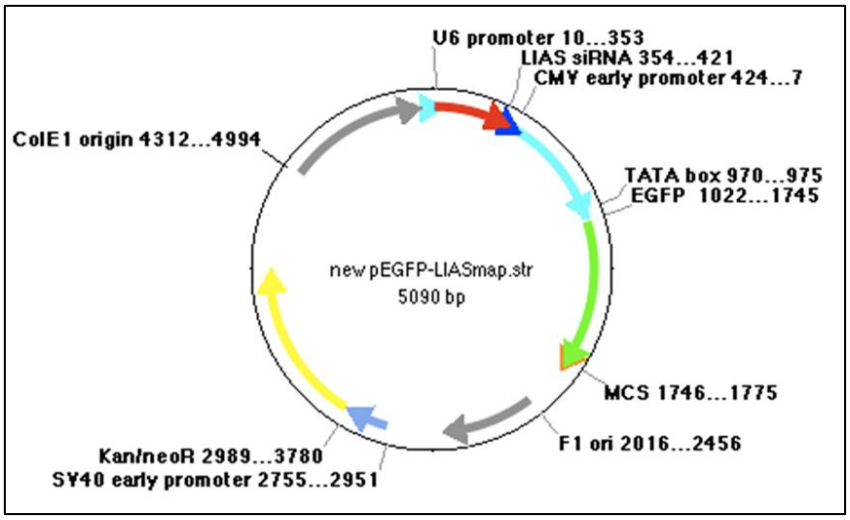

Figure 2.9: Representative example of the final product following vector construction. Illustrated in the figure is a GFP vector containing a shRNA construct for *LIAS* driven by the U6 promoter.

2.3.1.2 Transfection of NIH-3T3 cells with shRNA-expressing vectors

NIH-3T3 cells were transfected with the various shRNA-containing vectors using the METAFECTENE® Lipid Reagent. Transient and stable transfection experiments were performed concurrently and both were deemed successful by means of fluorescent microscopy (Fig. 2.10) and gene expression analysis (see section 2.3.1.3). Transfection efficiencies, as calculated with the Zeiss microscope, averaged above 70% for both the GFP and RFP vectors, although the former showed higher and more consistent transfection efficiencies. Selection for the stable transfections produced multiple colonies resistant to G418 when cultured in DMEM medium

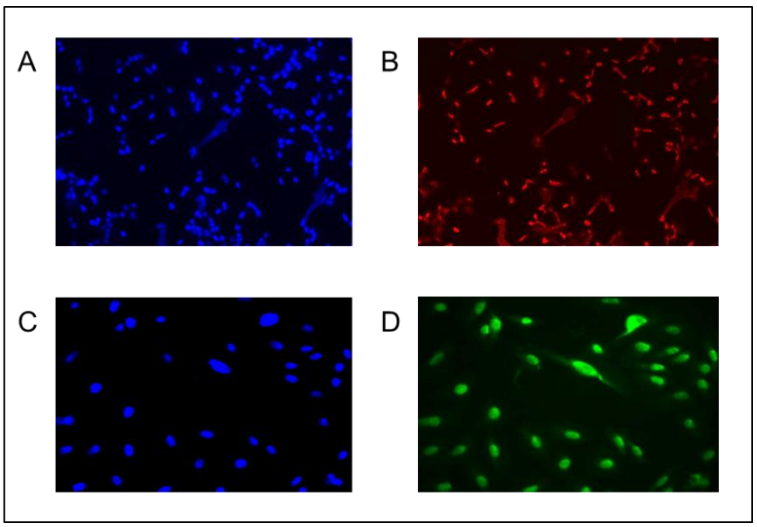

Figure 2.10: Representative photographs, taken with a Zeiss fluorescent microscope, of NIH-3T3 cells transfected with the shRNA-containing vectors. A – NIH-3T3 transfected cells counterstained with DAPI; B – NIH-3T3 cells transfected with RFP vector containing a shRNA for *LIAS*; C – NIH-3T3 transfected cells counterstained with DAPI; D – NIH-3T3 cells transfected with GFP vector containing a shRNA for *RPL9*.

supplemented with the antibiotic; thus also indicating the successful uptake of the vectors into the cells.

2.3.1.3 Validation of gene expression knockdown

Following successful transfection of the various vectors into NIH-3T3 cells, total RNA was extracted and cDNA was synthesised. The total RNA extraction generated pure, non-degraded RNA as revealed by the analysis with the Agilent 2100 Bioanalyzer (Fig. 2.11) and agarose gel electrophoresis. The cDNA synthesis reactions produced pure cDNA with high concentrations as determined by NanoDrop analysis.

In order to verify the successful gene expression knockdown of the candidate genes by the shRNA's, qPCR was performed to determine the relative expression levels of *LIAS*, *RPL9* and *CYPA* in the knockdown cell lines expressing the shRNA constructs for the respective genes. This technique is a modification of the traditional end-point PCR technique which allows for the concurrent detection and quantification of a DNA template in real time by means of fluorescent chemistries, such as SYBR® Green I (Pfaffl, 2001). More information regarding qPCR is available in chapter 4. The cDNA synthesised from the extracted total RNA was used as the template for the qPCR experiment and the results obtained were interpreted by the relative standard curve method. As required by this method, standard curves were constructed for both the reference genes as well as the target genes. These standard curves revealed reaction efficiencies ranging between 1.93-1.98 indicating near-optimal doubling of the template in each cycle.

The analysis revealed significant reductions in the expression levels for all three candidate genes in the knockdown cell lines, indicating a successful gene expression knockdown effect brought about by the shRNA constructs (Fig. 2.12). Cell lines transfected with the GFP vectors showed a

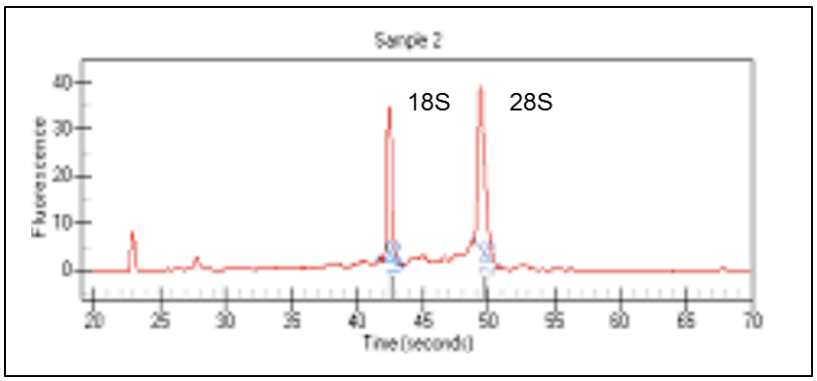

Figure 2.11: Representative example for determining the integrity of extracted total RNA as confirmed with the Agilent 2100 Bioanalyzer. The image shows the 18S and 28S peaks of RNA extracted from a *LIAS* knockdown cell line transfected with a GFP vector.

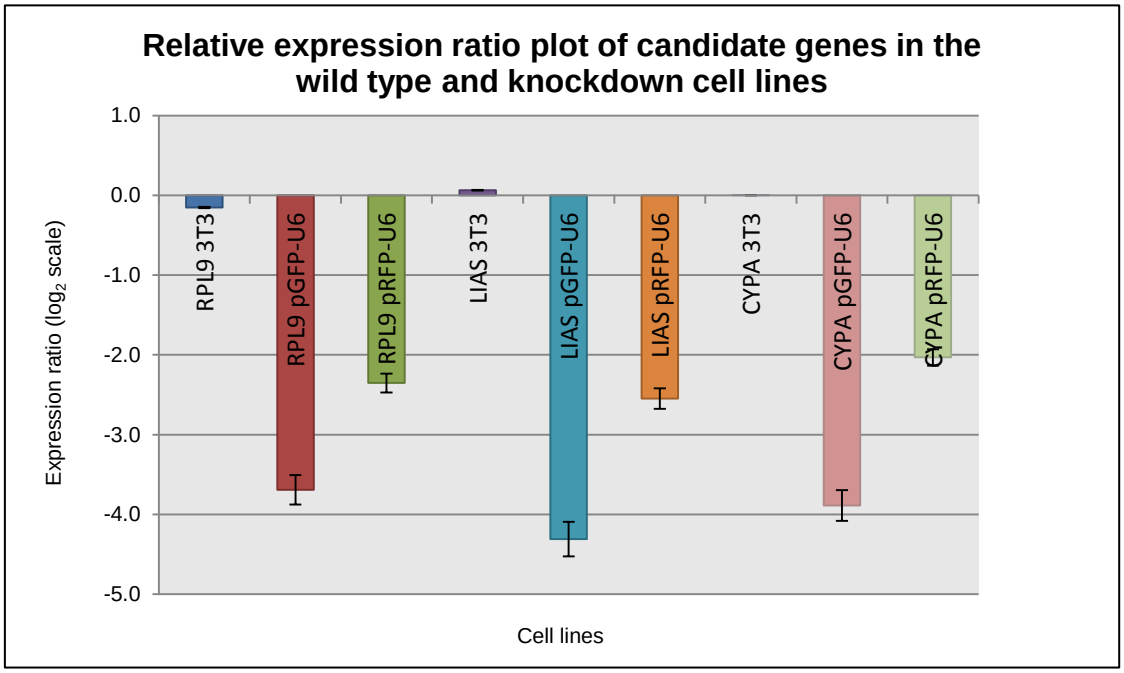

Figure 2.12: Relative expression ratio plot produced by the REST© software used for the analysis of the qPCR results for the validation of candidate gene expression knockdown. Bars indicate the ratios of the collective KD1 and KD2 expression levels, as measured in a $\log_2$ scale, for each candidate gene in the knockdown cell lines as compared to the normal expression levels of each gene in the wild type NIH-3T3 cells. Values are the averages ± standard error from duplicate experiments.

larger decrease in expression levels in comparison to the cell lines transfected with the RFP vectors; suggesting that even though the two expression vectors shared a promoter, the GFP vector facilitated higher expression of the shRNA constructs. Comparable results were obtained for both the KD1 and KD2 cell lines for each of the candidate genes, indicating that in each case both constructs successfully targeted the specific candidate gene.

2.3.2 Apoptosis assays

2.3.2.1 FACScan™ and CellQuest™ Pro analysis

Two apoptosis assays, namely APOPercentage™ and Caspase-3/CPP32, were performed to determine the level of apoptosis present in the knockdown cell lines following apoptosis induction with both C_2-ceramide and camptothecin. Cells were analysed with the automated flow cytometer FACScan™ system, which, in conjunction with the CellQuest™ Pro software allows for the quantification of live and dead cells. A number of 10 000 cells per sample (i.e. a collection of cells from a particular knockdown cell line treated with an apoptotic inducer and assayed by an apoptosis assay) were analysed for fluorescence by the FACScan™ system as they pass through a focussed laser beam in a moving fluid stream, one cell at a time. The CellQuest™ Pro software then uses the data generated by the FACScan™ system and produces single parameter histograms depicting two peaks representing the number of live (M1) and dead (M2) cells. Figure 2.13 shows a representative example of the results produced by the software. All the histograms for the *LIAS* knockdown cell lines showed a high M1 peaks with both C_2-ceramide and camptothecin apoptosis induction as assayed by both the APOPercentage™ and Caspase-3/CPP32 assays. The height of the peaks slightly declined with a corresponding increase in concentration of the apoptotic inducers; however it still remained higher than the M2 peak Histograms for the *CYPA* knockdown cell lines showed results similar to those of *LIAS*. High M1 peaks were observed in knockdown cell lines where apoptosis were induced by both C_2-ceramide and camptothecin and assayed by both APOPercentage™ and Caspase-3/CPP32 assays. These peaks also remained higher than the M2 peaks with increasing concentrations of the apoptotic inducer. These results are indicative of possible resistance to apoptosis based on the high amount of live cells present when compared to the results from the wild type NIH-3T3 cells, which showed increasingly higher M2 peaks upon apoptosis induction. In contrast to *LIAS* and *CYPA*, the histograms for the *RPL9* knockdown cell lines tended to resemble those of the wild type cells. M1 peaks decreased in height with increasing concentrations for both C_2-ceramide and camptothecin as assayed by both the APOPercentage™ and Caspase-3/CPP32 assay. These results thus suggest that *RPL9* knockdown cell lines are susceptible to apoptosis induction.

2.3.2.2 Analysis of results

Basic statistical analysis was performed in Microsoft® Excel® with the results obtained from the CellQuest™ Pro software in order to test for significant data. For this analysis, only results obtained from knockdown cell lines transfected with the GFP vectors carrying shRNA constructs for the respective candidate genes were used; these results were selected since these cell lines displayed a higher degree of gene expression knockdown as facilitated by the RNAi technique and also due to a higher level of overall consistency among the results obtained from these cell lines.The experiments were performed in triplicate and from these values the sample-based standard

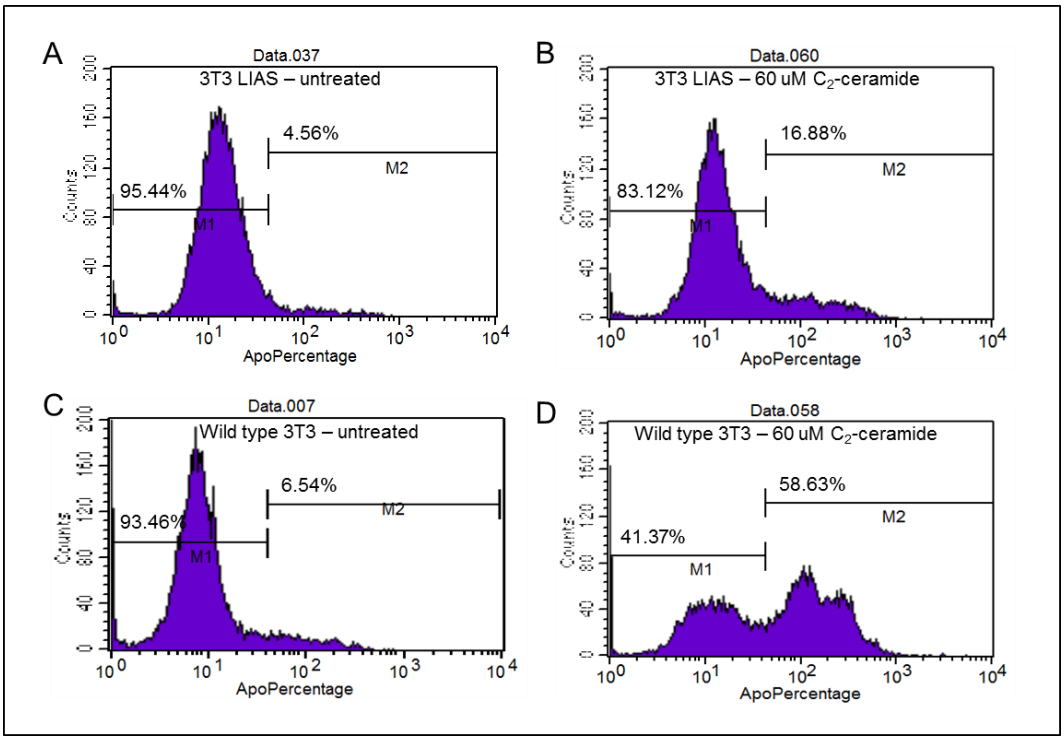

Figure 2.13: Representative example of results obtained from the CellQuest™ Pro software following flow cytometry. Figures illustrate the cell plots of wild type NIH-3T3 cells and cells transfected with GFP vector containing a *LIAS* shRNA construct, both assayed with the APOPercentage™ assay. A – untreated *LIAS* knockdown NIH-3T3 cells; B – *LIAS* knockdown NIH-3T3 cell treated with 60 µM C_2-ceramide; C – untreated wild type NIH-3T3 cells; D – Wild type NIH-3T3 cells treated with 60 µM C_2-ceramide. M1 – region showing live cells; M2 – region showing dead cells.

deviation and standard error of mean were calculated. Apart from a few exceptions, relatively small values were obtained with most ranging between zero and three. The two-sample F-test revealed that samples of both equal and unequal variances were present and based on these results the appropriate t-test was performed. The t-tests revealed significant values for both *LIAS* and *CYPA* knockdown cell lines when compared to the wild type NIH-3T3 cell line, however the *RPL9* knockdown cell lines had less significant values which decreased even more if a p-value of 0.001 were to be used. Table A1 and A2 in addendum A provides a summary of the descriptive statistic obtained in this analysis.

As with many molecular techniques, absolute specificity is fundamental to a successful RNAi experiment and the possibility that the experiment outcomes are a result of or influenced by some other off-target cross-reaction should always be considered. In this study, two separate knockdown cell lines for each candidate gene were created by designing two different siRNAs targeting the same gene. This methodology served to verify the specificity of the experiment; a validation method also suggested by Fraser (Fraser, 2004). Since both knockdown cell lines for each candidate gene behaved similarly when treated with the apoptotic inducers, it can be concluded that the effect seen after knockdown was not due to a cross reaction but that the knockdown of these genes were responsible to the changes in sensitivity to apoptosis induction.

APOPercentage™ assay

APOPercentage™ assays revealed significant resistance to apoptosis in *LIAS* and *CYPA* knockdown cell lines (Fig. 2.14-2.17). This can be seen in the remarkably slower decrease in live cells upon increasing concentrations of apoptotic inducers compared to that of the NIH-3T3 wild type cell line. In both *LIAS* and *CYPA* knockdown lines, the resistance effect was evident even at high concentrations of the inducers. While the percentage of live wild type cells dropped to between 7% and 21% at the highest concentration of the apoptotic inducers, the percentage of live cells in both *LIAS* and *CYPA* knockdown cell lines remained high, averaging at about 70%. On the other hand, *RPL9* knockdown cell lines displayed sensitivity to apoptosis by showing approximately the same trend as the wild type cell line (Fig. 2.18 and 2.19). The knockdown cell lines showed only a slightly higher percentage of live cells compared to that of the wild type at most of the concentration points, with the exception of the 80 µM C_2-ceramide concentration point where the amount of live knockdown cells were 17.65% higher. However, this effect was not seen in any of the camptothecin concentration points. With the exception of the above mentioned difference, both apoptotic inducers showed comparable results in terms of inducing apoptosis in the wild type cells and failing to induce apoptosis in the knockdown cell lines. In addition, KD1 and KD2 cell lines for each candidate gene also showed similar results; the highest differences in percentage of live cells between these two lines, across all genes, were 4.7% and 4.3% (Fig. 2.14 and 2.16, respectively). These were also the only two instances where the differences in percentages were higher than 3%.

Caspase-3/CPP32 Colourimetric Assay Kit

Results from the Caspase-3/CPP32 assay were comparable to that of the APOPercentage™ assay. *LIAS* and *CYPA* knockdown cells showed a substantially smaller and less rapid decline in the percentage of live cells over the range of increasing apoptotic inducer concentrations compared to the NIH-3T3 wild type cell lines (Fig. 2.20-2.23). The percentage of knockdown cells resisting apoptosis remained above 70% compared to the percentage of wild type cells which ranged between 9.6% and 14.6%; a smaller margin than observed in the APOPercentage™ assay results. The sensitivity of *RPL9* knockdown cell lines to apoptosis was also seen in the Caspase-3/CPP32 assay (Fig. 2.24 and 2.25). The knockdown cells followed the same declining trend as the wild type cells with only small differences in the percentage of live cells between the knockdown and wild type cell lines. A similar effect as seen in the APOPercentage™ assay at 80 µM C_2-ceramide was observed in the Caspase-3/CPP32 assay; although in this assay it occurred earlier, at 60 µM C_2-ceramide, and the difference between the knockdown and wild type cells averaged at 29.05%. Again, this was not seen at any camptothecin concentration points. Overall, both apoptotic inducers were effective in inducing apoptosis in wild type cells, while knockdown cell lines displayed comparable resistance to apoptosis upon induction of both chemicals. As in the

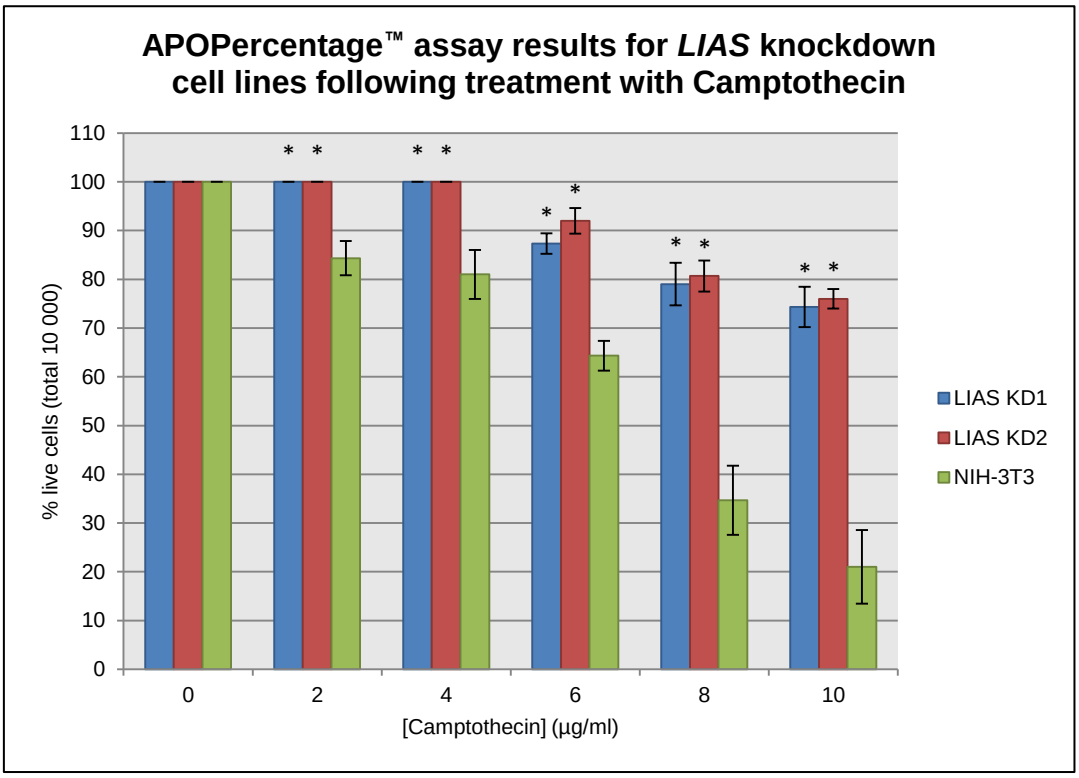

Figure 2.14: Results of testing for resistance to apoptosis in *LIAS* knockdown cell lines, as compared to wild type NIH-3T3 cells, by means of the APOPercentage™ assay following treatment of camptothecin for 24 hrs. Values are the averages ± standard deviation from triplicate experiments. * Indicates significantly different from wild type for $p < 0.05$. KD – knock down.

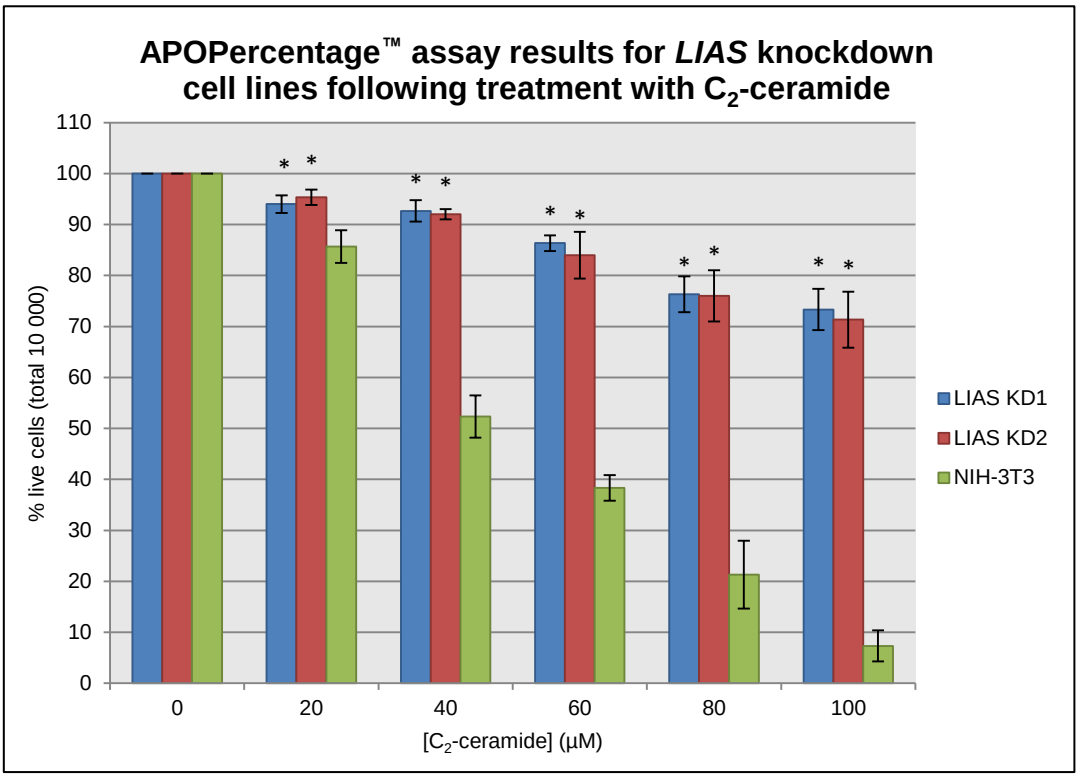

Figure 2.15: Results of testing for resistance to apoptosis in *LIAS* knockdown cell lines, as compared to wild type NIH-3T3 cells, by means of the APOPercentage™ assay following treatment of C_2-ceramide for 24 hrs. Values are the averages ± standard deviation from triplicate experiments. * Indicates significantly different from wild type for $p < 0.05$. KD – knock down.

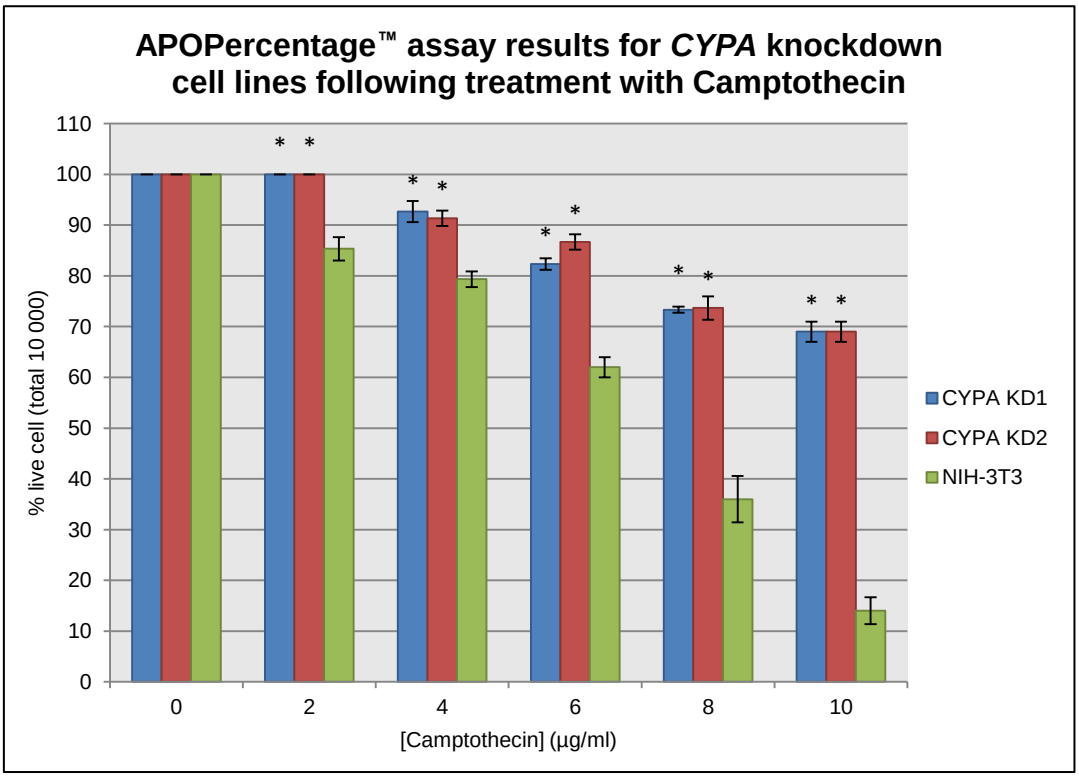

Figure 2.16: Results of testing for resistance to apoptosis in *CYPA* knockdown cell lines, as compared to wild type NIH-3T3 cells, by means of the APOPercentage™ assay following treatment of camptothecin for 24 hrs. Values are the averages ± standard deviation from triplicate experiments. * Indicates significantly different from wild type for $p < 0.05$. KD – knock down.

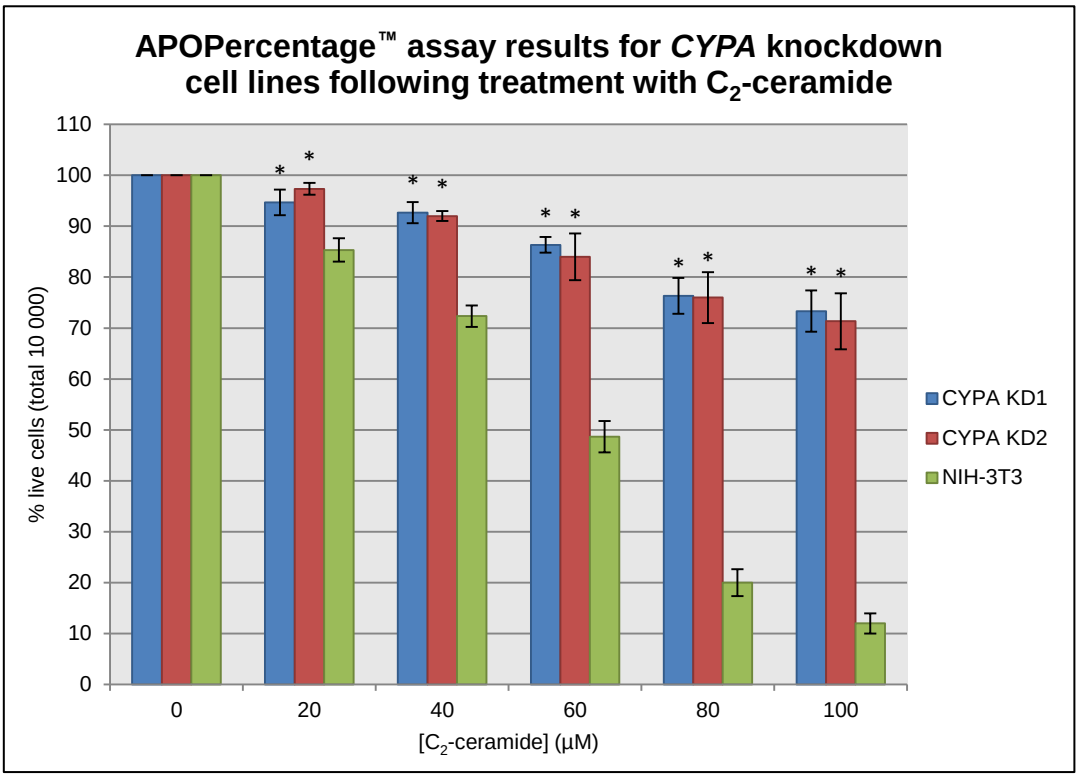

Figure 2.17: Results of testing for resistance to apoptosis in *CYPA* knockdown cell lines, as compared to wild type NIH-3T3 cells, by means of the APOPercentage™ assay following treatment of C_2-ceramide for 24 hrs. Values are the averages ± standard deviation from triplicate experiments. * Indicates significantly different from wild type for $p < 0.05$. KD – knock down.

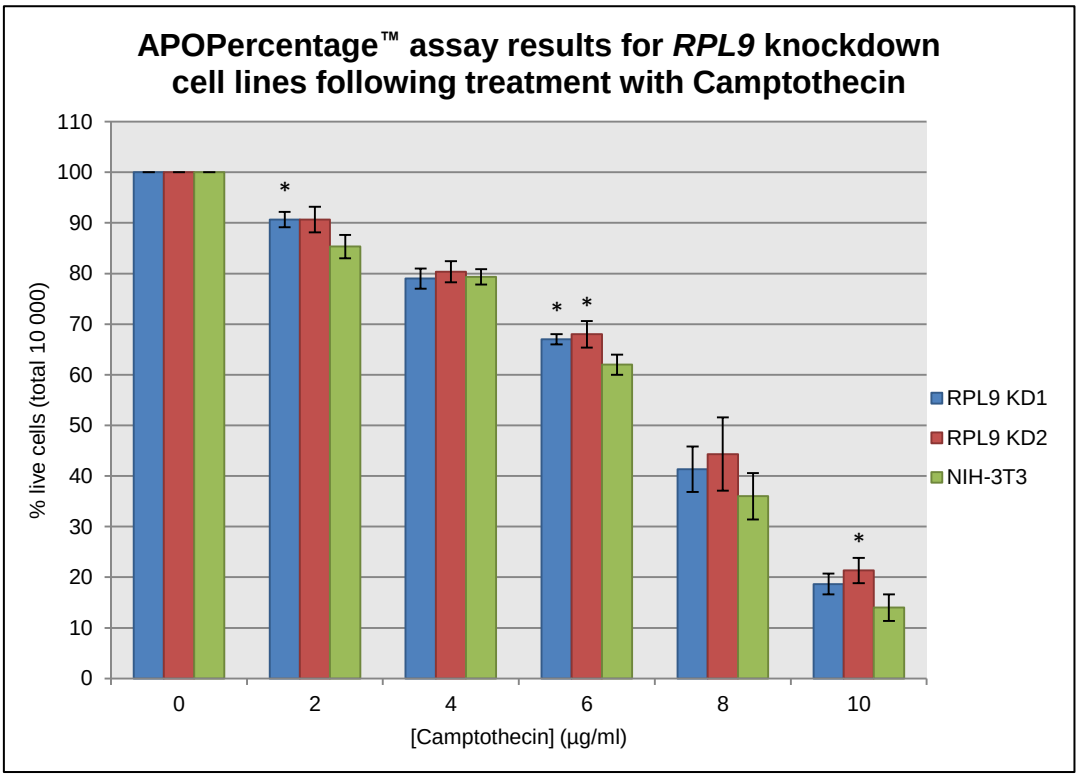

Figure 2.18: Results of testing for resistance to apoptosis in *RPL9* knockdown cell lines, as compared to wild type NIH-3T3 cells, by means of the APOPercentage™ assay following treatment of camptothecin for 24 hrs. Values are the averages ± standard deviation from triplicate experiments. * Indicates significantly different from wild type for $p < 0.05$. KD – knock down.

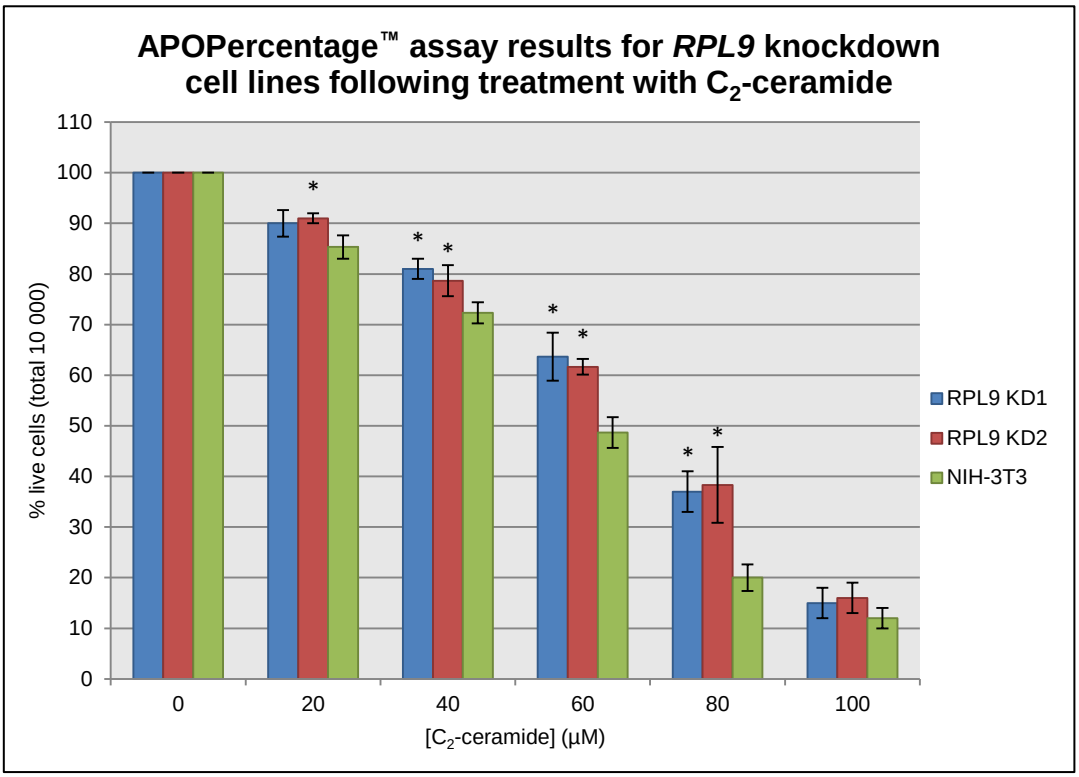

Figure 2.19: Results of testing for resistance to apoptosis in *RPL9* knockdown cell lines, as compared to wild type NIH-3T3 cells, by means of the APOPercentage™ assay following treatment of C_2-ceramide for 24 hrs. Values are the averages ± standard deviation from triplicate experiments. * Indicates significantly different from wild type for $p < 0.05$. KD – knock down.

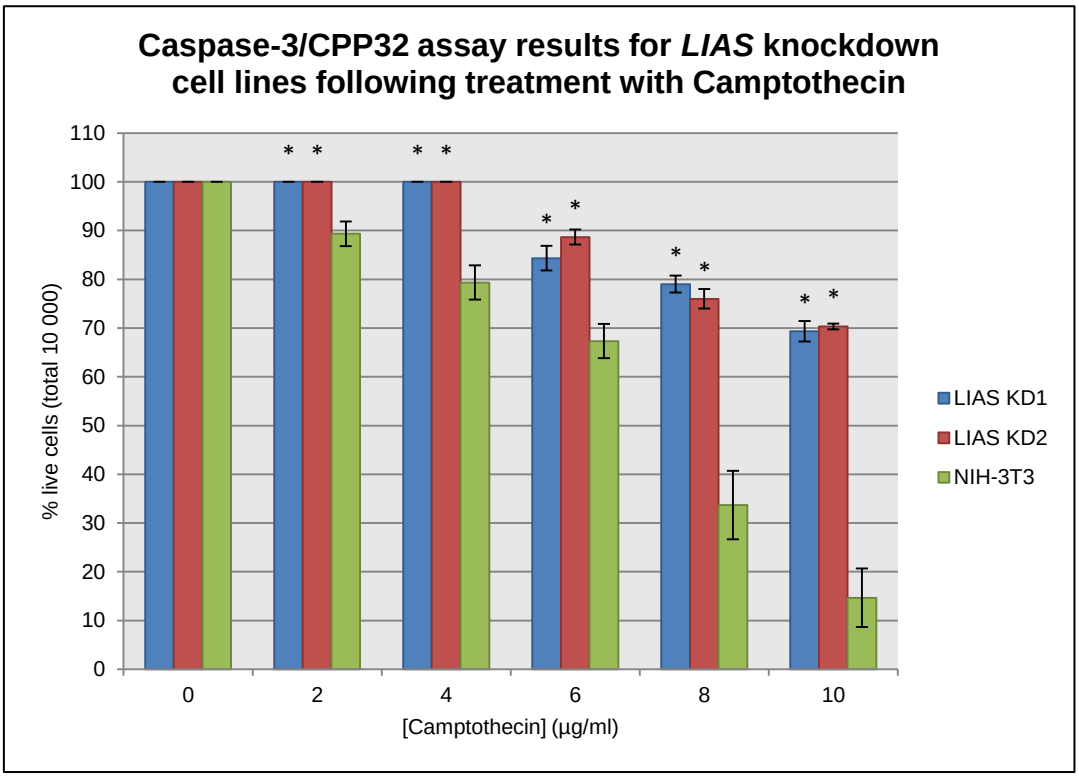

Figure 2.20: Results of testing for resistance to apoptosis in *LIAS* knockdown cell lines, as compared to wild type NIH-3T3 cells, by means of the Caspase-3/CPP32 assay following treatment of Camptothecin for 24 hrs. Values are the averages ± standard deviation from triplicate experiments. * Indicates significantly different from wild type for $p < 0.05$. KD – knock down.

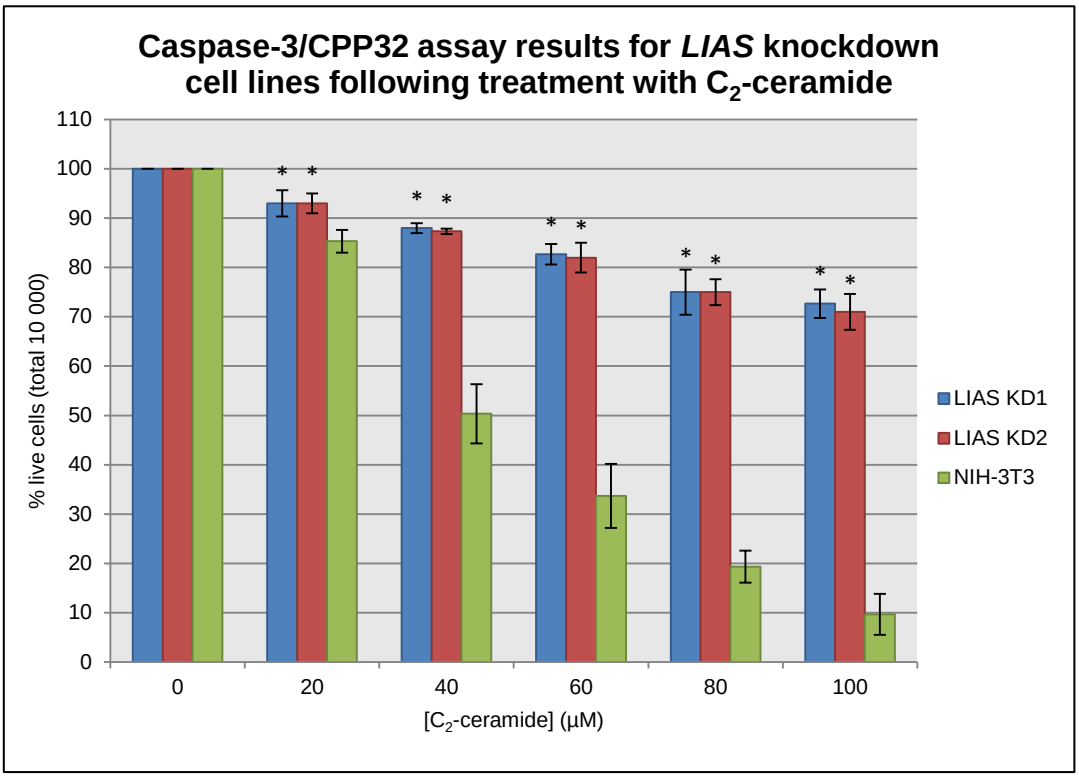

Figure 2.21: Results of testing for resistance to apoptosis in *LIAS* knockdown cell lines, as compared to wild type NIH-3T3 cells, by means of the Caspase-3/CPP32 assay following treatment of C_2-ceramide for 24 hrs. Values are the averages ± standard deviation from triplicate experiments. * Indicates significantly different from wild type for $p < 0.05$. KD – knock down.

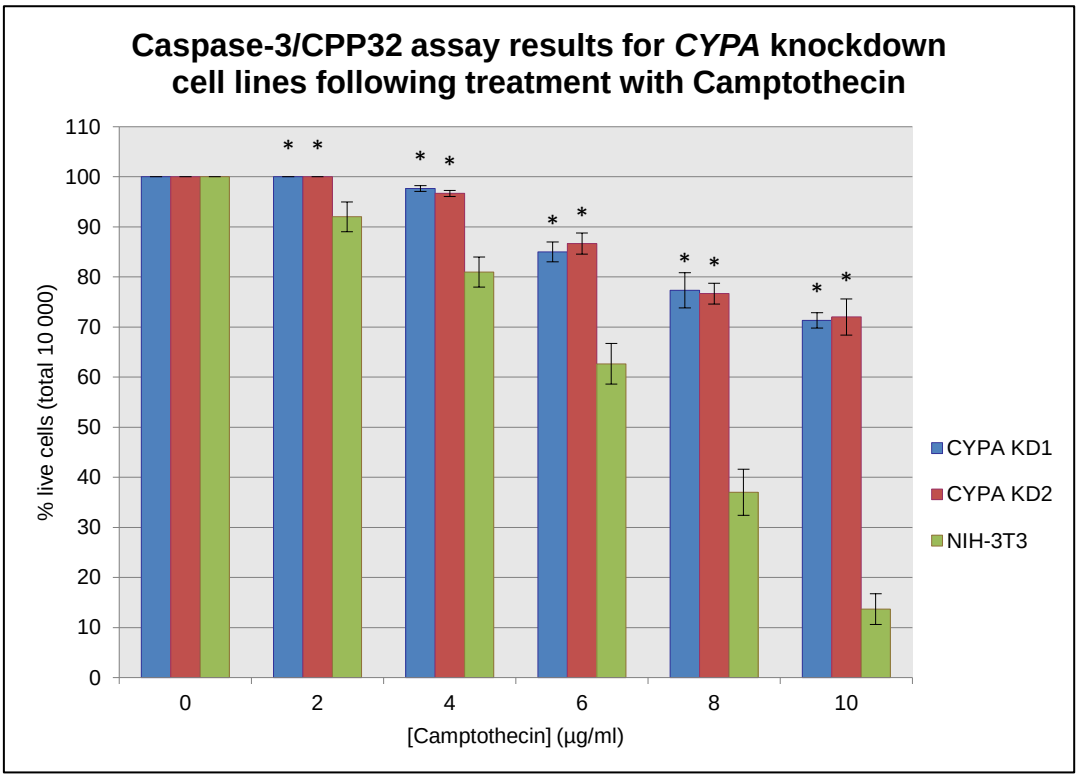

Figure 2.22: Results of testing for resistance to apoptosis in *CYPA* knockdown cell lines, as compared to wild type NIH-3T3 cells, by means of the Caspase-3/CPP32 assay following treatment of Camptothecin for 24 hrs. Values are the averages ± standard deviation from triplicate experiments. * Indicates significantly different from wild type for $p < 0.05$. KD – knock down.

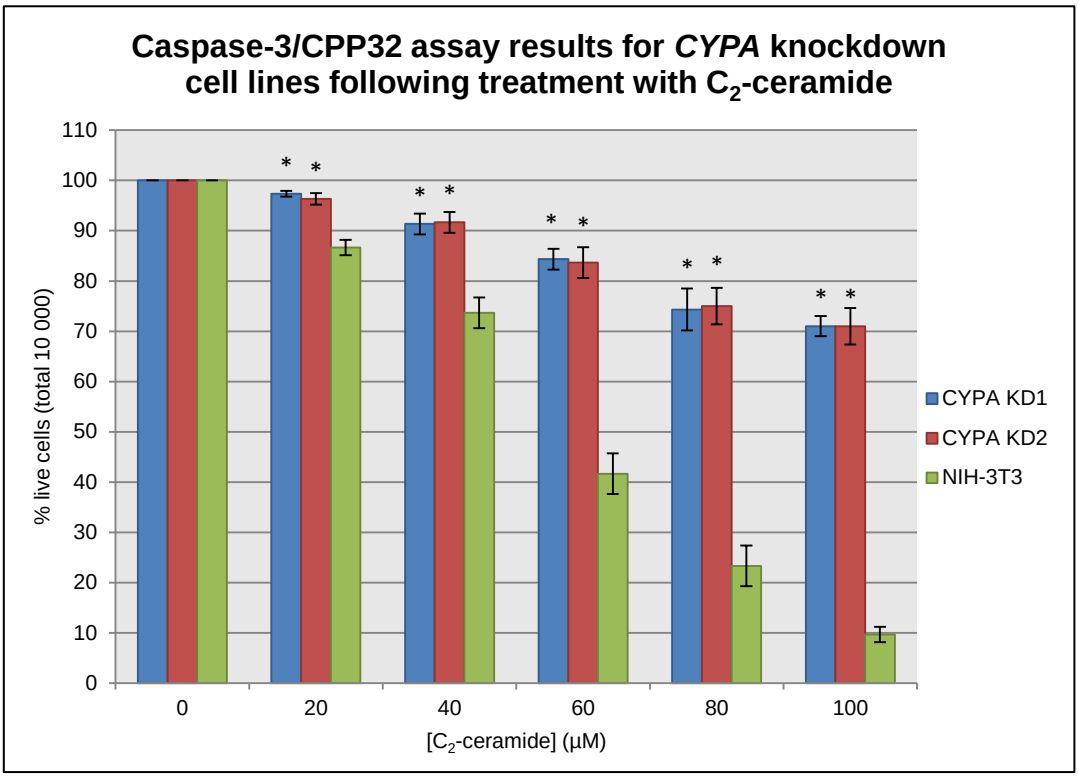

Figure 2.23: Results of testing for resistance to apoptosis in *CYPA* knockdown cell lines, as compared to wild type NIH-3T3 cells, by means of the Caspase-3/CPP32 assay following treatment of C_2-ceramide for 24 hrs. Values are the averages ± standard deviation from triplicate experiments. * Indicates significantly different from wild type for $p < 0.05$. KD – knock down.

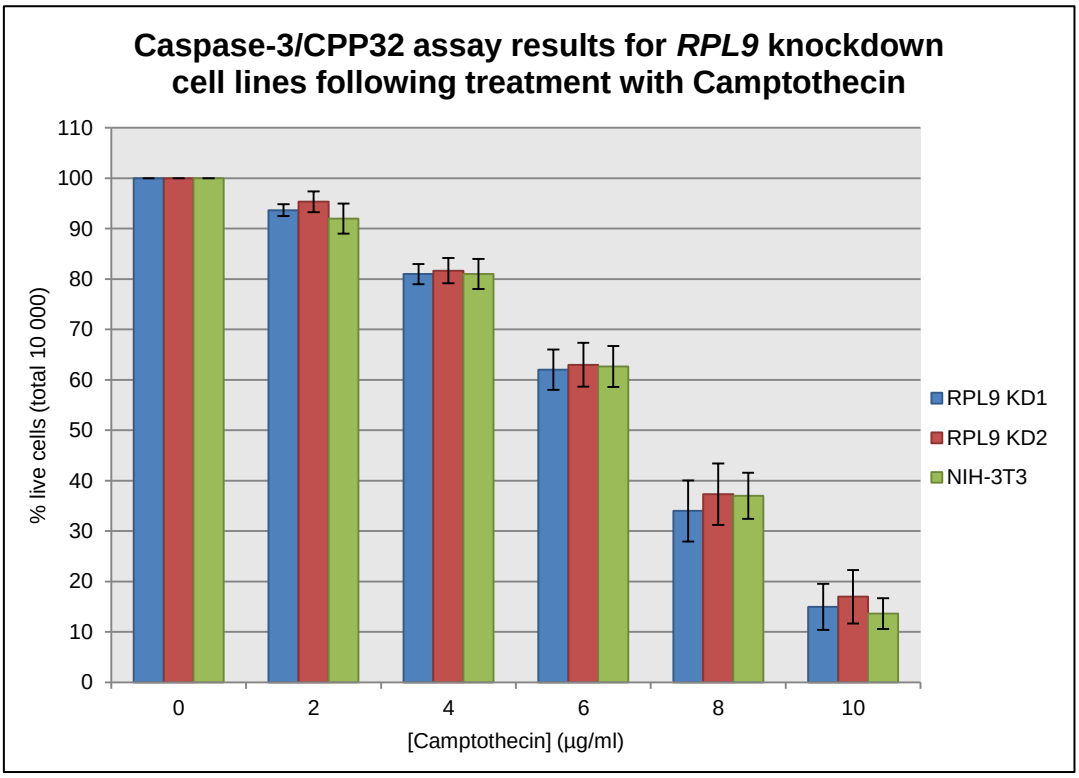

Figure 2.24: Results of testing for resistance to apoptosis in *RPL9* knockdown cell lines, as compared to wild type NIH-3T3 cells, by means of the Caspase-3/CPP32 assay following treatment of Camptothecin for 24 hrs. Values are the averages ± standard deviation from triplicate experiments. * Indicates significantly different from wild type for $p < 0.05$. KD – knock down.

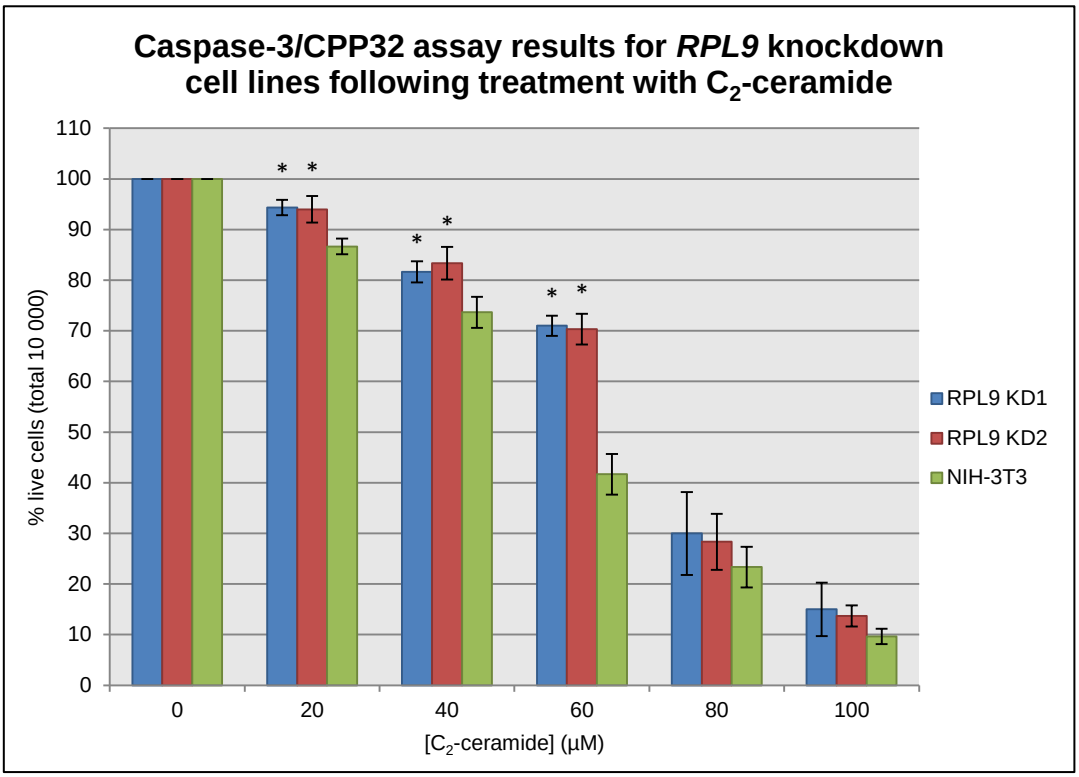

Figure 2.25: Results of testing for resistance to apoptosis in *RPL9* knockdown cell lines, as compared to wild type NIH-3T3 cells, by means of the Caspase-3/CPP32 assay following treatment of C_2-ceramide for 24 hrs. Values are the averages ± standard deviation from triplicate experiments. * Indicates significantly different from wild type for $p < 0.05$. KD – knock down.

APOPercentage™ assays, cells transfected with knockdown constructs one and two showed similar results, with only slight differences in the percentage of live cells and the two largest differences, 4.3% and 3.3%, also being the only two instances above 3% (Fig. 2.20 and 2.24 respectively).

2.4 Conclusions

Both *LIAS* and *CYPA* are relatively novel to apoptosis and specific roles for these genes in the apoptotic process are yet to be elucidated. This section aims to explore the possibility of a functional role for *LIAS* and *CYPA* in apoptosis and to possibly ascertain reasons why resistance to apoptosis would be associated with knockdown of these genes.

2.4.1 Potential roles for *LIAS* in apoptosis

The *LIAS* gene encodes for an enzyme known as lipoic acid synthetase (LIAS). This enzyme is located in the mitochondria where it fulfils a crucial role in the biosynthesis of α-lipoic acid (LA), which in turn is an essential co-factor for four multi-enzyme complexes, namely pyruvate dehydrogenase (PDH), α-ketoglutarate dehydrogenase (KGDH), the branched-chain α-keto acid dehydrogenase (BCKDH) complex and the glycine cleavage system (GCS) (Booker, 2004; Morikawa et al., 2001). Even though the exact biosynthetic pathway of LA remains unclear in mammalian cells, the pathway is well characterised in *E. coli* and thus served as a model for identifying homologs of the particular enzymes in various other species (see figure 2.26 and table 2.4) (Schonauer et al., 2009). Indeed, a yeast (LIP5) and mouse (Lias) homolog for LIAS have been identified (Morikawa et al., 2001; Sulo and Martin, 1993). In *E. coli*, the *de novo* synthesis of LA utilises octanoyl-acyl carrier protein (octanoyl-ACP) as a substrate (Cronan et al., 2005; Jordan and Cronan, 2003; Schonauer et al., 2009). To produce LA, LipA (the homolog for LIAS) catalyses the insertion of two sulphur atoms at positions C-6 and C-8 of octanoyl-ACP. This reaction can either precede or follow the transfer of octanoyl-ACP to a target protein, which is facilitated by the enzyme LipB. Target proteins are the E2 subunits and H-protein of the PDH, KGDH and BCKDH and GCS, respectively. An additional salvage pathway has also been described in *E. coli* that is associated with LA taken up exogenously by the cell. This pathway requires the action of the LplA enzyme and corresponding homologs has also been identified in mouse and human (Cronan et al., 2005; Jordan and Cronan, 2003; Schonauer et al., 2009).

The function of LIAS is clear enough, biosynthesis of LA, and the enzyme itself seems to have no other potential function or link to the apoptotic pathway. A more likely candidate though, is the product of LIAS's enzymatic function. *De novo* synthesis of LA takes place at the site where it is

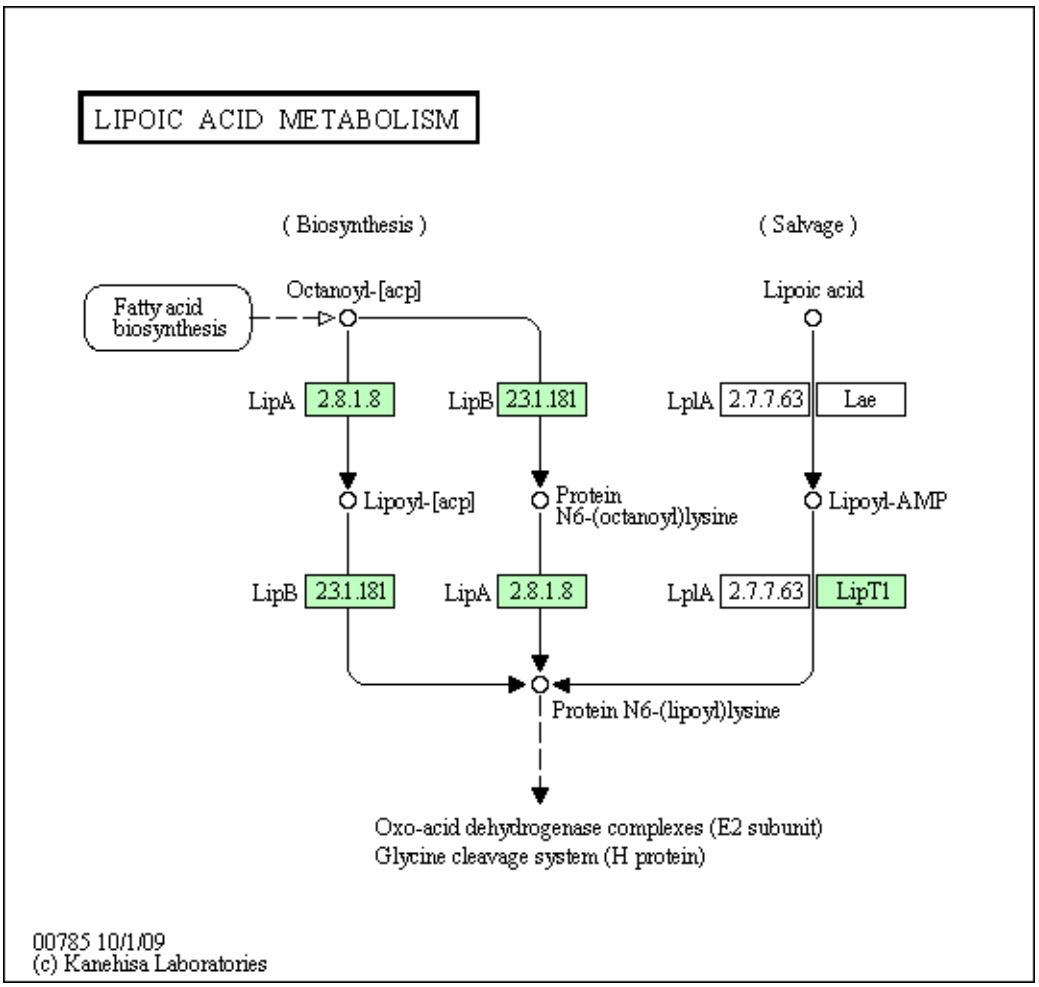

Figure 2.26: Pathway for LA metabolism according to the KEGG Pathway Database (hsa00785, accessed 25/07/2012)

Table 2.4: Homologs of enzymes involved in LA metabolism across various species[a]

Pathway	*Homo sapiens*	*Mus musculus*	*Saccharomyces cerevisiae*	*Escherichia coli*
De novo	LIAS	Lias	LIP5	LipA
De novo	LIPT2	Lipt2	LIP2	LipB
Salvage	LIPT1	Lipt1	AIM22 (putative)	LplA

[a]According to GeneCards® Database (accessed 25/07/2012)

needed as an essential co-factor (Cronan et al., 2005). PDH and KGDH are mitochondrial enzyme complexes that take part in the tricarboxylic acid cycle (TCA), while BCKDH and GCS is involved in the metabolism of branched-chain amino acids (leucine, isoleucine and valine) and the decarboxylation of glycine, respectively, in the same cellular compartment (Cronan et al., 2005; Perham, 2000). All four enzyme complexes are described as lipoyl dependent (Cronan et al., 2005).

PDH and KGDH represent key enzymes in the TCA cycle and both contribute to the production of NADH. In addition, PDH also serves as the link between glycolysis and the TCA cycle (Cronan et

al., 2005). Since PDH and KGDH can not function without LA as a co-factor, one can assume that a decrease in LA would significantly impair the activities of these enzyme complexes. In this case, decreased PDH and KGDH activity could result in decreased NADH levels and several studies has shown that this can lead to decreased NADH-linked (also referred to as state 3) respiration (Humphries et al., 1998; Lucas and Szweda, 1999; Nulton-Persson et al., 2003; Nulton-Persson and Szweda, 2001). Moreover, these groups also showed that inactivation of LA directly resulted in decreased NADH-linked respiration through inhibition of PDH and KGDH (Applegate et al., 2008; Humphries and Szweda, 1998). In addition, another group reported that silencing of *LIAS* by means of siRNA constructs resulted in decreased mitochondrial LA levels, including LA bound to the E2 subunits of PDH and KGDH (Padmalayam et al., 2009). Compromised NADH-linked respiration has the potential to negatively affect ATP synthesis; another consequence reported by one of the above mentioned groups (Nulton-Persson and Szweda, 2001). This in turn could result in the up-regulation of glycolysis in order to meet the energy demand of the cell. High glycolytic rates have been shown to successfully compensate for defective mitochondrial respiration in cells harbouring different mitochondrial backgrounds (von Kleist-Retzow et al., 2007). Even though the glycolytic pathway seems inadequate in meeting the energy demand of a cell since it only produces 2 moles ATP per mole glucose compared to the 36 moles ATP produced from respiration, the pathway can occur at a much faster rate the respiration, lending it the ability to sustain growth of even highly proliferating cells like lymphocytes and those of unicellular organisms like *S. cerevisiae* (Feron, 2009; Gatenby and Gillies, 2004; Ristow, 2006; Vander Heiden et al., 2009; Warburg, 1956).

The above mentioned cascade of events illustrates a phenotype similar to that seen in many tumours; a phenotype referred to as a Warburg effect. In 1956, Otto Warburg hypothesised that all cancers resulted from strikingly high rates of glycolysis in conjunction with attenuated mitochondrial respiration (Warburg, 1956). The latter part of his hypothesis was suggested to be the result of a “damaged respiration”; subsequently forcing the cell to compensate with increased glycolysis (DeBerardinis et al., 2008; Warburg, 1956). This unique phenotype results in the conversion of glucose to lactate, which is an expected outcome under hypoxic conditions; however, the phenotype is also present under normal oxygen tension and is thus described as anaerobic glycolysis (Tennant et al., 2009; Warburg, 1956; Wu et al., 2007). Two distinct characteristics of the Warburg effect represent potential mechanisms for resistance to apoptosis, especially with regards to the malignant transformation of cells. Firstly, high glycolytic rates result in the accumulation of lactic acid and subsequent acidification of the immediate extracellular environment (Gatenby and Gillies, 2004; Grinstein et al., 1989). This is facilitated by the activity of H^+ transporters, such as the Na^+/H^+ antiport, which functions to maintain normal intracellular pH by pumping H^+ ions out of the cell (Grinstein et al., 1989). Intracellular acidosis typically results in apoptosis, and up-regulation of H^+ transporters has been observed in tumour cells (Gatenby and

Gillies, 2004). In addition, the vacuolar H^+-ATPase transporter has been shown to provide resistance to apoptosis in neutrophils (Gatenby and Gillies, 2004; Gottlieb et al., 1995). Moreover, the activity of H^+ transporters has been suggested to play a vital role in cellular proliferative responses and is activated by various mitogens (Grinstein et al., 1989). An acidic extracellular environment has also been suggested to contribute to tumour invasion and metastasis (Gatenby and Gillies, 2004; Raghunand et al., 2003). Evidence supporting this statement includes increased activity of the vascular endothelial growth factor (VEGF), which plays a key role in angiogenesis, upon acidosis in human cancer cells and acid-mediated degradation of the extracellular matrix by cathepsins, as well as various other studies reporting increased invasion and metastatic abilities of cells cultured in acidic environments (Martínez-Zaguilán et al., 1996; Rozhin et al., 1994; Schlappack et al., 1991; Shi et al., 2001). In addition, acidosis can be mutagenic and potentially clastogenic (Gatenby and Gillies, 2004). The process of carcinogenesis is often described as somatic evolution; cells acquiring unique and beneficial mutations are selected for in a manner analogous to Darwinian evolution. Tumour cells are thus able to proliferate in an acidic microenvironment to which they are adapted, either through mutations or epigenetic changes, while normal cell populations are destroyed (Gatenby and Gillies, 2004).

A second characteristic present during a lack of LA, and also of the Warburg effect, that can potentially result in resistance to apoptosis is decreased NADH levels. During mitochondrial respiration, NADH is produced in the TCA cycle and is subsequently used to drive the flow of electrons through the electron transport chain (ETC) to produce ATP (Fernie et al., 2004). Complexes of the ETC are known sites of ROS production and constitute the primary intracellular source of oxygen radicals; thus, it would seem logical to expect reduced production of ROS under conditions of decreased NADH levels such as with a lack of LA availability (Cadenas and Davies, 2000; Turrens, 2003). Likewise, Nulton-Persson and colleague Sweda suggested that the inactivation of TCA enzymes generating reducing equivalents would limit the production of ROS, such as O_2^- and H_2O_2 (Nulton-Persson and Szweda, 2001). Moreover, by measuring metabolic rates and ROS production in resting and proliferating cells, Brand and colleague Hermfisse suggested that proliferating cells rely on the glycolytic breakdown of glucose to lactate to limit the production of ROS during the critical phases of DNA replication and cell division (Brand and Hermfisse, 1997). A role for ROS in apoptosis, as well as in its activation, is widely known (Cai and Jones, 1998; Chandra et al., 2000; Hampton and Orrenius, 1998). Several different ROS are known to induce apoptosis, while the generation of ROS has been reported in apoptosis induced by a variety of agents. In addition, antioxidants have been shown to effectively block apoptosis, while the broad-spectrum Bcl-2 anti-apoptotic protein also holds antioxidant properties (Cai and Jones, 1998; Chandra et al., 2000; Hampton and Orrenius, 1998). Thus, it would seem that one can suggest that the potentially limited production of ROS under conditions of LA deficiency could provide cells with the ability to resist ROS-mediated apoptosis. In addition to possibly limiting ROS

production, an aerobic glycolytic phenotype can also assist in the removal of ROS (Brand and Hermfisse, 1997; Nath et al., 1995; Spitz et al., 2000). Antioxidant properties in the form of H_2O_2 scavenging have previously been reported for the end product of glycolysis, namely pyruvate. Furthermore, glycolytic intermediates can also be redirected into the pentose phosphate pathway, producing nicotinamide adenine dinucleotide phosphate (reduced, NADPH), which by virtue of its redox status is able to provide reducing equivalents to other essential antioxidants, thus assisting the cells' natural antioxidant defence network (Brand and Hermfisse, 1997; Nath et al., 1995; Spitz et al., 2000; Vander Heiden et al., 2009). In contrast, it has also been shown that ROS are important mediators of mitogenic signalling in tumour cells; functioning to promote malignant transformation and cellular proliferation and suppressing apoptosis (Fruehauf and Meyskens, 2007). Various signalling pathways such as certain growth factor receptor pathways, cytokine and interleukin pathways engage ROS in some way or another (Finch et al., 2006; Fruehauf and Meyskens, 2007; Thannickal and Fanburg, 2000; Valko et al., 2006). In addition, ROS also promote tumorigenesis by damaging nucleic acids, proteins and lipids (Fruehauf and Meyskens, 2007; Valko et al., 2006). Removal of ROS seems to negatively affect tumour growth and proliferation, as shown by the overexpression of important components of the antioxidant defence network such as manganese superoxide dismutase (MnSOD), glutathione peroxidase and catalase in *in vitro* and *in vivo* studies (Finch et al., 2006; Liu et al., 2006; Ough et al., 2004). Being a potent antioxidant itself and, along with its redox partner dihydrolipoic acid (DHLA), being capable of regenerating another important antioxidant namely glutathione (Moini et al., 2002; Navari-Izzo et al., 2002), one can suggest that a lack of LA in the above mentioned scenario can have a negative impact on the cell's ability to remove ROS; thus resulting in a thriving ROS-mediated mitogenic signalling capacity able to withstand apoptosis.

The two scenarios mentioned above seem to contradict each other; is ROS harmful or beneficial to tumour cells? And what about normal cells? The answer might be both, although certain terms and conditions might apply. The effect of ROS on a cell seems to depend on the status (i.e. normal or malignant) of the cell and the initial redox status of that cell (Dozio et al., 2010; Fruehauf and Meyskens, 2007). For normal cells, low levels of ROS seems to be beneficial as it promotes physiological cell growth (Fruehauf and Meyskens, 2007; Trachootham et al., 2009). However, with increasing levels of ROS, damage to DNA and other essential molecules can occur, potentially resulting in the malignant transformation of the cell (Dozio et al., 2010; Fruehauf and Meyskens, 2007; Trachootham et al., 2009). Tumour cells display inherently higher levels of ROS which, in comparison with the low levels present in normal cells, enables mitogenic signalling and assists in cellular proliferation (Dozio et al., 2010; Fruehauf and Meyskens, 2007; Trachootham et al., 2009). Again, as with normal cells, too much ROS can also be harmful to tumour cells, and can potentially result in the induction of apoptosis (Fruehauf and Meyskens, 2007; Trachootham et al., 2009). These events have led to the proposal of two therapeutic strategies in terms of modulating ROS

levels for the treatment of cancer; to either remove ROS in order to dampen mitogenic signalling and inhibit proliferation or to increase ROS above the threshold in order to facilitate activation of apoptotic pathways (Dozio et al., 2010; Fruehauf and Meyskens, 2007; Shi et al., 2008).

Both therapeutic strategies seem to be applicable to LA, as reported by studies investigating the effect of its exogenous application to tumour cells. LA was shown to be capable of inducing apoptosis, although the particular mechanism differed with regards to the change in ROS levels (Dozio et al., 2010; Shi et al., 2008; Simbula et al., 2007; Wenzel et al., 2005). Some researchers reported that LA was able to induce apoptosis in tumour cells by indirectly increasing the production of ROS through facilitating increased mitochondrial respiration and electron flow through the ETC, while others reported a decrease in ROS preceding apoptosis (Dozio et al., 2010; Shi et al., 2008; Wenzel et al., 2005). Simbula and colleagues also reported an increase in ROS production upon LA treatment, but failed to speculate why (Simbula et al., 2007). In addition, LA failed to induce apoptosis in normal cells (Van de Mark et al., 2003; Wenzel et al., 2005). Most of these researchers made note of these contrasting effects and also attributed it to be subjective to the status of the cell, the inherent redox status as well as experimental conditions (Shi et al., 2008; Wenzel et al., 2005).

LA also functions as a co-factor for the H-protein in the GCS (Booker, 2004; Dinopoulos et al., 2005). This enzyme complex represents the major catabolic pathway for the amino acid glycine (Dinopoulos et al., 2005; Kikuchi et al., 2008). The pathway catalyses the oxidative cleavage of glycine to produce carbon dioxide, tetrahydrofolate and ammonium in a reversible reaction (Kikuchi et al., 2008). LA is covalently attached to the H-protein, designated as the carrier-protein, where it shuttles the reaction intermediate between the active sites of the other proteins that make up the enzyme complex in a manner that is similar to that seen in the keto acid dehydrogenase complexes (Kikuchi et al., 2008). Alternative pathways for glycine degradation do exist; however, the pathways seem to be limited in their capacity to degrade glycine when compared to the GCS (Kikuchi et al., 2008). Thus, adequate degradation of the amino acids needs to take place via the GCS, for which LA is required. LA deficiency can dramatically reduce the activity of the GCS; as supported by a case study by Hiraga and colleagues (1981). The group reported that a mutant H-protein devoid of LA exhibited only 4% specific activity when compared to that of a normal H-protein (Hiraga et al., 1981). In this particular case study, a patient presenting with this mutant H-protein suffered from non-ketotic hyperglycinemia (NKH), also known as glycine encephalopathy. Patients suffering from this autosomal recessive disease exhibit severe neurological symptoms including mental retardation, seizures, progressive lethargy and hypotonia and usually die while still in infancy (Dinopoulos et al., 2005; Kikuchi et al., 2008). The neurological symptoms are suggested to result from the interaction between the accumulated glycine and inhibitory neurons in the spinal cord and brain stem as well as interactions with *N*-methyl-$_D$-aspartate (NMDA) receptors in the cerebral cortex (Applegarth and Toone, 2006; Dinopoulos et al., 2005; Kikuchi et al., 2008).

It would seem reasonable to speculate that LA deficiency can potentially have pathological implications similar to that seen in patients with NKH, although the full complement of implications would most likely be limited to an *in vivo* environment and may not be applicable to a cell-culture based *in vitro* setting, as with this study. Neuronal cell lines could provide a more appropriate background to evaluate the effect of LA deficiency on NKH in an *in vitro* study. However, there seems to be no other possible connection between elevated glycine levels and resistance to apoptosis, suggesting that the apoptotic resistance seen in this study was not mediated by an effect on the GCS.

Finally, LA is also an essential co-factor for the E2 component of the BCKDH complex (Booker, 2004; Naik and Huang, 2004). This complex is responsible for the degradation of the branched-chain amino acids (BCAA), namely leucine, isoleucine and valine (Ribeiro et al., 2008; Ævarsson et al., 2000). Reduced functionality of the BCKDH complex results in the accumulation of the BCAA and their corresponding branched-chain keto-acids. A heritable genetic disease described by this pathophysiology has also been characterised and is referred to as maple syrup urine disease (MSUD) (Ribeiro et al., 2008; Ævarsson et al., 2000). Similarly to NKH, MSUD also presents with severe neurological deficits while the classical, and most severe form of the disease, displays a high fatality rate among infants (Ævarsson et al., 2000). Symptoms of MSUD include seizures, apnea, mental retardation, ataxia and psychomotor delay (Naik and Huang, 2004; Ribeiro et al., 2008). The molecular mechanisms behind MSUD are however still an uncertainty although complications such as neurotoxicity, demyelination and reduced mitochondrial respiration has been proposed (Jouvet et al., 2000; Ribeiro et al., 2008). MSUD displays significant mutational heterogeneity and include mutations in the E2 subunit of the complex, resulting in impaired or complete lack of function for this subunit (Herring et al., 1991; Naik and Huang, 2004). A deficiency for LA is likely to have a similar effect on the BCKDH; however, as noted with the GCS and NKH, it is likely that MSUD will only be expressed in full in an *in vivo* setting or partially in *in vitro* studies with neuronal cells. The same conclusion can thus be reached since it seems that there is no other link between apoptotic resistance and accumulated BCAA.

A significant amount of research spanning several decades provide valid arguments for the beneficial role of exogenously administered LA. This includes beneficial and preventative roles in diseases such as Alzheimer's, Parkinson's, Multiple Sclerosis, hemochromatosis, lipotoxicity, obesity, angiotensin II-induced renal injury and certain risk factors for cardiovascular diseases (Bharath et al., 2002; Holmquist et al., 2007; Kim et al., 2004; Lee et al., 2006; Marracci et al., 2002; Mervaala et al., 2003; Smith et al., 2004; Wollin and Jones, 2003). In addition, LA also shows great promise in diabetes-associated cataracts, nephropathy, atherosclerosis and cardiovascular complications (Obrosova et al., 1998; Obrosova et al., 2003; Smith et al., 2004; Yi and Maeda, 2006). Most of these researchers' suggestions are based on the antioxidant properties of LA and DHLA. However, studies investigating the effects of LA, or LIAS, deficiency are rare,

especially those not in conjunction with other illnesses. In 2011, Johannes Mayr and colleagues reported on the case of young boy diagnosed with LIAS deficiency (Mayr et al., 2011). Genetic analysis revealed a homozygous mutation in a highly conserved region of *LIAS* while immunoblot assays revealed a severe reduction in lipoylated PDH and KGDH. The group was however unable to determine the state of the GCS and BCKDH since a liver sample was not available. The child presented with seizures and muscle hypotonia as early as three days after birth, which progressively worsened. Additional symptoms included elevated glycine levels, pronounced lactic acidosis, poor feeding, brain edema, mild hypertrophic cardiomyopathy and severely retarded mental and motor development. The child succumbed to a severe respiratory tract infection at the age of four. The group suggested that the deficiency in functional LIAS resulted in a severe metabolic crisis, producing symptoms similar to that seen in NKH, which was subsequently complicated by brain damage caused by the edema (Mayr et al., 2011). In the same year, another group reported on the case study of 10 individuals from nine non-related families that presented with suspect symptoms (Navarro-Sastre et al., 2011). Lactic acidosis and hyperglycinemia were common among all the individuals, while major symptoms included a selection of neurological regression and encephalopathy, pulmonary hypertension and a failure to thrive. Symptoms presented very early in life and all individuals died before or at the age of 15 months. Genetic analysis revealed a common mutation in the *NFU1* gene which encodes the iron-sulphur cluster assembly protein NFU1. NFU1 was shown to be specifically required for the formation of the iron-sulphur cluster of LIAS; hence, the mutated NFU1 resulted in a significant reduction in LA synthesis and corresponding lipoylated proteins. Taking together their results, the group reported that the 10 individuals presented with biochemical features that correlates well with a deficiency in LA synthesis (Navarro-Sastre et al., 2011). Finally, a study by Yi and Maeda revealed that LIAS is required for the early embryonic development of mice by generating mice embryos carrying a null allele for *LIAS* (Yi and Maeda, 2005). Heterozygous mice expressing 50% of the normal mRNA levels were able to develop normally even though they presented with reduced glutathione levels. In contrast, mice embryos homozygous for the null allele failed to survive past 9.5 dpc (days post coitum). The timing of the lethal effect suggested that the lack of LA severely compromised the cellular metabolism of the embryo. The researchers speculated that LIAS is required for normal embryonic development due to LA's role as an essential cofactor but also partly due to its antioxidant properties (Yi and Maeda, 2005).

When taken together, the above mentioned studies clearly indicates that LIAS is required for normal early development in mammals, and that LIAS deficiency holds severe and lethal consequences. The fact that the individuals in the case studies survived the gestation period hints to some kind of bypass mechanism for the requirement of LIAS that is present in humans but absent in mice; a hint also alluded to by Navarro-Sastre and colleagues (Navarro-Sastre et al., 2011). When comparing these results to those obtained in this study, one can conclude that the

critical necessity for LIAS is most likely temporal, as well as cell and/or tissue type dependent. The affected stage of life in both the case studies and the murine study represented the early developmental stage, while the symptoms presented in the case studies were mostly of neurological descent. The reduced PDH activities coupled with lactic acidosis reported in the case studies supports the hypothesis that a deficiency in LIAS can results in cellular environments of an acidic nature; in non-developing tissues, this might potentially result in mutations favouring apoptotic resistance and malignant transformation. Deficiency in LIAS would also result in a diminished antioxidant network, as supported by the finding that heterozygous mice for the null allele displayed reduced glutathione levels. Whether this decrease can promote resistance to apoptosis in non-developing tissues through reduced mitogenic signalling or resistance to ROS-mediated apoptosis still needs to be confirmed.

In conclusion, even though the postulations made in this chapter of LIAS deficiency and its role in apoptosis resistance (or malignant transformation) are speculative, it provides a foundation that can be explored further in future work. This would most likely need to include the investigation of the effect of LIAS deficiency in different cell and tissue types and also *in vivo* models in order to determine whether a lack of LA is able to adequately lead to malignant tumour formation over longer period's of time.

2.4.2 Potential roles for *CYPA* in apoptosis

The second gene identified in this study to show a potential role in resistance to apoptosis is *CYPA*. This gene encodes a protein product of approximately 18 kDa in size, also designated as cyclophilin A (CYPA). The protein is ubiquitously expressed and is located in the cytosol (Galat, 1993). It belongs to the cyclophilin family which comprises of 15 members in humans, including CYPB, CYPC and CYPD (Zhu et al., 2007). Proteins in this family are referred to as peptidylproline *cis-trans*-isomerases (PPIases), since they catalyse the *cis-trans* transfiguration of peptidylproline bonds in their substrates, and have also been identified as targets for cyclosporine A (CsA), an immunosuppressive drug used in cases of organ transplant and graft versus host disease (Galat, 1993; Handschumacher et al., 1984). The binding affinity for CsA differs between the members of the family, with CYPA representing the major intracellular target (Galat, 1993; Wang and Heitman, 2005). Binding of CsA abolishes the PPIase activity of these proteins (Galat, 1993). The protein family maintains a high level of phylogenetic sequence conservation, suggesting an important physiological role; however, $CYPA^{-/-}$ embryonic stem cells develop and differentiate as normal, indicating that CYPA is not essential for mammalian cell viability (Colgan et al., 2000).

A major function for cyclophilins is made possible by their PPIase activity (Fig. 2.27). Although peptide bonds can exist in either a *trans* or *cis* configuration, the latter state is necessary for *de novo* protein folding as well as refolding following the transport of proteins across cellular

membranes (Wang and Heitman, 2005). Cyclophilins catalyse this isomerisation reaction, an otherwise rate-limiting step, by stabilising the transition state and accelerating the re-configuration (Wang and Heitman, 2005). Thus, cyclophilins are essential to various protein folding and modification processes, which includes the maturation of newly synthesised proteins, protein transport and the association of multiple proteins during complex formation as well as protein repair following damage by environmental stresses (Galat, 1993; Wang and Heitman, 2005; Yao et al., 2005). In particular, CYPA also exhibits certain immune-related functions; firstly as a potent chemo-attractant for leukocytes and monocytes and then also as mediator of human immunodeficiency virus (HIV)-1 infection (Sherry et al., 1992; Wang and Heitman, 2005; Xu et al., 1992; Yao et al., 2005). With the latter function, CYPA has been shown to promote the formation as well as infectivity of HIV-1 virions by interacting with the HIV-1 Gag protein, by means of CD147 interaction, or even both (Pushkarsky et al., 2001; Thali et al., 1994; Wang and Heitman, 2005; Yao et al., 2005).

Compared with *LIAS*, determining a potential role for *CYPA* in resistance to apoptosis might prove to be more straightforward, although some contrasting reports do exist. Numerous studies have reported a vital role for CYPA in the execution of apoptosis. Recombinant CYPA proteins were shown to possess nuclease activity capable of facilitating DNA degradation during apoptosis (Montague et al., 1994; Montague et al., 1997). The DNase activity were dependent on Ca^{2+}/Mg^{2+}, a characteristic commonly seen in apoptotic nucleases (Robertson et al., 2000; Samejima and Earnshaw, 2005). In addition, the DNase activity resulted in the production of 3'-OH termini, which serves as the foundation for apoptosis detection by means on the TUNEL assay, and was abrogated by compounds that prevent DNA degradation and apoptosis (Montague et al., 1994; Montague et al., 1997). Since the addition of CsA failed to prevent DNA degradation, it was also concluded that this characteristic was separate from the protein's isomerase activity. It was also hypothesised that CYPA does not act alone and might require a co-factor or additional protein to facilitate DNA degradation (Montague et al., 1997). Since then, a protein interaction has been established between CYPA and AIF (Candé et al., 2004). Through a series of experiments Candé and colleagues provided substantial evidence for the cooperation of these two proteins in the degradation of DNA and subsequent execution of apoptosis. The group showed that CYPA and AIF colocalised in the nucleus upon apoptosis induction and that a physical interaction was restricted to apoptotic cells. In accordance with the above mentioned studies, CsA had no effect on the CYPA-AIF interaction. Recombinant CYPA and AIF alone were unable to degrade naked supercoiled plasma DNA while a combination of the proteins resulted in non-specific DNA degradation. Levels of apoptosis in CYPA-deficient Jurkat cells were significantly lower compared to the wild type; a resistance that correlated with reduced large-scale DNA degradation. The same was true for cells devoid of AIF but expressing CYPA (Candé et al., 2004). Additional support for a direct CYPA-AIF interaction has been provided by other studies investigating the role of apoptosis

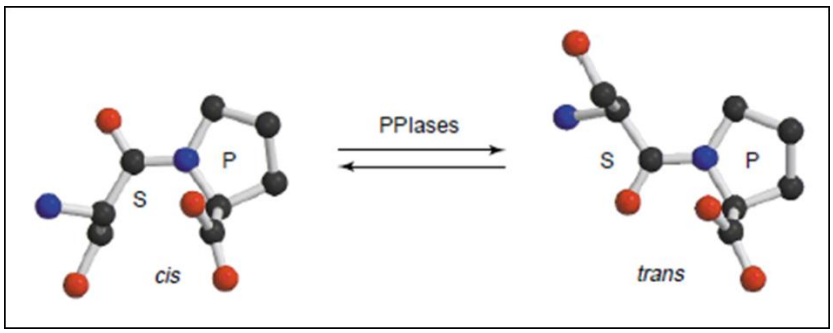

Figure 2.27: Illustration of the *cis-trans* isomerisation reaction catalysed by PPIases. P – proline; S – serine. Adapted from Lu et al., 2002.

in various diseases. In a mouse model for amyotrophic lateral sclerosis (ALS), a disease characterised by progressive motor neuron loss, CYPA was shown to colocalise with AIF in the nuclei of motor neurons in diseased mice (Tanaka et al., 2011). A lack of CYPA was also shown to be neuroprotective *in vivo* after exposure of *CYPA*$^{-/-}$ mice to cerebral hypoxia-ischemia (Zhu et al., 2007). The nuclear translocation of AIF was prevented in these mice while the translocation of CYPA was also prevented in AIF-deficient harlequin mice. The group also showed that the neuroprotective phenotype seen in CYPA deficient cells was not associated with other mitochondrial cell-death effectors, caspases or calpains, since none of these were affected by the lack of CYPA as compared with wild type cells (Zhu et al., 2007). The dependence of AIF on CYPA was also reported in yeast cells where disruption of the yeast CYPA homologue, *CPR1*, prevented cell death induced by the overexpression of the yeast AIF homologue, Aif1p (Wissing et al., 2004). This effect was specific to *CPR1* since disruption of the CYPB homologue, *CPR2*, failed to rescue cells from apoptosis (Wissing et al., 2004). In contrast to the interaction with AIF, a protein normally associated with caspase-independent apoptosis and where the interaction does not seem to involve isomerase activities, CYPA was also reported to be directly involved in apoptosis by facilitating caspase activation through its isomerase properties (Capano et al., 2002). In this *in vitro* study, CYPA expression was inhibited by treatment with antisense oligodeoxynucleotides. Upon apoptosis induction with a combination of glutamate and nitric oxide, this resulted in substantially decreased activation of caspases 8, 9 and 6, while a weaker effect was seen in the activation of caspase 3. Treatment of cells with CsA revealed comparable results and since CsA inhibits CYPA through binding its PPIase domain, this was indicative of the involvement of CYPA's isomerase activity. The authors suggested that CYPA is most likely a component in a complex involved in caspase processing (Capano et al., 2002). Taking together the above mentioned, CYPA seems to play a role in the execution of both caspase dependent and independent apoptosis, of which the involvement is of a pro-apoptotic nature. Based on this, it would seem likely that cells deficient in the CYPA protein would exhibit an inadequate apoptotic process, rendering the cell resistant to apoptotic induction.

Opposing roles for CYPA in terms of apoptosis and cellular proliferation is however apparent when taking into account studies measuring the expression of CYPA in cancer. Numerous studies have shown CYPA to be overexpressed in a variety of tumour cell lines and tissues, which includes cancers of the lung (non-small and small cell lung cancer), prostate, brain, pancreas, tongue and oesophagus (Campa et al., 2003; Choi et al., 2007; Huang et al., 2011b; Li et al., 2006; Qi et al., 2008; Shen et al., 2004; Sun et al., 2011; Yang et al., 2007). These opposing roles might however be dependent on the state of the cell. In order for CYPA to function as a pro-apoptotic protein, an association with AIF is required and, as shown by Candé and colleagues, CYPA is unable to induce DNA fragmentation on its own (Candé et al., 2004). On the other hand, AIF is located in the mitochondria under physiological conditions and is only released upon apoptotic induction, which can include induction by camptothecin and ceramide (Candé et al., 2004; Joza et al., 2009; Modjtahedi et al., 2006; Susin et al., 1999). MOMP facilitates the release of AIF, which in turn is under the stringent control of the Bcl-2 family proteins (Susin et al., 1999; Valero et al., 2011). As described in chapter one, anti-apoptotic Bcl-2 family members bind and inhibit the pro-apoptotic members of the family, preventing them from initiating MOMP (Coultas and Strasser, 2003; Hengartner, 2000). As part of the defence strategy against apoptosis, tumour cells often prevent MOMP, and subsequent release of the apoptogenic proteins from the mitochondrial intermembrane space, by changing the ratio of the Bcl-2 family proteins to favour the anti-apoptotic members (Aouacheria et al., 2007; Fulda, 2010; Valero et al., 2011). Thus AIF often remains confined in the mitochondria in tumour cells; which would mean that CYPA is unable to perform its apoptotic function. The increased expression levels of *CYPA* can also potentially be associated with a state of malignancy. Tumour cells often face hypoxic conditions and the ability to maintain a proliferative state during hypoxia is a characteristic that is associated with poor prognosis and resistance to anticancer therapies (Birner et al., 2000; Harris, 2002). During hypoxia, tumour cells make certain changes in order to adapt to the low availability of oxygen, and this includes altering gene expression patterns. The transcription factor hypoxia inducible factor 1α (HIF-1α) is a major player in facilitating this adaptation by activating the expression of numerous hypoxia responsive genes through the binding of hypoxia-response elements (HRE) in the promoter regions of these genes (Harris, 2002). *CYPA* is potentially regulated by HIF-1α due to the presence of a HRE in the promoter region of this gene (Choi et al., 2007). The same study also revealed an association between increased CYPA expression and hypoxia; an association that was mediated by HIF-1α. Increased HIF-1α activity has been associated with tumour progression and the corresponding gene is also commonly overexpressed in a variety of tumours (Zhong et al., 1999). Thus, these reports provide a potential foundation for the high levels of CYPA in tumour cells and tissues. A likely role for the up-regulation of CYPA in tumours is one that opposes its role in apoptosis, i.e. cellular proliferation. A study performed by Li and colleagues (2006) revealed that the exogenous administration of CYPA to pancreatic tumour cells resulted in significant increases in cellular proliferation (Li et al., 2006). This effect is however not restricted to tumour cells, since exogenous

CYPA was also able to significantly stimulate the proliferation of human aorta smooth muscle cells and human lung microvascular endothelial cells (Yang et al., 2005).

It is thus possible for CYPA to have opposing roles in the cell; roles that are determined by the state of a cell. Upon apoptosis induction in normal cells, like the cells used in this study, CYPA is likely to have an important cooperative function alongside AIF in the execution of apoptosis in such a way that without proper CYPA levels, apoptosis is likely to fail. However in tumour cells, where mechanisms to avoid apoptosis are set in motion, CYPA is left, and most likely induced, to fulfil other functions that might favour the tumour cell. A promising avenue for future studies would be to validate these statements in matched healthy and tumour sample sets from different types of tissues. In addition, the specific role for CYPA in tumour cells needs to validated in different tumour types.

2.5 References

Ævarsson, A., Chuang, J.L., Max Wynn, R., Turley, S., Chuang, D.T., and Hol, W.G. (2000). Crystal structure of human branched-chain α-ketoacid dehydrogenase and the molecular basis of multienzyme complex deficiency in maple syrup urine disease. Structure *8,* 277-291.

Andrieu-Abadie, N., and Levade, T. (2002). Sphingomyelin hydrolysis during apoptosis. Biochim. Biophys. Acta, Mol. Cell Biol. Lipids *1585,* 126-134.

Aouacheria, A., Cibiel, A., Guillemin, Y., Gillet, G., and Lalle, P. (2007). Modulating mitochondria-mediated apoptotic cell death through targeting of Bcl-2 family proteins. Recent Pat DNA Gene Seq *1,* 43-61.

Applegarth, D.A., and Toone, J.R. (2006). Glycine encephalopathy (nonketotic hyperglycinemia): comments and speculations. Am. J. Med. Genet. *140A,* 186-188.

Applegate, M.A.B., Humphries, K.M., and Szweda, L.I. (2008). Reversible inhibition of α-ketoglutarate dehydrogenase by hydrogen peroxide: glutathionylation and protection of lipoic acid. Biochemistry *47,* 473-478.

Berns, K., Hijmans, E.M., Mullenders, J., Brummelkamp, T.R., Velds, A., Helmerikx, M., Kerkhoven, R.M., Madiredjo, M., Nijkamp, W., Weigelt, B.*, et al.* (2004). A large-scale RNAi screen in human cells identifies new components of the p53 pathway. Nature *428,* 431-437.

Bharath, S., Cochran, B.C., Hsu, M., Liu, J., Ames, B.N., and Andersen, J.K. (2002). Pre-treatment with R-lipoic acid alleviates the effects of GSH depletion in PC12 cells: implications for Parkinson's disease therapy. Neurotoxicology *23,* 479-486.

Birner, P., Schindl, M., Obermair, A., Plank, C., Breitenecker, G., and Oberhuber, G. (2000). Overexpression of hypoxia-inducible factor 1α is a marker for an unfavorable prognosis in early-stage invasive cervical cancer. Cancer Res. *60,* 4693-4696.

Booker, S.J. (2004). Unraveling the pathway of lipoic acid biosynthesis. Chem. Biol. *11,* 10-12.

Brand, K., and Hermfisse, U. (1997). Aerobic glycolysis by proliferating cells: a protective strategy against reactive oxygen species. FASEB J. *11,* 388-395.

Cadenas, E., and Davies, K.J.A. (2000). Mitochondrial free radical generation, oxidative stress, and aging. Free Radical Biol. Med. *29,* 222-230.

Cai, J., and Jones, D.P. (1998). Superoxide in apoptosis. J. Biol. Chem. *273,* 11401-11404.

Campa, M.J., Wang, M.Z., Howard, B., Fitzgerald, M.C., and Patz, E.F. (2003). Protein expression profiling identifies macrophage migration inhibitory factor and cyclophilin A as potential molecular targets in non-small cell lung cancer. Cancer Res. *63,* 1652-1656.

Candé, C., Vahsen, N., Kouranti, I., Schmitt, E., Daugas, E., Spahr, C., Luban, J., Kroemer, R.T., Giordanetto, F., Garrido, C., *et al.* (2004). AIF and cyclophilin A cooperate in apoptosis-associated chromatinolysis. Oncogene *23,* 1514-1521.

Capano, M., Virji, S., and Crompton, M. (2002). Cyclophilin-A is involved in excitotoxin-induced caspase activation in rat neuronal B50 cells. Biochem. J. *363,* 29-36.

Caplen, N.J., Parrish, S., Imani, F., Fire, A., and Morgan, R.A. (2001). Specific inhibition of gene expression by small double-stranded RNAs in invertebrate and vertebrate systems. Proc. Natl. Acad. Sci. USA *98,* 9742-9747.

Casadaban, M.J., and Cohen, S.N. (1980). Analysis of gene control signals by DNA fusion and cloning in *Escherichia coli*. J. Mol. Biol. *138,* 179-207.

Chandra, J., Samali, A., and Orrenius, S. (2000). Triggering and modulation of apoptosis by oxidative stress. Free Radical Biol. Med. *29,* 323-333.

Chen, D., Daniel, K.G., Chen, M.S., Kuhn, D.J., Landis-Piwowar, K.R., and Dou, Q.P. (2005). Dietary flavonoids as proteasome inhibitors and apoptosis inducers in human leukemia cells. Biochem. Pharmacol. *69,* 1421-1432.

Choi, K.J., Piao, Y.J., Lim, M.J., Kim, J.H., Ha, J., Choe, W., and Kim, S.S. (2007). Overexpressed cyclophilin A in cancer cells renders resistance to hypoxia- and cisplatin-induced cell death. Cancer Res. *67,* 3654-3662.

Colgan, J., Asmal, M., and Luban, J. (2000). Isolation, characterization and targeted disruption of mouse Ppia: cyclophilin A is not essential for mammalian cell viability. Genomics *68,* 167-178.

Coultas, L., and Strasser, A. (2003). The role of the Bcl-2 protein family in cancer. Semin. Cancer Biol. *13,* 115-123.

Cronan, J.E., Zhao, X., and Jiang, Y. (2005). Function, attachment and synthesis of lipoic acid in *Escherichia coli*. In Advances in Microbial Physiology, Poole, Robert K. ed., (London, UK: Academic Press) pp. 103-146.

Daniel, K.G., Gupta, P., Harbach, R.H., Guida, W.C., and Dou, Q.P. (2004). Organic copper complexes as a new class of proteasome inhibitors and apoptosis inducers in human cancer cells. Biochem. Pharmacol. *67,* 1139-1151.

DeBerardinis, R.J., Lum, J.J., Hatzivassiliou, G., and Thompson, C.B. (2008). The Biology of cancer: metabolic reprogramming fuels cell growth and proliferation. Cell Metab. *7,* 11-20.

Dinopoulos, A., Matsubara, Y., and Kure, S. (2005). Atypical variants of nonketotic hyperglycinemia. Mol. Genet. Metab. *86,* 61-69.

Dozio, E., Ruscica, M., Passafaro, L., Dogliotti, G., Steffani, L., Pagani, A., Demartini, G., Esposti, D., Fraschini, F., and Magni, P. (2010). The natural antioxidant alpha-lipoic acid induces p27Kip1-dependent cell cycle arrest and apoptosis in MCF-7 human breast cancer cells. Eur. J. Pharmacol. *641,* 29-34.

Dykxhoorn, D.M., Novina, C.D., and Sharp, P.A. (2003). Killing the messenger: short RNAs that silence gene expression. Nat. Rev. Mol. Cell Biol. *4,* 457-467.

Elbashir, S.M., Harborth, J., Lendeckel, W., Yalcin, A., Weber, K., and Tuschl, T. (2001). Duplexes of 21 -nucleotide RNAs mediate RNA interference in cultured mammalian cells. Nature *411,* 494-498.

Fadok, V., Voelker, D., Campbell, P., Cohen, J., Bratton, D., and Henson, P. (1992). Exposure of phosphatidylserine on the surface of apoptotic lymphocytes triggers specific recognition and removal by macrophages. J. Immunol. *148,* 2207-2216.

Fernie, A.R., Carrari, F., and Sweetlove, L.J. (2004). Respiratory metabolism: glycolysis, the TCA cycle and mitochondrial electron transport. Curr. Opin. Plant Biol. *7,* 254-261.

Feron, O. (2009). Pyruvate into lactate and back: from the Warburg effect to symbiotic energy fuel exchange in cancer cells. Radiother. Oncol. *92,* 329-333.

Finch, J.S., Tome, M.E., Kwei, K.A., and Bowden, G.T. (2006). Catalase reverses tumorigenicity in a malignant cell line by an epidermal growth factor receptor pathway. Free Radical Biol. Med. *40,* 863-875.

Fraser, A. (2004). RNA interference: human genes hit the big screen. Nature *428,* 375-378.

Friesen, C., Fulda, S., and Debatin, K. (1999). Cytotoxic drugs and the CD95 pathway. Leukemia *13,* 1854-1858.

Fruehauf, J.P., and Meyskens, F.L. (2007). Reactive oxygen species: a breath of life or death? Clin. Cancer Res. *13,* 789-794.

Fulda, S. (2010). Evasion of apoptosis as a cellular stress response in cancer. Int. J. Cell Biol. *2010,* DOI:10.1155/2010/370835.

Galat, A. (1993). Peptidylproline cis-trans-isomerases: immunophilins. Eur. J. Biochem. *216,* 689-707.

Gatenby, R.A., and Gillies, R.J. (2004). Why do cancers have high aerobic glycolysis? Nat. Rev. Cancer *4,* 891-899.

Gavrieli, Y., Sherman, Y., and Ben-Sasson, S.A. (1992). Identification of programmed cell death in situ via specific labeling of nuclear DNA fragmentation. J. Cell Biol. *119,* 493-501.

Golstein, P. (1998). Cell death in us and others. Science *281,* 1283.

Gottlieb, R.A., Giesing, H.A., Zhu, J.Y., Engler, R.L., and Babior, B.M. (1995). Cell acidification in apoptosis: granulocyte colony-stimulating factor delays programmed cell death in neutrophils by up-regulating the vacuolar H^+-ATPase. Proc. Natl. Acad. Sci. USA *92,* 5965-5968.

Grinstein, S., Rotin, D., and Mason, M.J. (1989). Na^+/H^+ exchange and growth factor-induced cytosolic pH changes: role in cellular proliferation. Biochim. Biophys. Acta, Rev. Biomembr. *988,* 73-97.

Gurtu, V., Kain, S.R., and Zhang, G. (1997). Fluorometric and colorimetric detection of caspase activity associated with apoptosis. Anal. Biochem. *251,* 98-102.

Hammond, S.M.B., Bernstein, E., Beach, D. and Hannon, G.J. (2000). An RNA-directed nuclease mediates post-transcriptional gene silencing in Drosophila cells. Nature *404,* 293.

Hampton, M.B., and Orrenius, S. (1998). Redox regulation of apoptotic cell death. Biofactors *8,* 1-5.

Handschumacher, R., Harding, M., Rice, J., Drugge, R., and Speicher, D. (1984). Cyclophilin: a specific cytosolic binding protein for cyclosporin A. Science *226,* 544-547.

Hannon, G.J. (2002). RNA interference. Nature *418,* 244.

Hannun, Y., and Obeid, L. (2008). Principles of bioactive lipid signalling: lessons from sphingolipids. Nat. Rev. Mol. Cell Biol. *9,* 139-150.

Harris, A. (2002). Hypoxia - a key regulatory factor in tumour growth. Nat. Rev. Cancer *2,* 38-47.

Heinrich, M., Neumeyer, J., Jakob, M., Hallas, C., Tchikov, V., Winoto-Morbach, S., Wickel, M., Schneider-Brachert, W., Trauzold, A., Hethke, A., *et al*. (2004). Cathepsin D links TNF-induced acid sphingomyelinase to Bid-mediated caspase-9 and -3 activation. Cell Death Differ. *11,* 550-563.

Hengartner, M. (2000). The biochemistry of apoptosis. Nature *407,* 770-776.

Herring, W., Litwer, S., Weber, J., and Danner, D. (1991). Molecular genetic basis of maple syrup urine disease in a family with two defective alleles for branched chain acyltransferase and localization of the gene to human chromosome 1. Am. J. Hum. Genet. *48,* 342-350.

Hiraga, K., Kochi, H., Hayasaka, K., Kikuchi, G., and Nyhan, W.L. (1981). Defective glycine cleavage system in nonketotic hyperglycinemia: occurrence of a less active glycine decarboxylase and an abnormal aminomethyl carrier protein. J. Clin. Invest. *68,* 525-534.

Holen, T. (2005). Mechanisms of RNAi: mRNA cleavage fragments may indicate stalled RISC. J. RNAi Gene Silencing *1,* 21-25.

Holmquist, L., Stuchbury, G., Berbaum, K., Muscat, S., Young, S., Hager, K., Engel, J., and Münch, G. (2007). Lipoic acid as a novel treatment for Alzheimer's disease and related dementias. Pharmacol. Ther. *113,* 154-164.

Hsiang, Y.H., Hertzberg, R., Hecht, S., and Liu, L.F. (1985). Camptothecin induces protein-linked DNA breaks via mammalian DNA topoisomerase I. J. Biol. Chem. *260,* 14873-14878.

Huang, W., Chen, C., Lin, Y., and Lin, C. (2011a). Apoptotic sphingolipid ceramide in cancer therapy. J. Lipids *2011,* doi:10.1155/2011/565316.

Huang, C., Sun, Z., Zhao, Y., Chen, X., Jia, J., and Zhang, W. (2011b). Increased expression of peroxiredoxin 6 and cyclophilin A in squamous cell carcinoma of the tongue. Oral Dis. *17,* 328-334.

Humphries, K.M., and Szweda, L.I. (1998). Selective inactivation of alpha-ketoglutarate dehydrogenase and pyruvate dehydrogenase: reaction of lipoic acid with 4-hydroxy-2-nonenal. Biochemistry *37,* 15835-15841.

Humphries, K.M., Yoo, Y., and Szweda, L.I. (1998). Inhibition of NADH-linked mitochondrial respiration by 4-hydroxy-2-nonenal. Biochemistry *37,* 552-557.

Jordan, S.W., and Cronan, J.,John E. (2003). The *Escherichia coli* lipB gene encodes lipoyl (octanoyl)-acyl carrier protein:protein transferase. J. Bacteriol. *185,* 1582-1589.

Jouvet, P., Rustin, P., Taylor, D.L., Pocock, J.M., Felderhoff-Mueser, U., Mazarakis, N.D., Sarraf, C., Joashi, U., Kozma, M., Greenwood, K., *et al*. (2000). Branched chain amino acids induce apoptosis in neural cells without mitochondrial membrane depolarization or cytochrome C release: implications for neurological impairment associated with maple syrup urine disease. Mol. Biol. Cell *11,* 1919-1932.

Joza, N., Pospisilik, J.A., Hangen, E., Hanada, T., Modjtahedi, N., Penninger, J.M., and Kroemer, G. (2009). AIF: not just an apoptosis-inducing factor. Ann. N. Y. Acad. Sci. *1171,* 2-11.

Kikuchi, G., Motokawa, Y., Yoshida, T., and Hiraga, K. (2008). Glycine cleavage system: reaction mechanism, physiological significance, and hyperglycinemia. Proc. Japan Acad., Ser. B *84,* 246-263.

Kim, M., Park, J., Namkoong, C., Jang, P., Ryu, J., Song, H., Yun, J., Namgoong, I., Ha, J., Park, I.*, et al.* (2004). Anti-obesity effects of α-lipoic acid mediated by suppression of hypothalamic AMP-activated protein kinase. Nat. Med. *10,* 727-733.

Lee, Y., Naseem, R.H., Park, B., Garry, D.J., Richardson, J.A., Schaffer, J.E., and Unger, R.H. (2006). α-Lipoic acid prevents lipotoxic cardiomyopathy in acyl CoA-synthase transgenic mice. Biochem. Biophys. Res. Commun. *344,* 446-452.

Li, M., Zhai, Q., Bharadwaj, U., Wang, H., Li, F., Fisher, W.E., Chen, C., and Yao, Q. (2006). Cyclophilin A is overexpressed in human pancreatic cancer cells and stimulates cell proliferation through CD147. Cancer *106,* 2284-2294.

Liu, J., Du, J., Zhang, Y., Sun, W., Smith, B., Oberley, L., and Cullen, J. (2006). Suppression of the malignant phenotype in pancreatic cancer by overexpression of phospholipid hydroperoxide glutathione peroxidase. Hum. Gene Ther. *17,* 105-116.

Lu, K.P., Liou, Y., and Zhou, X.Z. (2002). Pinning down proline-directed phosphorylation signaling. Trends Cell Biol. *12,* 164-172.

Lucas, D.T., and Szweda, L.I. (1999). Declines in mitochondrial respiration during cardiac reperfusion: Age-dependent inactivation of α-ketoglutarate dehydrogenase. Proc. Natl. Acad. Sci. USA *96,* 6689-6693.

Marracci, G.H., Jones, R.E., McKeon, G.P., and Bourdette, D.N. (2002). Alpha lipoic acid inhibits T cell migration into the spinal cord and suppresses and treats experimental autoimmune encephalomyelitis. J. Neuroimmunol. *131,* 104-114.

Martínez-Zaguilán, R., Seftor, E.A., Seftor, R.E.B., Chu, Y., Gillies, R.J., and Hendrix, M.J.C. (1996). Acidic pH enhances the invasive behavior of human melanoma cells. Clin. Exp. Metastasis *14,* 176-186.

Mathias, S., Pena, L., and Kolesnick, R. (1998). Signal transduction of stress via ceramide. Biochem. J. *335,* 465-480.

Mayr, J., Zimmermann, F., Fauth, C., Bergheim, C., Meierhofer, D., Radmayr, D., Zschocke, J., Koch, J., and Sperl, W. (2011). Lipoic acid synthetase deficiency causes neonatal-onset epilepsy, defective mitochondrial energy metabolism, and glycine elevation. Am. J. Hum. Genet. *89,* 792-797.

Mervaala, E., Finckenberg, P., Lapatto, R., Muller, D.N., Park, J., Dechend, R., Ganten, D., Vapaatalo, H., and Luft, F.C. (2003). Lipoic acid supplementation prevents angiotensin II-induced renal injury. Kidney Int. *64,* 501-508.

Meyer, M., Essack, M., Kanyanda, S., and Rees, J.G. (2008). A low-cost flow cytometric assay for the detection and quantification of apoptosis using an anionic halogenated fluorescein dye. BioTechniques *45,* 317-320.

Modjtahedi, N., Giordanetto, F., Madeo, F., and Kroemer, G. (2006). Apoptosis-inducing factor: vital and lethal. Trends Cell Biol. *16,* 264-272.

Moini, H., Packer, L., and Saris, N.L. (2002). Antioxidant and prooxidant activities of α-lipoic acid and dihydrolipoic acid. Toxicol. Appl. Pharmacol. *182,* 84-90.

Montague, J.W., Gaido, M.L., Frye, C., and Cidlowski, J.A. (1994). A calcium-dependent nuclease from apoptotic rat thymocytes is homologous with cyclophilin: recombinant cyclophilins A, B, and C have nuclease activity. J. Biol. Chem. *269,* 18877-18880.

Montague, J.W., Hughes, F.M., and Cidlowski, J.A. (1997). Native recombinant cyclophilins A, B, and C degrade DNA independently of peptidylprolyl *cis-trans*-isomerase activity. J. Biol. Chem. *272,* 6677-6684.

Morikawa, T., Yasuno, R., and Wada, H. (2001). Do mammalian cells synthesize lipoic acid?: identification of a mouse cDNA encoding a lipoic acid synthase located in mitochondria. FEBS Lett. *498,* 16-21.

Naik, M.T., and Huang, T. (2004). Conformational stability and thermodynamic characterization of the lipoic acid bearing domain of human mitochondrial branched chain α-ketoacid dehydrogenase. Protein Sci. *13,* 2483-2492.

Nath, K.A., Ngo, E.O., Hebbel, R.P., Croatt, A.J., Zhou, B., and Nutter, L.M. (1995). alpha-Ketoacids scavenge H_2O_2 *in vitro* and *in vivo* and reduce menadione-induced DNA injury and cytotoxicity. Am. J. Physiol.: Cell Physiol. *268,* C227-C236.

Navari-Izzo, F., Quartacci, M.F., and Sgherri, C. (2002). Lipoic acid: a unique antioxidant in the detoxification of activated oxygen species. Plant Physiol. Biochem. *40,* 463-470.

Navarro-Sastre, A., Tort, F., Stehling, O., Uzarska, M., Arranz, J., del Toro, M., Labayru, M. ., Landa, J., Font, A., Garcia-Villoria, J.*, et al.* (2011). A fatal mitochondrial disease is associated with defective NFU1 function in the maturation of a subset of mitochondrial Fe-S proteins. Am. J. Hum. Genet. *89,* 656-667.

Novgorodov, S.A., Chudakova, D.A., Wheeler, B.W., Bielawski, J., Kindy, M.S., Obeid, L.M., and Gudz, T.I. (2011). Developmentally regulated ceramide synthase 6 increases mitochondrial Ca^{2+} loading capacity and promotes apoptosis. J. Biol. Chem. *286,* 4644-4658.

Nulton-Persson, A.C., and Szweda, L.I. (2001). Modulation of mitochondrial function by hydrogen peroxide. J. Biol. Chem. *276,* 23357-23361.

Nulton-Persson, A.C., Starke, D.W., Mieyal, J.J., and Szweda, L.I. (2003). Reversible inactivation of α-ketoglutarate dehydrogenase in response to alterations in the mitochondrial glutathione status. Biochemistry *42,* 4235-4242.

Obrosova, I., Cao, X., Greene, D.A., and Stevens, M.J. (1998). Diabetes-induced changes in lens antioxidant status, glucose utilization and energy metabolism: effect of DL-α-lipoic acid. Diabetologia *41,* 1442-1450.

Obrosova, I.G., Fathallah, L., Liu, E., and Nourooz-Zadeh, J. (2003). Early oxidative stress in the diabetic kidney: effect of DL-α-lipoic acid. Free Radical Biol. Med. *34,* 186-195.

Ough, M., Lewis, A., Zhang, Y., Hinkhouse, M.M., Ritchie, J.M., Oberley, L.W., and Cullen, J.J. (2004). Inhibition of cell growth by overexpression of manganese superoxide dismutase (MnSOD) in human pancreatic carcinoma. Free Radic. Res. *38,* 1223-1233.

Padmalayam, I., Hasham, S., Saxena, U., and Pillarisetti, S. (2009). Lipoic acid synthase (LASY): a novel role in inflammation, mitochondrial function, and insulin resistance. Diabetes *58,* 600-608.

Pattyn, F., Speleman, F., De Paepe, A., and Vandesompele, J. (2003). RTPrimerDB: the real-time PCR primer and probe database. Nucleic Acids Res. *31,* 122-123.

Perham, R.N. (2000). Swinging arms and swinging domains in multifunctional enzymes: catalytic machines for multistep reactions. Annu. Rev. Biochem. *69,* 961-1004.

Pfaffl, M.W. (2001). A new mathematical model for relative quantification in real-time RT–PCR. Nucleic Acids Res. *29,* DOI: 10.1093/nar/29.9.e45.

Pfaffl, M.W., Horgan, G.W., and Dempfle, L. (2002). Relative expression software tool (REST©) for group-wise comparison and statistical analysis of relative expression results in real-time PCR. Nucleic Acids Res. *30,* e36-e46.

Pfaffl, M.W., Tichopad, A., Prgomet, C., and Neuvians, T.P. (2004). Determination of stable housekeeping genes, differentially regulated target genes and sample integrity: BestKeeper – Excel-based tool using pair-wise correlations. Biotechnol. Lett. *26,* 509-515.

Pommier, Y. (2006). Topoisomerase I inhibitors: camptothecins and beyond. Nat. Rev. Cancer *6,* 789-802.

Pushkarsky, T., Zybarth, G., Dubrovsky, L., Yurchenko, V., Tang, H., Guo, H., Toole, B., Sherry, B., and Bukrinsky, M. (2001). CD147 facilitates HIV-1 infection by interacting with virus-associated cyclophilin A. Proc. Natl. Acad. Sci. USA *98,* 6360-6365.

Qi, Y., He, Q., Ma, Y., Du, Y., Liu, G., Li, Y., Tsao, G.S.W., Ngai, S.M., and Chiu, J. (2008). Proteomic identification of malignant transformation-related proteins in esophageal squamous cell carcinoma. J. Cell. Biochem. *104,* 1625-1635.

Raghunand, N., Gatenby, R.A., and Gillies, R.J. (2003). Microenvironmental and cellular consequences of altered blood flow in tumours. Br. J. Radiol. *76,* S11-S22.

Ribeiro, C., Sgaravatti, Â., Rosa, R., Schuck, P., Grando, V., Schmidt, A., Ferreira, G., Perry, M., Dutra-Filho, C., and Wajner, M. (2008). Inhibition of brain energy metabolism by the branched-chain amino acids accumulating in maple syrup urine disease. Neurochem. Res. *33,* 114-124.

Ristow, M. (2006). Oxidative metabolism in cancer growth. Curr. Opin. Clin. Nutr. Metab. Care *9,* 339-345.

Robertson, J.D., Orrenius, S., and Zhivotovsky, B. (2000). Review: nuclear events in apoptosis. J. Struct. Biol. *129,* 346-358.

Rozen, S., and Skaletsky, H. (2000). Primer3 on the WWW for general users and for biologist programmers. In Bioinformatics Methods and Protocols: Methods in Molecular Biology, Krawetz, S., and Misener, S. eds., (Totowa, NJ: Humana Press) pp. 365-386.

Rozhin, J., Sameni, M., Ziegler, G., and Sloane, B.F. (1994). Pericellular pH affects distribution and secretion of cathepsin B in malignant cells. Cancer Res. *54,* 6517-6525.

Rutz, S., and Scheffold, A. (2004). Towards *in vivo* application of RNA interference – new toys, old problems. Arthritis Res. Ther. *6,* 78-85.

Samejima, K., and Earnshaw, W.C. (2005). Trashing the genome: the role of nucleases during apoptosis. Nat. Rev. Mol. Cell Biol. *6,* 677-688.

Sashital, D.G., and Doudna, J.A. (2010). Structural insights into RNA interference. Curr. Opin. Struct. Biol. *20,* 90-97.

Schlappack, O., Zimmermann, A., and Hill, R. (1991). Glucose starvation and acidosis: effect on experimental metastatic potential, DNA content and MTX resistance of murine tumour cells. Br. J. Cancer *64,* 663-670.

Schonauer, M.S., Kastaniotis, A.J., Kursu, V.A.S., Hiltunen, J.K., and Dieckmann, C.L. (2009). Lipoic acid synthesis and attachment in yeast mitochondria. J. Biol. Chem. *284,* 23234-23242.

Shan, G. (2010). RNA interference as a gene knockdown technique. Int. J. Biochem. Cell Biol. *42,* 1243-1251.

Shen, J., Person, M.D., Zhu, J., Abbruzzese, J.L., and Li, D. (2004). Protein expression profiles in pancreatic adenocarcinoma compared with normal pancreatic tissue and tissue affected by pancreatitis as detected by two-dimensional gel electrophoresis and mass spectrometry. Cancer Res. *64,* 9018-9026.

Sherry, B., Yarlett, N., Strupp, A., and Cerami, A. (1992). Identification of cyclophilin as a proinflammatory secretory product of lipopolysaccharide-activated macrophages. Proc. Natl. Acad. Sci. USA *89,* 3511-3515.

Shi, Q., Le, X., Wang, B., Abbruzzese, J.,L., Xiong, Q., He, Y., and Xie, K. (2001). Regulation of vascular endothelial growth factor expression by acidosis in human cancer cells. Oncogene *20,* 3751-3756.

Shi, D., Liu, H., Stern, J.S., Yu, P., and Liu, S. (2008). Alpha-lipoic acid induces apoptosis in hepatoma cells via the PTEN/Akt pathway. FEBS Lett. *582,* 1667-1671.

Simbula, G., Columbano, A., Ledda-Columbano, G., Sanna, L., Deidda, M., Diana, A., and Pibiri, M. (2007). Increased ROS generation and p53 activation in α-lipoic acid-induced apoptosis of hepatoma cells. Apoptosis *12,* 113-123.

Smith, A.R., Shenvi, S.V., Widlansky, M., Suh, J.H., and Hagen, T.M. (2004). Lipoic acid as a potential therapy for chronic diseases associated with oxidative stress. Curr. Med. Chem. *11,* 1135-1146.

Spitz, D.R., Sim, J.E., Ridnour, L.A., Galoforo, S.S., and Lee, Y.J. (2000). Glucose deprivation-induced oxidative stress in human tumor cells: a fundamental defect in metabolism? Ann. NY Acad. Sci. *899,* 349-362.

Sulo, P., and Martin, N.C. (1993). Isolation and characterization of LIP5: a lipoate biosynthetic locus of *Saccharomyces cerevisiae*. J. Biol. Chem. *268,* 17634-17639.

Sun, S., Wang, Q., Giang, A., Cheng, C., Soo, C., Wang, C., Liau, L., and Chiu, R. (2011). Knockdown of CypA inhibits interleukin-8 (IL-8) and IL-8-mediated proliferation and tumor growth of glioblastoma cells through down-regulated NF-κB. J. Neuro-Oncol. *101,* 1-14.

Susin, S., Lorenzo, H., Zamzami, N., Marzo, I., Snow, B., Brothers, G., Mangion, J., Jacotot, E., Costantini, P., Loeffler, M.*, et al.* (1999). Molecular characterization of mitochondrial apoptosis-inducing factor. Nature *397,* 441-446.

Tanaka, H., Shimazaki, H., Kimura, M., Izuta, H., Tsuruma, K., Shimazawa, M., and Hara, H. (2011). Apoptosis-inducing factor and cyclophilin A cotranslocate to the motor neuronal nuclei in amyotrophic lateral sclerosis model mice. CNS Neurosci. Ther. *17,* 294-304.

Taraphdar, A., Roy, M., and Bhattacharya, R. (2001). Natural products as inducers of apoptosis: implication for cancer therapy and prevention. Curr. Sci. *80,* 1387-1396.

Tennant, D.A., Durán, R.V., Boulahbel, H., and Gottlieb, E. (2009). Metabolic transformation in cancer. Carcinogenesis *30,* 1269-1280.

Thali, M., Bukovsky, A., Kondo, E., Rosenwirth, B., Walsh, C., Sodroski, J., and Göttlinger, H. (1994). Functional association of cyclophilin A with HIV-1 virions. Nature *372,* 363-365.

Thannickal, V.J., and Fanburg, B.L. (2000). Reactive oxygen species in cell signaling. Am. J. Physiol.: Lung Cell. Mol. Physiol. *279,* L1005-L1028.

Todaro, G.J., and Green, H. (1963). Quantitative studies of the growth of mouse embryo cells in culture and their development into established cell lines. J. Cell Biol. *17,* 299-313.

Trachootham, D., Alexandre, J., and Huang, P. (2009). Targeting cancer cells by ROS-mediated mechanisms: a radical therapeutic approach? Nat. Rev. Drug Discovery *8,* 579-591.

Turrens, J.F. (2003). Mitochondrial formation of reactive oxygen species. J. Physiol. *552,* 335-344.

Tuschl, T. (2002). Expanding small RNA interference. Nat. Biotechnol. *20,* 446-448.

Valero, J.G., Sancey, L., Kucharczak, J., Guillemin, Y., Gimenez, D., Prudent, J., Gillet, G., Salgado, J., Coll, J., and Aouacheria, A. (2011). Bax-derived membrane-active peptides act as potent and direct inducers of apoptosis in cancer cells. J. Cell Sci. *124,* 556-564.

Valko, M., Rhodes, C.J., Moncol, J., Izakovic, M., and Mazur, M. (2006). Free radicals, metals and antioxidants in oxidative stress-induced cancer. Chem. Biol. Interact. *160,* 1-40.

Van de Mark, K., Chen, J.S., Steliou, K., Perrine, S.P., and Faller, D.V. (2003). α-Lipoic acid induces p27Kip-dependent cell cycle arrest in non-transformed cell lines and apoptosis in tumor cell lines. J. Cell. Physiol. *194,* 325-340.

Vander Heiden, M.G., Cantley, L.C., and Thompson, C.B. (2009). Understanding the Warburg effect: the metabolic requirements of cell proliferation. Science *324,* 1029-1033.

Vermes, I., Haanen, C., Steffens-Nakken, H., and Reutellingsperger, C. (1995). A novel assay for apoptosis flow cytometric detection of phosphatidylserine expression on early apoptotic cells using fluorescein labelled Annexin V. J. Immunol. Methods *184,* 39-51.

von Kleist-Retzow, J., Hornig-Do, H., Schauen, M., Eckertz, S., Dinh, T.A.D., Stassen, F., Lottmann, N., Bust, M., Galunska, B., Wielckens, K.*, et al.* (2007). Impaired mitochondrial Ca^{2+} homeostasis in respiratory chain-deficient cells but efficient compensation of energetic disadvantage by enhanced anaerobic glycolysis due to low ATP steady state levels. Exp. Cell Res. *313,* 3076-3089.

Wang, P., and Heitman, J. (2005). The cyclophilins. Genome Biol. *6,* 226.1-226.6.

Wang, Z., Liao, J., and Diwu, Z. (2005a). N-DEVD-N′-morpholinecarbonyl-rhodamine 110: novel caspase-3 fluorogenic substrates for cell-based apoptosis assay. Bioorg. Med. Chem. Lett. *15,* 2335-2338.

Wang, G., Silva, J., Krishnamurthy, K., Tran, E., Condie, B.G., and Bieberich, E. (2005b). Direct binding to ceramide activates protein kinase Cζ before the formation of a pro-apoptotic complex with PAR-4 in differentiating stem cells. J. Biol. Chem. *280,* 26415-26424.

Warburg, O. (1956). On the origin of cancer cells. Science *123,* 309-314.

Watanabe, M., Hitomi, M., van der Wee, K., Rothenberg, F., Fisher, S.A., Zucker, R., Svoboda, K.K.H., Goldsmith, E.C., Heiskanen, K.M., and Nieminen, A. (2002). The pros and cons of apoptosis assays for use in the study of cells, tissues, and organs. Microsc. Microanal *8,* 375-391.

Wenzel, U., Nickel, A., and Daniel, H. (2005). α-lipoic acid induces apoptosis in human colon cancer cells by increasing mitochondrial respiration with a concomitant O^{2-}-generation. Apoptosis *10,* 359-368.

Wissing, S., Ludovico, P., Herker, E., Büttner, S., Engelhardt, S.M., Decker, T., Link, A., Proksch, A., Rodrigues, F., Corte-Real, M.*, et al.* (2004). An AIF orthologue regulates apoptosis in yeast. J. Cell Biol. *166,* 969-974.

Wollin, S.D., and Jones, P.J.H. (2003). α-Lipoic acid and cardiovascular disease. J. Nutr. *133,* 3327-3330.

Wu, M., Neilson, A., Swift, A.L., Moran, R., Tamagnine, J., Parslow, D., Armistead, S., Lemire, K., Orrell, J., Teich, J., *et al*. (2007). Multiparameter metabolic analysis reveals a close link between attenuated mitochondrial bioenergetic function and enhanced glycolysis dependency in human tumor cells. Am J Physiol Cell Physiol *292,* C125-C136.

Xin, M., and Deng, X. (2006). Protein phosphatase 2A enhances the proapoptotic function of Bax through dephosphorylation. J. Biol. Chem. *281,* 18859-18867.

Xu, Q., Leiva, M.C., Fischkoff, S.A., Handschumacher, R.E., and Lyttle, C.R. (1992). Leukocyte chemotactic activity of cyclophilin. J. Biol. Chem. *267,* 11968-11971.

Yang, H., Li, M., Chai, H., Yan, S., Lin, P., Lumsden, A.B., Yao, Q., and Chen, C. (2005). Effects of cyclophilin A on cell proliferation and gene expressions in human vascular smooth muscle cells and endothelial cells. J. Surg. Res. *123,* 312-319.

Yang, H., Chen, J., Yang, J., Qiao, S., Zhao, S., and Yu, L. (2007). Cyclophilin A is upregulated in small cell lung cancer and activates ERK1/2 signal. Biochem. Biophys. Res. Commun. *361,* 763-767.

Yao, Q., Li, M., Yang, H., Chai, H., Fisher, W., and Chen, C. (2005). Roles of cyclophilins in cancers and other Oorgan systems. World J. Surg. *29,* 276-280.

Yi, X., and Maeda, N. (2005). Endogenous production of lipoic acid is essential for mouse development. Mol. Cell. Biol. *25,* 8387-8392.

Yi, X., and Maeda, N. (2006). α-Lipoic acid prevents the increase in atherosclerosis induced by diabetes in apolipoprotein E–deficient mice fed high-fat/low-cholesterol diet. Diabetes *55,* 2238-2244.

Yu, J., DeRuiter, S.L., and Turner, D.L. (2002). RNA interference by expression of short-interfering RNAs and hairpin RNAs in mammalian cells. Proc. Natl. Acad. Sci. USA *99,* 6047-6052.

Zhang, H., Kasibhatla, S., Wang, Y., Herich, J., Guastella, J., Tseng, B., Drewe, J., and Cai, S.X. (2004). Discovery, characterization and SAR of gambogic acid as a potent apoptosis inducer by a HTS assay. Bioorg. Med. Chem. *12,* 309-317.

Zhong, H., De Marzo, A.M., Laughner, E., Lim, M., Hilton, D.A., Zagzag, D., Buechler, P., Isaacs, W.B., Semenza, G.L., and Simons, J.W. (1999). Overexpression of hypoxia-inducible factor 1α in common human cancers and their metastases. Cancer Res. *59,* 5830-5835.

Zhu, C., Wang, X., Deinum, J., Huang, Z., Gao, J., Modjtahedi, N., Neagu, M.R., Nilsson, M., Eriksson, P.S., Hagberg, H., *et al.* (2007). Cyclophilin A participates in the nuclear translocation of

apoptosis-inducing factor in neurons after cerebral hypoxia-ischemia. J. Exp. Med. *204,* 1741-1748.

Chapter 3: A bioinformatic approach to identifying novel candidate genes involved in apoptosis

3.1 Introduction

The field of bioinformatics has flourished in recent years along with the increase in genomic and proteomic data (Perez-Iratxeta et al., 2007). Data-intensive research has spurred the development of computational methods to ease analysis and databases, especially those of a cross-disciplinary nature, to serve as resources by collecting and integrating data. Indeed, the use of databases has increased significantly in the past decade (Perez-Iratxeta et al., 2007). Databases come in all shapes and sizes, and two examples are protein interaction and pathway databases. These databases are valuable tools that allow for genes and proteins to be organised within their larger biological context, making it possible for inferences to be made regarding their role in, for example, pathogenesis (Romero et al., 2004).

Even though significant progress has been made in the understanding of apoptosis, a level of uncertainty remains, especially with regards to the regulatory mechanisms of apoptosis and its implications for disease (Ola et al., 2011). The identification of novel candidate genes or proteins that may potentially have a role in apoptosis is not only important for expanding our knowledge on the process but may also be important for the therapeutic potential of apoptosis; if these candidates were found to have some kind of regulatory effect on apoptosis, they could become potential targets for the development of therapeutic drugs.

By investigating the protein interactions of a novel candidate, clues can be obtained to its molecular function and regulation. Similarly, identifying associated cellular pathways would reveal the functional environment of a candidate. As mentioned previously, protein interaction and pathway databases can greatly assist in this annotation of novel candidates. These databases can contain experimentally verified data retrieved from published literature or predicted data, and even though verified data would be of more noteworthy value, predicted data provides a framework for future experimental studies.

The aim of this chapter is thus two-fold; firstly, to identify additional potential candidate genes involved in apoptosis by analysing nucleotide sequences obtained from the promoter-trap mutagenesis experiments performed in the pilot study. This was achieved by means of Basic Local Alignment Search Tool (BLAST) searches. Secondly, to perform a bioinformatic analyses on candidate genes identified in the pilot study, as well as candidate genes identified by the first aim. For this analyses, possible interacting proteins and a potential role in cellular pathways were investigated by means of a variety of freely available web-based databases; databases IntAct (Kerrien et al., 2012), STRING (Jensen et al., 2009), BioGRID (Stark et al., 2006), DOMINE

(Raghavachari et al., 2008; Yellaboina et al., 2011) and I2D (Brown and Jurisica, 2005; Brown and Jurisica, 2007) were used to identify possible interacting proteins, while the KEGG (Kanehisa and Goto, 2000; Kanehisa et al., 2012), Reactome (Croft et al., 2011; Matthews et al., 2009), HumanCyc (Romero et al., 2004) and UniPathway (Morgat et al., 2012) databases were used to investigate a potential role for the candidate genes in cellular pathways. Below follows a brief description of each of these databases, as well as a description for GeneCards®, a database commonly used throughout the methodology of this chapter.

GeneCards® (http://www.genecards.org/):

Established in 1997 by the Weizmann Institute of Science in collaboration with Life Map Sciences Incorporated, the GeneCards® database aimed to integrate data generated by the human genome project which was subsequently scattered over various specialised databases (Rebhan et al., 1997). The latest database version (v. 3), released in 2010, boasts with more than 73 000 entries which includes cards for all known and predicted protein coding genes as well as pseudo- and RNA genes (Safran et al., 2010). Genome, transcriptome, proteome, function and disease data is sourced from more than 80 different electronic resources, including large public databases like ENSEMBL, UniProtKB, National Centre for Biotechnology Information (NCBI) and HUGO Gene Nomenclature Committee (HGNC). In addition, this human gene database takes it one step further by listing known orthologs and paralogs and providing links to reagents and products specific to your gene of interest. A section listing interactions and/or associations with various drugs and chemical compounds is also included. The GeneCards® database provides the researcher with a multifaceted tool that allows for the characterisation of genes from a nucleotide sequence starting point, beyond the analysis of gene expression and protein modification, right up to viewing implicated cellular pathways and identifying involvement in diseases, all the while providing molecular tools to aid research (Safran et al., 2010).

IntAct (http://www.ebi.ac.uk/intact/):

Hosted by the European Bioinformatics Institute, the IntAct database is a freely available protein interaction database that collects and collates data from literature and direct data submissions. Each data entry is curated and checks are performed on a database level before the final entry is submitted (Kerrien et al., 2012). In addition, the original author is consulted before the submission and the entry is manually updated in the case of comments from the author. IntAct is compliant with HUPO-PSI data standards and is also a member of the IMEx consortium, employing IMEx annotation standards to the majority of the protein-protein interaction data. Although the database focusses on protein-protein interactions, referencing more than 57 000 proteins (as of September 2011), the database also branches out to protein interactions with small molecules, nucleic acids and genes (Kerrien et al., 2012). IntAct can be searched by using a protein's gene name, PubMed ID, UniProtKB accession number or UniProtKB ID.

STRING (http://string-db.org/):

The Search Tool for the Retrieval of Interacting Genes/Proteins (STRING) is a comprehensive visual database that integrates information on known and predicted protein interactions (Jensen et al., 2009; Szklarczyk et al., 2011). The database is unique in its visual representation of a specified protein's interaction network, which can be altered by repositioning the implicated proteins or by removing or adding additional proteins. STRING employs a variety of evidence types, which includes experimental data, co-expression data, homology data and data obtained from text-mining. Confidence scores for an interaction are obtained by combining the probabilities from the different evidence types while correcting for the probability of randomly observing an interaction. The user can choose to remove a certain evidence type from the analysis and can also set a threshold confidence score for the analysis; thus making it possible to balance different levels of accuracy and coverage. Another strength of the database is that it covers a vast variety of organisms; in fact, the latest version covers more than 1100 completely sequenced organisms (Jensen et al., 2009; Szklarczyk et al., 2011).

BioGRID (http://thebiogrid.org/):

The Biological General Repository for Interaction Datasets (BioGRID) database was first released in 2002 and has since been modified and expanded on several occasions (Breitkreutz et al., 2008; Stark et al., 2006; Stark et al., 2011). The database aims to capture and organise protein and genetic interaction data, especially those obtained from high-throughput studies. BioGRID places special attention on interaction data from *S. cerevisiae* and *Schizosaccharomyces pombe* by maintaining the data with monthly updates to provide a near-complete representation of all interactions available in literature. Additional focus is placed on interactions in a human platform, for obvious biomedical reasons. Other model organisms covered by the database include *Macaca mulatta*, *M. musculus*, *D. melanogaster*, *Arabidopsis thaliana* and *Bacillus subtilis* (Breitkreutz et al., 2008; Stark et al., 2006; Stark et al., 2011).

DOMINE (http://domine.utdallas.edu/cgi-bin/Domine):

The DOMINE database represents a thorough collection of known and predicted protein domain-domain interactions (Raghavachari et al., 2008; Yellaboina et al., 2011). A number of different computational approaches aimed at inferring domain-domain interactions have been developed due to the fact that interactions inferred from structural data can explain only a limited number of protein interactions. With this in mind, DOMINE utilises 15 different data sources, of which two provides known interactions inferred from 3D structures. Predicted domain-domain interactions obtained from computational approaches is also assigned confidence scores. Simply put, the individual approaches are weighted based on how well their predictions are confirmed by others; this allows for the calculation of a confidence score by summing the weights from each approach

that predicted a particular interaction. Based on the confidence score, predicted interactions can be classified as either of high, medium or low confidence (Raghavachari et al., 2008; Yellaboina et al., 2011).

I2D (http://ophid.utoronto.ca/ophidv2.201/):

Formerly known as OPHID, the I2D, or Interologous Interaction Database, aims to elaborate the human interactome by supplementing the experimentally verified protein interactions with predicted interactions (Brown and Jurisica, 2005; Brown and Jurisica, 2007). As the name suggests, the database was constructed using an interologous approach; protein interactions from model organisms were transferred to human orthologs by utilising the BLASTp tool in combination with a reciprocal best-hit tactic (the top hit identified in a BLASTp search with the model organism protein had to produce a top hit that matched the original query protein when BLAST searched in the reverse direction). The model organisms used in the construction of the database included *M. musculus*, *D. melanogaster*, *C. elegans* and *S. cerevisiae*. Three evidence types, namely domain co-occurrence, gene co-expression and Gene Ontology (GO) term similarity, were used as support for the predicted interactions. As with all predicted interactions, these interactions needs to be experimentally verified, however increasing evidence suggests the protein-protein interactions are conserved through evolution (Brown and Jurisica, 2005; Brown and Jurisica, 2007).

KEGG (http://www.genome.jp/kegg/):

Throughout the years the Kyoto Encyclopaedia of Genes and Genomes (KEGG) database has become synonymous with the visualisation and elucidation of cellular pathways. The database is a comprehensive resource that integrates genomic, chemical and systemic functional information based on experimentally verified data (Kanehisa and Goto, 2000; Kanehisa et al., 2012). KEGG houses 15 different databases covering three focus areas, namely systems information (e.g. KEGG PATHWAY, KEGG DISEASE and KEGG BRITE), genomic information (e.g. KEGG GENOME, KEGG GENES and KEGG ORTHOLOGY) and chemical information (e.g. KEGG REACTION, KEGG ENZYME and KEGG COMPOUND). In-house software is used to manually draw the graphical representations of the pathways maps in KEGG PATHWAY (Kanehisa and Goto, 2000; Kanehisa et al., 2012).

Reactome (http://www.reactome.org):

Reactome is a freely available and open source database for human processes and pathways (Croft et al., 2011; Matthews et al., 2009). Pathways are manually curated and peer-reviewed, and annotations are cross-referenced with a variety of established bioinformatic databases, such as NCBI Entrez Gene, UniProt, KEGG COMPOUND and GO. Reactome pathways are also expanded to include processes such as the transport of proteins between cellular compartments and by including a variety of entities such as macromolecular complexes, small molecules, proteins and

nucleic acids. External databases, such as IntAct, BioGRID and STRING, are also consulted to provide molecular interaction data for pathway construction (Croft et al., 2011; Matthews et al., 2009).

HumanCyc (http://humancyc.org/):

HumanCyc is a database for human metabolic pathways and forms part of the larger BioCyc collection (Romero et al., 2004). The database was constructed with the PathoLogic component of the Pathway Tools Software (Karp et al., 2002), a reusable software package able to create a type of model-organism database called a pathway/genome database (PGDB) (Romero et al., 2004). The PathoLogic component utilises the annotated genome of an organism to create a new PGDB (Karp et al., 2002). HumanCyc contains 305 metabolic pathways; curation, however, is an on-going process, leaving many of the pathways predicted (Romero et al., 2004). Although, as with predicted protein interactions, these predicted pathways based on the human genome provides a framework for the elucidation of interactions, and subsequent pathways, on an experimental level.

UniPathway (http://www.grenoble.prabi.fr/obiwarehouse/unipathway):

UniPathway is a resource for the exploration of metabolic pathways (Morgat et al., 2012). The database is completely manually curated, using primary literature as a source as well as external databases such as KEGG and MetaCyc. In addition, all reactions in UniPathway are linked to the corresponding entries in UniProtKB. A key concept in the database is that of UniPathway Linear Subpathway (ULS), which represents a set of enzymatic reactions known to occur in linear sequence with no known variance. These ULSs are used as building blocks upon which larger pathways is assembled while species-specific pathway variants form alternative paths through connected ULSs (Morgat et al., 2012).

3.2 Materials and methods

3.2.1 Identification of potential candidate genes

A local alignment search was performed with eight sequences obtained from the promoter-trap mutagenesis experiments performed in the pilot study. The sequences were named as follows: MMJ304(BF)3'41, MMJ304G, MMJ308BFG, SEJJ302 BOTT3'41, SEJJ302 TOP3'41, SEJJ3021034, SWJ612MF43 and SWJ612TF43. The search was performed by utilising the BLASTn tool located on the NCBI webpage (http://blast.ncbi.nlm.nih.gov/). The search was conducted against the human genomic and transcript database while default options for the remaining parameters were selected. The top hit from each BLAST search were investigated further by submitting the identified gene(s) to a search in the GeneCards® database. This was done in order to elucidate the molecular function of the gene(s) and also to determine if the gene(s)

had any established associations with apoptosis or cancer. Characteristics of interest included cellular location of the corresponding protein, molecular function, participation in a molecular process, possible involvement in cellular pathways, protein-protein interactions, domains present in the corresponding protein and the presence of transcription factor binding sites in the promoter region of the gene.

By assessing the results from the BLAST searches in terms of E-values (expect values), bit scores and percentage identities and the information obtained from the GeneCards® searches, two candidate genes were selected to undergo further bioinformatic analyses as described in section 3.2.2.

3.2.2 Bioinformatic analysis of selected candidate genes

A total of four candidate genes, two identified in the pilot study and two identified as described in section 3.2.1, were subjected to further bioinformatic analyses. For these analyses, freely available web-based databases were used to investigate possible protein interactions for the candidate genes' corresponding proteins as well as to identify any potential involvement in cellular pathways. A variety of databases were used for these analyses, and this includes IntAct, STRING, BioGRID, DOMINE and I2D for protein interactions and KEGG, Reactome, HumanCyc and UniPathway for the pathway analysis. This selection of databases was chosen based on three reasons; firstly, to include both experimentally verified and computationally predicted data; secondly, these databases exhibit different features (especially the pathway databases); and lastly, because the databases are constructed differently (especially the protein interaction databases). Default parameters were selected for all database searches performed with the exception of the STRING database. Here, the text-mining evidence type were removed from the analysis since this feature functions as an "automatic key-word" search in abstracts of published literature and can thus result in false positives. In addition, a confidence score of 0.500 was selected in order to restrict the results to interactions with a higher confidence level (default value is 0.4).

The results obtained from the searches conducted in the protein interaction and pathway databases were investigated further in order to determine their relevance to this study. In terms of the protein interaction data, the molecular function for each interactant, as generated by all of the databases, were searched for in either GeneCards®, NCBI Entrez Gene, UniProtKB or InterPro. Only those functioning in processes such as apoptosis, cell death, cell survival, cell differentiation, cell division or cell cycle control, or those described as an oncogene or tumour suppressor, were deemed relevant. The same criteria were used to determine the relevance of the each pathway generated by the pathway databases.

3.3 Results and Discussion

3.3.1 Identification of potential candidate genes

The BLAST searches performed with the nucleotide sequences obtained from the pilot study produced alignments to either refseq mRNA sequences or genomic contigs (table 3.1). Each alignment produced one candidate gene, with the exception of sequence SWJ612MF43, where two genes were identified, namely *autophagy protein 5* (*ATG5*) and *cAMP-specific 3',5'-cyclic phosphodiesterase 7B* (*PDE7B*). Due to the nature of the promoter-trap mutagenesis experiments, this could indicate that the two genes share a promoter. Both *ATG5* and *PDE7B* are located on chromosome 6, however, they are located at different regions (*ATG5* – 6q21 and *PDE7B* – 6q23-24) and thus the possibility remains that instead of sharing a common promoter, these genes share a similar stretch of nucleotides in their promoter regions. The true nature for this phenomenon was however not investigated since it was outside the scope of this project. An interesting result was observed in the alignments of sequences MMJ304(BF)3'41 and SEJJ302 BOTT3'41; both of these alignments identified the same candidate gene, namely *AHNAK nucleoprotein* (*AHNAK*). The fact that this gene was identified twice, and was thus knocked-down in two different cell populations which showed resistance to apoptosis in the promoter-trap mutagenesis experiments performed the pilot study, provides increased support for *AHNAK* to potentially be involved in apoptosis. This phenomenon also occurred with sequences MMJ304G and MMJ308BFG. In this case, *lipoic acid synthetase* (*LIAS*) was identified as the candidate gene. In addition to the above mentioned statement, this observation provides even more support for a possible involvement in apoptosis since *LIAS* was also identified as a candidate gene in the pilot study. In terms of the E-values produced by each of the alignments, statistically significant results were obtained for three alignments, namely those of sequences MMJ304G, MMJ308BFG and SEJJ3021034. These alignments identified *LIAS* and *serum amyloid A-like 1* (*SAAL1*) as candidate genes. The remaining alignments produced unfavourable E-values and could be an indication of false positives. Overall, the lengths of the alignments were relatively short, ranging between 21 and 67 nucleotides, which can be attributed to the inverse-PCR technique used in the pilot study. This technique has however been improved since then and a subsequent study performed by a fellow researcher following the same protocol for BLAST analysis produced alignments which were considerably longer (Molenaar, 2012). The percentage identities for the alignments averaged at 89.67%; gaps present in the alignments could potentially be explained by the fact that the BLAST searches were performed against the human genomic and transcript databases.

Table 3.1: Results obtained from the BLAST searches performed with sequences isolated from the pilot study

Sequence	Candidate gene	Accession number	Bit score (Total)	E-value¥	Alignment Identity§ (%)
MMJ304(BF)3'41	*AHNAK nucleoprotein* (*AHNAK*) (transcript variant 1)	NM_001620.1	39.2 (42)	2.8	24/26 (93%)
MMJ304G	*Lipoic acid synthetase* (*LIAS*) (transcript variant 1)	NM_006859.2	60.8 (66)	1E-06	46/55 (84%)
	Lipoic acid synthetase (*LIAS*) (transcript variant 2)	NM_194451.1	60.8 (66)	1E-06	46/55 (84%)
MMJ308BFG	*Lipoic acid synthetase* (*LIAS*)	NT_016297.16	62.6 (68)	4E-07	53/67 (80%)
	Lipoic acid synthetase (*LIAS*)	NW_001838902.1	62.6 (68)	4E-07	53/67 (80%)
SEJJ302 BOTT3'41	*AHNAK nucleoprotein* (*AHNAK*) (transcript variant 1)	NM_001620.1	39.2 (42)	4.9	24/26 (93%)
SEJJ302 TOP3'41	*6-phosphofructo-2-kinase/fructo-2,6-bisphosphatase 3* (*PFKFB3*)	NT_008705.16	42.8 (46)	0.38	26/28 (93%)
	6-phosphofructo-2-kinase/fructo-2,6-bisphosphatase 3 (*PFKFB3*)	NW_001837931.2	42.8 (46)	0.38	26/28 (93%)
SEJJ3021034	*Serum amyloid A-like 1* (*SAAL1*)	NT_009237.18	53.6 (58)	2E-04	37/42 (89%)
	Serum amyloid A-like 1 (*SAAL1*)	NW_001838022.2	53.6 (58)	2E-04	37/42 (89%)
SWJ612MF43	*Autophagy protein 5* (*ATG5*)	NT_025741.15	42.8 (46)	0.32	31/36 (87%)
	cAMP-specific 3',5'-cyclic phosphodiesterase 7B (*PDE7B*)	NT_025741.15	39.2 (42)	3.8	21/21 (100%)
	Autophagy protein 5 (*ATG5*)	NW_001838990.2	42.8 (46)	0.32	31/36 (87%)
	cAMP-specific 3',5'-cyclic phosphodiesterase 7B (*PDE7B*)	NW_001838990.2	39.2 (42)	3.8	21/21 (100%)
SWJ612TF43	*Gamma-glutamyl hydrolase* (*GGH*)	NM_003878.2	39.2 (42)	3.8	24/26 (93%)

¥ - Expect value; § - nucleotide alignment identity (amount of identical nucleotides out of the total amount of nucleotides in the alignment)

The seven candidate genes identified by the BLAST searches were investigated by means of the GeneCards® searchable database in order to assign basic functional annotations. This characterisation would ultimately assist in the selection of candidate genes for further study. Characteristics such as molecular function, molecular process, cellular pathways and protein interactions were important, although additional characteristics were also determined to provide a more complete overview of each candidate gene. The results of this investigation can be found in table 3.2; however, even though the table contains complete information for most of the characteristics, it must still be regarded as a summary of the information available on the GeneCards® database, especially with regards to the predicted transcription factor binding sites.

Basic functional annotations could be assigned to the majority of the candidate genes and a relatively large amount of heterogeneity between the genes could be observed in terms of molecular function and process involvement. With regards to the cellular pathways, most of the candidate genes were either involved in a metabolic pathway or a type of signalling pathway. In contrast to the rest of the candidate genes, very little information could be obtained for *SAAL1*. The GeneCards® database revealed no known specific function or cellular pathways for this gene.

Potential links to apoptosis could be ascertained for some of the candidate genes. Determining the molecular function for *ATG5* revealed that this gene is required for autophagy, a type of cell death, and may also potentially be involved in the modification of the cytoskeleton during apoptosis. As mentioned in chapter 1, morphological characteristics of apoptosis include cellular contraction, nuclear disintegration, cellular fragmentation and the formation of apoptotic bodies; characteristics such as these all involve modifications of the cytoskeleton (Ndozangue-Touriguine et al., 2008). Further support for a potential role in apoptosis is obtained from protein-protein interactions with caspase 8 and FADD, two proteins essential to the extrinsic pathway of apoptosis, as well as the predicted presence of a p53 transcription factor binding site in the promoter region for *ATG5*. A protein-protein interaction with caspase 8 was also revealed for *PFKFB3*, in addition to an interaction with TRADD, another protein involved in the extrinsic apoptotic pathway. The promoter region of *PFKFB3* is also suggested to contain a binding site for c-Myc, a transcription factor that is known to play a role in cell proliferation and apoptosis (Nieminen et al., 2007). The candidate gene *GGH* was shown to be involved in the biosynthetic pathway of folate. This reveals a potential link to apoptosis since folate is necessary for the biosynthesis of purines and is thus vital for DNA synthesis and repair as well as maintaining the stability and integrity of DNA. Folate deficiency is known to increase the presence of DNA strand breaks and may also induce apoptosis (Novakovic et al., 2006). With regards to *PDE7B*, this gene functions to hydrolyse cyclic adenosine monophosphate (cAMP) and is thus central to its regulation. cAMP is an important second messenger molecule implicated in multiple signalling pathways and physiological processes and through these, cAMP is said to have both an anti-apoptotic and pro-apoptotic impact (Dou and Wang, 2010).

Table 3.2: Results obtained from the Genecards® database for each candidate gene identified by the BLAST searches

Characteristic	Summary of GeneCards® results
	AHNAK nucleoprotein (*AHNAK*)
Alternative names	*Desmoyokin; neuroblast differentiation-associated protein AHNAK*
Cellular location of protein	Nucleus
Molecular function	May be required for neuronal cell differentiation; protein binding
Molecular process	Nervous system development
Cellular pathways	Phospholipase C signalling
Protein domains	PDZ
Protein-protein interactions	EGFR; IL6; DYSF; S100A10; HDAC2; CDKN2A
Predicted transcription factor binding sites	CREB; p53; c-Myc; NFκB
	Lipoic acid synthetase (*LIAS*)
Alternative names	*Lipoate synthase; lipoyl synthase*
Cellular location of protein	Mitochondrion
Molecular function	α-lipoic acid synthesis; sulphur insertion in lipoate-dependent enzymes; transferase activity; metal ion binding
Molecular process	Inflammatory response; response to oxidative stress; lipoate biosynthetic process
Cellular pathways	Lipoic acid metabolism; metabolic pathways; protein modification
Protein domains	Aldolase-type TIM barrel; radical SAM; elongator protein 3/MiaB/NifB
Protein-protein interactions	MCM2; OGDH; DLST; HSPD1; LIPT1; LIPT2
Predicted transcription factor binding sites	CREB; p53; c-Jun; GCNF; CUTL1

EGFR – epidermal growth factor receptor; IL6 – interleukin 6; DYSF – dysferlin; S100A10 – S100 calcium binding protein A10; HDAC2 – histone deacetylase 2; CDKN2A – cyclin dependent kinase inhibitor 2A; CREB – cAMP responsive element binding protein; NFκB – nuclear factor kappa B; MCM2 – minichromosome maintenance complex component 2; OGDH – oxoglutarate dehydrogenase; DLST – dihydrolipoamide S-succinyltransferase; HSPD1 – heat shock 60kDa protein 1; LIPT1 – lipoyltransferase 1; LIPT2; lipoyltransferase 2; GCNF – germ cell nuclear factor; CUTL1 – cut-like homeobox 1.

Table 3.2 continued

Characteristic	Summary of GeneCards® result
6-phosphofructo-2-kinase/fructo-2,6-bisphosphatase 3 (*PFKFB3*)	
Alternative names	*6-phosphofructo-2-kinase/fructose-2,6-bisphosphatase*
Cellular location of protein	Cytosol
Molecular function	Synthesis and degradation of fructose-2,6-bisphosphate; kinase activity; protein binding; hydrolase activity
Molecular process	Glycolysis; carbohydrate metabolic process
Cellular pathways	AMPK signalling; fructose and mannose metabolism
Protein domains	6-phosphofructo-2-kinase; histidine phosphatase superfamily clade-1
Protein-protein interactions	CASP8; TRADD; HIF1A; CDK1; GCK; PPARG
Predicted transcription factor binding sites	PPARγ1; PPARγ2; SRF; CREB; Chx10; c-Myc; c-Jun; p300
	Serum amyloid A-like 1 (*SAAL1*)
Alternative names	*FLJ41463; SPACIA1*
Cellular location of protein	Extracellular region
Molecular function	Binding
Molecular process	Acute-phase response
Cellular pathways	-
Protein domains	Armadillo-like helical; armadillo-type fold
Protein-protein interactions	USP19; MARK3; PHLDA3
Predicted transcription factor binding sites	NRSF form 1; NRSF form 2; c-Myc; ZEB1; CUTL1; NRF-2

CASP8 – caspase 8; TRADD – tumour necrosis factor receptor type 1 (TNFR1)-associated death domain protein; HIF1A – hypoxia inducible factor 1-alpha; CDK1 – cyclin dependent kinase 1; GCK – glucokinase; PPARG – peroxisome proliferator-activated receptor gamma; PPARγ1 – peroxisome proliferator-activated receptor gamma 1; PPARγ2 – peroxisome proliferator-activated receptor gamma 2; SRF – serum response factor; CREB – cAMP responsive element binding protein; Chx10 – Ceh-10 homeodomain-containing homolog; USP19 – ubiquitin specific peptidase 19; MARK3 – MAP/microtubule affinity-regulating kinase 3; PHLDA3 – pleckstrin homology-like domain, family A, member 3; NRSF – neuron restrictive silencer factor; ZEB1 – zinc finger E-box binding homeobox 1; CUTL1 – cut-like homeobox 1; NRF-2; nuclear respiratory factor 2.

Table 3.2 continued

Characteristic	Summary of GeneCards® results
Autophagy protein 5 (*ATG5*)	
Alternative names	*Apoptosis specific protein; autophagy related 5 homolog (S. cerevisiae)*
Cellular location of protein	Cytosol; autophagic vacuole; protein complex
Molecular function	Required for autophagy; possible role in modification of cytoskeleton during apoptosis; protein binding
Molecular process	Autophagy; blood vessel remodelling; negative regulation of apoptosis; heart contraction
Cellular pathways	Regulation of autophagy; RIG-I-like receptor signalling pathway; shigellosis
Protein domains	Autophagy-related protein 5
Protein-protein interactions	SIRT1; FADD; CASP8; RIPK1; ATG12; ATG10
Predicted transcription factor binding sites	ATF-2; p53; Hlf; c-Jun; NFIL3
cAMP-specific 3',5'-cyclic phosphodiesterase 7B (*PDE7B*)	
Alternative names	*Phosphodiesterase 7B; rolipram-insensitive phosphodiesterase type 7*
Cellular location of protein	Cytosol
Molecular function	Hydrolyses cAMP; phosphoric diester hydrolase activity; 3',5'-cyclic nucleotide phosphodiesterase activity
Molecular process	Signal transduction; synaptic transmission
Cellular pathways	cAMP-signalling; protein kinase A signalling; GPCR signalling; purine metabolism
Protein domains	3',5'-cyclic nucleotide phosphodiesterase; HD/PDEase
Protein-protein interactions	ADK; GUK1; GMPR; ITPA; ADCY1
Predicted transcription factor binding sites	Chx10; POU2F1; ALX1

SIRT1 – sirtuin 1; FADD – Fas-associated death domain protein; CASP8 – caspase 8; RIPK1 – receptor interacting serine/threonine-protein kinase 1; ATG12 – autophagy protein 12; ATG10 – autophagy protein 10; ATF-2 – activating transcription factor 2; Hlf – hepatic leukaemia factor; NFIL3 – nuclear factor interleukin 3 regulated; cAMP – cyclic adenosine monophosphate; GPCR – G-protein coupled receptor; ADK – adenosine kinase; GUK1 – guanylate kinase 1; GMPR – guanosine monophosphate reductase; ITPA – inosine triphosphatase; ADCY1 – adenylate cyclase 1; Chx10 – Ceh-10 homeodomain-containing homolog; POU2F1 – POU class 2 homeobox 1; ALX1 – ALX homeobox 1.

Table 3.2 continued

Characteristic	Summary of GeneCards® result
	Gamma-glutamyl hydrolase (*GGH*)
Alternative names	*Conjugase; gamma-Glu-X-carboxypeptidase*
Cellular location of protein	Extracellular region; lysosome; cytosol; melanosome
Molecular function	Hydrolysis of folylpoly-gamma-glutamates; exopeptidase activity; omega peptidase activity; hydrolase activity; gamma-glutamyl-peptidase activity
Molecular process	Glutamine metabolic process; response to zinc ion; response to insulin stimulus; response to ethanol
Cellular pathways	Folate biosynthesis
Protein domains	Peptidase C26, gamma-glutamyl hydrolase; peptidase C26
Protein-protein interactions	MYC; CEBPA; GH1; GSTM1; GSTK1; MGST1
Predicted transcription factor binding sites	c-Jun; p53; ATF-2; CUTL1; DDIT3; Chx10

MYC – Myc proto-oncogene protein; CEBPA – CCAAT/enhancer binding protein (C/EBP) alpha; GH1 – growth hormone 1; GSTM1 – glutathione S-transferase mu 1; GSTK1 – glutathione S-transferase kappa 1; MGST1 – microsomal glutathione S-transferase 1; ATF-2 – activating transcription factor 2; CUTL1 – cut-like homeobox 1; DDIT3 – DNA-damage-inducible transcript 3; Chx10 – Ceh-10 homeodomain-containing homolog.

Based on the results obtained from the BLAST and GeneCards® searches, two candidate genes were selected for further bioinformatic analysis, namely *AHNAK* and *SAAL1*. Even though the alignments for *AHNAK* were short and presented with high E-values, the gene was also identified in the BLAST searches performed by a fellow researcher (Molenaar, 2012). These searches were also performed with sequences obtained from promoter-trap mutagenesis experiments and as mentioned previously, the alignments were considerably longer. The alignment to the *AHNAK* gene was 152 bp in length and had an E-value of 4×10^{-57} (Fig. 3.1). In addition, the BLAST searches were performed against both the mouse and human genomic and transcript databases. These results confirm *AHNAK* as a candidate gene. The GeneCards® search revealed predicted transcription factor binding sites for p53 and c-Myc and the gene is suggested to play a role in neuronal cell differentiation. As mentioned previously, very little information was obtained for *SAAL1* with the GeneCards® search, although the gene is predicted to have a transcription factor binding site for c-Myc. *SAAL1* was however also identified as a candidate gene by a fellow researcher (Fig. 3.2) (Molenaar, 2012). In addition to the significant results obtained from the BLAST searches, these two genes were selected based on their novelty to the apoptotic process, as confirmed with the GeneCards® search. Further bioinformatic analysis with databases containing known and predicted data may thus potentially assist in the functional annotation of these genes, especially for *SAAL1*, and may provide more substantial links to apoptosis.

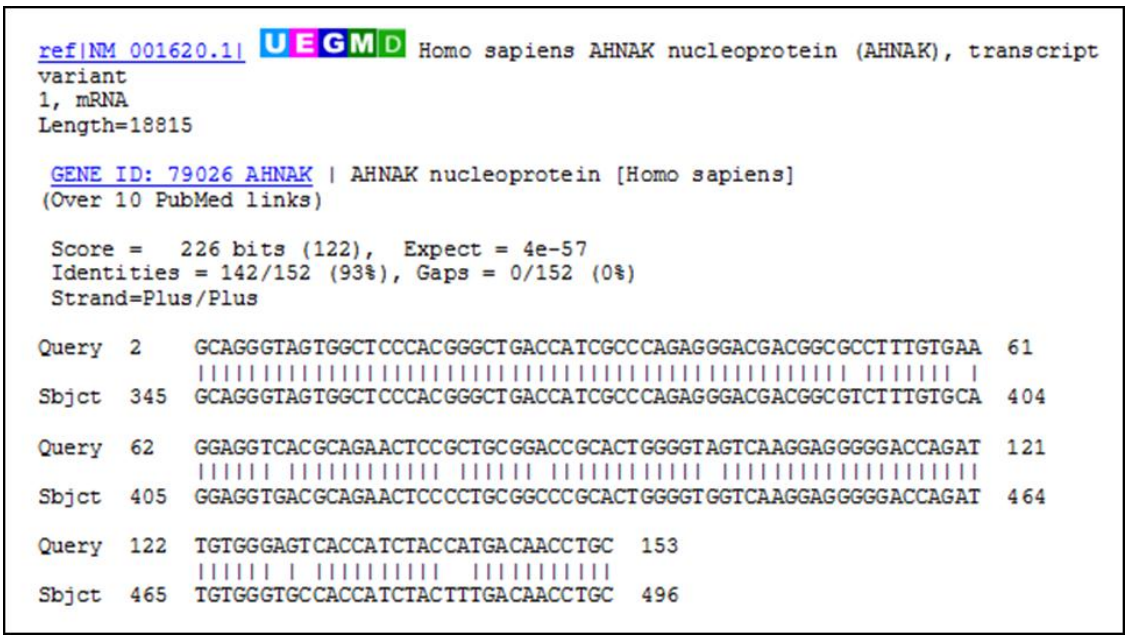

Figure 3.1: BLAST search results of sequence RM118 showing verification of *AHNAK* as a candidate gene. Sequence was obtained from promoter-trap mutagenesis experiments and BLAST searched against the human genomic and transcript database using the BLASTn tool in the NCBI webpage.

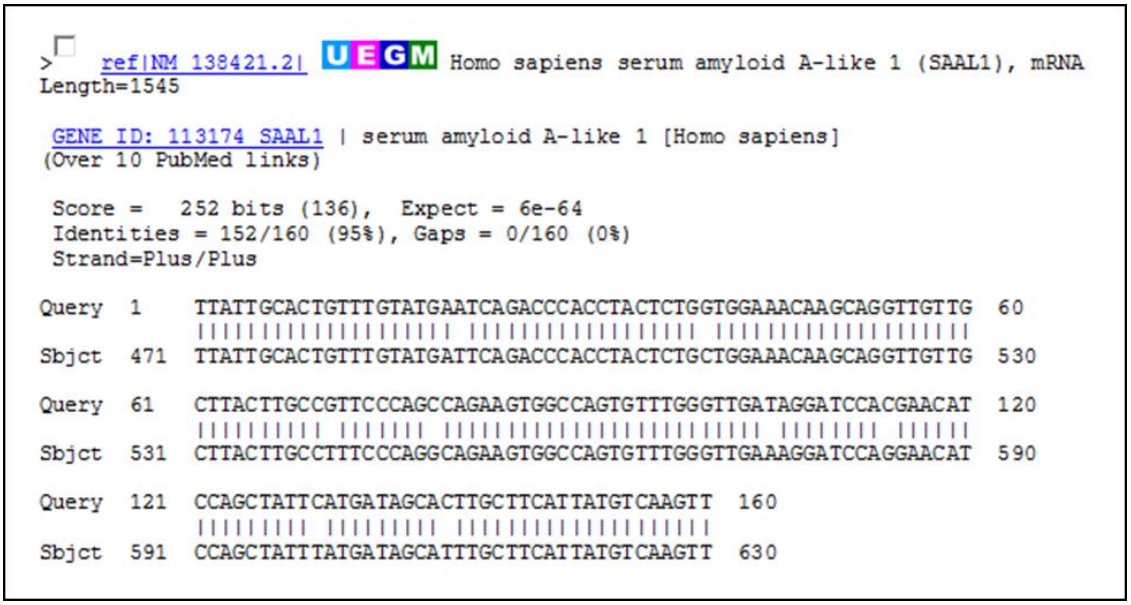

Figure 3.2: BLAST search result of sequence RM289 showing verification of *SAAL1* as a candidate gene. Sequence was obtained from promoter-trap mutagenesis experiments and BLAST searched against the human genomic and transcript database using the BLASTn tool in the NCBI webpage.

3.3.2 Bioinformatic analysis of selected candidate genes

Bioinformatic analyses investigating potential protein-protein interactions and cellular pathways were performed for four candidate genes. In addition to *AHNAK* and *SAAL1*, *LIAS* and *CYPA* were selected for these analyses. These genes were identified in the pilot study and, unlike *RPL9*, the apoptotic resistance effect accompanying the knockdown of these genes were verified in diploid mouse cells, as described in chapter 2. The results obtained from the analysis were further

investigated by determining the molecular function or role of each protein interactant or cellular pathway by means of searches in either the GeneCards®, NCBI Entrez Gene, UniProtKB or InterPro databases.

Investigating the protein interactions for AHNAK revealed a total of 153 interactions across all five databases (table 3.3). These included a combination of 52 known and 101 predicted interactions. Several interactions presenting a potential link to apoptosis were also found; in total, 12 different interacting proteins were identified in addition to four domain signatures. Based on the results obtained from the databases, it would seem that AHNAK might have an impact on apoptosis by playing a role in control of cellular growth and survival, since several of the protein interactants function in these processes. For instance, AHNAK was shown to interact with both the human and mouse homologs of cyclin dependent kinase 1 (CDK1) as well as cyclin dependent kinase 2 (CDK2). These proteins are crucial to the control of the cell cycle and are known to phosphorylate proteins such as p53, the Myc proto-oncogene protein (MYC) and the baculoviral IAP repeat containing 5 (BIRC5) protein, which is a member of the inhibitor of apoptosis (IAP) family. CDK1 has the ability to trigger apoptosis upon DNA damage by phosphorylating Bcl-X_L, while phosphorylation of caspase 8 by CDK1 inhibits its activation and subsequent apoptosis. An interaction with a related protein, cyclin dependent kinase inhibitor 2A (CDKN2A), was also revealed. Referred to as a tumour suppressor, this protein promotes apoptosis by sequestering and inhibiting Mdm2 p53 E3 ubiquitin protein ligase homolog (MDM2), the protein responsible for p53 degradation. Other interactants that function in cellular growth and survival include epidermal growth factor receptor (EGFR), MYC, cell division cycle 5-like protein (CDC5L), v-akt murine thymona viral oncogene homolog 1 (AKT1), S100 calcium binding protein B (S100B) and tyrosine-protein kinase Yes (YES1). The EGFR activates numerous signalling cascades, including the Ras, AKT and protein kinase C (PKC) pathways, which regulate cell growth and survival. The MYC protein functions in the regulation of gene transcription and may promote the transcription of growth-related genes. CDC5L is a DNA binding protein participating in the control of the cell cycle and may also potentially be a transcription factor. AKT1 has been shown to regulate numerous processes, including metabolism, growth, proliferation, angiogenesis and cell survival. The protein is also capable of preventing apoptotic induction through inhibiting components of the apoptotic machinery by means of phosphorylation. S100B participates in the control of cell cycle progression and differentiation and has been associated with certain diseases including type I diabetes, Alzheimer's disease, amyotrophic lateral sclerosis, melanomas and other neoplastic diseases. Lastly, the non-receptor protein tyrosine kinase YES1 plays a role in regulating cell-cell adhesion, cytoskeleton remodelling and apoptosis as well as cellular differentiation, growth and survival. It also participates in the FasL signalling pathway and mediates AKT-mediated cell migration. Among all of the interactions that suggested a potential role for AHNAK in the regulation of cell growth and survival, only two were predicted interactions, namely those with Cdk1 (the mouse homolog of

Table 3.3: Results obtained from the bioinformatic analysis investigating the protein interactions for AHNAK

	All interactions					Interactions with possible ties to apoptosis	
Database	No. of inter-actions	Known/ experimental	Predicted	Interactant from human	Interactant from other organism	No. of inter-actions	Interactants
IntAct	17	5	12¥	7	10	4	Cdk1; EGFR; MYC; CDC5L
STRING	5	5	-	5	-	4	CDKN2A; AKT1; S100B; XRCC4
BioGRID	21	21	-	16	5	4	CDK2; CDK1; EGFR; S100B
DOMINE	98	9	23 HCP; 11 MCP; 55 LCP	N/A	N/A	4	Protein kinase C-terminal; protein-tyrosine phosphatase, receptor/non-receptor type; leucine-rich repeat; pleckstrin homology domain
I2D	12	12	-	12	-	6	EGFR; S100B; YES1; APC; XRCC4; CDKN2A

HCP – high confidence predictions; MCP – medium confidence predictions; LCP – low confidence predictions; N/A – not applicable; ¥ - interactions expanded by spoke model; Cdk1 – Cyclin dependent kinase 1 (mouse); EGFR – epidermal growth factor receptor; MYC – Myc proto-oncogene protein; CDC5L – cell division cycle 5-like protein; CDKN2A – cyclin dependent kinase inhibitor 2A; AKT1 – v-akt murine thymona viral oncogene homolog 1; S100B – S100 calcium binding protein B; XRCC4 – X-ray repair complementing defective repair in Chinese hamster cells 4; CDK2 – cyclin dependent kinase 2; CDK1 – cyclin dependent kinase 1 (human); YES1 – tyrosine-protein kinase Yes; APC – adenomatous polyposis coli protein.

human CDK1) and MYC, which were identified by the IntAct database following the spoke expansion model. This model uses an algorithm to expand the interactions in a protein complex, identified by experimental methods such as tandem affinity purification, into a set of artefactually created binary interactions. Since this model assumes that every prey molecule interacts with the bait molecule, these interactions needs to be verified. The remaining two interactions that link AHNAK to apoptosis is the X-ray repair complementing defective repair in Chinese hamster cells 4 (XRCC4) protein and the adenomatous polyposis coli (APC) protein. XRCC4 is essential to non-homologous end joining, a process that repairs double strand DNA breaks and is required for normal development and tumour suppression, while APC is described as a tumour suppressor due to its role in processes such as transcriptional regulation, cell adhesion and migration as well as apoptosis. Four domain interactions was revealed for the PDZ domain located in AHNAK, including an interaction of medium confidence for the pleckstrin homology domain and high confidence interactions for the remaining three domains. The results obtained from the DOMINE database supports those obtained from the other databases since the majority of these domains implicate the interacting proteins identified by the other databases. The protein kinase C-terminal domain is found in protein kinases, enzymes responsible for the phosphorylation of proteins, and is thus associated with cellular processes such as differentiation, division, proliferation and apoptosis. In addition, the protein-tyrosine phosphatase receptor/non-receptor type domain which catalyses the opposite reaction of that of the protein kinase C-terminal domain, is also associated with the same cellular processes. The pleckstrin homology domain supports a protein-protein interaction with AKT1, since this domain is found in this AKT1. Lastly, the leucine-rich repeat domain can be found in a variety of proteins, including those involved in DNA repair and apoptosis. Even though potential links to apoptosis was found for AHNAK with the protein interaction databases, the search for cellular pathways was unsuccessful. AHNAK was not found to be involved in any cellular pathways by all four databases, indicating that the individual binary interactions for AHNAK still needs to be expanded and incorporated into cellular pathway databases.

As with the initial GeneCards® search, the database searches for *SAAL1* revealed very little information. No cellular pathways was identified with the pathway databases and, compared to *AHNAK*, considerably less protein interactions was identified (table 3.4). Across the databases, the number of protein interactions identified ranged between one and seven, while the DOMINE database did not produce any results. Only three protein interactions proved to be of relevance to apoptosis, namely those with ubiquitin specific peptidase 19 (USP19), pleckstrin homology-like domain family A member 3 (PHLDA3) and neural precursor cell expressed developmentally down-regulated 4 E3 ubiquitin protein ligase (NEDD4). Interactions with PHLDA3 and NEDD4 were both known, while the interaction with USP19 was identified by the spoke expansion model by the IntAct database. However, known interactions between SAAL1 and USP19 were identified by other databases, thus confirming this interaction. In total, USP19 was identified by four databases, while

Table 3.4: Results obtained from the bioinformatic analysis investigating the protein interactions for SAAL1

	All interactions					Interactions with possible ties to apoptosis	
Database	No. of inter-actions	Known/ experimental	Predicted	Interactant from human	Interactant from other organism	No. of inter-actions	Interactants
IntAct	5	3	2¥	3	2	2	USP19; PHLDA3
STRING	1	1	-	1	-	1	USP19
BioGRID	7	7	-	6	1	2	NEDD4; USP19
DOMINE	-	-	-	-	-	-	-
I2D	4	4	-	4	-	2	USP19; PHLDA3

¥ - interactions expanded by spoke mode; USP19 – ubiquitin specific peptidase 19; PHLDA3 – pleckstrin homology-like domain family A member 3; NEDD4 – neural precursor cell expressed, developmentally down-regulated 4, E3 ubiquitin protein ligase.

PHLDA3 was identified twice and NEDD4 only once. The deubiquitinating enzyme USP19 regulates the degradation of numerous proteins as well as the stability of two members of the IAP family, namely BIRC2 and BIRC3. It is also associated with the regulation of the cell cycle by promoting the degradation of cyclin-dependent kinase inhibitor 1 B (CDKN1B). The PHLDA3 protein is suggested to be a tumour suppressor. The protein is directly regulated by p53 and functions by inhibiting AKT1 translocation and activation. PHLDA3 thus mediates p53-dependent apoptosis by means of AKT1 inhibition. Lastly, NEDD4 is an ubiquitin-protein ligase and regulates the degradation of proteins by means of ubiquitination. NEDD4 targets the degradation of insulin-like growth factor 1 receptor (IGF1R) and fibroblast growth factor receptor 1 (FGFR1). The former is referred to as an anti-apoptotic agent since it enhances cell survival, while the latter is involved in cellular differentiation, proliferation and migration. NEDD4 also regulates the degradation of the EGFR. Based on these interactions, one can suggest that SAAL1 may also have an impact on apoptosis by regulating cell survival since this seems to represent a common theme among the protein interactions.

Among the four databases used for the identification of cellular pathways, only Reactome yielded results for CYPA. A total of nine pathways were identified; however, none of these seem to implicate CYPA in apoptosis. The majority of the pathways support an immunological function for CYPA, especially with regards to HIV infection. CYPA was shown to take part in the early phase of the HIV life cycle (REACT_6266.5) while five other pathways identified by the database clustered beneath this pathway. In addition, CYPA was also shown to take part in apolipoprotein B mRNA-editing, enzyme-catalytic, polypeptide-like 3G (APOBEC3G)-mediated resistance to HIV-1 infection (REACT_9406.2). The basigin interactions pathway was also identified; here, CYPA binds basigin to form the basigin precursor molecule (REACT_12560.3). Lastly, the platelet degranulation pathway was identified where CYPA is inferred to be one of the cytosolic components released from the platelet cell (REACT_318.7). Based on the descriptions of these pathways, there seems to be no link to apoptosis for CYPA. The database searches for protein interactions was however more successful (table 3.5). A total of 238 interactions were identified across all five databases, of which the majority were known interactions. The I2D database identified the largest amount of interactions, that is, 78 interactions of which only one was predicted. Among the interactions showing potential links to apoptosis were some that were identified more than once by different databases, and thus the investigation identified 26 different protein interactants with potential links to apoptosis. As with the other candidate genes, a common theme is also present among the identified protein interactants; many of these proteins are involved in cellular proliferation and survival as well as processes associated with DNA damage, including preventing, inducing or repairing damage. The protein interactant with the most pronounced association with apoptosis also conforms to this theme, namely apoptosis inducing factor 1 mitochondrial (AIFM1), or AIF. This interaction was identified with both the human and mouse homologs by the IntAct database.

Table 3.5: Results obtained from the bioinformatic analysis investigating the protein interactions for CYPA

	All interactions					Interactions with possible ties to apoptosis	
Database	No. of inter-actions	Known/ experimental	Predicted	Interactant from human	Interactant from other organism	No. of inter-actions	Interactants
IntAct	46	19	27¥	32	14	8	GABARAP; APP; H2AFX; AIFM1; Cdk1; Aifm1; RAD52; PCNA
STRING	15	14	1*	15	-	3	APP; RB1; PCNA
BioGRID	47	47	-	38	9	7	CDK2; COPS5; Cdk1; H2AFX; PAF; MAD2L1BP; PCNA
DOMINE	52	5	7 HCP; 11 MCP; 29 LCP	N/A	N/A	4	Histone core; leucine-rich repeat; cell division binding GTP binding; histone H4 acetyltransferase, NuA4 complex, Eaf6
I2D	78	77	1	78	-	17	PDPK1; FOXO3; GABARAP; APP; RB1; H2AFX; DDIT3; PRKAA2; TRAF2; STK4; PRKAA1; STK3; SQSTM1; STK11; RB1CC1; RASSF5; ATG5

HCP – high confidence predictions; MCP – medium confidence predictions; LCP – low confidence predictions; N/A – not applicable; ¥ - interactions expanded by spoke mode; * - based on co-expression evidence type; GABARAP – gamma-aminobutyric acid receptor-associated protein; APP – amyloid beta A4 protein; H2AFX – histone H2A.x; AIFM1 – apoptosis-inducing factor 1, mitochondrial; Cdk1 – cyclin dependent kinase 1 (mouse); Aifm1 – apoptosis inducing factor 1, mitochondrial (mouse); RAD52 – DNA repair protein RAD52 homolog; PCNA – proliferating cell nuclear antigen; RB1 – retinoblastoma 1; CDK2 – cyclin dependent kinase 2; COPS5 – COP9 constitutive photomorphogenic homolog subunit 5; PAF – PCNA-associated factor; MAD2L1BP – mitotic arrest deficient 2-like protein 1 (MAD2L1)-binding protein; PDPK1 – 3-phosphoinositide-dependent protein kinase 1; FOXO3 – forkhead box protein 3; DDIT3 – DNA-damage-inducible transcript 3; PRKAA2 – 5'-AMP-activated protein kinase catalytic subunit alpha-2; TRAF2 – tumour necrosis factor (TNF)-receptor associated factor 2; STK4 – serine/threonine protein kinase 4; PRKAA1 – 5'AMP-activated protein kinase catalytic subunit alpha-1; STK3 – serine/threonine protein kinase 3; SQSTM1 – sequestosome-1; STK11 – serine/threonine protein kinase 11; RB1CC1 – retinoblastoma 1 (RB1)-inducible coiled coil protein 1; RASSF5 – ras association domain-containing protein 5; ATG5 – autophagy protein 5.

AIF is a major facilitator of caspase-independent apoptosis by binding to and fragmenting chromosomal DNA in a sequence-independent matter. AIF is also capable of activating caspase 7, thus amplifying the apoptotic process. The kinases Cdk1 and CDK2 were also identified and as mentioned previously, these proteins are important regulators of the cell cycle as well as the activity of p53 and BIRC5 by means of phosphorylation. The variant histone H2A.x (H2AFX) is present in a subset of nucleosomes. In general, histones are important regulators of transcription and are also involved in DNA replication, DNA repair and the maintenance of chromosomal stability. The DNA repair protein RAD52 homolog (RAD52) functions in genetic recombination and DNA repair by participating in the repair of double-stranded breaks. Proliferating cell nuclear antigen (PCNA) is vital to the DNA damage response by positioning itself at the replication fork and coordinating DNA replication with DNA repair and DNA damage tolerance pathways. Retinoblastoma 1 (RB1) is a well-known tumour suppressor and functions by regulating entry into cell division. The RB1-inducible coiled-coil protein 1 (RB1CC1) was also identified by the databases. This protein is a DNA-binding transcription factor and an important regulator of the RB1 pathway. Another protein interactant involved in cell division is mitotic arrest deficient-like 1 (MAD2L1)-binding protein (MAD2L1BP). This protein may be involved in the silencing of the spindle checkpoint, thus allowing mitosis to proceed. Referred to as a master kinase, 3-phosphoinositide-dependent protein kinase 1 (PDPK1) plays a vital role in the control of cell proliferation and survival by phosphorylating and subsequently activating AKT1. The DNA-damage-inducible transcript 3 (DDIT3) is a transcription factor and member of the CCAAT/enhancer-binding protein (C/EBP) family. DDIT3 prevents the binding of C/EBP transcription factors to DNA and also promotes apoptosis. Both the 5'-AMP-activated protein kinase catalytic subunit alpha 1 (PRKAA1) and 2 (PRKAA2) were identified by the protein interaction databases. As their names suggests, these proteins form the catalytic subunit of the AMP-activated protein kinase (AMPK), an essential regulator of cell growth and proliferation upon energy-deficient circumstances. The kinase is known to phosphorylate numerous proteins, including p53. Tumour necrosis factor (TNF) receptor-associated factor 2 (TRAF2) plays a key role in regulating cellular survival and apoptosis by regulating the activation of nuclear factor kappa B (NFκB) and Jun N-terminal kinase (JNK). The protein also has the ability to prevent the degradation of BIRC2 and BIRC3. The I2D database identified interactions with three serine/threonine kinases (STK), namely STK3, STK4 and STK11, and all three are pro-apoptotic kinases. STK3 and STK4 are stress-activated kinases that, upon apoptotic stimuli, translocate to the nucleus to induce chromatin condensation and DNA fragmentation. They are also capable of inhibiting AKT1. STK11 is referred to as a tumour suppressor kinase and is known to play a role in DNA damage response and apoptosis. STK11 is also a mediator of p53-mediated apoptosis. Finally, sequestosome 1 (SQSTM1) is potentially involved in cellular differentiation and apoptosis by regulating the activation of NFκB. Other protein interactants that can be associated with apoptosis by means other than cellular proliferation and DNA damage processes include gamma-

aminobutyric acid receptor-associated protein (GABARAP), amyloid beta A4 protein (APP), COP9 constitutive photomorphogenic homolog subunit 5 (COPS5), PCNA-associated factor (PAF), forkhead box protein 3 (FOXO3), Ras association domain-containing protein 5 (RASSF5) and autophagy protein 5 (ATG5). GABARAP is involved in the transport of GABA receptors and plays a role in apoptosis. APP is associated with pathways known to induce apoptosis, such as the JNK-interacting protein (JIP)-mediated pathway. The COPS5 protein is likely a subunit of the COP9 signalosome complex (CSN) which is known to play a role in the phosphorylation of p53 and c-Jun, a proto-oncogene. PAF is likely to provide protection from cell death induced by UV-light. FOXO3 is a transcription factor known to induce apoptosis in the absence of survival factors. As mentioned previously ATG5 may be involved in apoptosis through modifications of the cytoskeleton. Lastly, RASSF5 is described as a tumour suppressor. The DOMINE databases also identified domain interactions for the pro-isomerase domain located in CYPA that may provide links to apoptosis. Two of these domain interactions are associated with and the modification of histones. The histone core domain is found in numerous histone proteins while the histone H4 acetyltransferase Nu4 complex Eaf6 family signature is associated with the acetylation of histones and is thus involved in regulation of transcription, DNA damage response and cell cycle control. Another family signature, cell division protein GTP binding, is involved in cell cycle control, while the leucine-rich repeat, as mentioned previously, can be associated with apoptosis.

Compared to those of *AHNAK* and *CYPA*, fewer results were obtained from the bioinformatic analysis for *LIAS*. Investigating the cellular pathways for LIAS identified a single pathway representing lipoic acid metabolism, as revealed by KEGG (hsa00785), HumanCyc (HS04528) and UniPathway (UPA00538). This pathway entails the biosynthesis of lipoic acid and subsequent lipoylation of lipoate-dependent enzymes, in which LIAS plays a central role. However, as with CYPA, there seems to be no link to apoptosis. With regards to the protein interactions, 63 interactions were identified of which the majority were predicted interactions (table 3.6). Both the IntAct and BioGRID databases failed to produce any results and only four proteins interactions were identified that revealed potential links to apoptosis. These interactions were predicted by the STRING and I2D databases. Cyclin-dependent kinase 5 (CDK5) regulatory associated protein 1 (CDK5RAP1) is a specific inhibitor of CDK5 and plays an important role in cell cycle arrest in neurons and is also known to phosphorylate p53 and regulate Bcl-2. The DNA replicating licensing factor MDM2 (MDM2) is essential for the control of DNA replication initiation and elongation and is required for cell division. The protein interactant with the most pronounced association with apoptosis is likely to be that of guanine nucleotide-binding protein subunit beta-2-like 1 (GNB2L1). This protein is capable of inducing apoptosis by disrupting the interaction between Bcl-2L and Bax, thereby promoting Bax oligomerisation. Finally, protein arginine N-methyltransferase 1 (PRMT1) is an arginine methyltransferase capable of inhibiting signal transducer and activator of transcription

Table 3.6: Results obtained from the bioinformatic analysis investigating the protein interactions for LIAS

	All interactions					Interactions with possible ties to apoptosis	
Database	No. of inter-actions	Known/ experimental	Predicted	Interactant from human	Interactant from other organism	No. of inter-actions	Interactants
IntAct	-	-	-	-	-	-	-
STRING	31	3	28*	31	-	1	CDK5RAP1
BioGRID	-	-	-	-	-	-	-
DOMINE	19	5	3 HCP; 11 LCP	N/A	N/A	-	-
I2D	13	-	13	13	-	3	MCM2; GNB2L1; PRMT1

HCP – high confidence predictions; LCP – low confidence predictions; N/A – not applicable; * - based on neighbourhood, fusion, co-occurrence, homology and co-expression evidence types; CDK5RAP1 – cyclin dependent kinase 5 regulatory associated protein 1; MCM2 – minichromosome maintenance complex 2; GNB2L1 – guanine nucleotide-binding protein subunit beta-2-like 1; PRMT1 – protein arginine N-methyltransferase 1.

1 (STAT1), a transcription factor involved in the regulation of cellular differentiation, growth and survival.

3.4 Conclusions

Since the start of the bioinformatics era, this continually expanding field of study has made significant contributions to the understanding of the genome, including the analysis of high-throughput data, assigning gene/protein annotations, building and exploring protein structures and providing knowledgebases that conveniently collects and integrate biological data while making it available to the everyday researcher. In particular, databases have been created covering almost every area of research and have become valuable tools that aid and complement molecular techniques. As described in this chapter, a bioinformatic approach was used to identify candidate genes with a potential role in apoptosis. Nucleotide sequences, obtained from the promoter-trap mutagenesis experiments performed in the pilot study, were analysed by means of the BLASTn tool to identify gene-specific sequences within the nucleotide sequences. The identified candidate genes were investigated by means of the GeneCards® database, and two candidate genes, *AHNAK* and *SAAL1*, were selected for further analysis based on their novelty to the apoptotic process. In addition, two candidate genes, *LIAS* and *CYPA*, previously identified in the pilot study were also included. A total of nine databases were selected to investigate protein interactions and cellular pathways for the four selected candidate genes with the aim of identifying a potential role for these genes in apoptosis.

The BLAST analysis were successful for only three alignments, however results obtained in a study performed by a fellow researcher supported the identification of *SAAL1* and *AHNAK* as candidate genes (Molenaar, 2012). The fact that three of the candidate genes, namely, *LIAS*, *SAAL1* and *AHNAK*, were identified more than once in the BLAST searches performed with nucleotide sequences, whether in this study, the study performed by the fellow researcher or in the pilot study, provides increasing support for a potential role for these genes in apoptosis.

The bioinformatic analysis investigating protein interactions and cellular pathways were successful, albeit more for *AHNAK* and *CYPA* than for *SAAL1* and *LIAS*. The use of a number of different databases provided a good representation of the available data and even though some interactions or pathways were identified more than once by different databases, the majority were identified by only a single database. This highlights the heterogeneity present in the construction of bioinformatic databases and the different results they produce; it would thus seem advantageous to use more than one database when investigating a particular area of interest. A combination of both known, or experimentally verified, and predicted interactions was obtained by the protein interaction databases. Known interactions are of course important when expanding and exploring the larger biological context of a particular protein, but predicted interactions might prove to be of more value when annotating a gene with little known information or when assigning a gene/protein

to a new pathway/process. Predicted protein interactions provide clues to the function of a protein and may also implicate the protein in a cellular pathway. In addition, predicted interactions provide a foundation for molecular techniques that aims to experimentally ascertain an annotation for a gene/protein. In this study, the majority of the protein interactions identified for LIAS were predicted, including those with potential links to apoptosis. Even though a known function for LIAS exists, as confirmed by the results obtained from the cellular pathway investigation, these predicted interactions may suggest additional functions for LIAS.

Several potential links to apoptosis were identified for the candidate genes, although they remain to be verified experimentally especially since the majority of them were of an indirect nature. An indirect link refers to a protein interactant which is primarily involved in a different process or pathway but can also have an impact on the apoptotic process, whether this impact would be consequence of the protein's primary role or not. In contrast, direct links would be to proteins which are primarily involved in the apoptotic process itself, either as an inducer or mediator. Examples of the indirect links are the commonly identified cyclin dependent kinases, PRMT1, RAD52, USP19, EGFR and many others. Examples of direct links would be AIFM1, FOXO3, STK3 and STK4. In general, a common theme was present among the majority of the protein interactants for the candidate genes. Most of these proteins were involved cell cycle control, cellular proliferation, growth and survival. A number of transcriptional regulators were also identified. This observation highlights the fact that even though a core set of apoptotic molecules exist, the process can be affected by a multitude of other proteins. In addition it also supports the reality the cell death and cell proliferation/survival is a tightly regulated and complex balance beam.

Future applications of the results described in this chapter include perhaps additional bioinformatic analyses, investigating other areas of interest such as gene expression and transcriptional regulation. Indeed, exploring these results by means of molecular techniques would assist in verifying the candidate genes' involvement in apoptosis as well as aiding in their annotation, especially with regards to *SAAL1* and *LIAS*.

3.5 References

Breitkreutz, B., Stark, C., Reguly, T., Boucher, L., Breitkreutz, A., Livstone, M., Oughtred, R., Lackner, D.H., Bähler, J., Wood, V., *et al*. (2008). The BioGRID interaction database: 2008 update. Nucleic Acids Res. *36,* D637-D640.

Brown, K.R., and Jurisica, I. (2005). Online predicted human interaction database. Bioinformatics *21,* 2076-2082.

Brown, K., and Jurisica, I. (2007). Unequal evolutionary conservation of human protein interactions in interologous networks. Genome Biol. *8,* R95.1-R95.11.

Croft, D., O'Kelly, G., Wu, G., Haw, R., Gillespie, M., Matthews, L., Caudy, M., Garapati, P., Gopinath, G., Jassal, B.*, et al.* (2011). Reactome: a database of reactions, pathways and biological processes. Nucleic Acids Res. *39,* D691-D697.

Dou, A., and Wang, X. (2010). Cyclic adenosine monophosphate signal pathway in targeted therapy of lymphoma. Chin. Med. J. (Beijing, China, Engl. Ed.) *123,* 95-99.

Jensen, L.J., Kuhn, M., Stark, M., Chaffron, S., Creevey, C., Muller, J., Doerks, T., Julien, P., Roth, A., Simonovic, M., *et al*. (2009). STRING 8 - a global view on proteins and their functional interactions in 630 organisms. Nucleic Acids Res. *37,* D412-D416.

Kanehisa, M., and Goto, S. (2000). KEGG: Kyoto Encyclopedia of Genes and Genomes. Nucleic Acids Res. *28,* 27-30.

Kanehisa, M., Goto, S., Sato, Y., Furumichi, M., and Tanabe, M. (2012). KEGG for integration and interpretation of large-scale molecular data sets. Nucleic Acids Res. *40,* D109-D114.

Karp, P.D., Paley, S., and Romero, P. (2002). The Pathway Tools software. Bioinformatics *18,* S225-S232.

Kerrien, S., Aranda, B., Breuza, L., Bridge, A., Broackes-Carter, F., Chen, C., Duesbury, M., Dumousseau, M., Feuermann, M., Hinz, U.*, et al.* (2012). The IntAct molecular interaction database in 2012. Nucleic Acids Res. *40,* D841-D846.

Matthews, L., Gopinath, G., Gillespie, M., Caudy, M., Croft, D., de Bono, B., Garapati, P., Hemish, J., Hermjakob, H., Jassal, B.*, et al.* (2009). Reactome knowledgebase of human biological pathways and processes. Nucleic Acids Res. *37,* D619-D622.

Molenaar, N. (2012). Identification of novel genes involved in resistance to apoptosis. Unpublished Hons. dissertation. Stellenbosch: University of Stellenbosch.

Morgat, A., Coissac, E., Coudert, E., Axelsen, K.B., Keller, G., Bairoch, A., Bridge, A., Bougueleret, L., Xenarios, I., and Viari, A. (2012). UniPathway: a resource for the exploration and annotation of metabolic pathways. Nucleic Acids Res. *40,* D761-D769.

Ndozangue-Touriguine, O., Hamelin, J., and Bréard, J. (2008). Cytoskeleton and apoptosis. Biochem. Pharmacol. *76,* 11-18.

Nieminen, A., Partanen, J., and Klefstrom, J. (2007). c-Myc blazing a trail of death: coupling of the mitochondrial and death receptor apoptosis pathways by c-Myc. Cell Cycle *6,* 2464-2472.

Novakovic, P., Stempak, J.M., Sohn, K., and Kim, Y. (2006). Effects of folate deficiency on gene expression in the apoptosis and cancer pathways in colon cancer cells. Carcinogenesis *27,* 916-924.

Ola, M., Nawaz, M., and Ahsan, H. (2011). Role of Bcl-2 family proteins and caspases in the regulation of apoptosis. Mol. Cell. Biochem. *351,* 41-58.

Perez-Iratxeta, C., Andrade-Navarro, M.A., and Wren, J.D. (2007). Evolving research trends in bioinformatics. Briefings Bioinf. *8,* 88-95.

Raghavachari, B., Tasneem, A., Przytycka, T.M., and Jothi, R. (2008). DOMINE: a database of protein domain interactions. Nucleic Acids Res. *36,* D656-D661.

Rebhan, M., Chalifa-Caspi, V., Prilusky, J., and Lancet, D. (1997). GeneCards: integrating information about genes, proteins and diseases. Trends Genet. *13,* 163.

Romero, P., Wagg, J., Green, M., Kaiser, D., Krummenacker, M., and Karp, P. (2004). Computational prediction of human metabolic pathways from the complete human genome. Genome Biol. *6,* R2.1-R2.17.

Safran, M., Dalah, I., Alexander, J., Rosen, N., Iny Stein, T., Shmoish, M., Nativ, N., Bahir, I., Doniger, T., Krug, H.*, et al.* (2010). GeneCards Version 3: the human gene integrator. Database *2010,* doi: 10.1093/database/baq020.

Stark, C., Breitkreutz, B., Reguly, T., Boucher, L., Breitkreutz, A., and Tyers, M. (2006). BioGRID: a general repository for interaction datasets. Nucleic Acids Res. *34,* D535-D539.

Stark, C., Breitkreutz, B., Chatr-aryamontri, A., Boucher, L., Oughtred, R., Livstone, M.S., Nixon, J., Van Auken, K., Wang, X., Shi, X.*, et al.* (2011). The BioGRID interaction database: 2011 update. Nucleic Acids Res. *39,* D698-D704.

Szklarczyk, D., Franceschini, A., Kuhn, M., Simonovic, M., Roth, A., Minguez, P., Doerks, T., Stark, M., Muller, J., Bork, P., *et al*. (2011). The STRING database in 2011: functional interaction networks of proteins, globally integrated and scored. Nucleic Acids Res. *39,* D561-D568.

Yellaboina, S., Tasneem, A., Zaykin, D.V., Raghavachari, B., and Jothi, R. (2011). DOMINE: a comprehensive collection of known and predicted domain-domain interactions. Nucleic Acids Res. *39,* D730-D735.

Chapter 4: Investigating the gene expression of the novel candidate genes in two cancer cell lines

4.1 Introduction

Quantitative PCR (qPCR), or real-time PCR, is a modification of the traditional end-point PCR technique that allows for the concurrent detection and quantification of a DNA template in real time (Pfaffl, 2001). Following its first report in 1993, qPCR has since become the method of choice for measuring gene expression; however, its usefulness is not restricted to gene expression studies (Derveaux et al., 2010; Higuchi et al., 1993). Other applications of qPCR includes the validation of gene expression microarrays, copy number determination for genomic or viral DNA, allelic discrimination assays and mutation detection (Arya et al., 2005; Valasek and Repa, 2005). The ability of qPCR to produce accurate results across a dynamic range of several log orders of magnitude, as well as its impressive sensitivity and precision, are three important advantages of qPCR (Arya et al., 2005; Wong and Medrano, 2005). In addition, relatively high-throughput can also be obtained with the proper instrumentation (Wong and Medrano, 2005).

Central to the qPCR technique is the use of fluorescent chemistries that bind to the template in either a non-specific or specific manner. The most popular non-specific chemistry used today is SYBR® Green I. This intercalating dye emits its fluorescent signal upon binding to the minor groove of double-stranded DNA (dsDNA) in a sequence-independent manner (Arya et al., 2005; Morrison et al., 1998). The dye is relatively cheap and can be incorporated into established and optimised protocols (Bustin and Nolan, 2004). A major disadvantage of SYBR® Green I is however nested within its nature; since the dye binds non-specifically to dsDNA, fluorescent signals are also emitted upon binding to miss-primed amplification products and primer-dimers. This necessitates a melting curve analysis, plotting fluorescence as a function of temperature, in order to determine the presence of the target amplicon by means of its melting temperature (T_M) (Arya et al., 2005; Kubista et al., 2006). Specific chemistries entail the design and synthesis of sequence-specific fluorescently-labelled probes, which can prove to be very costly (Bustin and Nolan, 2004). However, since the emission of a fluorescent signal is dependent on the annealing of the probe to the specific target, potential false signals are avoided (Arya et al., 2005; Bustin and Nolan, 2004). In addition, the specificity of the probes make them amendable to multiplex reactions where multiple probes labelled with different fluorescent dyes can be included in one reaction (Arya et al., 2005). The majority of these chemistries are designed around fluorescence resonance energy transfer (FRET) between a quencher and donor dye as the basis of its detection method (Bustin and Nolan, 2004). Examples of specific chemistries include Taqman® probes, dual hybridisation probes, molecular beacons and scorpions (Arya et al., 2005; Wong and Medrano, 2005).

The amplification process in qPCR follows the same phases as traditional PCR, and it is in the exponential phase, when optimal doubling of the template takes place in the absence of any limiting conditions, that quantification of the template takes place (Arya et al., 2005; Ginzinger, 2002). Early in the exponential phase, an arbitrary threshold is set by the instrument based on the baseline of the experiment, the initial cycles where the accumulating fluorescence remains beneath the instrument's limit of detection. As amplification proceeds, a cycle is reached where the fluorescent signal exceeds the threshold; a point that is defined as the cycling threshold, or C_T, value. The C_T values can then be extrapolated back to determine the initial amount of the template; the lower the C_T value, the higher the amount of template present at the start of amplification (Fig. 4.1) (Arya et al., 2005; Ginzinger, 2002).

Three quantification strategies are commonly used to interpret the data generated by qPCR. The first method is referred to as absolute quantification, or the standard curve method, and is generally performed when the actual amount of the template needs to be measured such as in the determination of viral load in a diseased sample (Arya et al., 2005). In this method, the concentration of a target in an unknown sample is calculated from a standard curve generated by a set of standards for the specific target (Arya et al., 2005; Wong and Medrano, 2005). The remaining two methods are based on relative quantification, that is, the amount of template present in a sample is determined relative to that of a reference, which is normally a constitutively expressed reference gene (Valasek and Repa, 2005). In the relative standard curve method, otherwise known as the Pfaffl method, standard curves are also constructed for each of the target and reference genes, however, the curves are only used to the determine the efficiency of the qPCR reaction. The efficiency value is then incorporated into the calculation for the expression of a target gene relative to that of the reference gene(s) (Pfaffl, 2001). Due to the requirement of standard curves, the first two methods can be quite laborious and time consuming, especially when a large number of target genes are being investigated (Schmittgen and Livak, 2008). Lastly, the comparative C_T method, or delta-delta C_T method, was used in this study. This method is simpler when compared to the other two methods since it does not require the construction of standard curves; instead, it assumes a PCR efficiency of 100% or a value of two (i.e. optimal doubling of the PCR template in each cycle), which is then used for the calculation of relative gene expression. In addition, this method also assumes that the efficiencies of the reference gene(s) are similar to those of the target genes (Arya et al., 2005; Schmittgen and Livak, 2008). Thus, in order for this method to give an accurate ratio of the expression of a target gene relative to that of a reference gene, these two assumptions must hold true (Schmittgen and Livak, 2008). This is possible, for example, when using established and optimized primers and qPCR protocols where efficiencies have been calculated previously and shown to be comparable.

This part of the study aimed to determine the relative expression of the novel candidate genes, *LIAS*, *CYPA*, *AHNAK* and *SAAL1*, in two cancer cell lines compared to matching control cell lines.

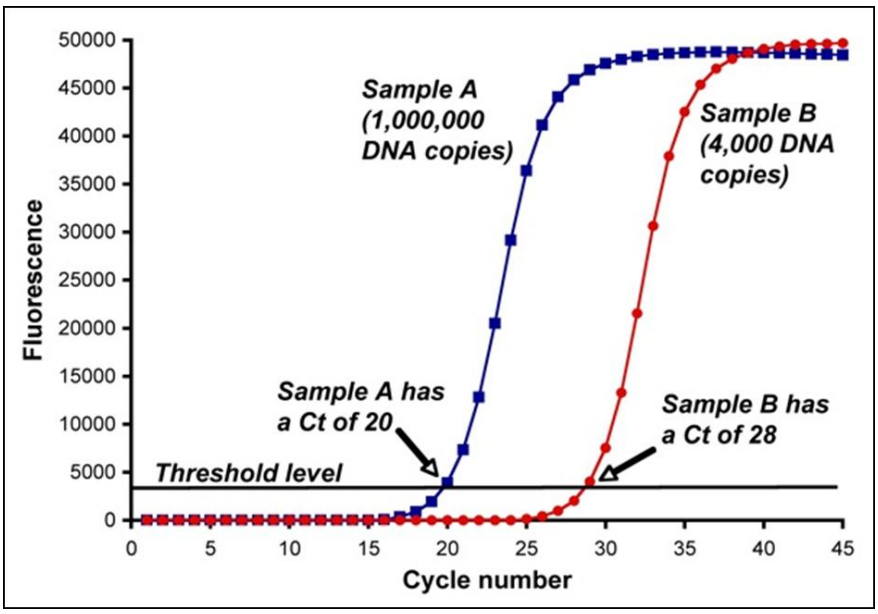

Figure 4.1: Illustration of an amplification plot obtained in qPCR depicting the estimation of the C_T value. Obtained from http://www.langfordvets.co.uk/lab_pcr_ct_values.htm.

This was done to aid in the characterisation of these genes and to determine whether they are differentially regulated in cancer. Since resistance to apoptosis is a central characteristic of tumours, this could also assist in the characterisation of the candidate genes in apoptosis resistance.

4.2 Materials and methods

4.2.1 Total RNA extraction and cDNA synthesis

The sample material used in this part of the study originated from four cell lines, cultured and maintained at the UWC. These samples consisted of two cancer cell lines, namely Caki-1 (kidney cancer sample) and A549 (lung cancer sample), and two control cell lines, namely HEK293T (normal kidney sample) and MRC-5 (normal lung sample). Total RNA, extracted as described in section 2.2.1.6, was provided the collaborator Dr M. Meyer at the UWC.

For cDNA synthesis, the Transcriptor First Strand cDNA Synthesis kit from Roche Applied Sciences was used and performed as described in section 2.2.1.7. A NanoDrop Spectrophotometer was used to determine the concentration, as well as integrity, of the synthesised cDNA. A 250 ng/µl dilution was prepared for each of the samples which were kept at 4°C during use.

4.2.2 Quantitative PCR

Quantitative PCR was performed to measure the expression levels of seven target genes and two reference genes. Target genes consisted of the four candidate genes, namely *LIAS*, *CYPA*, *AHNAK* and *SAAL1*, and also included three genes known to be involved in the apoptotic process, namely *Bcl2* and *caspase 3* (*casp3*) and *9* (*casp9*). The selected reference genes were *GAPDH* and *ubiquitin C* (*UBC*). The qPCR reactions were performed on the Applied Biosystems StepOnePlus™ (Life Technologies™) instrument at the Central Analytical Facility, University of Stellenbosch. The reactions were prepared with the KAPA SYBR® FAST qPCR Kit Master Mix (2 x) ABI Prism™ (KAPA Biosystems) at a 1 x final concentration, to which specific primers and 250 ng template cDNA were added; a final volume of 20 µl was obtained by the addition of ultrapure water. All primers were used at a final concentration of 200 nM, with the exception of the *CYPA* primers where a final concentration of 100 nM was used. Primer sequences and T_A's are listed in table 4.1. All reactions were performed in triplicate and non-template controls were included to control for contamination. The cycling parameters used for all qPCR reactions consisted of an initial enzyme activation step of 3 min at 95°C followed by a two-step cycling protocol with denaturation and annealing/elongation steps of 3 s at 95°C and 30 s at the primer-specific T_A, respectively, which was repeated 45 times. A melt curve, ranging from 58°C to 95°C, was also performed after completion of the cycling protocol. Gel electrophoresis (50 min at 120 V) was performed with the qPCR amplification product on a 1.5% agarose gel.

Since the primers used for the qPCR reactions have been optimised and successfully used before, the comparative C_T method was used for the analysis of the qPCR results. This was done by making use of the freely available REST-384© (v. 1) software package (Pfaffl et al., 2002). This software performs a group-wise comparison between data for a sample and control group and performs a randomisation test to test for significant expression ratios. For the analysis, an assumed PCR efficiency of two was selected and the data was tested for significance by performing the recommended 2000 randomisations.

4.3 Results and discussion

4.3.1 Quantitative PCR

During this part of the study, the relative expression levels of seven target genes were determined with qPCR; these genes are *LIAS*, *CYPA*, *AHNAK*, *SAAL1*, *Bcl-2*, *casp3* and c*asp9*. In addition, the *UBC* and *GAPDH* genes were also included to serve as reference genes. Intact and pure cDNA, as determined by the NanoDrop spectrophotometer, was used as the template material for the qPCR reactions. The samples originated from two cancer cell lines and two matched control cell lines. The use of sample matched controls allows for a comparison to be drawn between the

Table 4.1: Details of primers used for qPCR experiments

Gene	Primer orientation	Primer sequence (5'-3')	Primer length (bp)	Primer T_A (°C)	Product size (bp)
GAPDH	F	TGATGACATCAAGAAGGTGGTGAAG	25	60	240
	R	TCCTTGGAGGCCATGTGGGCCAT	23		
UBC	F	CGGTGAACGCCGATGATTAT	20	60	124
	R	ATCTGCATTGTCAAGTGACGA	21		
LIAS	F	GCAACAATGAAAGCACTTCGTT	22	60	176
	R	ACCAAAGGGCCACTTGCAGTA	21		
CYPA	F	GTTCTTCGACATTGCCGTCG	20	62	212
	R	ACTTGCCACCAGTGCCATTA	20		
SAAL1	F	TTGACAGCCTCATTCGGGTC	20	60	206
	R	CTTTACTCCCTGAGCCACCG	20		
AHNAK	F	CAGTGTGCCCTCTGCCAATA	20	60	210
	R	CCAGGCCCCTGAACATCAAT	20		
Casp3	F	GGCCTGCCGTGGTACAGAAC	20	60	187
	R	CAGCATGGCACAAAGCGACTG	21		
Casp9	F	AGGCCCCATATGATCGAGGA	20	60	193
	R	TCGACAACTTTGCTGCTTGC	20		
Bcl2	F	GTCATGTGTGTGGAGAGCGT	20	60	192
	R	AGTCTTCAGAGACAGCCAGGA	20		

F – forward; R – reverse; bp – base pair; T_A – annealing temperature; °C – degrees Celcius.

normal and malignant state of a particular cell line. The quantification of each gene was performed in triplicate in order to control for variation between reactions. For the most part, near-identical results were obtained from the triplicate reactions for each of the genes investigated as revealed by the amplification plots (Fig. 4.2). A melt curve was also performed on completion of the amplification cycling protocol. By measuring the fluorescence during a gradual increase in temperature, a specific T_M is obtained for each amplification product in a sample; thus, if more than one product is present, for example in the case of non-specific binding by the primers or the formation of primer-dimers, more than one peak will be obtained. This additional step is especially important when using non-specific DNA-binding dyes such as SYBR® Green since the dye emits a fluorescent signal upon binding to any dsDNA template (Arya et al., 2005; Kubista et al., 2006). All triplicate reactions for each of the genes investigated revealed a single peak upon the melt curve analysis (Fig. 4.2).

The selection of an appropriate constitutively expressed reference gene for qPCR analysis is of utmost importance. Since even minor, but inevitable, inter-sample variances can easily affect the

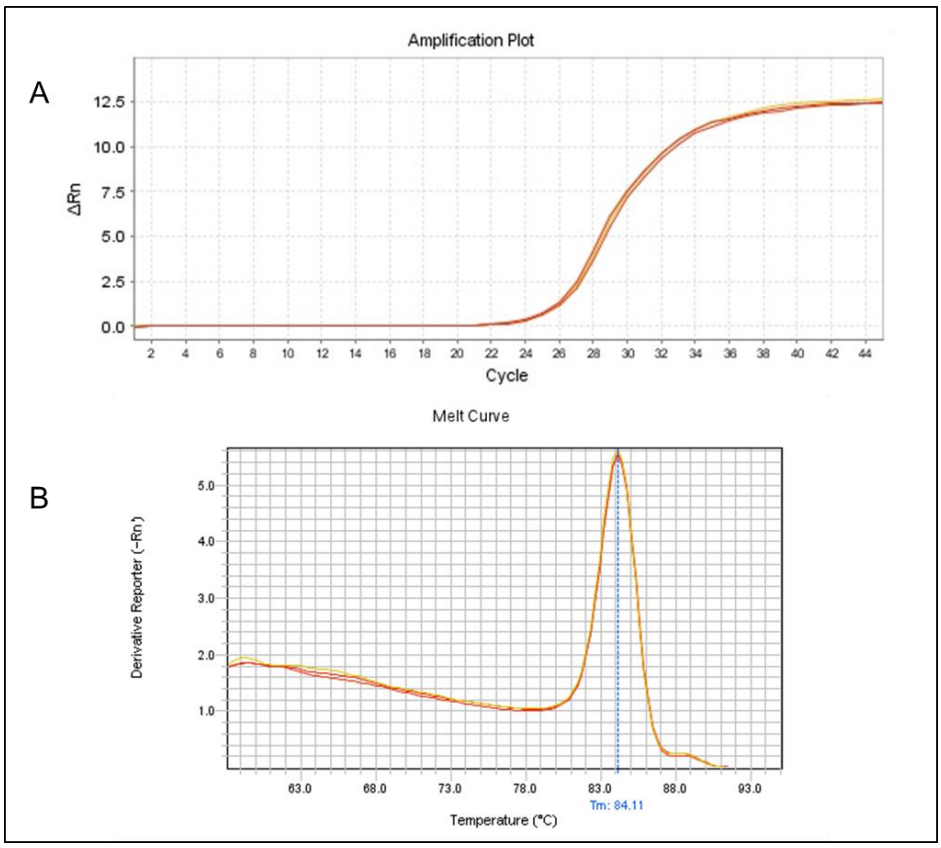

Figure 4.2: Representative example of an amplification plot (A) and melt curve (B) obtained during the qPCR reactions. The triplicate reactions for *LIAS* quantification in the lung cancer sample are displayed. Rn – normalised fluorescence.

reliability of qPCR results, it is necessary to compensate for these differences by submitting all samples to normalisation with a reference gene (Arya et al., 2005; VanGuilder et al., 2008). An appropriate reference gene would exhibit constant expression in all tissues and under all conditions and would thus allow for the comparison of samples (Kubista et al., 2006; VanGuilder et al., 2008). Quite a large selection of reference genes is available today; however, many have been shown to be regulated in some tissues or under certain conditions (Arya et al., 2005; Pfaffl et al., 2004). In this study, two genes, namely *UBC* and *GAPDH*, were selected as reference genes and were quantified in triplicate in all four samples. However, upon inspection of the results, differential expression was noted by investigating the amplification plots of both genes; large deviations in C_T values was seen between the kidney control and kidney cancer samples for *UBC*, while *GAPDH* displayed large C_T value deviations between the lung cancer and lung control samples. These results suggested regulation of *UBC* and *GAPDH* in these specific cancer samples. Based on the results, it was decided to use *UBC* as a reference gene for the lung samples only and *GAPDH* only for the kidney samples.

The results obtained from the qPCR reactions were analysed in the REST-384© software package by following the comparative C_T method for relative gene expression quantification. This method could be used since the gene-specific primers used in the qPCR reactions have been optimised before, achieving comparable PCR efficiencies (table A3). The fold change and absolute regulation

ratio, as well as the $\log_2$ value of the absolute regulation ratio, was calculated for each of the target genes. The software also tested for significant results by means of randomisation tests; target genes with a p-value less than 0.05 were deemed as showing significantly different gene expression in the cancer samples when compared to the matched control samples. In the lung cancer versus lung control samples, *AHNAK* (~ 600 fold) and *Bcl-2* (~ 4 fold) showed significant up-regulation while *LIAS* (~ 24 fold) and *Casp9* (~ 37 fold) showed significant down-regulation (table 4.2 and figure 4.3). *CYPA* (~ 1.5 fold) and *SAAL1* (~ 1.2 fold) also showed slight up-regulation with *Casp3* (~ 1 fold) showing levels very similar to those in the control sample; however, these results were not statistically significant as determined by the randomisation tests. In contrast, all seven target genes (ranging between ~ 5 fold and ~ 96 fold) showed significant up-regulation in the kidney cancer sample when compared to the kidney control sample (table 4.3 and figure 4.4).

4.4 Conclusions

The relative gene expression of seven target genes was successfully measured by means of qPCR and analysed by the comparative C_T method with REST-384©. The majority of the results revealed significant differential gene regulation in the two cancer cell lines as compared to the two control cell lines.

Analysis of the relative expression of *Bcl-2* revealed significant up-regulation in both the lung and kidney cancer samples (tables 4.2-4.3 and figures 4.3-4.4). This result is expected, since the gene has been shown to be overexpressed in numerous tumours, including cancers of the kidneys, breast, central nervous system, prostate and larynx (Placzek et al., 2010; Trask et al., 2002; Yoshino et al., 2006). Overexpression of *Bcl-2* has also been associated with resistance to apoptosis, especially in cases of cytotoxic drug-resistant tumours (Azmi et al., 2011; Igney and Krammer, 2002). However, it is important to remember that *Bcl-2* is not the only anti-apoptotic Bcl-2 family member. Recently, a gene expression profile survey was conducted with all six anti-apoptotic Bcl-2 family members across 68 cancer cell lines covering eight different tissue types; when compared to the other family members, particularly *Mcl-1* and *Bcl-X_L*, relatively low levels of *Bcl-2* expression was observed and severe overexpression seemed to be limited to leukaemia cell lines (Placzek et al., 2010). These results suggest that when investigating the mechanism of apoptotic resistance in a particular cancer cell line or tissue, it is important to not limit the search to *Bcl-2* but to also consider other members of the family such as *Mcl-1* and *Bcl-X_L*.

Contrasting results were obtained for both *casp3* and *casp9*. Significant down-regulation was observed for *casp9* in the lung cancer sample with *casp3* showing levels very similar to the control sample (table 4.2 and fig. 4.3). In contrast, significant up-regulation was observed for both genes in the kidney cancer sample (table 4.3 and fig. 4.4). It would be expected for both of these

Table 4.2: Descriptive results for the analysis of the relative gene expression of the seven target genes in the lung cancer sample as compared to the lung control sample

Gene	Sample	Mean C_T	Std. error	Fold change	p-value	Log_2 value	Log_2 std. error
LIAS	Control	20.21	0.12	-23.945	0.001	-4.582	7.749
	Cancer	24.38	0.08				
CYPA	Control	27.74	0.01	1.493	0.514	0.578	3.098
	Cancer	26.75	0.09				
AHNAK	Control	33.90	0.01	595.665	0.046	9.218	4.731
	Cancer	24.27	0.01				
SAAL1	Control	32.42	0.32	1.184	0.595	0.243	1.802
	Cancer	31.76	0.11				
Casp3	Control	27.12	0.12	-1.053	0.882	-0.075	3.329
	Cancer	26.78	0.08				
Casp9	Control	22.04	0.06	-36.716	0.024	-5.198	9.172
	Cancer	26.82	0.03				
Bcl2	Control	25.14	0.04	3.815	0.046	1.932	1.937
	Cancer	22.80	0.07				

C_T – threshold cycle; Std. – standard.

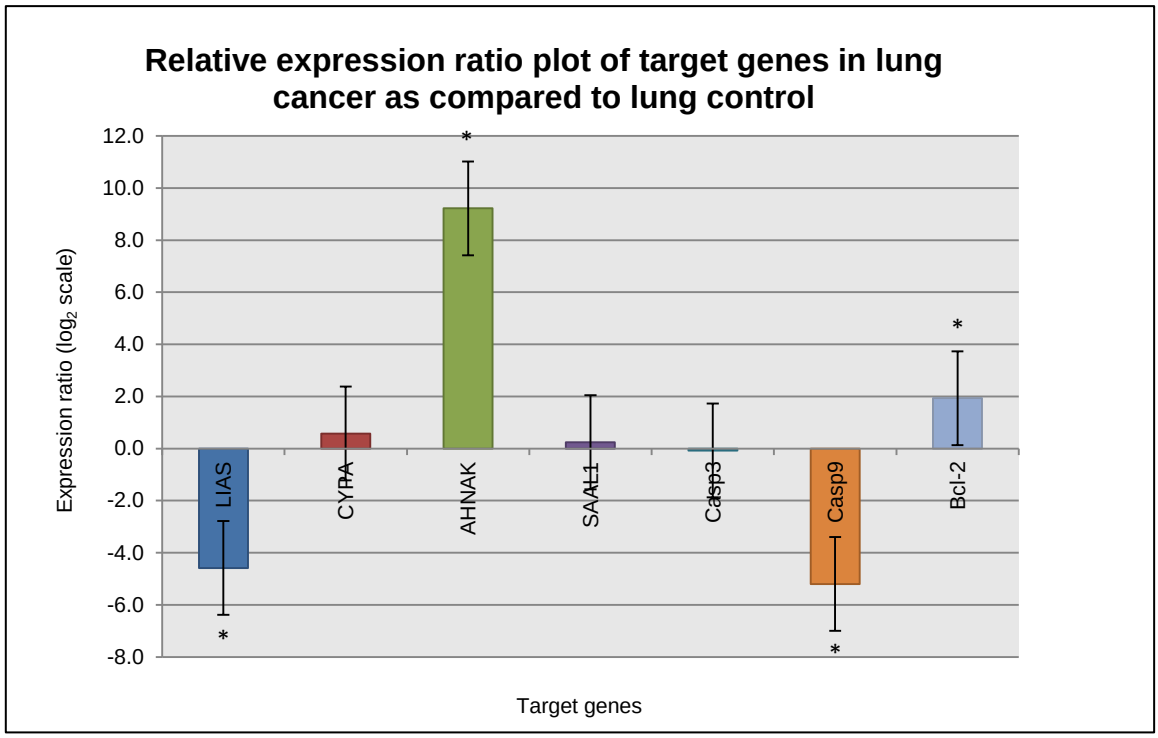

Figure 4.3: Relative expression ratio plot produced by the REST-384© software showing the absolute regulation of the target genes in a log_2 scale in lung cancer as compared to lung control. Values are the averages ± standard error of triplicate experiments. Target gene expression was normalised with the *UBC* reference gene. * indicates significant results for $p < 0.05$.

Table 4.3: Descriptive results for the analysis of the relative gene expression of the seven target genes in the kidney cancer sample as compared to the kidney control sample

Gene	Sample	Mean C_T	Std. error	Fold change	p-value	Log_2 value	Log_2 std. error
LIAS	Control	30.70	0.08	14.496	0.027	3.858	1.693
	Cancer	27.77	0.31				
CYPA	Control	26.31	0.07	70.189	0.001	6.133	2.745
	Cancer	21.14	0.11				
AHNAK	Control	29.42	0.06	95.538	0.001	6.578	2.411
	Cancer	23.77	0.01				
SAAL1	Control	31.13	0.21	4.702	0.001	2.233	0.501
	Cancer	29.83	0.04				
Casp3	Control	29.08	0.07	9.460	0.001	3.242	0.395
	Cancer	26.77	0.08				
Casp9	Control	30.74	0.23	45.615	0.001	5.511	2.926
	Cancer	26.16	0.05				
Bcl2	Control	26.39	0.02	73.534	0.001	6.200	2.527
	Cancer	21.12	0.10				

C_T – threshold cycle; Std. – Standard.

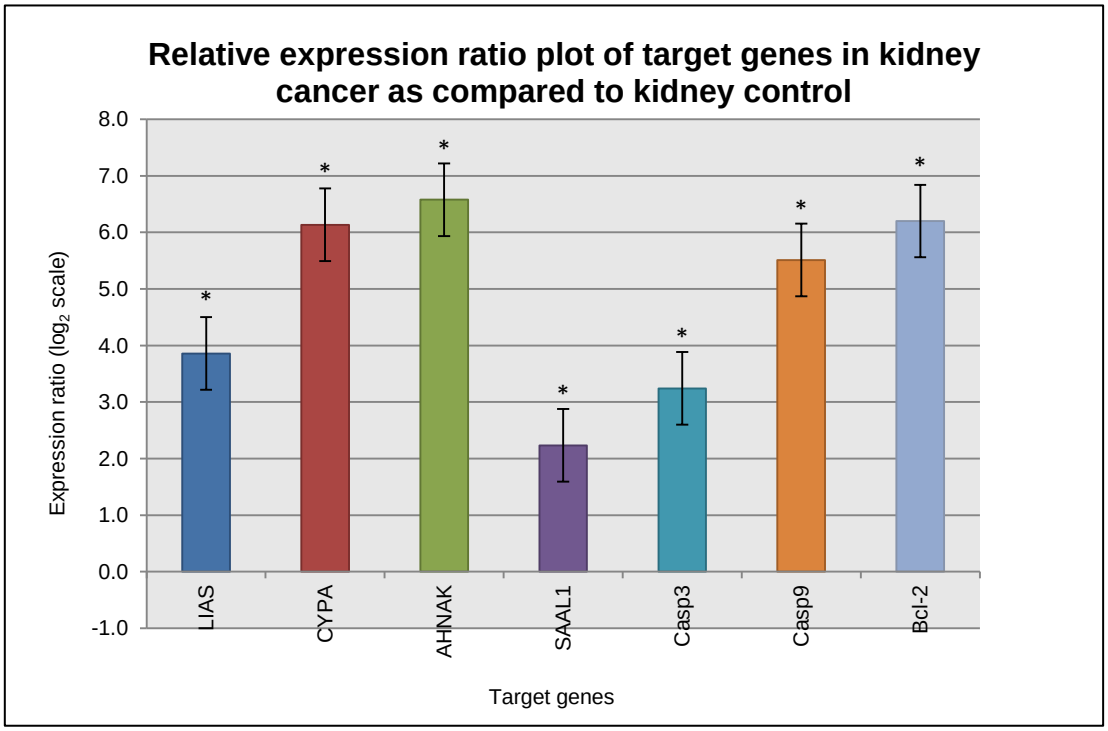

Figure 4.4: Relative expression ratio plot produced by the REST-384© software showing the absolute regulation of the target genes in a log_2 scale in kidney cancer as compared to kidney control. Values are the averages ± standard error of triplicate experiments. Target gene expression was normalised with the *GAPDH* reference gene. * indicates significant results for $p < 0.05$.

genes to display decreased expression in the cancer samples since this observation has been noted before in hepatocellular carcinoma, prostate and breast cancer for *casp3* and prostate and colon cancer for *casp9* (Huang et al., 2010; Nassar et al., 2008; Rodríguez-Berriguete et al., 2012; Sträter et al., 2010). However, variable levels of caspase expression in cancers are possible; *casp9* was shown to be up-regulated in the lymphocytes of breast cancer patients while no significant changes was seen for *casp1*, *casp3* and *casp9* expression in prostate cancer tissues when compared to normal tissues (Khanna et al., 2004; Winter et al., 2001). In addition, apoptosis mediated by caspases can also be prevented by mechanisms downstream of transcriptional regulation. Members of the IAP family function to bind and inhibit caspases, including *casp3* and *casp9*, and have been reported to be overexpressed in several cancers (Mita et al., 2008; Nachmias et al., 2004; Tamm et al., 2000). It would thus seem advantageous to investigate the expression of these proteins in cases where caspase gene expression in cancer cell lines or tissues revealed up-regulation or no significant changes in order to determine if post-transcriptional apoptotic resistance mechanisms are in place. Interestingly, alternative splicing of *casp9* have been shown to produce both an anti-apoptotic and pro-apoptotic variant (Goehe et al., 2010). In non-small cell lung carcinoma cells, increased expression of the casp9b variant maintained the tumourigenic capacity of the cells and also resulted in decreased casp9 apoptotic activity. The altered mRNA processing resulted from the up-regulation of the heterogeneous nuclear ribonucleoprotein L (hnRNP L) which interacted with the exonic splicing silencer (Goehe et al., 2010).

In terms of the novel candidate genes, some contrasting results between the lung and kidney cancer samples were also obtained. Analysis of the relative gene expression for *LIAS* showed significant down-regulation in the lung cancer sample but significant up-regulation in the kidney cancer sample (tables 4.2-4.3 and figures 4.3-4.4). As mentioned in chapter 2, a definitive role for *LIAS* in cancer is yet to be established, although possible ties are discussed. Reports of *LIAS* gene expression in cancers in literature are scarce; however two studies have identified *LIAS* as a potential tumour antigen by means of serological studies (Hishizawa et al., 2005; Ito et al., 2004). By screening a cDNA expression library, originating from a leukaemic cell line, with autologous plasma obtained from a patient with adult T cell leukaemia (ATL), *LIAS* was identified as tumour antigen and relative expression of the gene was determined (Hishizawa et al., 2005). *LIAS* showed variable gene expression in human T-cell leukaemia cell lines and decreased expression in chronic and acute ATL (Hishizawa et al., 2005). By using a similar strategy, *LIAS* was also identified a potential tumour antigen in bladder cancer (Ito et al., 2004). The isolated clones in the cDNA expression library was a close partial match to human *LIAS* while a protein BLAST search (NCBI) revealed 87% identity to mouse *LIAS*. Again, *LIAS* gene expression was evaluated by means of qPCR and was shown to be up-regulated in various bladder cancer cell lines and tissues as well as gastric and renal cell cancer tissues compared to various normal tissues. Northen blot analysis

revealed similar results (Ito et al., 2004). Finally, *LIAS* was also shown to be up-regulated in a peripheral blood B-lymphocyte cell line in response to ionising radiation (Lin et al., 2007).

CYPA showed significant up-regulation in kidney cancer but only slight up-regulation in lung cancer (tables 4.2-4.3 and figures 4.3-4.4). Nevertheless, an up-regulation is to be expected. Numerous other studies have shown *CYPA* to be up-regulated in a variety of cancers and, as discussed in chapter 2, *CYPA* might have a proliferative function in tumour cells. A similar observation was seen in the relative expression of *SAAL1*. Significant up-regulation was measured in the kidney cancer sample while only a slight up-regulation was detected in the lung cancer sample (tables 4.2-4.3 and figures 4.3-4.4). However, in the case of *SAAL1*, there are no expected results and its molecular function is unknown. A gene expression profile in type 2 diabetes mellitus patients revealed decreased *SAAL1* gene expression when compared to control subjects (Manoel-Caetano et al., 2012). Recently, a large-scale RNAi screen identified *SAAL1* as a downstream target in p53-p21 and p16-pRB pathways (Rovillain et al., 2011). The results obtained for *SAAL1* in these two studies were however not discussed by the authors, who, due to the size of the studies, only discussed the main and most noteworthy results. Even though *SAAL1* was identified as a downstream target of the abovementioned pathways, its functional role within the pathways needs to be established in order to determine how this could potentially be associated with apoptosis or cancer. A more tangible association for *SAAL1* with a disease state was however recently identified. Sato and colleagues reported the overexpression of *SAAL1* in the inflamed foot joints of a collagen-induced arthritic mice model and in human rheumatoid- and osteoarthritis patients (Sato et al., 2011). More specifically, the up-regulation was exhibited by synovial fibroblasts in the inner layer of the synovial membrane. In addition, the thickness of the synovial lining was shown to correlate with *SAAL1* overexpression and the gene was suggested to be involved in the progression of synovitis (Sato et al., 2011).

The final target gene *AHNAK* revealed similar results in the analysis its relative expression; a significant up-regulation in both the lung and kidney cancer samples (tables 4.2-4.3 and figures 4.3-4.4). Even though its molecular function is still unknown, the gene is potentially involved in cell migration based on expression studies. A transcriptome and proteome analysis of six human metastatic tumour cell lines identified *AHNAK* to be essential for actin cytoskeleton dynamics, pseudopod protrusion and tumour cell migration and invasion (Shankar et al., 2010). *AHNAK* was also identified in a gene expression profile of gastric cancer tissues as one of the few genes shown to be up-regulated in tumours with perineural invasion compared to tumours without (Jhawer et al., 2009). Furthermore, *AHNAK* was suggested to be of considerable relevance to angiotropism and extravascular migratory metastasis when a gene expression profile of metastatic melanoma tissues was constructed (Lugassy et al., 2011). In addition, an up-regulation in *AHNAK* gene expression was also observed in the cell membrane of migratory mesenchymal cells during embryonic development (Kingsley et al., 2001).

The qPCR technique used in this part of the study offered a specific and sensitive method for the measurement of the relative gene expression of the four novel candidate genes as well as three additional genes known to be involved in apoptosis. Significant differential expression in the cancer samples were obtained for the majority of the genes and the expression levels of several genes were supported by studies in literature. Promising avenues to explore in future work would be to repeat this work in tumour tissues and to include more genes known to be involved in apoptosis to potentially construct a gene expression profile of a particular cancer. This, for example, could assist in the generation of custom arrays which could potentially be used for diagnostic purposes. Investigating and comparing the gene expression of a novel candidate gene in these profiles could assist in their characterisation and potentially identify pathways of apoptotic resistance and/or tumour progression. In addition, the use of these candidate genes as potential biomarkers in cancer could also be investigated. For example, a gene like *SAAL1* only showed up-regulation in kidney cancer, but not in lung cancer, whereas *LIAS* showed down-regulation in lung cancers, but up-regulation in kidney cancers. This data is completely novel and could be a valuable source as potential markers for cancer.

4.5 References

Arya, M., Shergill, I., Williamson, M., Gommersall, L., Arya, N., and Patel, H. (2005). Basic principles of real-time quantitative PCR. Expert Rev. Mol. Diagn. *5,* 209-219.

Azmi, A.S., Wang, Z., Philip, P.A., Mohammad, R.M., and Sarkar, F.H. (2011). Emerging Bcl-2 inhibitors for the treatment of cancer. Expert Opin. Emerging Drugs *16,* 59-70.

Bustin, S., and Nolan, T. (2004). Pitfalls of quantitative real-time reverse-transcription polymerase chain reaction. J. Biomol. Tech. *15,* 155-166.

Derveaux, S., Vandesompele, J., and Hellemans, J. (2010). How to do successful gene expression analysis using real-time PCR. Methods *50,* 227-230.

Ginzinger, D.G. (2002). Gene quantification using real-time quantitative PCR: an emerging technology hits the mainstream. Exp. Hematol. *30,* 503-512.

Goehe, R.W., Shultz, J.C., Murudkar, C., Usanovic, S., Lamour, N.F., Massey, D.H., Zhang, L., Camidge, D.R., Shay, J.W., Minna, J.D., *et al*. (2010). hnRNP L regulates the tumorigenic capacity of lung cancer xenografts in mice via caspase-9 pre-mRNA processing. J. Clin. Invest. *120,* 3923-3939.

Higuchi, R., Fockler, C., Dollinger, G., and Watson, R. (1993). Kinetic PCR analysis: real-time monitoring of DNA amplification reactions. Biotechnology *11,* 1026-1030.

Hishizawa, M., Imada, K., Sakai, T., Ueda, M., Hori, T., and Uchiyama, T. (2005). Serological identification of adult T-cell leukaemia-associated antigens. Br. J. Haematol. *130,* 382-390.

Huang, H., Zhang, X., Zhou, H., Xue, Y., Dong, Q., Ye, Q., and Qin, L. (2010). Expression and prognostic significance of osteopontin and caspase-3 in hepatocellular carcinoma patients after curative resection. Cancer Sci. *101,* 1314-1319.

Igney, F., and Krammer, P. (2002). Death and anti-death: tumour resistance to apoptosis. Nat. Rev. Cancer *2,* 277-288.

Ito, K., Fujita, T., Akada, M., Kiniwa, Y., Tsukamoto, M., Yamamoto, A., Matsuzaki, Y., Matsushita, M., Asano, T., Nakashima, J.*, et al.* (2004). Identification of bladder cancer antigens recognized by IgG antibodies of a patient with metastatic bladder cancer. Int. J. Cancer *108,* 712-724.

Jhawer, M., Coit, D., Brennan, M., Qin, L., Gonen, M., Klimstra, D., Tang, L., Kelsen, D., and Shah, M. (2009). Perineural invasion after preoperative chemotherapy predicts poor survival in patients with locally advanced gastric cancer: gene expression analysis with pathologic validation. Am. J. Clin. Oncol. *32,* 356-362.

Khanna, A.K., Plummer, M., Sadasiwan, C., Purdy, A., and Walker, A. (2004). Differential expression of peroxisome proliferator-activated receptor (alpha and gamma), chemokines, integrins, and caspases in normal and breast cancer tissues. Proc. Amer. Assoc. Cancer Res. *2004,* 808.

Kingsley, P.D., McGrath, K.E., Maltby, K.M., Koniski, A.D., Ramchandran, R., and Palis, J. (2001). Subtractive hybridization reveals tissue-specific expression of AHNAK during embryonic development. Dev. Growth Differ. *43,* 133-143.

Kubista, M., Andrade, J.M., Bengtsson, M., Forootan, A., Jonák, J., Lind, K., Sindelka, R., Sjöback, R., Sjögreen, B., Strömbom, L., *et al*. (2006). The real-time polymerase chain reaction. Mol. Aspects Med. *27,* 95-125.

Lin, R., Sun, Y., Li, C., Xie, C., and Wang, S. (2007). Identification of differentially expressed genes in human lymphoblastoid cells exposed to irradiation and suppression of radiation-induced apoptosis with antisense oligonucleotides against caspase-4. Oligonucleotides *17,* 314-326.

Lugassy, C., Lazar, V., Dessen, P., van den Oord, J.J., Winnepenninckx, V., Spatz, A., Bagot, M., Bensussan, A., Janin, A., Eggermont, A.M., *et al*. (2011). Gene expression profiling of human angiotropic primary melanoma: selection of 15 differentially expressed genes potentially involved in extravascular migratory metastasis. Eur. J. Cancer *47,* 1267-1275.

Manoel-Caetano, F.S., Xavier, D.J., Evangelista, A.F., Takahashi, P., Collares, C.V., Puthier, D., Foss-Freitas, M.C., Foss, M.C., Donadi, E.A., Passos, G.A., *et al*. (2012). Gene expression profiles

displayed by peripheral blood mononuclear cells from patients with type 2 diabetes mellitus focusing on biological processes implicated on the pathogenesis of the disease. Gene *511,* 151-160.

Mita, A.C., Mita, M.M., Nawrocki, S.T., and Giles, F.J. (2008). Survivin: key regulator of mitosis and apoptosis and novel target for cancer therapeutics. Clin. Cancer Res. *14,* 5000-5005.

Morrison, T., Weis, J., and Wittwer, C. (1998). Quantification of low-copy transcripts by continuous SYBR Green I monitoring during amplification. BioTechniques *24,* 954-962.

Nachmias, B., Ashhab, Y., and Ben-Yehuda, D. (2004). The inhibitor of apoptosis protein family (IAPs): an emerging therapeutic target in cancer. Semin. Cancer Biol. *14,* 231-243.

Nassar, A., Lawson, D., Cotsonis, G., and Cohen, C. (2008). Survivin and caspase-3 expression in breast cancer: correlation with prognostic parameters, proliferation, angiogenesis, and outcome. Appl. Immunohistochem. Molecul. Morphol. *16,* 113-120.

Pfaffl, M.W. (2001). A new mathematical model for relative quantification in real-time RT–PCR. Nucleic Acids Res. *29,* DOI: 10.1093/nar/29.9.e45.

Pfaffl, M.W., Horgan, G.W., and Dempfle, L. (2002). Relative expression software tool (REST©) for group-wise comparison and statistical analysis of relative expression results in real-time PCR. Nucleic Acids Res. *30,* e36-e46.

Pfaffl, M.W., Tichopad, A., Prgomet, C., and Neuvians, T.P. (2004). Determination of stable housekeeping genes, differentially regulated target genes and sample integrity: BestKeeper – Excel-based tool using pair-wise correlations. Biotechnol. Lett. *26,* 509-515.

Placzek, W., Wei, J., Kitada, S., Zhai, D., Reed, J., and Pellecchia, M. (2010). A survey of the anti-apoptotic Bcl-2 subfamily expression in cancer types provides a platform to predict the efficacy of Bcl-2 antagonists in cancer therapy. Cell Death Dis. *1,* DOI:10.1038/cddis.2010.18.

Rodríguez-Berriguete, G., Galvis, L., Fraile, B., de Bethencourt, F.R., Martínez-Onsurbe, P., Olmedilla, G., Paniagua, R., and Royuela, M. (2012). Immunoreactivity to caspase-3, caspase-7, caspase-8, and caspase-9 forms is frequently lost in human prostate tumors. Hum. Pathol. *43,* 229-237.

Rovillain, E., Mansfield, L., Lord, C., Ashworth, A., and Jat, P. (2011). An RNA interference screen for identifying downstream effectors of the p53 and pRB tumour suppressor pathways involved in senescence. BMC Genomics *12,* 355-367.

Sato, T., Fujii, R., Konomi, K., Yagishita, N., Aratani, S., Araya, N., Aono, H., Yudoh, K., Suzuki, N., Beppu, M.*, et al.* (2011). Overexpression of SPACIA1/SAAL1, a newly identified gene that is

involved in synoviocyte proliferation, accelerates the progression of synovitis in mice and humans. Arthritis Rheum. *63,* 3833-3842.

Schmittgen, T., and Livak, K. (2008). Analyzing real-time PCR data by the comparative C_T method. Nat. Protoc. *3,* 1101-1108.

Shankar, J., Messenberg, A., Chan, J., Underhill, T.M., Foster, L.J., and Nabi, I.R. (2010). Pseudopodial actin dynamics control epithelial-mesenchymal transition in metastatic cancer cells. Cancer Res. *70,* 3780-3790.

Sträter, J., Herter, I., Merkel, G., Hinz, U., Weitz, J., and Möller, P. (2010). Expression and prognostic significance of APAF-1, caspase-8 and caspase-9 in stage II/III colon carcinoma: caspase-8 and caspase-9 is associated with poor prognosis. Int. J. Cancer *127,* 873-880.

Tamm, I., Kornblau, S.M., Segall, H., Krajewski, S., Welsh, K., Kitada, S., Scudiero, D.A., Tudor, G., Qui, Y.H., Monks, A., *et al*. (2000). Expression and prognostic significance of IAP-family genes in human cancers and myeloid leukemias. Clin. Cancer Res. *6,* 1796-1803.

Trask, D.K., Wolf, G.T., Bradford, C.R., Fisher, S.G., Devaney, K., Johnson, M., Singleton, T., and Wicha, M. (2002). Expression of Bcl-2 family proteins in advanced laryngeal squamous cell carcinoma: correlation with response to chemotherapy and organ preservation. Laryngoscope *112,* 638-644.

Valasek, M.A., and Repa, J.J. (2005). The power of real-time PCR. Advan. in Physiol. Edu. *29,* 151-159.

VanGuilder, H., Vrana, K., and Freeman, W. (2008). Twenty-five years of quantitative PCR for gene expression analysis. BioTechniques *44,* 619-626.

Winter, R.N., Kramer, A., Borkowski, A., and Kyprianou, N. (2001). Loss of caspase-1 and caspase-3 protein expression in human prostate cancer. Cancer Res. *61,* 1227-1232.

Wong, M., and Medrano, J. (2005). Real-time PCR for mRNA quantitation. BioTechniques *39,* 75-85.

Yoshino, T., Shiina, H., Urakami, S., Kikuno, N., Yoneda, T., Shigeno, K., and Igawa, M. (2006). Bcl-2 expression as a predictive marker of hormone-refractory prostate cancer treated with taxane-based chemotherapy. Clin. Cancer Res. *12,* 6116-6124.

Chapter 5: Conclusions

5.1 Final remarks and conclusions

Apoptosis represents a finely orchestrated and highly conserved natural form of cell death (Fadeel and Orrenius, 2005; Kam and Ferch, 2000). It is executed in one of three pathways and can be induced by a variety of stimuli (Elmore, 2007). In spite of its opposing role, the importance of apoptosis has been equalled to that of mitosis and the process, which is mediated by numerous genes and proteins, is thus highly regulated (Elmore, 2007; Fadeel and Orrenius, 2005). Apoptosis is vital for the preservation of cell and tissue homeostasis but also performs several defensive and protective functions (Elmore, 2007). However, altered or deregulated apoptosis can have severe pathological consequences and apoptosis has been shown to play a central role in several diseases, including neurological and autoimmune diseases as well as many cancers (Adams and Cory, 2007; Kam and Ferch, 2000). Consequently, the search for apoptotic-based therapies has received much attention and of vital importance to this quest is the elucidation and characterisation of the specific mediators of apoptosis and their regulation. Even though much progress has been made since apoptosis's initial description in 1972, more research is needed to fully understand the complete cascade of molecular events that make up apoptosis (Elmore, 2007; Kerr et al., 1972; Ola et al., 2011). Thus, this study aimed to assist in this characterisation, as well as to identify novel candidate genes potentially involved in resistance to apoptosis. These genes could also serve as potential targets for apoptosis-based therapeutic strategies.

The first objective of this study was to verify the involvement of three novel candidate genes in resistance to apoptosis induced by C_2-cermaide and camptothecin. These candidate genes were identified in a previously performed pilot study where apoptosis-resistant phenotypes were observed in CHO cells following promoter-trap mutagenesis by means of retroviral integration in the promoter sequences for each of the respective candidate genes. Since the pilot study made use of a haploid model, the results obtained needed to be verified in a diploid model. This was performed in the current study, in addition to using a more specific technique of gene knockdown in case the observed phenotype resulted from some other consequence from the technique used in the pilot study. The current study successfully verified the results obtained from the pilot study for two of the candidate genes, namely *LIAS* and *CYPA*. Following gene knockdown by means of RNAi, cells displayed significant levels of apoptosis resistance as measured by the apoptosis assays (Fig. 2.14-2.17 and 2.20-2.23). However, the results obtained for the third candidate gene, *RPL9*, contrasted the results obtained in the pilot study. Knockdown cell lines for this gene displayed sensitivity to apoptosis induction comparable to that shown by the wild type cells (Fig. 2.18-2.19 and 2.24-2.25). These results excluded *RPL9* as a candidate gene. *RPL9* was most likely identified in the pilot study due to the fact that the gene's chromosomal location is adjacent to *LIAS*; hence, the apoptotic resistance phenotype observed in the pilot was in fact attributed to

knockdown of *LIAS*. Since these two genes share a bi-directional promoter, the inverse PCR technique could have amplified sequences from the *RPL9* gene adjacent to the promoter and to *LIAS*. Comparable results were obtained for both apoptosis assays performed, confirming apoptosis as the mode of cell death. Comparable results were also obtained for both of the apoptotic inducers, indicating that the observed apoptotic resistance phenotype was not restricted to a specific inducer. This is important to consider since the molecular events of apoptosis that ensues following induction can differ between different stimuli (Fulda, 2010; Kam and Ferch, 2000; Kolesnick and Krönke, 1998); hence the resistance phenotype is not restricted to certain set of molecular events. Furthermore, comparable results were also obtained for both knockdown cell lines generated for each of the candidate genes, confirming the specificity of the RNAi technique. Possible links to the apoptotic process for *LIAS* and *CYPA* are discussed in section 2.4. Even though no direct links to apoptosis were identified for *LIAS*, possible sequences of events that may potentially lead to apoptosis resistance are described. These involve the deregulation of metabolic processes and of ROS. In both cases, restoring the normal levels of *LIAS*, and thus LA, might restore sensitivity to apoptosis. As mentioned, the exogenous application of LA was shown to be capable of inducing apoptosis in tumour cells (Dozio et al., 2010; Shi et al., 2008; Simbula et al., 2007; Wenzel et al., 2005). Interestingly, LA was however unable to induce apoptosis in normal cells (Van de Mark et al., 2003; Wenzel et al., 2005). This observation alludes to a potential anticancer therapeutic capacity for *LIAS*/LA; tumour cells are targeted and sensitised to apoptosis, while the surrounding normal cells are unaffected. This is in contrast to many traditional anticancer therapies, where normal tissues are often destroyed along with the tumour which can result in serious complications and side-effects (Nussbaumer et al., 2011). Additionally, this also suggests the expression of a cancer-specific epitope which is not recognised by LA treatment in normal cells. A more direct link to apoptosis was however identified for *CYPA*. Previous studies have shown a functional association with AIF, and it is through this association that CYPA contribute to DNA fragmentation during apoptosis (Candé et al., 2004; Tanaka et al., 2011; Wissing et al., 2004; Zhu et al., 2007). Specifically, Candé et al. (2004) reported resistance to apoptosis in cells deficient of *CYPA*, thus supporting the results obtained in this study. In addition, several other studies have reported overexpression of *CYPA* in tumour cells and that knockdown of *CYPA* expression results in apoptosis (Choi et al., 2007; Li et al., 2006; Sun et al., 2011; Yang et al., 2007). This observation also alludes to a potential anticancer therapeutic capacity for *CYPA*, similar to *LIAS*; while knockdown of *CYPA* results in apoptosis in tumour cells, normal cells become resistant to apoptosis. However, the 'side-effects' of *CYPA* knockdown in normal cells would have to be investigated *in vivo*.

During the course of this study, a bioinformatic approach was used to identify and characterise novel candidate genes possibly involved in resistance to apoptosis. Candidate genes were identified by performing BLAST searches with nucleotide sequences obtained from the pilot study.

This resulted in the identification of two additional novel candidate genes, namely *AHNAK* and *SAAL1*. As mentioned in section 3.4, these candidate genes, as well as *LIAS*, were identified more than once by the BLAST searches. Future work would be to generate stable knockdown cell lines for *AHNAK* and *SAAL1* using a diploid model to verify their involvement in apoptotic resistance. A total of four candidate genes, namely *LIAS*, *CYPA*, *AHNAK* and *SAAL1* were subjected to further bioinformatic analysis in order to aid in their characterisation and to ascertain possible links to apoptosis by investigating the protein interactions and cellular pathway involvement for each of the candidate genes. Results obtained from the bioinformatic analysis for *LIAS* and *CYPA* supported the findings discussed in section 2.4. Interacting proteins for LIAS, as revealed by the STRING database, included the PDH, KGDH, BCKDH and GCS complexes (data not shown). In addition, the search for cellular pathways produced the metabolic pathway for LIAS. For CYPA, both the human and mouse AIF protein homologs were identified as interacting proteins (table 3.5). In terms of *AHNAK* and *SAAL1*, the bioinformatic analyses confirmed the novelty of these genes to the apoptotic process and no definitive function for these genes in apoptosis could be established. For all four candidate genes, possible links to apoptosis were however noted upon investigating the interacting proteins for each of the genes. These interactions provide promising avenues which can be explored in future studies by additional bioinformatic analyses or experimental methods.

The final objective of this study was to investigate the gene expression levels of the candidate genes in normal and cancer cell lines. This was achieved by performing qPCR, a sensitive and reliable technique capable of quantifying the expression of a target gene in real time (Pfaffl, 2001). The comparative C_T method was used for the analysis of the qPCR results which was normalised against one of two reference genes. The relative gene expression of three additional genes, namely *Bcl-2*, *casp3* and *casp9*, was also investigated. Even though these genes are known to be involved in apoptosis and have been extensively investigated in cancer, it remains important to characterise these genes and their protein products since they represent promising targets for the development of apoptotic-based therapies. In particular, investigating the gene and protein expression of *Bcl-2*, and its anti-apoptotic family members, in different cancer cell lines and tissues can assist in the optimisation of therapeutic strategies targeting the anti-apoptotic Bcl-2 family members, such as the SMI's described in chapter 1 (section 1.2.6). The up-regulation of *LIAS* observed in the kidney cancer sample (Fig. 4.4) was supported by studies in literature also reporting increased gene expression. However, the down-regulation of *LIAS* observed in the lung cancer sample (Fig. 4.3) supported the results obtained in chapter 2 where decreased expression levels maintained cell survival (Fig. 2.14-2.15 and 2.20-2.21). These observations warrant further investigation especially since a definitive role for *LIAS* in apoptosis and/or cancer progression is yet to be established. In addition, it should be noted that this paradox could have been influenced by the heterogeneity seen in different types of cancer, possible differences between cultured cancer cell lines and tumour tissues and between different stages of tumour development as well

as the possibility of a dual role for these genes that depends on the disease state and cellular environments.

SAAL1 was shown to be up-regulated in both cancers (Fig. 4.3 and 4.4) and this was supported by a recent study which suggested that increased *SAAL1* gene expression is needed for synoviocyte proliferation (Sato et al., 2011). As discovered during the bioinformatic analysis in chapter 3, very little information about *SAAL1* is available and this was also observed in a literature search for the gene. To our knowledge, this is the first report of *SAAL1* gene expression in cancer. The increased *CYPA* gene expression observed in the cancer cell lines (Fig. 4.3 and 4.4) is also supported by numerous other studies in literature. Possible reasons for this up-regulation in cancer are discussed in section 2.4.2, as well as how knockdown of *CYPA* could still potentially result in resistance to apoptosis. These reasons are intertwined with a protein interaction with AIF and based on this, it would be interesting to investigate the gene and protein expression, as well as protein localisation, of CYPA and AIF in various cancer and control tissues. Lastly, *AHNAK* was found to be overexpressed in both the lung and kidney cancer samples. Again, this was also supported by studies in literature which also suggested a role for *AHNAK* in cell migration and metastasis of tumours. This suggestion is in turn supported by a protein interaction identified by the bioinformatic analysis performed in chapter 3; a known interaction between AHNAK and YES1 was revealed by the I2D database (table 3.3). YES1 is known to play a role in cell-cell adhesion and cytoskeleton remodelling and is also mediator of AKT-mediated cell migration. It would thus seem that AHNAK and YES1 could function together in promoting cell migration and tumour metastasis. However, this would also contrast the results obtained in chapter 2; thus, further investigation is warranted.

In conclusion, this study identified two novel candidate genes, namely *AHNAK* and *SAAL1*, potentially involved in the resistance to apoptosis. In addition, results obtained for two candidate genes identified in a previously performed pilot study, *LIAS* and *CYPA*, were also verified. Differential expression of these genes in cancer is also reported. Results obtained during this study can aid in the complete characterisation and functional annotation of these genes. Potential ties to apoptosis and associations with cancer are discussed for all four candidate genes and the possibilities of therapeutic strategies for anticancer treatments involving these candidate genes are noted.

5.2 References

Adams, J., and Cory, S. (2007). The Bcl-2 apoptotic switch in cancer development and therapy. Oncogene *26,* 1324-1337.

Candé, C., Vahsen, N., Kouranti, I., Schmitt, E., Daugas, E., Spahr, C., Luban, J., Kroemer, R.T., Giordanetto, F., Garrido, C., *et al*. (2004). AIF and cyclophilin A cooperate in apoptosis-associated chromatinolysis. Oncogene *23,* 1514-1521.

Choi, K.J., Piao, Y.J., Lim, M.J., Kim, J.H., Ha, J., Choe, W., and Kim, S.S. (2007). Overexpressed Cyclophilin A in cancer cells renders resistance to hypoxia- and cisplatin-induced cell death. Cancer Res. *67,* 3654-3662.

Dozio, E., Ruscica, M., Passafaro, L., Dogliotti, G., Steffani, L., Pagani, A., Demartini, G., Esposti, D., Fraschini, F., and Magni, P. (2010). The natural antioxidant alpha-lipoic acid induces p27Kip1-dependent cell cycle arrest and apoptosis in MCF-7 human breast cancer cells. Eur. J. Pharmacol. *641,* 29-34.

Elmore, S. (2007). Apoptosis: a review of programmed cell death. Toxicol. Pathol. *35,* 495-516.

Fadeel, B., and Orrenius, S. (2005). Apoptosis: a basic biological phenomenon with wide-ranging implications in human disease. J. Intern. Med. *258,* 479-517.

Fulda, S. (2010). Evasion of apoptosis as a cellular stress response in cancer. Int. J. Cell Biol. *2010,* 370835-1-370835-6.

Kam, P.C.A., and Ferch, N.I. (2000). Apoptosis: mechanisms and clinical implications. Anaesthesia *55,* 1081-1093.

Kerr, J., Wyllie, A., and Currie, A. (1972). Apoptosis: a basic biological phenomenon with wide-ranging implications in tissue kinetics. Br. J. Cancer *26,* 239-257.

Kolesnick, R.N., and Krönke, M. (1998). Regulation of ceramide production and apoptosis. Annu. Rev. Physiol. *60,* 643-665.

Li, M., Zhai, Q., Bharadwaj, U., Wang, H., Li, F., Fisher, W.E., Chen, C., and Yao, Q. (2006). Cyclophilin A is overexpressed in human pancreatic cancer cells and stimulates cell proliferation through CD147. Cancer *106,* 2284-2294.

Nussbaumer, S., Bonnabry, P., Veuthey, J., and Fleury-Souverain, S. (2011). Analysis of anticancer drugs: a review. Talanta *85,* 2265-2289.

Ola, M., Nawaz, M., and Ahsan, H. (2011). Role of Bcl-2 family proteins and caspases in the regulation of apoptosis. Mol. Cell. Biochem. *351,* 41-58.

Pfaffl, M.W. (2001). A new mathematical model for relative quantification in real-time RT–PCR. Nucleic Acids Res. *29,* DOI: 10.1093/nar/29.9.e45.

Sato, T., Fujii, R., Konomi, K., Yagishita, N., Aratani, S., Araya, N., Aono, H., Yudoh, K., Suzuki, N., Beppu, M., *et al.* (2011). Overexpression of SPACIA1/SAAL1, a newly identified gene that is involved in synoviocyte proliferation, accelerates the progression of synovitis in mice and humans. Arthritis Rheum. *63,* 3833-3842.

Shi, D., Liu, H., Stern, J.S., Yu, P., and Liu, S. (2008). Alpha-lipoic acid induces apoptosis in hepatoma cells via the PTEN/Akt pathway. FEBS Lett. *582,* 1667-1671.

Simbula, G., Columbano, A., Ledda-Columbano, G., Sanna, L., Deidda, M., Diana, A., and Pibiri, M. (2007). Increased ROS generation and p53 activation in α-lipoic acid-induced apoptosis of hepatoma cells. Apoptosis *12,* 113-123.

Sun, S., Wang, Q., Giang, A., Cheng, C., Soo, C., Wang, C., Liau, L., and Chiu, R. (2011). Knockdown of CypA inhibits interleukin-8 (IL-8) and IL-8-mediated proliferation and tumor growth of glioblastoma cells through down-regulated NF-κB. J. of Neuro-Oncol. *101,* 1-14.

Tanaka, H., Shimazaki, H., Kimura, M., Izuta, H., Tsuruma, K., Shimazawa, M., and Hara, H. (2011). Apoptosis-inducing factor and cyclophilin A cotranslocate to the motor neuronal nuclei in amyotrophic lateral sclerosis model mice. CNS Neurosci. Ther. *17,* 294-304.

Van de Mark, K., Chen, J.S., Steliou, K., Perrine, S.P., and Faller, D.V. (2003). α-Lipoic acid induces p27Kip-dependent cell cycle arrest in non-transformed cell lines and apoptosis in tumor cell lines. J. Cell. Physiol. *194,* 325-340.

Wenzel, U., Nickel, A., and Daniel, H. (2005). α-lipoic acid induces apoptosis in human colon cancer cells by increasing mitochondrial respiration with a concomitant O_2^--generation. Apoptosis *10,* 359-368.

Wissing, S., Ludovico, P., Herker, E., Büttner, S., Engelhardt, S.M., Decker, T., Link, A., Proksch, A., Rodrigues, F., Corte-Real, M., *et al.* (2004). An AIF orthologue regulates apoptosis in yeast. J. Cell Biol. *166,* 969-974.

Yang, H., Chen, J., Yang, J., Qiao, S., Zhao, S., and Yu, L. (2007). Cyclophilin A is upregulated in small cell lung cancer and activates ERK1/2 signal. Biochem. Biophys. Res. Commun. *361,* 763-767.

Zhu, C., Wang, X., Deinum, J., Huang, Z., Gao, J., Modjtahedi, N., Neagu, M.R., Nilsson, M., Eriksson, P.S., Hagberg, H., *et al.* (2007). Cyclophilin A participates in the nuclear translocation of apoptosis-inducing factor in neurons after cerebral hypoxia-ischemia. J. Exp. Med. *204,* 1741-1748.

Addendum A

Table A1: Descriptive statistics for APOPercentage™ assay as calculated with Microsoft® Excell®

Apoptotic inducer	Inducer concentration	Averages¥	Standard deviation§	F-test*	T-test¤
		LIAS KD1			
Camptothecin	0	100.00	0.00	N/A	N/A
	2	100.00	0.00	0.00	0.02
	4	100.00	0.00	0.00	0.02
	6	87.33	2.08	0.32	4.21E-04
	8	79.00	4.36	0.27	7.68E-04
	10	74.33	4.16	0.23	4.30E-04
C_2-ceramide	0	100.00	0.00	N/A	N/A
	20	94.00	1.73	0.23	0.02
	40	92.67	2.08	0.20	1.15E-04
	60	86.33	1.53	0.27	9.35E-06
	80	76.33	3.51	0.22	2.25E-04
	100	73.33	4.04	0.36	2.28E-05
		LIAS KD2			
Camptothecin	0	100.00	0.00	N/A	N/A
	2	100.00	0.00	0.00	0.02
	4	100.00	0.00	0.00	0.02
	6	92.00	2.65	0.43	2.90E-04
	8	80.67	3.21	0.17	5.15E-04
	10	76.00	2.00	0.07	2.59E-04
C_2-ceramide	0	100.00	0.00	N/A	N/A
	20	95.33	1.53	0.18	9.28E-03
	40	92.00	1.00	0.06	8.82E-05
	60	84.00	4.58	0.23	1.11E-04
	80	76.00	5.00	0.36	3.41E-04
	100	71.33	5.51	0.24	6.12E-05
		NIH-3T3 (for comparison with *LIAS* KD cell lines)			
Camptothecin	0	100.00	0.00		
	2	84.33	3.51		
	4	81.00	5.00		
	6	64.33	3.06		
	8	34.67	7.09		

Apoptotic inducer	Inducer concentration	Averages[¥]	Standard deviation[§]	F-test*	T-test[¤]
	10	21.00	7.55		
C_2-ceramide	0	100.00	0.00		
	20	85.67	3.21		
	40	52.33	4.16		
	60	38.33	2.52		
	80	21.33	6.66		
	100	7.33	3.06		
			RPL9 KD1		
Camptothecin	0	100.00	0.00	N/A	N/A
	2	90.67	1.53	0.30	0.03
	4	79.00	2.00	0.37	0.83
	6	67.00	1.00	0.20	0.02
	8	41.33	4.51	0.49	0.22
	10	18.667	2.08	0.38	0.07
C_2-ceramide	0	100.00	0.00	N/A	N/A
	20	90.00	2.65	0.43	0.08
	40	81.00	2.00	0.48	6.52E-03
	60	63.67	4.73	0.29	9.90E-03
	80	37.00	4.00	0.30	3.57E-03
	100	15.00	3.00	0.31	0.22
			RPL9 KD2		
Camptothecin	0	100.00	0.00	N/A	N/A
	2	90.67	2.52	0.46	0.05
	4	80.33	2.08	0.35	0.54
	6	68.00	2.65	0.36	0.04
	8	44.33	7.23	0.29	0.17
	10	21.33	2.52	0.48	0.03
C_2-ceramide	0	100.00	0.00	N/A	N/A
	20	91.00	1.00	0.16	0.02
	40	78.67	3.06	0.32	0.04
	60	61.67	1.53	0.20	2.74E-03
	80	38.33	7.51	0.11	0.02
	100	16.00	3.00	0.31	0.13
			NIH-3T3 (for comparison with *RPL9* KD cell lines)		
Camptothecin	0	100.00	0.00		

Apoptotic inducer	Inducer concentration	Averages[¥]	Standard deviation[§]	F-test*	T-test[¤]
	2	85.33	2.31		
	4	79.33	1.53		
	6	62.00	2.00		
	8	36.00	4.58		
	10	14.00	2.65		
C_2-ceramide	0	100.00	0.00		
	20	85.33	2.31		
	40	72.33	2.08		
	60	48.67	3.06		
	80	20.00	2.65		
	100	12.00	2.00		
			CYPA KD1		
Camptothecin	0	100.00	0.00	N/A	N/A
	2	100.00	0.00	0.00	8.16E-03
	4	92.67	2.08	0.35	8.64E-04
	6	82.33	1.55	0.25	1.08E-04
	8	73.33	0.58	0.02	5.06E-03
	10	69.00	2.00	0.36	8.74E-06
C_2-ceramide	0	100.00	0.00	N/A	N/A
	20	94.67	2.52	0.46	9.09E-03
	40	92.67	2.08	0.50	2.80E-04
	60	86.33	1.53	0.20	4.43E-05
	80	76.33	3.51	0.36	2.44E-05
	100	73.33	4.04	0.20	1.92E-05
			CYPA KD2		
Camptothecin	0	100.00	0.00	N/A	N/A
	2	100.00	0.00	0.00	8.16E-03
	4	91.33	1.53	0.50	6.52E-04
	6	86.67	1.53	0.37	7.06E-05
	8	73.67	2.31	0.20	2.20E-04
	10	69.00	2.00	0.36	8.74E-06
C_2-ceramide	0	100.00	0.00	N/A	N/A
	20	97.33	1.15	0.20	1.29E-03
	40	92.00	1.00	0.19	1.23E-04
	60	84.00	4.58	0.31	3.73E-04

Apoptotic inducer	Inducer concentration	Averages[¥]	Standard deviation[§]	F-test*	T-test[¤]
	80	76.00	5.00	0.22	6.79E-05
	100	71.33	5.51	0.12	6.21E-05
NIH-3T3 (for comparison with *CYPA* KD cell lines)					
Camptothecin	0	100.00	0.00		
	2	85.33	2.31		
	4	79.33	1.53		
	6	62.00	2.00		
	8	36.00	4.58		
	10	14.00	2.65		
C_2-ceramide	0	100.00	0.00		
	20	85.33	2.31		
	40	72.33	2.08		
	60	48.67	3.06		
	80	20.00	2.65		
	100	12.00	2.00		

[Camptothecin] – µg/ml; [C_2-ceramide] – µM; ¥ - Average values from triplicate experiments; § - Sample based estimate of standard deviation; * - Two sample F-test for variances. Based on the p-value generated by this test, the appropriate t-test was selected. ¤ - Two sample t-test assuming equal variances for F-test p-value ≥ 0.05 and two sample t-test assuming unequal variances for F-test p-value <0.05. Data was seen as statistically significant (compared with wild type NIH-3T3 data) for t-test p-value < 0.05.

Table A2: Descriptive statistics for the Caspase-3/CPP32 assay as calculated with Microsoft® Excell®

Apoptotic inducer	Inducer concentration	Averages¥	Standard deviation§	F-test*	T-test¤
			LIAS KD1		
Camptothecin	0	100.00	0.00	N/A	N/A
	2	100.00	0.00	0.00	0.02
	4	100.00	0.00	0.00	9.49E-03
	6	84.33	2.52	0.34	2.42E-03
	8	79.00	1.73	0.06	4.09E-04
	10	69.33	2.08	0.11	1.20E-04
C_2-ceramide	0	100.00	0.00	N/A	N/A
	20	93.00	2.65	0.43	0.02
	40	88.00	2.00	0.03	8.66E-03
	60	82.67	2.08	0.09	2.41E-04
	80	75.00	4.58	0.32	6.67E-05
	100	72.67	2.89	0.32	2.75E-05
			LIAS KD2		
Camptothecin	0	100.00	0.00	N/A	N/A
	2	100.00	0.00	0.00	0.02
	4	100.00	0.00	0.00	9.49E-03
	6	88.67	1.53	0.16	6.45E-04
	8	76.00	2.00	0.08	5.53E-04
	10	70.33	0.58	0.01	3.92E-03
C_2-ceramide	0	100.00	0.00	N/A	N/A
	20	93.00	2.00	0.43	0.01
	40	87.33	0.58	0.01	8.81E-03
	60	82.00	3.00	0.18	3.07E-04
	80	75.00	2.65	0.40	2.06E-05
	100	71.00	3.61	0.43	4.26E-05
			NIH-3T3 (for comparison with *LIAS* KD cell lines)		
Camptothecin	0	100.00	0.00		
	2	89.33	2.52		
	4	79.33	3.51		
	6	67.33	3.51		
	8	33.67	7.02		
	10	14.67	6.03		

Apoptotic inducer	Inducer concentration	Averages[¥]	Standard deviation[§]	F-test*	T-test[¤]
C_2-ceramide	0	100.00	0.00		
	20	85.33	2.31		
	40	50.33	6.03		
	60	33.67	6.51		
	80	19.33	3.21		
	100	9.67	4.16		
			RPL9 KD1		
Camptothecin	0	100.00	0.00	N/A	N/A
	2	93.67	1.15	0.13	0.42
	4	81.00	2.00	0.31	1.00
	6	62.00	4.00	0.49	0.85
	8	34.00	6.08	0.36	0.53
	10	15.00	4.58	0.31	0.70
C_2-ceramide	0	100.00	0.00	N/A	N/A
	20	94.33	1.53	0.50	3.55E-03
	40	81.67	2.08	0.32	0.02
	60	71.00	2.00	0.20	3.54E-04
	80	30.00	8.19	0.20	0.27
	100	15.00	5.29	0.08	0.17
			RPL9 KD2		
Camptothecin	0	100.00	0.00	N/A	N/A
	2	95.33	2.08	0.33	0.19
	4	81.67	2.52	0.41	0.78
	6	63.00	4.36	0.46	0.93
	8	37.33	6.11	0.36	0.94
	10	17.00	5.29	0.25	0.40
C_2-ceramide	0	100.00	0.00	N/A	N/A
	20	94.00	2.65	0.25	0.01
	40	83.33	3.21	0.47	0.02
	60	70.33	3.06	0.36	6.08E-04
	80	28.33	5.51	0.35	0.27
	100	13.67	2.08	0.35	0.06
			NIH-3T3 (for comparison with *RPL9* KD cell lines)		
Camptothecin	0	100.00	0.00		
	2	92.00	3.00		

Apoptotic inducer	Inducer concentration	Averages[¥]	Standard deviation[§]	F-test*	T-test[¤]
	4	81.00	3.00		
	6	62.67	4.04		
	8	39.00	4.58		
	10	13.67	3.06		
C_2-ceramide	0	100.00	0.00		
	20	86.67	1.53		
	40	73.67	3.06		
	60	41.67	4.04		
	80	23.33	4.04		
	100	9.67	1.53		
			CYPA KD1		
Camptothecin	0	100.00	0.00	N/A	N/A
	2	100.00	0.00	0.00	0.04
	4	97.67	0.58	0.04	0.01
	6	85.00	2.00	0.20	1.01E-03
	8	77.33	3.51	0.37	2.68E-04
	10	71.33	1.53	0.20	8.14E-06
C_2-ceramide	0	100.00	0.00	N/A	N/A
	20	97.33	0.58	0.13	3.48E-04
	40	91.33	2.08	0.32	1.16E-03
	60	84.33	2.08	0.21	8.38E-05
	80	74.33	4.16	0.49	1.09E-04
	100	71.00	2.00	0.37	1.88E-06
			CYPA KD2		
Camptothecin	0	100.00	0.00	N/A	N/A
	2	100.00	0.00	0.00	0.04
	4	96.67	0.58	0.04	0.01
	6	96.67	2.08	0.21	7.94E-04
	8	76.67	2.08	0.17	1.67E-04
	10	72.00	3.61	0.42	2.83E-05
C_2-ceramide	0	100.00	0.00	N/A	N/A
	20	96.33	1.15	0.36	9.43E-04
	40	91.67	2.08	0.32	1.08E-03
	60	83.67	3.06	0.36	1.37E-04
	80	75.00	3.61	0.44	7.86E-05

Apoptotic inducer	Inducer concentration	Averages[¥]	Standard deviation[§]	F-test*	T-test[¤]
	100	71.00	3.61	0.15	1.1E-05
NIH-3T3 (for comparison with *CYPA* KD cell lines)					
Camptothecin	0	100.00	0.00		
	2	92.00	3.00		
	4	81.00	3.00		
	6	62.67	4.04		
	8	37.00	4.58		
	10	13.67	3.06		
C_2-ceramide	0	100.00	0.00		
	20	86.67	1.53		
	40	73.67	3.06		
	60	41.67	4.04		
	80	23.33	4.04		
	100	9.67	1.53		

[Camptothecin] – µg/ml; [C_2-ceramide] – µM; ¥ - Average values from triplicate experiments; § - Sample based estimate of standard deviation; * - Two sample F-test for variances. Based on the p-value generated by this test, the appropriate t-test was selected. ¤ - Two sample t-test assuming equal variances for F-test p-value ≥ 0.05 and two sample t-test assuming unequal variances for F-test p-value <0.05. Data was seen as statistically significant (compared with wild type NIH-3T3 data) for t-test p-value < 0.05.

Table A3: Previously calculated qPCR efficiencies of primers for target genes and reference genes

Gene	Lung control	Lung cancer	Kidney control	Kidney cancer
GAPDH	1.97	1.95	1.96	1.95
UBC	1.94	1.97	1.95	1.94
LIAS	1.95	1.93	1.92	1.95
CYPA	1.95	1.94	1.94	1.97
AHNAK	1.92	1.94	1.94	1.95
SAAL1	1.92	1.93	1.94	1.92
Casp3	1.96	1.95	1.93	1.94
Casp9	1.93	1.95	1.95	1.93
Bcl-2	1.95	1.98	1.94	1.98